
**Gallab Bander S. Alotaibi**

# The UK saltmarsh elevations and Ecosystem Services

A thesis submitted for the degree of

Master of Philosophy

The School of Environmental Sciences, University of East Anglia,
Norwich, Norfolk, England

January 2024

**Declaration**

This research described in this is, to the best of my knowledge, original except where due reference is made.

**Gallab Bander S Alotaibi**

**Abstract**

Saltmarshes are ecologically important and provide diverse ecosystem services, including protection of shorelines, carbon sequestration, and wildlife habitat provision. Assessments of saltmarsh ecosystem services often consider them homogeneous, ignoring differences within and between marshes. This research examined the extent to which saltmarsh elevations and local tidal levels altered estimates of ecosystem service provision for 35 UK saltmarshes. LiDAR derived Digital Terrain Models (DTMs) gave reliable estimates of sediment surface elevation with an accuracy of better than 20cm. Most of the area of marshes in the South of the UK, from the Tees Estuary on the East Coast moving clockwise to the Dovey Estuary on the West coast lies at or below the level of MHWS, often with a sub-horizontal platform lying just below MHWS. These marshes make a substantial contribution to coastal protection during normal conditions by dissipating wave energy, but their contribution in reducing flooding risks is less important during storm surge events when they may be submerged to a depth of more than 2m. In the northern UK, substantial areas of marsh occur above the level of MHWS, potentially playing a bigger role in dissipating wave energy during storm surges, but the areas of land vulnerable to coastal flooding are much smaller here. The proportion of low marsh is small at most sites in the UK. The majority of saltmarsh area is predicted to have relatively high redox values and emissions of the greenhouse gases methane and nitrous oxide will therefore be low. Rapid sedimentation occurs mainly on low marshes, and rates of carbon burial will be overestimated if this is not taken into account. Mechanisms of sedimentation and vegetation succession appear to be variable and unstable, whether across the whole saltmarsh or in different parts in an individual marsh.

**Acknowledgment**

First and foremost, I am extremely grateful to my primary supervisor, Prof. Alastair Grant for his invaluable advice, continuous support, and patience during my PhD study. His immense knowledge and plentiful experience have encouraged me in all the time of my academic research and daily life. I would also like to express gratitude to my second supervisor, Dr. Iain Lake for his treasured support and his advice during my PhD study.

Mom and Dad, thank you for being there whenever I need it, and even I thought I did not need it. Thank you for teaching respect, confidence and proper etiquette. You are the best parent in the world, and I owe my success to you. I promise, I will always be by your side whenever you need me.

I would like also to thank my darling wife, Kayidah. Thank you for taking care of us, making us smile no matter how bad the day was. You make me feel loved every day. I'm blessed to have you. To my children, Bandar and Layan, watching you grow up in the UK, learn different languages, and explore the world has been an inspiration to me. Thank you both.

My gratitude extends to my brothers and my sisters, and their wonderful families for the encouragement throughout my studies.

I would like to thank, Dr. Hussein Aldosari for his support during my PHD study. You spent long time helping me when I started my journey, My gratitude for you.

Thanks, are also due to friends and office-mates Dr. Abdulaziz Almohyawi, Mr Hamadan Alzahrani, Dr. Elizabeth Duxbury, and especially Dr. Solomon Udochi for his support with R Programming.

Finally, I wish to thank the Government of Saudi Arabia for providing me with the scholarship to undertake my studies at the University of East Anglia.

## Table of content

### Contents

**List of figures**

**Chapter One**



**Chapter Two**

**Chapter Three**

**Chapter Four**

**Chapter Five**

List of Tables

**Chapter one**



**Chapter Two**



**Chapter Three**



**Chapter Four**

**Chapter Five**

## Chapter One

## General Introduction

### 1.1 Saltmarsh ecology of the United Kingdom

Saltmarshes are saline intertidal areas which have been colonised by halophytic herbs, grasses and low growing shrubs (Mitsch and Gosselink, 2007 ). They primarily occur in sheltered embayment's and estuaries in temperate latitudes, where vegetation stabilises sediments which are usually muddy (Boorman *et al.*, 1996, Mount *et al.*, 2010, Siemes *et al.*, 2020). They experience periodic flooding due to tidal fluctuations (Prahalad *et al.*, 2019), and occur approximately between mean high water of spring and neap tides in the intertidal zone (Figure 1.1) (Adnitt, 2007), although halophytic vegetation can occur at elevations that are flooded by the tide only a few times a year. The composition of saltmarsh vegetation is influenced by climate and complicated interactions between regularity of tidal inundation, wind and wave action, movements of relative sea level, deposition of suspended sediments, salinity, size of sediment particles, slope and interactions between the colonising plants, sometimes modulated by herbivores (Boorman, 2003b, Doody, 2008).

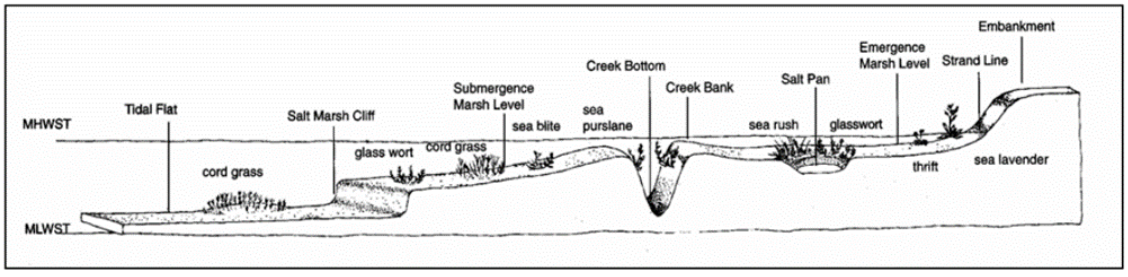


Figure 1.1 the physiographical features of saltmarsh (Adnitt, 2007).

Intertidal environments, which include mud flats and saltmarshes, deliver a wide range of ecosystem services. Salt marshes are increasingly recognized as resilient and sustainable supplements to traditional engineering structures for protecting coasts against flooding

(Mitsch and Gosselink, 2007 ). Globally, ecosystem services provided by saline and estuarine marshes include provisioning such as fuel, food and fibre; inducing service regulation for the cycling of nutrients; regulation of atmospheric and climatic conditions; processing of waste; regulation of diseases; regulation of flood hazards; and services that are cultural such as recreation, amenities and aesthetic values (Assessment, 2005, Costanza *et al.*, 2008). They act as fish, crab, and animal nursery areas, providing both food and shelter for them. Some birds may inhabit in or near saltmarshes because the marsh provides abundant food sources (Prahalad and Pearson, 2013). Barbier *et al.*, (2011) summarised ecosystems services and saltmarsh processes and functions (as shown in Table 1.1). Although marshes occupy only a small proportion (4%) of the total land area on Earth, they are associated with a substantial global value and also make a contribution to the national economy (Barbier, Hacker *et al.*, 2011). Across the UK, the contribution of intertidal environments has been ranked at an estimated £48 billion, or 3.46% of the national income (Jones *et al.*, 2011b).

Table 1.1. Ecosystem services, processes and functions for saltmarshes (Barbier, Hacker *et al.*, 2011).

| **Ecosystem services** | **Ecosystem processes and functions** |
|---|---|
| Food and raw material | Generates diversity and biological productivity |
| Coastal protection | Dissipate or attenuate waves |
| Erosion control | Stabilises sediment by protect structure of vegetation roots. |
| Water purification | Purifies water by particle deposition. |
| Carbon sequestration | Generates biological activity, biogeochemical activity and sedimentation. |
| Conservation of fishers | Provides habitat and nursey ground. |
| Tourism, education, recreation and research | Considers to be suitable habitat for diverse fauna and flora. |

According to (Alongi, 1998, Chen *et al.*, 2021, Gu *et al.*, 2021), saltmarshes and mudflats which are intertidal environments are considered as some of the most productive biologically on earth. They are able to accumulate significant levels of particulate organic matter from estuaries, rivers and the ocean (Abril *et al.*, 2002). Intertidal sediments store some of the organic material, including reactive nutrients from particles and the accreted sediments sequester large carbon (C), nitrogen (N) and phosphorous (P), including nutrients discharged to the environment in wastewater and agriculture. Some of the

nutrients are recycled and returned to coastal systems and estuaries, while others are permanently buried (Abril, Nogueira *et al.*, 2002, Andrews *et al.*, 2006, Andrews *et al.*, 2000, Jickells *et al.*, 2000). This has led to an interest in the potential of coastal wetland systems to sequester large amounts of carbon, potentially mitigating the consequences of anthropogenic carbon dioxide emissions (Craft *et al.*, 2003, Livesley and Andrusiak, 2012, Santin *et al.*, 2009, Shepherd *et al.*, 2007).

In the UK, saltmarshes have been categorised into three broad types: ungrazed marsh in the South-East England, grazed marsh in the Irish Sea coast of England and Wales and marshes at the head of sea lochs on the West coast of Scotland (Adam, 1978). The total area of UK saltmarshes is estimated to be between 40,000 to 45,000 ha (Burd, 1989, Jones, Angus *et al.*, 2011a). Table 1.2 gives estimates made by (Boorman, 2003a) based on data from (Burd, 1989). Saltmarshes are particularly widely distributed particularly in Essex, Norfolk, Lancashire, Hampshire and North Kent (May and Hansom, 2003), and the largest five sites (Wash, Inner Solway, Morecambe Bay, Burry estuary, Dee estuary) are responsible for 1/3 of the total UK population (Burd, 1989). However, the extent of saltmarshes is currently less than in the past due to human activity, such as reclamation for agricultural use and industrial development (Morris *et al.*, 2004).

Table 1.2 Distribution of saltmarsh sites in the UK, showing distribution of sites by size (cited in (Boorman, 2003a).

| Region | Area (ha) | Sites > 100ha | Sites < 10ha | All Sites | Av. area (ha) |
|---|---|---|---|---|---|
| England | 32,500 | 59 | 16 | 120 | 270.8 |
| Scotland | 6,748 | 14 | 280 | 380 | 17.8 |
| Wales | 6,089 | 8 | 15 | 57 | 106.8 |
| N. Ireland* | 239 | 0 | 6 | 15 | 15.9 |
| Total | 45,337 | 81 | 304 | 577 | 78.6 |

* Refers to designated saltmarsh sites only

Saltmarshes occur in Northern Ireland's sea loughs, the large low-lying land estuaries in eastern and northwest England and in Wales, with minute areas in southern England estuaries and the firths of eastern and southwest Scotland. Small saltmarsh sites (embayments and beaches) in sea lochs are characteristic of northwest Scotland. An estimate made is that at the mean high-water line, 3% of the Scottish coastline, 24% of the English coastline and 11% of the Welsh coastline is made up of saltmarsh (GROUP, 1999, Posford, 1998). The distinct zonation patterns and low species diversity of saltmarsh vegetation have made them ideal subjects for investigations that aim to demonstrate how gradients in the environment and competitive interactions with other plant species on saltmarshes may create plant community patterns. Experimental manipulations of these ecosystems readily allows examination of the association between biotic and abiotic factors in explaining the permanence and development of the various distributional patterns ((CCP), 2021, Bertness, 1991, Pennings *et al.*, 2003, Silvestri and Marani, 2004, Vince and Snow, 1984).

Although these strong environmental gradients on saltmarshes are well known, many studies of ecosystem services delivered by saltmarshes have treated them as a homogeneous object, neglecting variation within and between sites (Adams *et al.*, 2012, Ford *et al.*, 2012, King and Lester, 1995, Martin *et al.*, 2010, Möller and Spencer, 2002, Möller *et al.*, 1999). They assume that a square metre of saltmarsh is the same, and that its delivery of ecosystem services can be calculated in the same way wherever it is. However, ecological characteristics of saltmarshes vary substantially with elevation. There are also important differences in biogeochemical functioning between low shore and high shore of saltmarshes. A pioneer marsh has largely anoxic sediments, whereas a mature saline marsh that is high on the shore usually has oxic sediments, although sediments continue to be

anoxic on high marshes where there is a transition to freshwater marshes, usually dominated by *Phragmites* (Mossman *et al.*, 2012a, Mossman *et al.*, 2020). Therefore, it is crucial to take into account elevation changes across saltmarsh when we calculate ecosystem services delivered by saltmarshes.

### 1.2 Saltmarsh elevation

Saltmarshes develop relatively high in the tidal frame where sediments are sufficiently stable to allow vegetation succession to begin (Doody, 2008). The regularity of tidal inundation is a key influence on the areas above this. Inundation by tides affects abiotic conditions and therefore plant distributions (Mossman, Grant *et al.*, 2020, Xie *et al.*, 2019), and interactions between species (Hacker and Bertness, 1999). Inundation frequency and duration are strongly correlated with elevation (Mossman, Grant *et al.*, 2020) but significant differences in the relationship between frequency of tidal inundation and elevation occur between sites, as tidal range is variable depending on geographical location (Shepard *et al.*, 2011). In intertidal habitat creation schemes, knowledge of tidal elevations can help in predicting ecological development (Crooks *et al.*, 2002, Dawe *et al.*, 2000).

Mean high water of neap tides (MHWN) varies from 1.17 metres to 6.7 metres above Ordnance Datum Newlyn (ODN), which corresponds to mean sea level in the UK. The range of mean high-water tides of spring (MHWS) varies from 2 metres at Portland to more than 12 metres in the Bristol Channel (https://southwalesports.co.uk/Marine_Information/Marine_Information/Bristol_Channel_Tides/;(NTSLF, 2020)). This range can vary significantly on smaller spatial scales. A delay in high tides can be observed as high water crosses large areas or travels along shallow channels of almost flat marsh lands, particularly in estuaries and inlets (Healey *et al.*, 1981). The association between tidal levels and elevation can change over distances that are relatively short. For instance, (Van der Molen, 1997) observed variations in the mean high water levels reaching 80cm over distances that were shorter than 15 km in Cape Cod Bay, USA, where there is an average tidal range of three metres. (Mossman *et al.* 2012 a) observed differences of 70 cm over distances of 40 km in the height of MHWS along the

North Norfolk coast, and they also observed smaller scale variations in the elevation of MHWN caused by local topography.

In Cromer (Norfolk, UK), the difference between predicted and observed tidal heights could be substantial. The average (±SD) variation between predicted and observed tides was 0.16 ± 0.20 m, with tides that were individual ranging up to 1.29 metres higher and 0.83 metres lower than was predicted. The identified levels of high water which were assessed at sites of saltmarshes on the North Norfolk coast were strongly correlated with those observed at Cromer (Mossman, Davy *et al.*, 2012b). It is therefore important that tidal heights at a site should be correlated with observed data collected and recorded by a permanent tide gauge rather than with predicted tides. For example, (Goodwin and Mudd, 2019) reported that MHWS at Morecambe Bay saltmarsh was at 3.3 m (ODN) using Heysham tide gauge data which is 15 Km away from that marsh, but the nearest location where tidal data are available is Arnside (5 km away) where the MHWS is at an elevation of 5.33 m ODN.

Low-elevation marshes are often associated with high mineral sedimentation rates where there is sufficient availability of sediments (Rosencranz *et al.*, 2017). The greater submergence of the low marsh provides more opportunity for sediment to settle out of suspension, while deposition rates are lowest in marshes in high elevations which are flooded rarely (Cahoon and Reed, 1995, Marion *et al.*, 2009, Pethick, 1981, Temmerman *et al.*, 2003). Diverse factors also affect vertical marsh accretion, including age of marsh (increase in level of marsh within the tidal frame), relative sea level, compaction and reclamation frequency (Brown *et al.*, 1999).

### 1.3 Saltmarsh elevation and vegetation

Intertidal environments including saltmarshes were examined ecogeomorphologically in different aspect in the field and laboratory. Recently remote sensing has become an effective approach for examining, monitoring and maintaining saltmarshes in large scale (Chust *et al.*, 2008, Krolik-Root *et al.*, 2015, Mitasova *et al.*, 2010).

In saltmarshes, the presence of vegetation helps to dissipate wave energy, which can be reduced by 82% in saltmarshes compared with only 29% over bare tidal flats, although the extent of the reduction in incident wave energy may be lower under storm conditions (Möller, Spencer *et al.*, 1999). Wave energy is dissipated by up to 50% under average tidal inundation depths in the first 10–20 m of a surface of saltmarsh that is vegetated (Möller, 2006). (Möller *et al.*, 2014) examined wave dissipation in water depths of 2 m in a large flume, finding a maximum 19.5% reduction of wave height across 40m of marsh for waves with an amplitude of 0.3 m, but lower dissipation than this for both larger and smaller waves.

The proportional sediment surface elevation in saltmarsh landscapes is a variable which is substantial and that defines the frequency duration of the tidal inundation of these habitats, which ultimately control the productivity of the community of saltmarsh plants (Morris *et al.*, 2002). Salt Marsh vegetation comprises primarily emergent aquatic macrophytes with at least 10% cover, especially saline or halophytic species (NatureServe, 2022). Salt marsh macrophytes under natural conditions are generally divided into five macrophytes zones from low to high elevation: (1) the pioneer macrophyte zone, (2) the low tide beach zone, (3) the middle tide beach zone, (4) the high tide beach zone and (5) the transition zone. The main features of macrophytes at the lower elevations are salt tolerance and flood resistance. Pioneer macrophytes gradually transition to higher

elevations as mesophytes (Boorman, 2003a). There will also be largely distributions of halophyte on saltmarshes and their distributions are highly associated to the tidal frame elevation and microtopography is of greater importance in regulating halophyte distribution than previously recognized. (Hladik and Alber, 2012, Mossman, Grant *et al.*, 2020).

Halophytes inhibit coastal saltmarshes as they are able to tolerate the physical environment, in particular, salinity and tidal inundation. The distribution of species may be changed by inter-species interactions (Bertness and Ellison, 1987, Pennings and Callaway, 1992), but elevation within the tidal frame determines inundation frequency and duration which directly impacts on plants and indirectly alters a suite of other environmental variables which affect plant physiology and ultimately occurrence (Bockelmann *et al.*, 2002, Chapman, 1960, Mossman, Grant *et al.*, 2020, Zedler *et al.*, 1999).

### 1.4 Remote sensing data

Over the years, the utilisation of remote sensing (RS) to inform management of wetlands has grown significantly since the mid-1970s when there was exclusive use of aerial photographs. Satellite RS technology is considered one of the tools which is most effective for large-scale vegetation mapping, particularly to control and monitor the distribution pattern of saltmarsh vegetation (Gao and Zhang, 2006). It has been applied to characterise various wetlands, such as saltmarshes, saltpans and tidal flats (Bhuvaneswari *et al.*, 2011). It has provided useful data pertaining to the change in vegetation in wetlands, over time, and across a large scale. (Sghair and Goma, 2013) used remote sensing (Landsat TM and aerial photographs) and GIS, combined with ground truth, to assess wetland vegetation changes in two contrasting wetland sites in the UK: a freshwater wetland at Wicken Fen between 1984 and 2009, and saltmarsh wetland between 1988 and 2009 in Caerlaverock Reserve. The study clearly showed the ability of the RS/GIS approach, using both satellite imagery and aerial photography, to detect spatial and temporal variation in two different wetland vegetation types. This can subsequently generate information which is valuable to facilitate the conservation and management of wetland habitats.

RS technology has the ability to take a comprehensive view of spatial data and control dynamic spatiotemporal shifts in saltmarsh vegetation. For example, (Arzandeh and Wang, 2003) monitored the recent growth of an invasive species by utilising diverse satellite images, including Landsat thematic mapper (TM), Satellite pour observation de la Terre (SPOT) and Indian Remote Sensing Satellite (IRS). Laba *et al.*, (2008) used high-resolution QuickBird imagery and Earth Resources Data Analysis (ERDAS) software to generate maps of invasive plants in the Hudson River National Estuarine Research Reserve. RS has been used to extract information about wave mechanism and process of coastal habitat (Mani

and Parthasarathy, 2006), storm impact on coastline (Nayak *et al.*, 2001), sea grass and mangrove ecosystem (Dahdouh-Guebas, 2002). Multispectral imagery which has a high spatial resolution has important benefits for eco-geomorphological evaluation and modelling, and high-resolution of Airborne Imaging Multispectral Sensor AIMS-1 imagery obtained from RS improved characterisation of ditches, panes and drained ponds in saltmarsh (Mani and Parthasarathy, 2006).

Most science organisations in the world utilise high-spatial-resolution accurate digital elevation models (DEMs) for developing mapping, and they have become extremely important for many applications, including; control of flooding, management of forests and urban planning (Lim *et al.*, 2003). New applications of geo-positioning have been developed using LIDAR (light detection and ranging) DEMs (James *et al.*, 2006, Laporte-Fauret *et al.*, 2020, Matso *et al.*, 2019, Miller *et al.*, 2007, Rodarmel *et al.*, 2006). Measurements for the characterisation and monitoring of coastal environments widely use LIDAR technology (Chust, Galparsoro *et al.*, 2008, Krolik-Root, Stansbury *et al.*, 2015, Mitasova, Hardin *et al.*, 2010), which allows DEMs to be developed even when site access is prohibited (Montané and Torres, 2006).

DEMs derived from LIDAR have been utilised in conjunction with geographic information systems (GIS) to generate metrics for landscapes which may be used to predict distribution of plants (Hladik and Alber, 2014). In one of the most successful applications of RS, a study combined distance to channel and size of channels in order to quantify the impact of tidal channels, thereby, predicting the probability of species in saltmarshes with 90% accuracy (Sanderson *et al.*, 2001). Other landscape metrics of upland areas, such as slope and distance, have also been included in some analyses (Andrew and Ustin, 2009, Griffin *et al.*, 2011, Sellars and Jolls, 2007). Many researchers have combined elevation with field

measurements of edaphic variables successfully including lower salinity, lower soil moisture, and reduced soil nutrients (Byrd and Kelly, 2006, Lang *et al.*, 2010), as simple elevation correlations and/or metrics for distance alone have not fully explained zonation of plants in saltmarshes (Silvestri *et al.*, 2005, Zedler, Callaway *et al.*, 1999).

In tidal environments such as saltmarshes, determining elevation by LIDAR has been successful (Farris *et al.*, 2019), with vertical resolutions as low as 5.0 centimetres (Goetz *et al.*, 2010, Lohani and Mason, 2001, Montané and Torres, 2006), and this data is enormously valuable on a system-wide scale (Thomas *et al.*, 2010).

Previous studies reveal the importance of RS technique of facilitating information gathering of intertidal environments including saltmarshes.

### 1.5 Accuracy and precision of LIDAR

Airborne LiDAR systems emit short laser pulses and thereafter, the reflected light is captured using photodiode detectors. The distance to the target (range) can be estimated by calculating the laser flight time propagating through the medium, with the assumption that light travels in a known constant speed within the medium (Glennie *et al.*, 2013, Williams *et al.*, 2013). LiDAR technology has become an integral source of surface elevation data and provides valuable information to facilitate investigation on the effects of the rise of sea level on coastal ecosystems and the impact of tidal inundation on vegetation (Titus and Anderson, 2009).

LIDAR provides accuracy and resolution (El-Sheimy *et al.*, 2005), providing more accurate information than high-resolution aerial photographs and Google Earth reveals (Sadr, 2016). Digital elevation models (DEMs) encompass two types of elevation model Digital Surface Models (DSM) and Digital Terrain Models (DTM). Currently, geospatial analysis has facilitated the mapping of features that are complicated and located above the ground (e.g. areas that are built up) by producing DSMs which capture the built-up and natural earth-surface features, and DTMs that characterise topography or elevation of the bare-earth (Li *et al.*, 2004).

Saltmarsh topography can be successfully characterised by LiDAR data (Wang *et al.*, 2009). However, derived elevation products obtained from LIDAR vary between types of surfaces, specifically in environments that include vegetation that is dense in nature (Hladik and Alber, 2012, Schmid *et al.*, 2011). So, in places with trees and vegetation, LIDAR has the ability to remove isolated trees, but continuous vegetation is probably impossible, because all the instruments captured the top of the vegetation, and LIDAR algorithm is unable to remove continuous vegetation (Anders *et al.*, 2019). Removing creeks would, in principle,

be feasible using an algorithm that water always flows downhill, but saltmarsh pans are going to be more difficult, because they are not connected to anything else (Hladik *et al*., 2013).

Elevation accuracy in low-lying areas such as saltmarshes by using DTMs can help saltmarsh managers perfect their approach to evaluating saltmarsh changes (Fernandez *et al.*, 2017). Although accuracy of LIDAR-derived digital terrain models (DTMs) vary in saltmarshes is insufficient to distinguish topographic structures for determining flooding arising from tides or patterns in vegetation (Hladik and Alber, 2012, Krolik-Root, Stansbury *et al.*, 2015), it is more accurate than of determining the elevations of saltmarshes in flats that are of an intertidal nature, salt pans and low-density short (<0.2 m height) plant habitats (Fernandez *et al.*, 2017), and in large expanses of saltmarsh, high accuracy (82%) can be obtained by using object-based image analysis with high-resolution habitat classification.

### 1.6 Using landcover maps to define saltmarsh extent

Data from land cover play a key role in a large number of research studies on Earth system (Yang *et al.*, 2013). Earth system models are completed by the essential input of land cover (Dai *et al.*, 2003, Jung *et al.*, 2006, Liu *et al.*, 1997) or models on habitats (Liang *et al.*, 2010, Özesmi and Mitsch, 1997, Pearson *et al.*, 2004, Yu *et al.*, 2015). Land cover is further deemed fundamental for the design and administration of natural resources (Gong, 2012, LaFontaine *et al.*, 2015, Pauleit and Duhme, 2000, Zhong *et al.*, 2012).

Many users consider land cover maps that are global as essential baseline data sources [such as the United Nation's Millennium Ecosystem Assessment (Assessment, 2005), the World Conservation Monitoring Centre (WCMC) and the Global Environmental Outlook project (UNEP, 2002)]. The applications of these users are also highly diversified and lead to modelling of climate change, sustainable development and forest cover estimation. For instance, global circulation models (GCMs) utilise land cover types and also use vegetation static models. In simulations of dynamic models, the model predictions can be verified using land cover (Foley *et al.*, 1998).

In the UK map on land cover, more than 50% of the land area is cultivated (Arable and Horticulture also Improved Grassland, 51%) or created (" Built-up Zones and Gardens" (6%)). The remainder is semi natural vegetation, with forests covering 12% of the UK – divided equally between Broadleaved Forest and Coniferous Forest. The remaining 30% of the UK is divided between Coastal (1%), Semi-natural prairie and Mountain, heath and marsh (Rowland *et al.*, 2017).

Rowland, Morton *et al.*, (2017) indicated that in the UK LCM 2015 enhance the complexity of discovering zones that are representative and that are adequately sized to undertake classification based on spectral characteristics. Cawkwell *et al.*, (2007), report that

saltmarsh habitats can be reasonably identified using land cover data and saltmarsh vegetation was also fairly well separated from the non-saltmarsh vegetation (Kumar and Sinha, 2014).

### 1.7 Thesis aims, objectives and hypotheses

The assessment of ecosystem services provided by saltmarshes does not consider the substantial heterogeneity of their ecology and biogeochemical functioning, particularly that driven by their elevation in the tidal frame. Therefore, the core objective of this research was to evaluate the degree to which considering saltmarsh elevations alters estimates of the ecosystem services that exist in the UK.

The study objectives were formulated as follows:

(i) To determine the distribution of elevations that occur on a sample of UK saltmarshes.

(ii) To relate these elevations to local tidal levels on each marsh.

(iii) To predict the likely effectiveness of wave dissipation across the elevation profile of saltmarsh.

(iv) To evaluate the contribution of saltmarshes to sea defence, and the extent to which this is modulated by their elevation.

(v) To evaluate to what extent the implications of saltmarsh elevation alter greenhouse gas (GHG) emissions and carbon burial that occur on the sample of the UK saltmarshes.

The study addresses these by:

Assessing the accuracy of elevation data for saltmarshes determined using high resolution differential Global Positioning System (GPS). Quantifying the distribution of elevations that occur on a sample of UK saltmarshes using landcover maps determined from (RS) data combined with elevation data obtained using Lidar (chapters 2 and 3). Investigating tidal elevations observations and evaluate saltmarshes contribution as a sea defence using elevation data obtained combined with tidal data obtained in the main saltmarshes of the

UK (chapter 3). Modelling wave dissipation across the elevation gradients that occur saltmarshes using elevation data and tidal heights to determine water depths (chapter 4). Evaluating biogeochemical functions that occur on samples of UK saltmarshes using data on their elevation and geomorphological history and data on the relationship between elevation and sediment redox potential (Chapter 5). Discussing the contribution of elevation in saltmarshes by bringing together the findings of the chapters (chapter 6).

## Chapter Two

## Characterising saltmarshes using remote sensing data

### 2.1 Introduction

The coverage of wetlands is almost 10% of the terrestrial area of land in the British and Irish landscape (Dawson *et al.*, 2003). These environments include rivers, ponds, lakes and ditches that are saturated with marshes and water permanently and may also be flooded for extended time periods (Polunin and Walters, 1985). Saltmarsh, as a part of wetlands, consists of four core types; low, pioneer, upper or high marsh and transitional marsh (Adnitt, 2007), and this environment is geomorphologically complicated due to the distribution of creeks and tidal channels (Esselink *et al.*, 1998, French and Spencer, 1993, Leonard, 1997, Reed *et al.*, 1999).

Elevation is a critical variable in saltmarshes even though the elevation range on these systems is small (Mckee and Patrick, 1988). Therefore, small elevation changes can influence the general vegetation and marsh extent (Zedler, Callaway *et al.*, 1999), and marshes may reveal changes and patchiness that are substantial due to the subtle sensitivity of vegetation to elevation differences (Cahoon and Lynch, 1997, Titus and Anderson, 2009).

((CCP), 2021, Boorman *et al.*, 2002, Boorman, Pakeman *et al.*, 1996, Boorman, 1999, Burger *et al.*, 2019, Thomas, Buckland *et al.*, 2010) indicated that low marshes, patchiness of vegetation is well recognised and the presence of pans is very well documented, and their formation relatively well understood (Perillo and Iribarne., 2003). However, there is also small-scale heterogeneity of vegetation on many high marshes, for reasons that are not fully understood (Adam, 2002). For example, in *Phragmites* communities in the high marsh there is mineral and organic sediment trapping greater than *Spartina* communities and also

control of invasive of *Phragmites australis* influenced by relative sea level rise may enhance erosion (Rooth and Stevenson, 2000). This makes them ecologically more interesting and will lead to heterogeneity in greenhouse gas production which will be discussed later on briefly in chapter 5.

Elevation has a major impact on saltmarsh ecology and biogeochemistry (Cahoon and Lynch, 1997, Mckee and Patrick, 1988, Titus and Anderson, 2009, Zedler, Callaway *et al.*, 1999) and therefore on the delivery of ecosystem services. Therefore, there is need to correctly determine elevations relative to terrestrial datum and subsequently, identify the association between the elevations of saltmarshes and frequency of inundation. Navarro et al., (2021) provide a comprehensive set of coastal land-cover uses and land change information for the south-eastern coast of Australia, with a focus on coastal wetland (mangrove and saltmarsh) ecosystems and they mention that maps obtained in their study have the potential to provide local and statewide managers with an effective method for quantifying the gains and losses of coastal wetlands in south-eastern Australia.

### 2.1.1 Airborne Light Detection and Ranging (LIDAR) for saltmarshes

Airborne Light Detection and Ranging (LIDAR) data allows the delineation of an accurate model of the earth surface. The particular data is obtained (thousands of times per second) using rapidly reflected laser pulses at the ground surface. Laser energy is reflected back from the vegetation canopy and ground surface. These data allow the construction of a Digital Surface Model (DSM) from which a Digital Terrain Model (DTM) can be calculated by making some assumptions about the shape of the ground surface and the likely morphologies of vegetation and buildings (Digimap EDINA, 2021, (https://digimap.edina.ac.uk/)).

LIDAR has been applied for detection and mapping intertidal vegetation to assess saltmarsh vegetation and intertidal habitat in the Canadian Gulf of St. Lawrence (Collin *et al.*, 2010), and was used to map and examine flooding in coastal regions which is induced by a surge in Cádiz Bay (SW Spain) (Raji *et al.*, 2011). Imagery which is multispectral in nature is combined with LIDAR has been used to analyse geomorphologically the saltmarsh feature distribution at the Great Marsh, Massachusetts, USA (Millette *et al.*, 2010). High resolution LIDAR data has been adopted for vegetation classification and determination of the height of vegetation for marshes in the vicinity of Lake Hatchineha in Florida, USA (Genç *et al.*, 2004).

The majority of work developing algorithms to construct DTMs from DSMs has been carried out on terrestrial environments, and it is not clear how well these algorithms will operate on saltmarshes. However (Beumier, 2008) obtained good results for the removal of small buildings or woods where the terrain is rather flat and DTMs enable to estimating the minimum bias in ground elevation across saltmarsh (Wang, Menenti *et al.*, 2009). Moreover, they have been significantly improved for the identification and characterisation of the geospatial distribution of pans, ponds that are drained, and ditches across the surface of the marsh by dividing each feature according to their elevation (Millette *et al.*, 2010).

### 2.1.2 Aims of the study

In this study we have:

(i) Used the UK Land Cover Map data as the most comprehensive standard dataset on saltmarsh extent in the UK (Rowland *et al.*, 2017).

(ii) Critically evaluated the accuracy of this classification by a process of expert judgement using aerial photographs; and where available, detailed ecological surveys; photos or personal knowledge of the marshes as will be seen below (Fig. 2.8; 2.9 and Table 2.1).

(iii) Assessed the ability to obtain accurate data on saltmarsh elevation from Lidar data by comparing the derived DTM with the underlying DSM to identify whether algorithms designed for terrestrial environments work on saltmarshes.

(iv) Compared the DTM with high resolution GPS measurements to assess the accuracy of the DTM.

## 2.2 Method

Thirty-five saltmarsh sites were identified from around the English, Scottish and Welsh coasts using geographic information system GIS (ArcGIS 10.6.1) (Fig 2.1). They were chosen to cover all the areas of the UK where there are substantial areas of saltmarsh and to represent locations where LIDAR data were available, ideally at 0.25 m resolution. However, for some sites, the available LIDAR data had pixel sizes of 0.5 or 1m (Table 2.1). We avoided including managed retreat sites, although accidental retreat sites at Tollesbury and Streat are included. Thirteen sites were examined to compare LIDAR-derived DSMs and DTMs (Fig 2.5). We illustrate this approach using the Stiffkey site as example, with the remaining sites provided in appendix to Chapter 2) Moreover, we used photoshop program to combine saltmarsh terrain with land cover of the marsh to generate 3D terrain generator (Fig 2.3, Stiffkey site as example, see more in appendix to Chapter 2). LIDAR data originally collected by the Environment Agency in England and Wales and Scottish Natural Heritage (SNH) in Scotland were obtained from Digimap (https://digimap.edina.ac.uk/). DTM and DSM data were downloaded in 2018 and saved as raster files (see table 2.1). These data files were imported and analysed using statistical programs both Matlab, (R2016B) and R 3.5.0 version Core team in 2018, (Pinheiro *et al.*, 2018), using the raster, rgdal, rgeos, magick, imager and ggplot2 packages (Barthelme, 2017, Bivand *et al.*, 2015, Bivand and Rundel, 2017, Hadley, 2016, Hijmans *et al.*, 2017, Jeroen, 2018). The DTM and DSM were compared for Thirteen sites CrablyCreek, Dengie, Donna Nook, Fambridge, Foulton Hall, Hamford Water, Llanrhidian, Stiffkey, Sudbourne, Tollesbury, Undy, Warham, and Welwick All these sites are located in the East of England except Undy and Llanrhidian which are located in the West of England and South Wales respectively. Figure 2.1 displays the location of the saltmarshes in the UK.

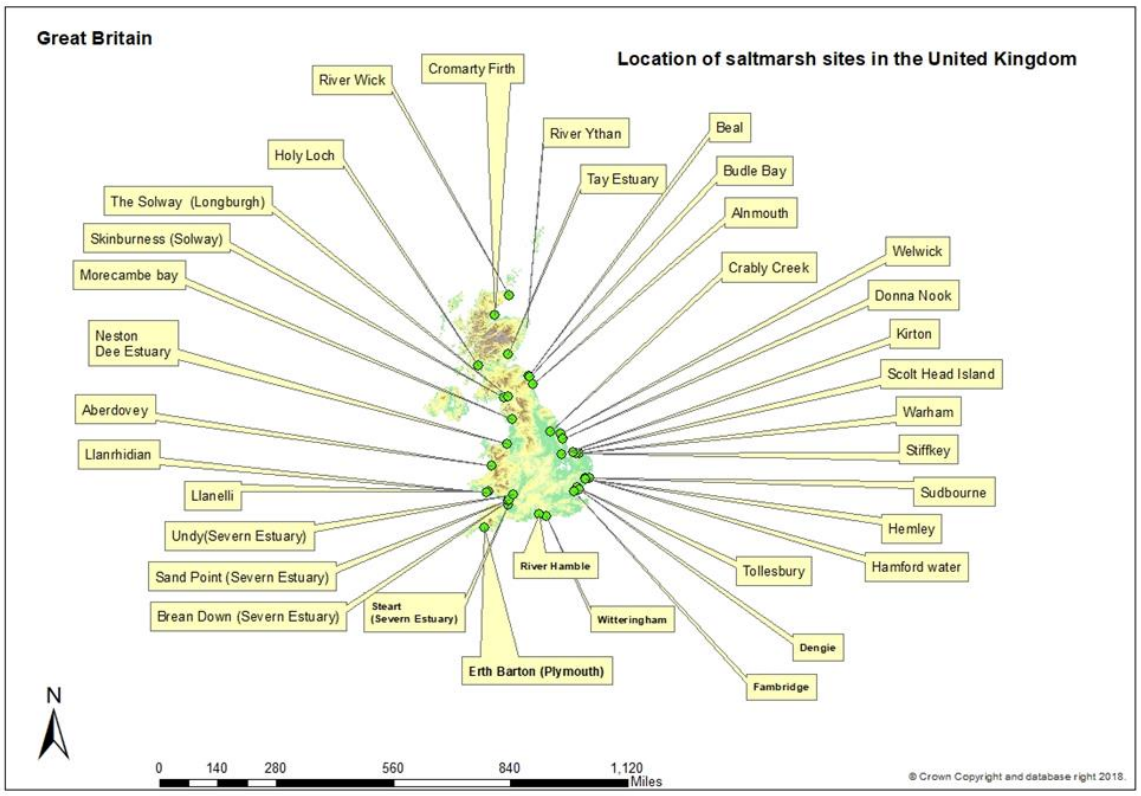


Figure 2.1 Location of saltmarsh sites studied in the United Kingdom. The map was produced ArcGIS Desktop 10.3.

These sites are variable and contain different structures but both Undy and Llanrhidian have high elevations relative to other sites (see result section chapter 3). A number of transects were randomly defined across these saltmarshes, stretching from the sand or mudflat beyond the marsh's seaward edge to the seawall or rising ground at the marsh's landward edge. Elevations of the DTM were plotted against those of the DSM and both were plotted against distance along transect to examine the differences (more details in results section) using Matlab commands (Matlab, R2016B, see scripts in appendix to Chapter 2). The DTM and DSM were also plotted as colour coded maps (Fig 2.5, 6 and 7, Stiffkey site as example, see more in appendix to chapter 2).

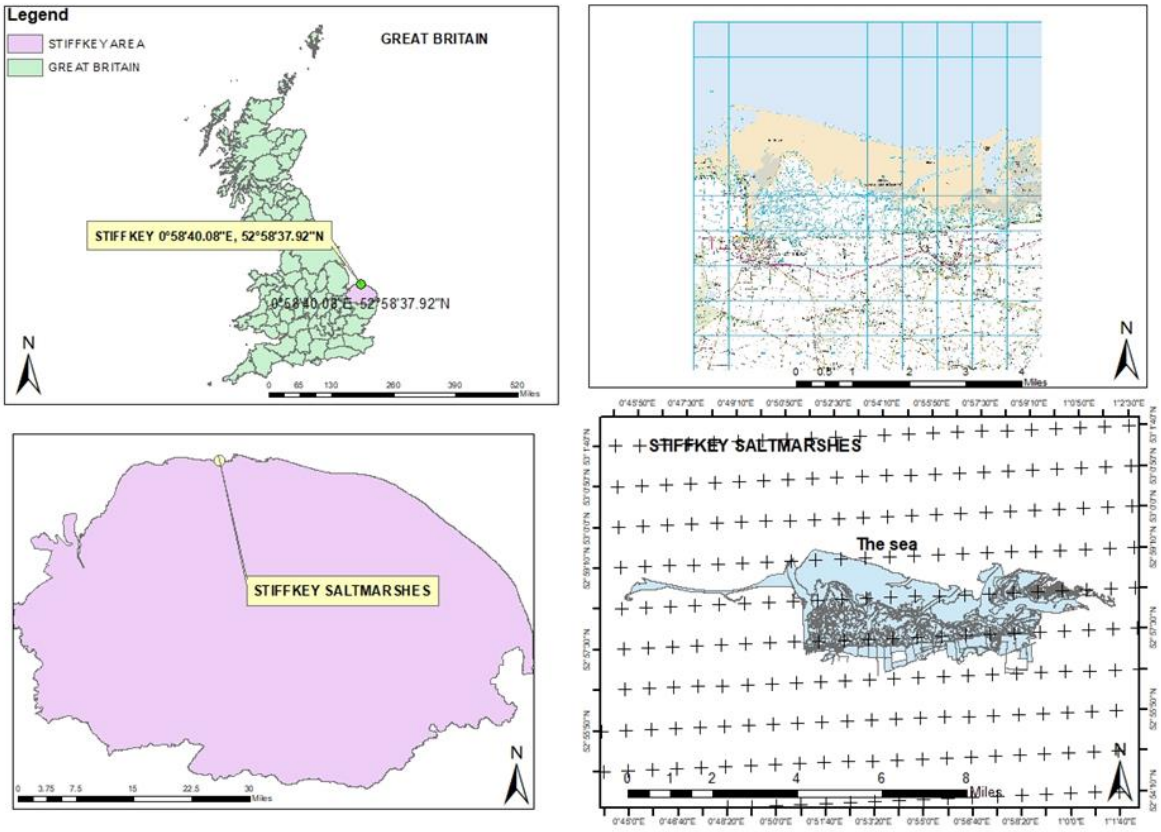


Figure 2.2 A map detail of Stiffkey saltmarsh. The map was produced Arc GIS Desktop 10.3.

The initial assessment of the comparison between DTM and DSM indicated that DTM was observed to be more reliable than DSM in estimating the elevations of the surface of the sediment on the marsh closely to the reality (Fig. 2.5, 6 and 7). So, for the remaining sites, only the DTM was examined. Vertical orthorectified aerial photographs with 25 cm were obtained from Edina Digimap (https://digimap.edina.ac.uk/) to view detailed aerial imagery at various fixed scales (Fig 2.10, Stiffkey as an example). Photographs of other sites are in appendix to Chapter 2.

The accuracy of the DTM data was assessed based on the differences between GPS and DTM elevations across saltmarsh at Stiffkey and Warham. Field work to compare lidar data with directly measured elevations was conducted on both the Stiffkey and Warham saltmarshes. Elevation was measured at 297 points randomly chosen locations along transects using high resolution differential Global Positioning System (GPS) (Topcon Hyper

V, Topcon, Newbury, UK) with a horizontal and vertical resolution of +/- 3 mm and +/- 3.5 mm respectively (Fig 2.4). Longitude and latitude of each GPS measurement were used to extract the corresponding elevations of the closest pixel in the LIDAR DTM, and this was compared with the field GPS measurements. Figure 2.2 displays a map of Stiffkey saltmarsh that was generated using ARC GIS desktop.

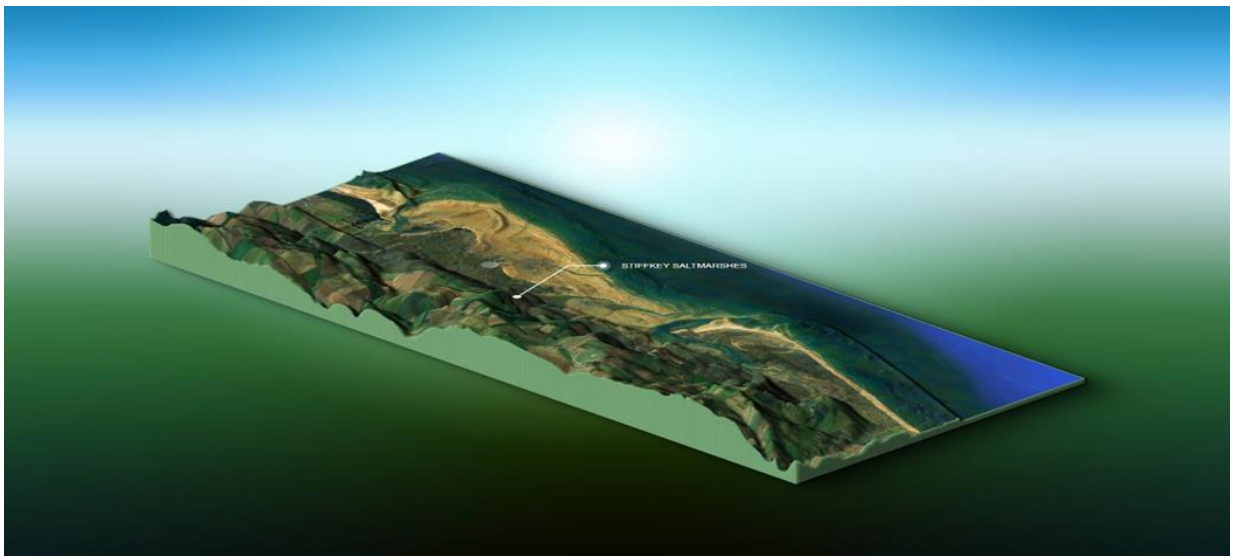


Figure2.3 Stiffkey saltmarsh 3D terrain generator


Figure 2.4 Global Positioning System (GPS) (Topcon Hyper V, Topcon).

In addition, the UK landcover map for 2015 (LCM), published in 2017 (Rowland, *et al.*, 2017) was obtained from UK Centre for Ecology and Hydrology (CEH, 2018). This was generated from over seventy satellite images acquired in summer and winter by the Landsat-Thematic Map (TM5), Satellite Pure Observation dele Teree (SPOT-4) and SPOT-5 and Indian Remote Sensing Satellite (IRS)-LISS3 sensors. The pixel size for these satellites is 20-30m. Advanced Wide Field Sensor (AWIFS) with a pixel size of 60m was used when other imagery was unavailable. Polygons identified as saltmarsh were extracted from the landcover map, then cropped and overlain onto the aerial photographs. These were examined visually to assess the accuracy of the landcover map. Initial inspection showed that a small number of polygons had been incorrectly identified as saltmarsh. These, which represented only 1 - 2 % of the “saltmarsh” polygons, were most frequently areas of coastal freshwater grazing marsh, rough grassland or arable land adjacent to the coast, or areas of

seagrass or algal growth on intertidal mudflats. They were removed manually (see table 2.1), then the LIDAR data files were masked with the remaining polygons to extract elevations corresponding to areas of saltmarshes (Figure 2.8 and 9, Warham as example, see more in appendix to Chapter 2). Analyses were carried out in R 3.5.0 version (Pinheiro, Bates *et al.*, 2018) using the raster, rgdal, rgeos, magick, imager and ggplot2 packages (Barthelme, 2017, Bivand, Keitt *et al.*, 2015, Bivand and Rundel, 2017, Hadley, 2016, Hijmans, van Etten *et al.*, 2017, Jeroen, 2018). We used packages for following procedures:

- read raster, tiff, text, shape and images files, and overlay them to allow visual inspection of the data.
- Maximize the extent of the marsh area from 1 $km^2$ to cover most of the marsh by emerging more than 1 $km^2$, depending on the availability of the data from the source.
- Combined LCM and LIDAR data to identify the limitation of saltmarsh area and removed non-marsh area, and then extracting saltmarsh elevation.

Displaying saltmarsh area images and histogram of saltmarsh elevation relative to tidal heights.

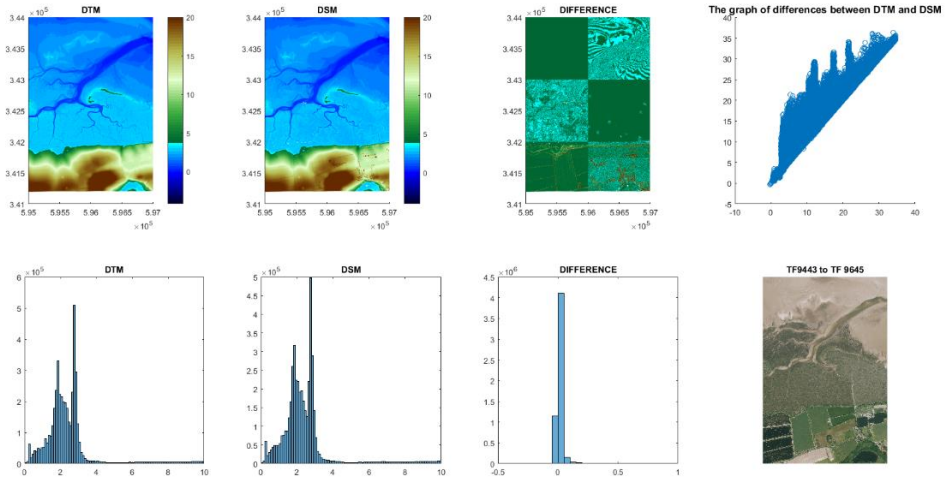


Figure 2.5The differences in saltmarsh elevation between DTM and DSM at Stiffkey.

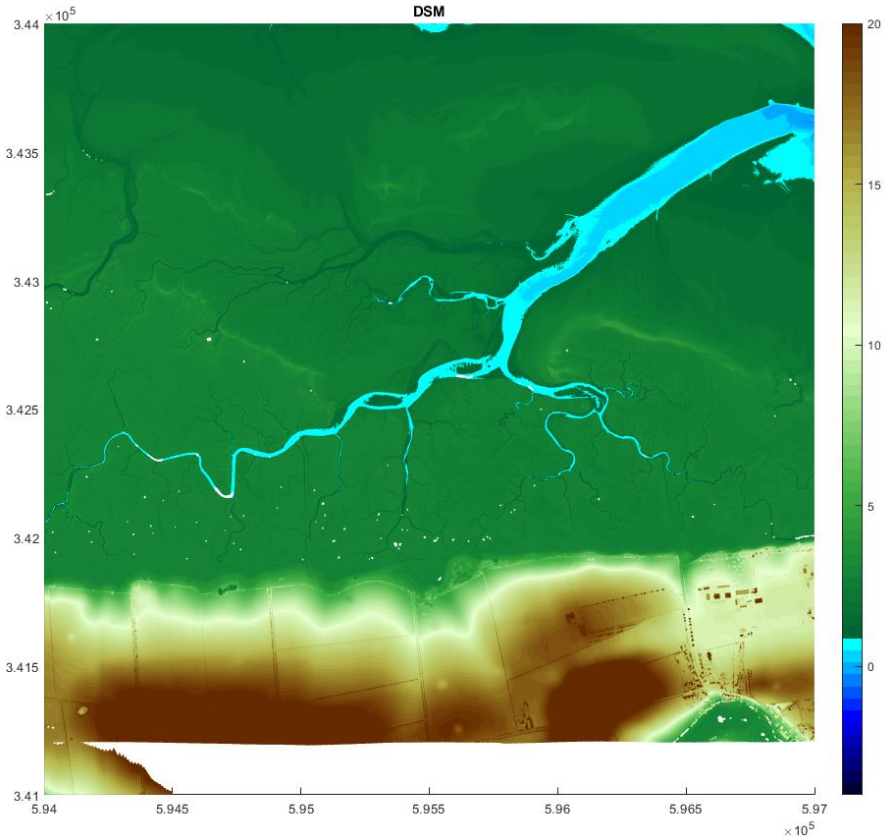


Figure 2.6 A map of elevation of the marsh (DSM) at Stiffkey. Note that, the white patches are.

refere to NAN in the data (https://digimap.edina.ac.uk/)

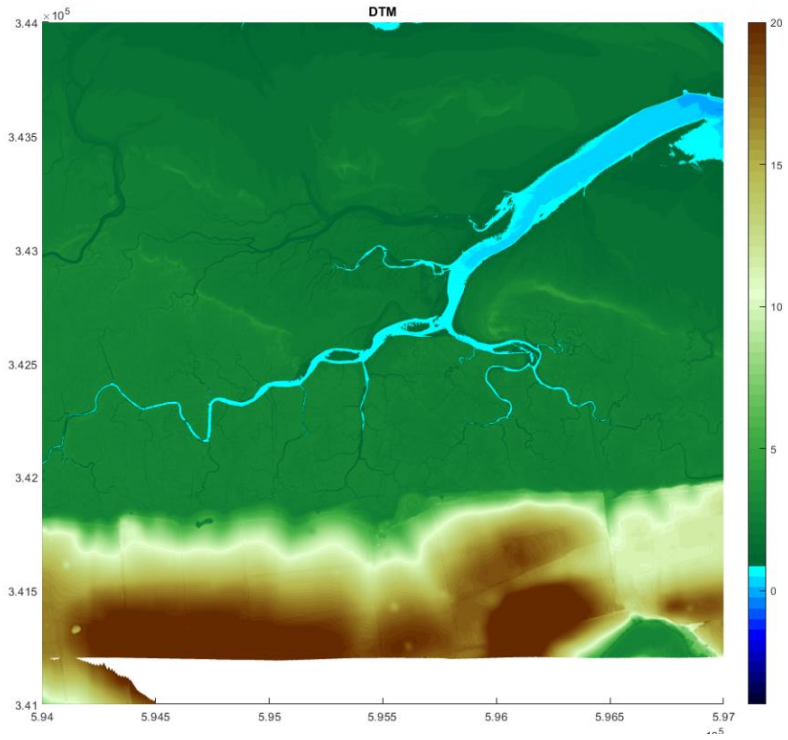


Figure 2.7 A map of elevation of the marsh (DTM) at Stiffkey (https://digimap.edina.ac.uk/).

In figure 2.8 below, an aerial photograph of all polygons obtained from the landcover map at the Warham saltmarsh is presented. However, after removal of some of the polygons from the LCM, the remainder polygons corresponding to the area in Warham saltmarsh were generated as displayed in figure 2.9 below after the problematic polygons have been removed.

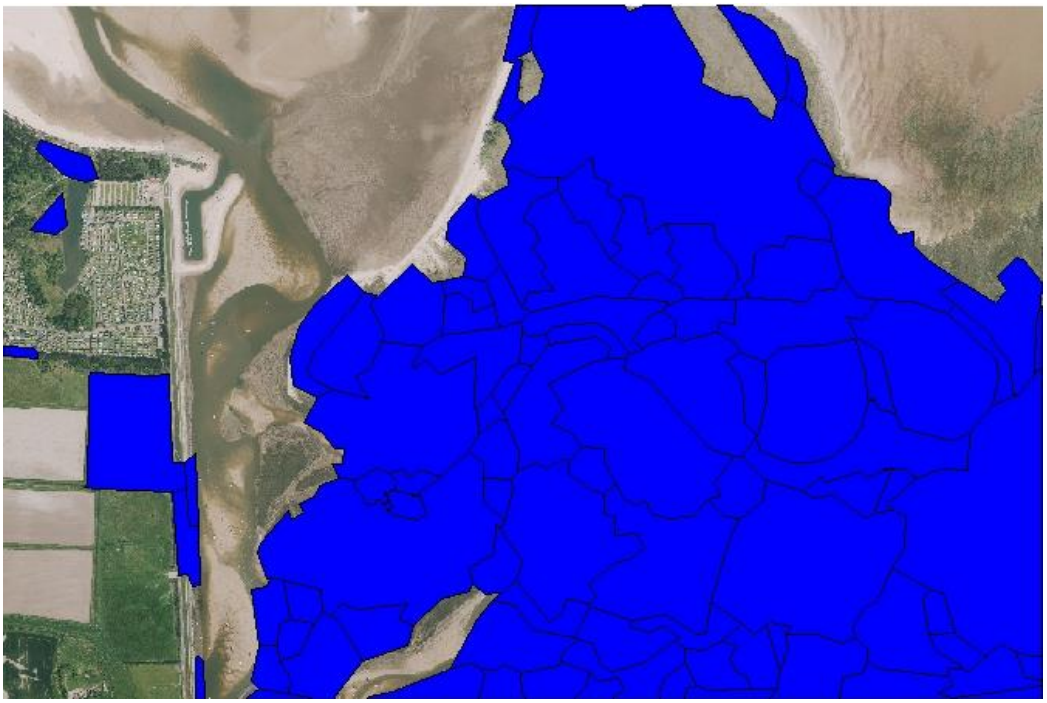

Figure 2.8 Aerial photograph representing all polygons at Warham identified as saltmarsh in the UK landcover map (https://digimap.edina.ac.uk/).

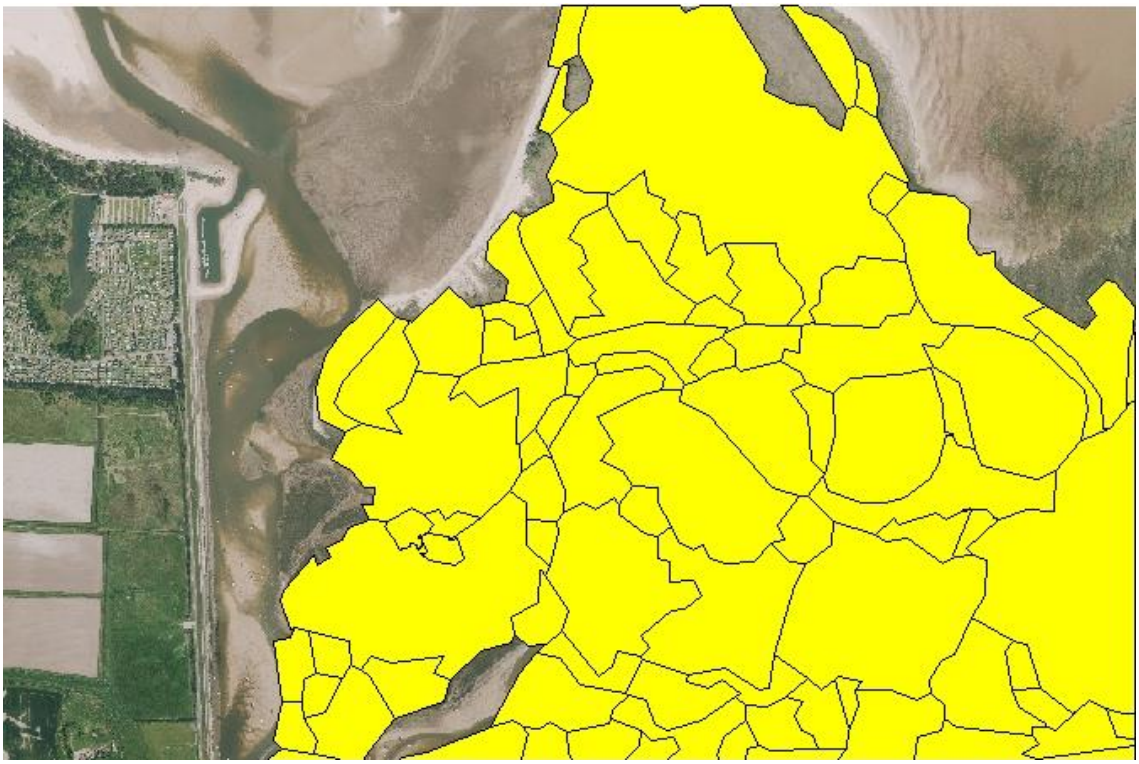

Figure 2.9 Saltmarsh polygons remaining at Warham after manual removal of incorrectly designated polygons (https://digimap.edina.ac.uk/).

In figure 2.10, an aerial photograph of the Stiffkey saltmarsh at 25cm resolution is displayed.

Figure 2.10 Aerial photograph with 25 cm resolution of saltmarsh at Stiffkey (https://digimap.edina.ac.uk/).

In table 2.1 below, the data specification for study sites including UK Ordinance survey involving 1km grid squares is included. The resolution of LIDAR images and UK land cover map of the polygon numbers that were manually removed are also detailed.

Table 2.1 Data specification for study sites, including UK Ordnance Survey 1km grid squares included resolution of the LIDAR image (m) and UK land cover map Polygon numbers that were manually excluded.

| Site name | UK Ordnance Survey 1km squares | Resolution of the LIDAR image(m) | Excluded 2015 Land Cover Map Polygon numbers |
|---|---|---|---|
| Crably Creek | SE9027, SE9127 | 0.25 | 2711048, 2172324<br>5275733, 5849579 |
| Welwick | TA3218, TA3219, TA3318,<br>TA3319, TA3418, TA3419 | 0.25 | 4798177, 2903927,<br>6139836 |
| Donna Nook | TA3900, TA3901 | 0.25 | 3697587, 3644914,<br>3289651 |
| Frampton | TF3738, TF3838,<br>TF3938, TF4038 | 0.25 | 4802614, 2772162, 4828916, 5999893,<br>1974226, 2000719, 5473809, 487370,<br>4245686, 5946990, 3486953, 5955407,<br>1481924, 6685071, 2325624, 4524392,<br>91958, 3592400 |
| Scolt Head Island | TF8045, TF8046,<br>TF8145, TF8146 | 1 | 6026216, 403457, 6008466, 340245, 5104862,<br>6297812, 2212129, 5236413, 4376853, 6671835,<br>5060527, 3723865, 2606577, 2225262, 271795,<br>3763198, 987229, 4644791, 1825002, 840384,<br>566523, 1750486 |
| Warham | TF9144, TF9145, TF9244,<br>TF9245, TF9344, TF9345 | 1 | 1114334, 223946, 6487234, 4197826,<br>5350524, 4602882, 2061903 |
| Stiffkey | TF9544, TF9545, TF9644,<br>TF9645, TF9744, TF9745 | 1 | _____ |
| Orfordness | TM4349 | 1 | 1085140, 3433015, 3921125, 6664321, 4131686, 690456,<br>3558535, 5288769, 5932468, 6268666, 5169330, 3137183,<br>1301261, 6690787, 6453302, 2947270, 5906202, 895145 |
| Hemley | TM2941, TM2942 | 0.25 | 5406, 1038574, 6142802, 5399923, 4998747, 3380025 |

| Site name | UK Ordnance Survey 1km squares | Resolution of the LIDAR image (m) | Excluded 2015 Land Cover Map Polygon numbers |
|---|---|---|---|
| Hamford Water | TM2223, TM2224, TM2225, TM2226, TM2227, TM2323, TM2324, TM2325, TM2326, TM2327, TM2423, TM2424, TM2425, TM2426, TM2427 | 1 | 564896, 5373843, 4789263, 1722613, 6090361, 4637084, 4657509, 1287659, 1842306, 110671, 3347459, 1531269, 242069, 2408418, 6690406, 2840494, 57907, 1689715, 2880817, 6116512, 4432262, 3689494 |
| Tollesbury | TL9610, TL9611, TL9612, TL9710, TL9711, TL9712 | 0.25 | 4425967, 5327008, 5426374, 3163209, 274879, 6663918, 2170856, 880668, 749029, 4038521, 5380025, 3669486, 1379869, 4064979, 3242384, 5841246, 157554, 1557667, 1222220, 3181544, 5037103, 3505418 |
| Dengie | TM0200, TM0201, TM0202, TM0203, TM0300, TM0301, TM0302, TM0303 | 1 | _____ |
| Fambridge | TQ8396, TQ8397, TQ8496, TQ8497, TQ8596, TQ8597 | 0.25 | 420695, 2513192, 1979292 |
| Witteringham | SZ7698, SZ7699, SZ7799, SZ7798 | 1 | 1783799, 2941210, 1783797, 3677699 |
| River Hamble | SU4808 | 1 | 5256286, 5018976, 204361, 5266605, 2688807, 1767683, 3978150, 4966399, 530624, 951713, 5993246, 1256582, 6572954 |
| Erth Island (Plymouth)* | SX3756 | 1 | 580796, 884750, 1884366, 2937056, 5831268, 1685358, 3463018 |
| Steart (Severn Estuary)* | ST2845, ST2846 | 0.50 | 1625, 4104340, 736117, 95217, 1580338, 5343648, 1791827, 938243, 253337, 4843558, 3264869, 2096124, 549731, 1841357, 3659517, 2859444, 4238690, 95218, 1107357, 3735537, 6314075, 5568911 |

| Site name | UK Ordnance Survey 1km squares | Resolution of the LIDAR image (m) | Excluded 2015 Land Cover Map Polygon numbers |
|---|---|---|---|
| Brean Down (Severn Estuary) * | ST3058 | 1 | 6630926, 1264603, 3896560, 5094970, 1865491, 5501632, 1017139, 6253009, 128265, 3805940, 6095286 |
| Sand Point (Severn Estuary) * | ST3265, ST3365 | 1 | 476006, 5674466, 3159824, 2081414, 1660065, 4023524, 5817135, 6728319 |
| Undy (Severn Estuary) | ST4485, ST4585 | 1 | 2237001, 2360762, 5490896, 2675778 |
| Llanelli | SS5496, SS5497, SS5596, SS5597, SS5696, SS5697, SS5796, SS5797 | 1 | 2176008, 5922349, 1174818, 4910653, 5779134, 475760, 1148271, 3463907, 791779, 4864748, 2897003, 1806843 |
| Llanrhidian | SS4593, SS4594, SS4693, SS4694, SS4793, SS4794, SS4893, SS4894, SS4993, SS4994, SS5093, SS5094 | 1 | 6464267, 701565, 3674494, 1148290, 6554659, 2686495, 2544434, 3306031, 4175085, 391616, 6095352, 2537396, 121965, 1606674, 5753024, 6517026, 3607261, 332600, 2608124, 6211666 |
| Dovey Estuary | SN6393, SN6394, SN6395, SN6396, SN6397, SN6493, SN6494, SN6495, SN6496, SN6497, SN6593, SN6594, SN6595, SN6596, SN6597 | 1 | 2123715, 728657, 5317547, 3201840, 5840472, 5972116, 3420042, 393717, 5053948, 2702467, 3044350, 6054562, 6472720, 728645, 3761476, 5027711, 1738452, 4018060, 4701560, 5423164, 4814267, 4974997, 6261564, 6502646, 2319359, 271969, 43821, 5254052 |
| Neston Dee Estuary | SJ2672, SJ2673, SJ2674, SJ2675, SJ2676, SJ2677, SJ2772, SJ2773, SJ2774, SJ2775, SJ2776, SJ2777, SJ2872, SJ2873, SJ2874, SJ2875, SJ2876, SJ2877 | 1 | 262009, 2841865, 5892525, 4766083 |

| Site name | UK Ordnance Survey 1km squares | Resolution of the LIDAR image (m) | Excluded 2015 Land Cover Map Polygon numbers |
|---|---|---|---|
| Morecambe Bay | SD4670, SD4671, SD4672, SD4673, SD4770, SD4771, SD4772, SD4773, SD4870, SD4871, SD4872, SD4873 | 0.25 | 4045742, 815149 |
| Skinburness (Solway) | NY1355, NY1356, NY1357, NY1455, NY1456, NY1457, NY1555, NY1556, NY1557, NY1655, NY1656, NY1657, NY1755, NY1756, NY1757, NY1855, NY1856, NY1857, NY1955, NY1956, NY1957 | 1 | 767006, 4808344, 6477172, 5450611, 2756349, 2688144, 5387331, 2494607, 3887622, 4545008, 3608816, 466832 |
| Longburgh ( Solway) | NY2959, NY2960, NY2961, NY2962, NY2963, NY2964, NY3059, NY3060, NY3061, NY3062, NY3063, NY3064, NY3159, NY3160, NY3161, NY3162, NY3163, NY3164, NY3259, NY3260, NY3261, NY3262, NY3263, NY3264, NY3359, NY3360, NY3361, NY3362, NY3363, NY3364 | 1 | 5792170, 5571525, 5334602, 3523465, 914482, 2888209, 5186937, 5081541, 235607, 3840960, 229635 |
| Holy Loch | NS1581, NS1582 | 1:1 000 | _____ |
| River Wick | ND35SW, ND35SE | 1 | _____ |
| Cromarty Firth | NH7570 | 1:1 000 | _____ |
| River Ythan | SU4808 | 1 | _____ |
| Tay Estuary | NO2015, NO2020, NO2515, NO2520 | 1 | _____ |

| Site name | UK Ordnance Survey 1km squares | Resolution of the LIDAR image (m) | Excluded 2015 Land Cover Map Polygon numbers |
|---|---|---|---|
| Beal | NU0840, NU0841, NU0940, NU0941 | 1 | 4708500, 3315922, 50842, 5008676, 1526154, 6340427, 6303285, 3577701, 2668107, 4062741, 1421209, 4851277, 2737707, 6421542, 1983698, 4053680, 658930, 5013138, 5956291, 5605236, 5298284 |
| Budle Bay | NU1434, NU1435, NU1534, NU1535 | 1 | 2062694, 6709396, 3684392, 167369, 777715, 6419660, 6540708, 2904646, 5377853, 171872, 2221394, 3434988, 5114192, 2921602, 3062137, 66396, 5666732, 4641061, 2300348, 167368 |
| Alnmouth | NU2410 | 1 | 4855702, 421423, 6272181, 6351810, 4119568, 1404104, 5324833, 3829523, 1513659, 4036283, 1456398, 2777524, 1698242, 5561857, 1957180, 2252290, 5524310, 1667461, 1930622, 2353047, 483526, 1618950 |

## 2.3 Results

There was close agreement between the DSM and DTM across the saltmarsh (t-test, $r^2$ = 0.988, $p<0.05$), (Fig. 2.12) and their differences were close to zero (Figure 2.5), and the DTM is virtually always lower than the DSM. There are also some differences between DTM and DSM in the areas of rough grassland and shrubs and through creeks. Although there are some pixels in which the DSM is higher than the DTM along the transects across the saltmarshes (Fig 2.11 a), the largest differences between the DSM and the DTM occur in the areas of rough grassland and shrubs above the highest elevations of the saltmarshes. The trees and shrubs such as gorse (*Ulex europeaus*) are removed successfully from the DTM. For example, at Stiffkey it is apparent that the DTM removed shrubs elevations along the section at the landward edge of the transect (Fig. 2.11b).

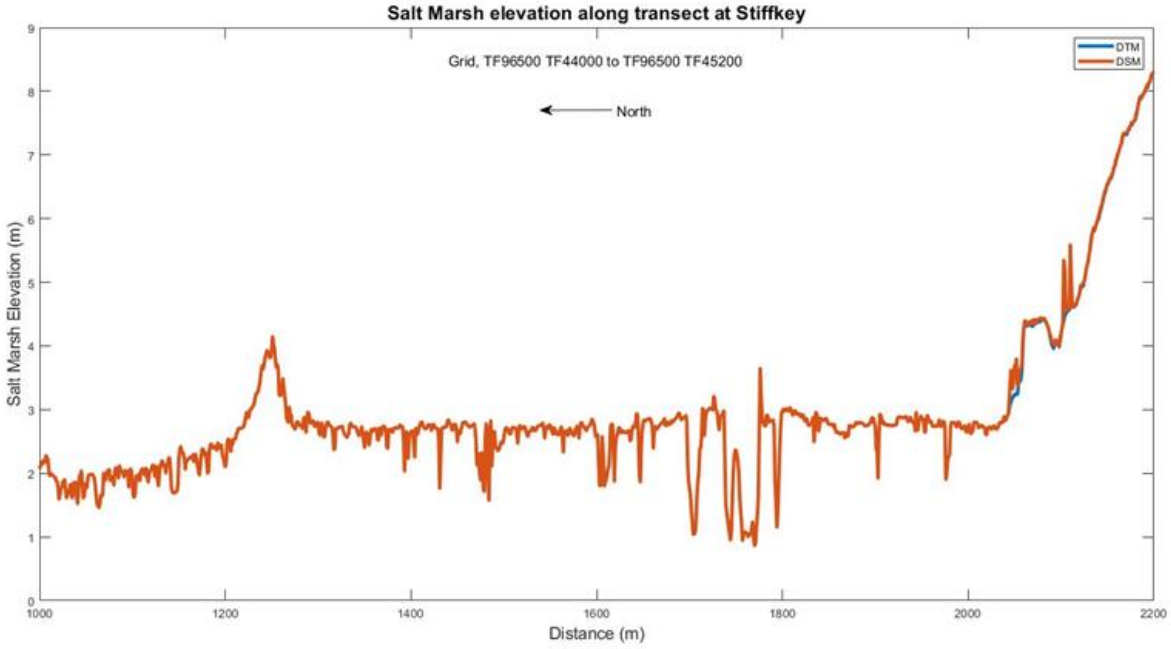


Figure 2.11a salt marsh elevation (DTM &DSM) along transect across saltmarsh at Stiffkey

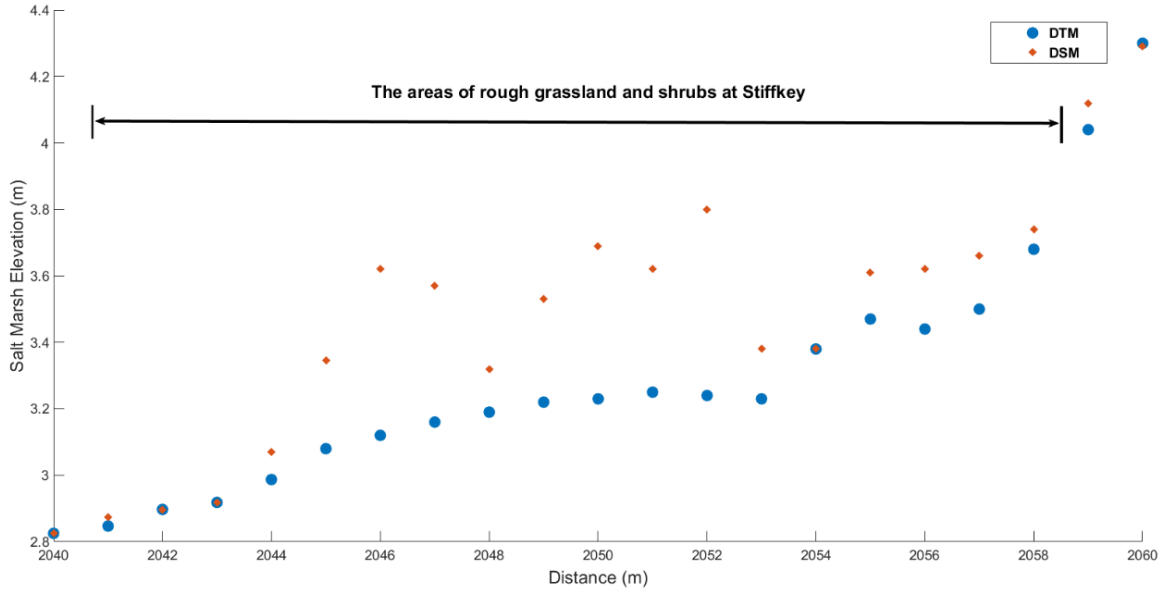


Figure 2.11. salt marsh elevation (DTM &DSM) in the areas of rough grassland and shrubs at Stiffkey.

The DSM is slightly higher than DTM (Figure 2.11c) which highlights slightly changes in elevation between DTM and DSM across the saltmarsh vegetation.

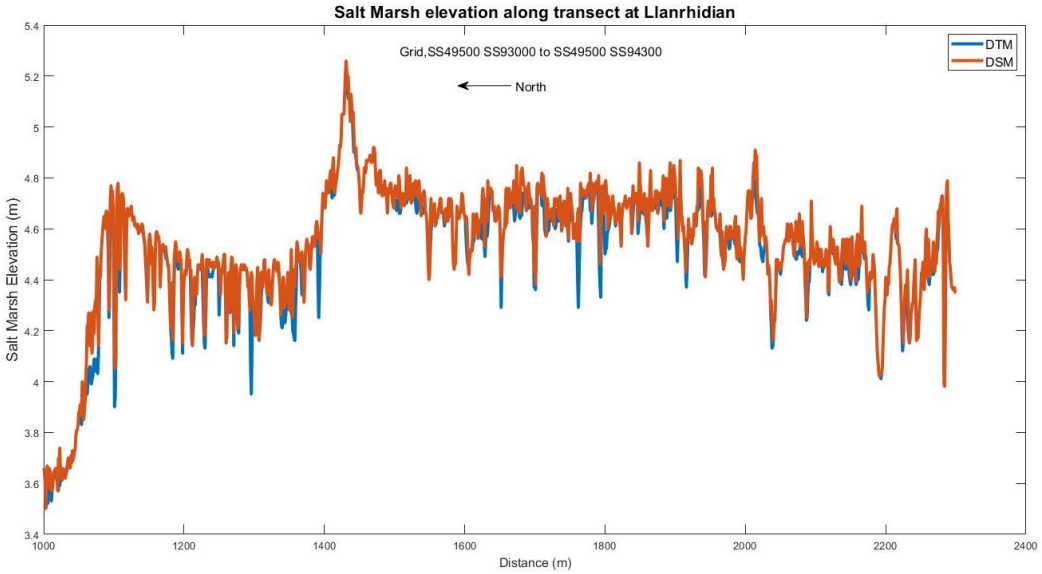


Figure 2.11b salt marsh elevation (DTM &DSM) along transect across saltmarsh at Llarnhidian.

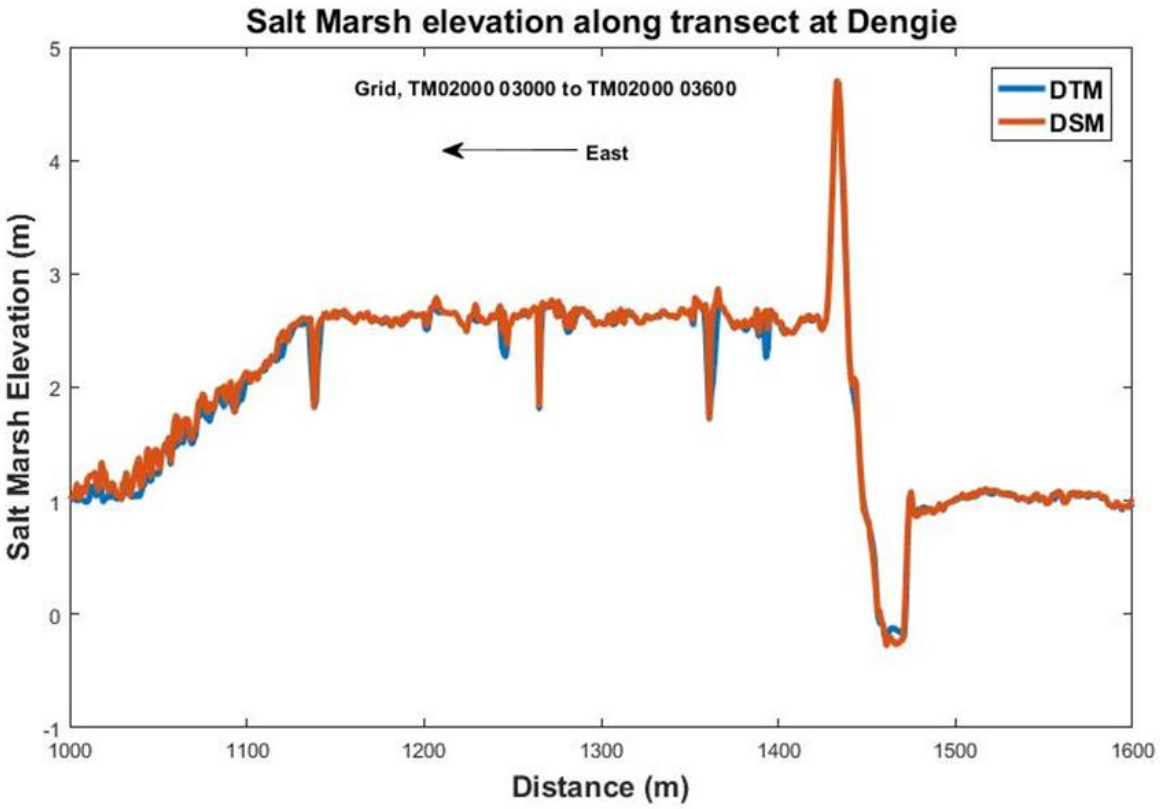


Figure 2.11c salt marsh elevation (DTM &DSM) along transect across saltmarsh at Dengie.

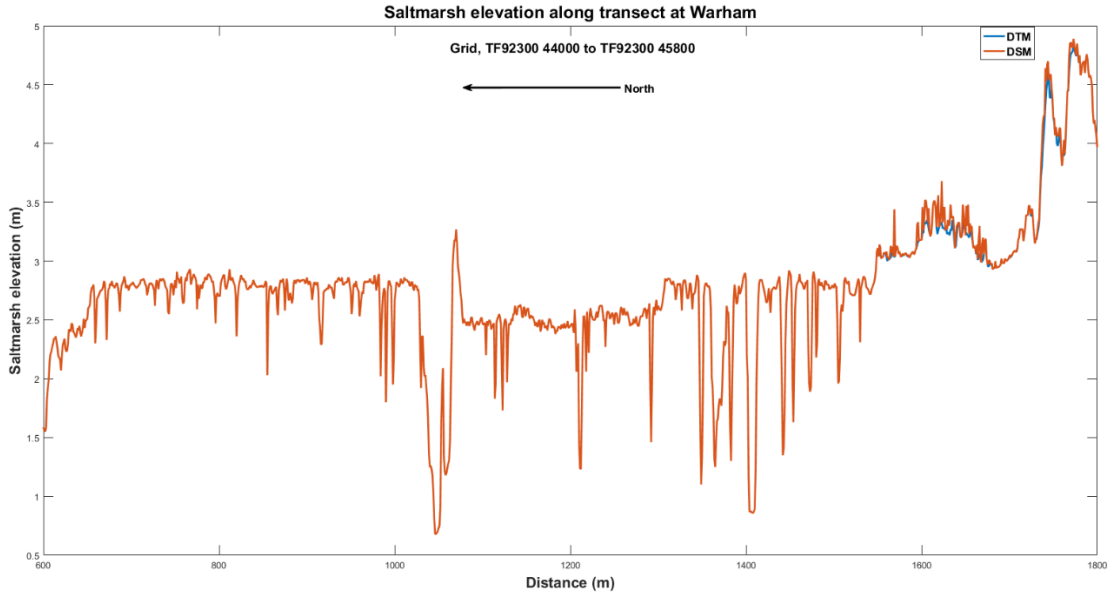


Figure 2.11 d salt marsh elevation (DTM &DSM) along transect across saltmarsh at Warham.

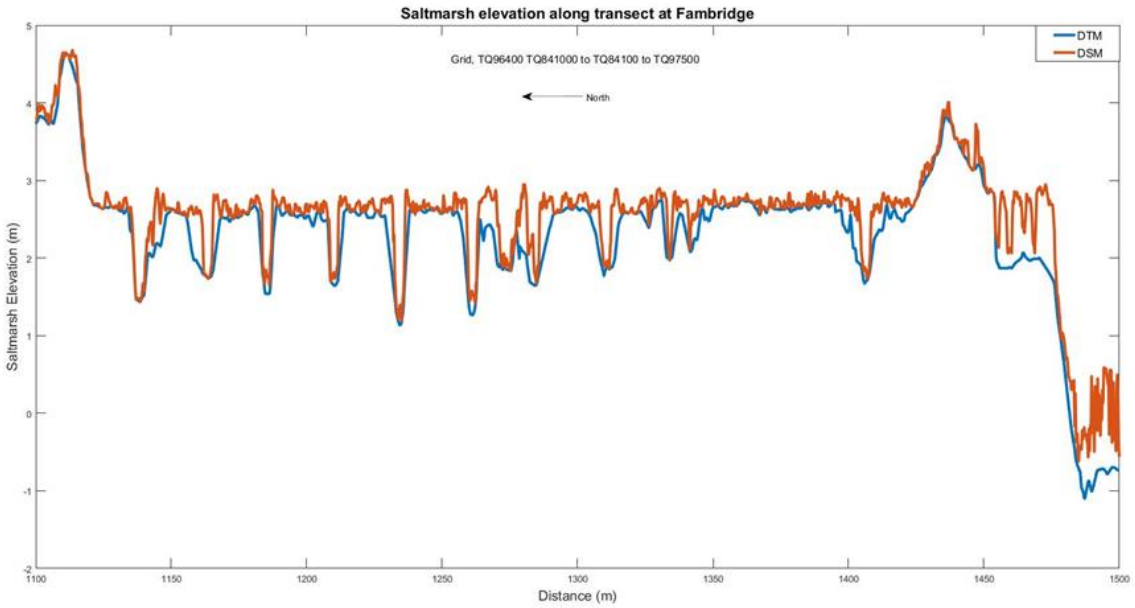


Figure 2.11e salt marsh elevation (DTM &DSM) along transect across saltmarsh at Fambridge.

The DTM estimates elevations with water bodies but in some parts of saltmarshes it might be joining small creeks and pans up through transect. However, the DSM fails to estimate a surface elevation in creeks and sets the elevation to NaN (plotted in white on the DSM, Figure 2.6), whereas the DTM algorithm makes reasonable estimates of the elevations of the bottoms of the creeks (Fig. 2.11b). In some cases where creek meanders surround an area of higher marsh or mudflat on three sides, the DTM algorithm may incorrectly subtract the elevated area from the DSM, leading to an overestimate of creek area and volume (Fig. 2.11b).

There was largely agreement between the DTM and the DSM of estimating elevation along transect through shingle ridge at Stiffkey (Figure 2.11 a) at approximately 1250 m of a distance and also through cliff at Dengie (Figure 2.11 c) at approximately 1180 m of a distance along transect. However, there will be slightly differences through cliff such as Llarnhidian saltmarsh (Fig 2.11b) at approximately 1450 m of a distance along transect.

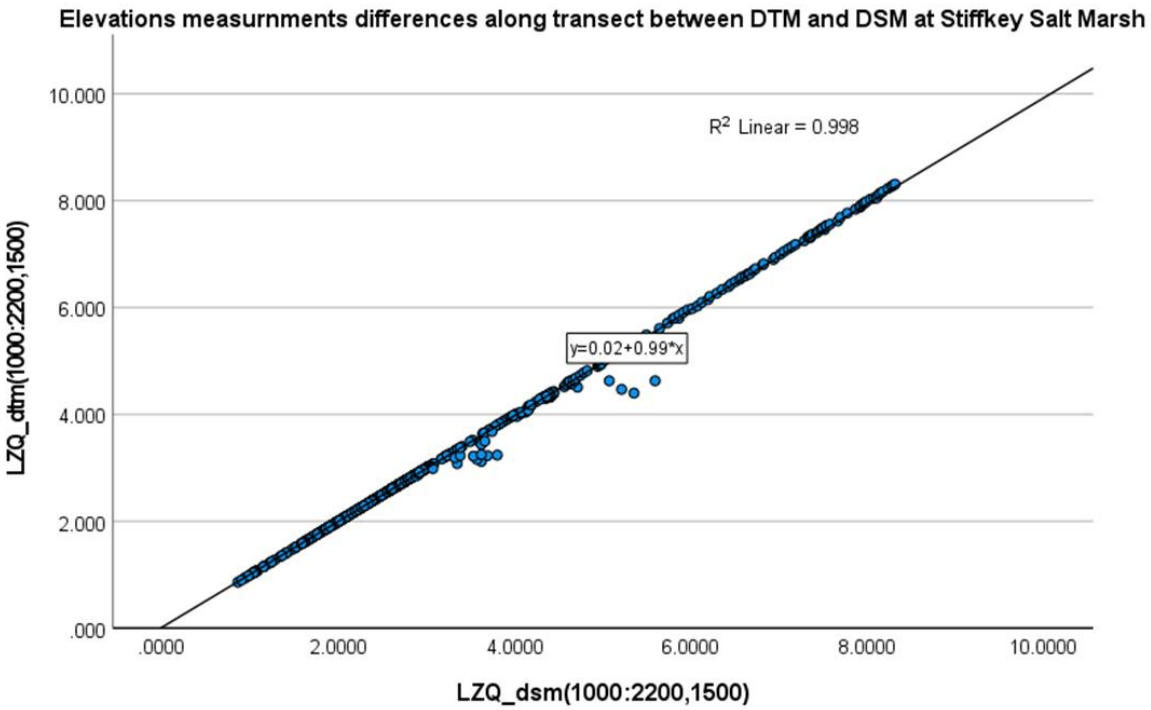


Figure 2.12 the differences of estimating elevations of the surface of the sediment on the marsh between DTM and DSM along transect at Stiffkey.

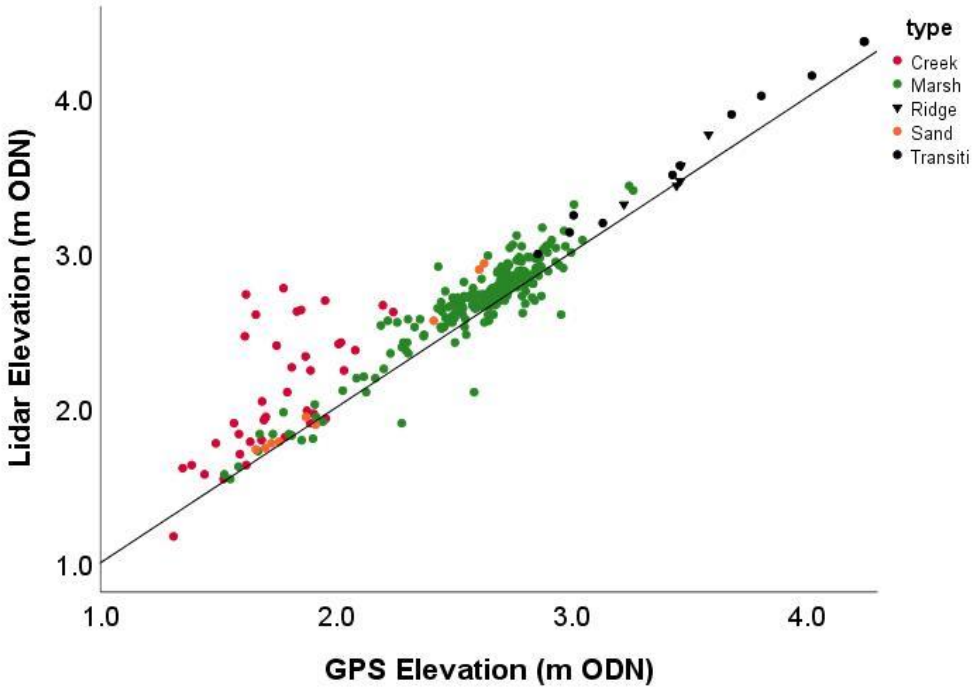


Figure 2.13 Plot of Lidar DTM elevation against elevations obtained using high resolution GPS at Stiffkey and Warham saltmarshes to illustrate the accuracy of the DTM.

GPS estimates of elevation on the salt marsh surface at 297 points of saltmarsh at Stiffkey and Warham were very similar to those from LIDAR data, with the majority of differences being less than 20 cm (Fig 2.13). Therefore, the DTM seems to be more reliable to estimate elevation of sediment surface in the marsh. However, the DTM underestimates the full depth of some creeks by between 30 and 80 cm in creeks (Fig 2.13). This may in part be due to movement of creeks between the dates on which the LIDAR and GPS data were acquired, but visual comparisons of DTMs and DSMs indicates that in at least some cases, creeks are being incorrectly removed by the algorithm that generates the DTM.

Salt marshes examined here have quite extensive platforms that are close to horizontal, with much steeper gradients both on the pioneer zone and the upper marsh. For example, Figures 2.11 a, b, c, d and e show cross sections of the marsh at Stiffkey and Warham in North Norfolk; at Dengie and Fambridge in Essex, and at Llarnhidian in Swansea. At Stiffkey, a platform occurs at an elevation of 2.75m ODN (Fig 2.11a), just below the elevation of MHWS (2.81m ODN at this site). At the landward edge of the marsh there is a steep gradient, rising from around MHWS to above the level of the highest recorded storm surge at this site (5.34 m ODN), (Spencer *et al.*, 2015) over a distance of only 100 m. Despite there being no artificial sea wall at this site at Stiffkey, the more steeply sloping pioneer marsh is to seawards of a small shingle ridge, but a similar pattern occurs on other marshes (e.g. Fig 2.11c example, Llarnhidian salt marsh) and in other cases, a small cliff exists at the marsh edge with mudflat to seawards (Fig 2.11c example, Dengie salt marsh). At Fambridge, Essex the marsh is now badly eroding along the lines of field drains that were constructed after reclamation, and the DTM algorithm does not correctly identify the heights of the areas that have not been eroded (Fig. 2.11e).

## 2.4 Discussion

In line with previous studies (Fernandez *et al.*, 2017, Hopkinson *et al.*, 2004, Schmid *et al.*, 2011) there was quite close agreement between the DSM and DTM across the saltmarsh. However, there are very small differences in elevation between DTM and DSM (Fig. 2.5). These differences might reflect the canopy height of the vegetation, because of vegetation height and density play a role in variations between DTM and DSM in saltmarsh area (Brovelli *et al.*, 2004, Rosso *et al.*, 2006). The DTM algorithm is unable to remove the effect of continuous vegetation across saltmarshes, but it was successfully able to remove shrubs such as *Sueada vera* from the DSM above the highest elevations of the saltmarshes (Fig 2.11a in landward edge at Stiffkey). Another aspect is that for saltmarshes elevations of a few tens of cm, as that can have a big impact on vegetation and sediment waterlogging. For terrestrial environments, the overall differences in elevation are much bigger so removing vegetation that is 10-20 cm high is much less important.

Elevation measurements within water bodies on saltmarshes including creeks and pans might be difficult (French and Spencer, 1993, Reed, Spencer *et al.*, 1999) but the DTM provided good information of the elevations of the bottom of the creeks across saltmarsh. However, DTM might be joining small creeks and pans up through transect across saltmarsh (Figure 2.11b and 2.11b1) and estimated these elevations as sediment surface elevation of saltmarsh. This might be due to very small differences in elevations, but (Fernandez-Nunez, Burningham *et al.*, 2017) indicated that the accuracy of DTM is around 84 % in classifying saltmarsh feature recognition in ponds and small creeks, so this is reasonable reason of joining small creeks and pans up through small creeks.

By contrast, the DSM fails to estimate surface elevation in creeks and sets the elevation to NaN (plotted in white on the DSM, Figure 2.6 ), this might occur particularly in the DSM due

to inability of laser beam to discriminate creeks from saltmarsh surface (Jacobsen and Lohmann, 2003). For shingle ridges (Fig 2.11a, at Stiffkey), and cliffs at the edge of marshes (Fig 2.11c, at Dengie) both the DTM and the DSM were largely agreement of estimating elevations. This might be due to the DSM estimates the position of the surface, whether this is vegetation or sediment, then the DTM tries to remove objects that stick up above the surrounding area (Li, Zhu *et al.*, 2004).

Most of the differences between GPS and LIDAR data were less than 20 cm (Fig 2.13). This confirmed that the accuracy of the DTM decreases approximately 10 cm compared to the reality (Salach *et al.*, 2018) as we find that the sediment surface is going to be around 10-20cm lower than the DTM. Moreover, LIDAR offers accuracies better than 20 cm even without vegetation correction (Chassereau *et al.*, 2011, Sadro *et al.*, 2007, Wang, Menenti *et al.*, 2009). However, the DTM underestimates the full depth of some creeks by between 30 and 80 cm (Fig 2.13). This may in part be due to movement of creeks (Nemmaoui *et al.*, 2019) between the dates on which the LIDAR and GPS data were acquired, but visual comparisons of DTMs and DSMs indicates that in at least some cases, creeks are being incorrectly removed by the algorithm that generates the DTM.

Textbook diagrams of saltmarshes often show an approximately uniform gradient running from the level of the highest tides down to the pioneer zone, although this is dissected by creeks and pans (Boorman, 2003b), Fig 2.1; (Burd, 1989) Fig 1. However, many of the marshes examined here have quite extensive platforms that are close to horizontal, with much steeper gradients both on the pioneer zone and the upper marsh, and platforms of these marshes often occur at or below an elevation of MHWS particularly in the East and South of England. For example, at Stiffkey a platform occurs at an elevation of 2.75m ODN (Fig 2.11a), just below the elevation of MHWS (2.81m ODN at this site). Although our

estimates are higher than the elevations of marshes by (Pethick, 1981) in North Norfolk, they are similar to elevations estimated by (French, 1993). At Dengie, a platform occurs at 2.48m ODN elevation (Fig 2.11c) just below MHWS (2.57m ODN at this site), and this elevation was measured by Moller (2006) at 2.4–2.7m O.D. In some sites, such as North Fambridge (Fig 2.11e), there are frequent changes in elevation. This is a marsh that was reclaimed then regenerated as saltmarsh after accidental dike breach by the great storm in 1897 (Crooks *et al.*, 2002).

Based on our analysis and the differences between GPS and DTM elevations across saltmarsh at Stiffkey and Warham, the DTM is extremely valuable for comparing marsh features, and it is more reliable than the DSM to estimate elevation of sediment surface in the marsh with accuracy less than 20 cm. So, the DTM gives an accurate elevation, but one that is slightly higher than the sediment surface, as a result of continuous vegetation.

## 2.5 Conclusion

In this chapter, findings obtained showed that LIDAR worked quite well in the generation of the DTM and DSM models. In particular, the results showed that the DTM facilitated the removal of rough grassland and shrub from the DSM above the highest elevations of the saltmarshes. In turn, this led to the successful estimation of the surface of the sediment. The DTM can be used to provide precisely good information for saltmarsh elevations and clearly determine existing differences. Concerning GPS, it is noteworthy mentioning that the actual sediment surface is consistently lower than the DTM in 20cm. Furthermore, findings showed that although the accuracy of the UK Landcover map (LCM) data is very good, improvements in quality can be obtained through manual checking of its classification against aerial photographs. In the following calculations, evaluations and quantifications in the next chapters of this study we interested in sediment surface measurement. Therefore, any underestimation of creek depth does not affect the conclusions of this work as we focus entirely on the DTM data.

## Chapter three

## Tidal elevations of UK saltmarshes and implications for their potential contribution to sea defence

### 3.1 Introduction

Intertidal environments, such as saltmarshes, mangroves and mud flats, deliver a wide range of ecosystem services and make a significant contribution to global and national economies (Barbier *et al*., 2011). In the UK, their value has been estimated as £48 billion, or 3.46% of the national income (Jones *et al*., 2011). An important role of saltmarshes is in helping to ensure protection of communities in coastal areas and economic assets from flooding, the risks of which are increasing because of sea-level rise and changes in shorelines (Gedan *et al.*, 2011, Morgan *et al.*, 2009, Woodruff *et al.*, 2013).

King and Lester, (1995) argued that an 80 m width of saltmarsh in front of a seawall reduced the height of wall needed as an effective sea defence from 12m to 3m. This claim, and the reduction in construction costs that it implies, has been very influential on UK coastal defence policy Environment Agency (EA), 2007 (e.g., Dixon et al., 1998; Jones et al., 2011; Foster et al., 2013). Wetlands can also play a role in reducing peak water levels of storm surges as they move inland, with reported reductions varying between 1.7 and 25 cm per km of marsh (Gedan et al., 2011; Leonardi et al.,2018), but this is not our focus here.

Wave energy dissipation is greatest in shallow water (Saket *et al.*, 2018), so intertidal vegetation, such as saltmarshes and mangroves, increase the amount of dissipation that occurs by stabilising sediments relatively high in the tidal frame (Krauss *et al.*, 2009, Sheng *et al.*, 2012, Wamsley *et al.*, 2010), thus reducing water depths during high tide. The vegetation itself may also contribute to wave energy dissipation by increasing bed friction (Garzon *et al.*, 2019, Möller, Spencer *et al.*, 1999, van Rooijen *et al.*, 2018).

One modelling study (Brampton, 1992) predicted that the reduction of the height of waves over an 80-metre-wide saltmarsh was 40%. Diverse empirical studies have quantified wave reduction heights that occur as waves propagate across intertidal vegetation. (Möller, Spencer *et al.*, 1999) found that wave height reduction across 200 m of saltmarsh averaged at 63%, although this percentage was smaller than expected based on extrapolations of (Brampton, 1992) modelling results, as most energy dissipation occurred over the first 10 to 50 metres of the surface of the salt-marsh.

Although the effectiveness of saltmarshes in dissipating wave energy depends strongly upon the depth of water over the marsh, empirical studies almost inevitably collect data during normal tidal conditions rather than during rare storm surges. An exception is (Möller, Kudella *et al.*, 2014) who examined wave dissipation in water depths of 2 m in a large flume, finding a maximum 19.5% reduction of wave height across 40m of marsh for waves with an amplitude of 0.3 m, but lower dissipation than this for both larger and smaller waves.

In most cases, the use of traditional surveying equipment has been predominant for most researchers whereby, the elevation of sites is determined by using conventional equipment (Millard et al., 2013). The use of High-resolution differential GPS provides accurate data to do elevation surveys (Ganju et al., 2020), but the data are still limited to point measurements across the whole marsh. Instead, remote sensing technologies (LIDAR) data gives much more dense spatial coverage (Ekberg *et al.,* 2017), over short period of time, and determines how effectively vegetation can be removed (DiGiacomo et al., 2020).

To extrapolate these studies to understand what may happen during storm surges, when water levels are markedly higher, we need to know the depth of water that occurs over saltmarshes during storm surges. We have good data on heights of normal tides and storm

surges relative to land for a number of locations, but saltmarshes are often some distance away from these standard ports. Also, the elevation that corresponds to a particular tidal elevation, such as the level of mean high water of spring tides, can change rapidly over relatively short distances (Mossman, Davy *et al.*, 2012b). In consequence, with the exception of a small number of sites where workers studying saltmarshes have deployed tide gauges nearby (Gray and Bunce, 1972a; b, Gray and Scott, 1977), we usually do not know the exact tidal elevation of saltmarshes.

We use publicly available LIDAR data in this study to quantify the elevation of saltmarshes at sites from across the UK relative to the national elevation datum (ODN; based on mean sea level in Newlyn, Cornwall). We combine this with data on heights of storm surges, spring and neap tides from nationally maintained datasets (Nationally Data List, 2017) and our own data collected using depth sensing data loggers (Mossman, Davy *et al.*, 2012b). This allows us to determine the elevations of saltmarshes relative to mean spring and neap tides. This in turn allows us to predict water depths over saltmarshes during storm surge conditions and thus to assess the extent to which they mitigate flood risk during the rare storm surge events during which most coastal flooding occurs.

### 3.1.1 Aims of the Study

The aims of this study are:

(i) To characterise the elevations of 35 saltmarshes around the UK relative to a terrestrial datum (ODN) and relative to the elevations reached by normal high tides and by storm surges.

(ii) Thus, to investigate the extent to which saltmarshes around the UK may contribute to flood protection and coastal defence by reducing wave energy during normal and storm surge conditions.

The objectives of this study are:

(i) Using a Digital Terrain Model (DTM) based on LIDAR data across saltmarshes and the landcover polygons of the UK to extract elevation of saltmarshes for thirty-five sites around the UK.,

(ii) To combine saltmarsh polygons from the UK landcover map with DTM data for each saltmarsh site to characterise the elevation relative to ODN of each saltmarsh site; to determine the range of elevations occurring at each site.

(iii) To determine the elevations of mean high water of spring and neap tides (MHWS and MHWN) for each saltmarsh site, and the height of extreme storm surges above these levels. Thus determine the relationship between marsh elevation and critical tidal levels and the likely depth of water above the marshes during storm surges.

### 3.2 Method

Following the methods in chapter 2, thirty-five sites were identified to extract elevations corresponding to areas of saltmarshes (Figure 2.1, see chapter 2). These sites encompass the range of saltmarshes present around the UK. From the previous chapter (chapter 2), we found that Digital Terrain Model (DTM) is a more accurate indicator than Digital Surface Model (DSM) for measuring elevations of the sediment of saltmarsh. Therefore, elevations of saltmarshes were generated and determined from DTM data. Analyses of these data were carried out in R 3.5.0 using the raster, rgdal, rgeos, magick, imager and ggplot2 packages (Barthelme, 2017, Bivand, Keitt *et al.*, 2015, Bivand and Rundel, 2017, Hadley, 2016, Hijmans, van Etten *et al.*, 2017, Jeroen, 2018). Site information has been explained in detail in chapter 2. In addition, saltmarsh elevations were extracted and converted into histograms (details in chapter 2). The histograms are displayed in this chapter where the distribution of elevations across the saltmarsh area at each site is observed (for example, figure 3.1 which shows the histogram of Stiffkey). The proportion of the areas of the marsh above the level of MHWS and below the level of MHWN was also calculated (Table 3.1 (record 7 for Stiffkey), Figure 3.2 and Figure 3.3 for Stiffkey as an example).

To simplify direct comparison of the height of marsh platforms between sites, we have standardised the tidal elevations so that 0 corresponds to MHWN and 1 corresponds to MHWS, using the formula:

Tidal height = (Elevation relative to ODN − MHWN)／(MHWS−MHWN), (Mossman, Davy *et al.*, 2012b), and these are included in (Table 3.1 and; Figure 3.20; Figure 3.21).

With one exception, elevations corresponding to MHWS and MHWN were obtained from tidal measurements made on that marsh or nearby by (Mossman, Davy *et al.*, 2012b) or from nearby ports where tidal data have been published UK Hydrographic Office (2014).

Two sites (Erth Island and Neston) were located approximately equidistant between standard ports, which gave rather different estimates of these elevations. For these sites, both values are provided in (Table 3,1). MHWS is defined as "the height of the average throughout the year (when the average maximum declination of the moon is 23.5°) of two successive high waters during those periods of 24 hours when the range of the tide is at its greatest (NTSLF, 2020). Whereas MHWN is the equivalent value for successive high waters when the tidal range is at its smallest. In a full year's data of tidal heights from Cromer, Norfolk, UK, MHWS corresponded to the 98th highest tide out of 705 and MHWN to the 601st (Mossman et al, 2012a). We therefore approximated MHWS as the 13.9th percentile of the observed high tides and MHWN as the 85.2 percentile when other estimates were not available or were unreliable. For the Sudbourne (Orford Ness) marsh, the value of 1.2m ODN for MHWS at Orford Quay given by UK Hydrographic Office (2014) appears to be incorrect, as it is much lower than the elevation of the marsh platform. Tidal heights for Orford Ness (indicated by Orford Quay in Table 3.1) were calculated from one year of water level data (1st May 2018 to 30th April 2019) provided by the UK Environment Agency, giving elevations of MHWN and MHWS of 1.02 m and 1.48 m ODN, respectively.

Heights of the ten highest water levels ever recorded at 39 tide gauges around the UK, and heights of MHWS were obtained from the UK National Tide and Sea Level Facility (NTSLF, 2020). These gauges were installed after the 1953 North Sea storm surge, and the summary values cover the period up until the end of 2012, so do not include either the 1953 or 2013 surges. Data on the heights of these events was obtained from (Spencer, Brooks *et al.*, 2015). Hourly water level data for Cuxhaven, Germany, were downloaded from https://uhslc.soest.hawaii.edu/data/. Hourly data higher than the immediately preceding

and following values were taken as representing levels of high tides, with the level of MHWS estimated as described above.

## 3.3 Results

### 3.3.1 Saltmarsh heights for some individual sites

Detail elevation data is presented from six contrasting sites to illustrate the range of marsh morphologies observed and the spatial distribution of different elevations across each marsh.

#### 3.3.1.1 Stiffkey Marsh

As illustrated in (Fig 2.11a, see chapter 2), much of the surface at Stiffkey consists of a sub-horizonal platform lying just below the height of MHWS. A histogram of elevations across the whole Stiffkey marsh is shown in figure 3.1 below.

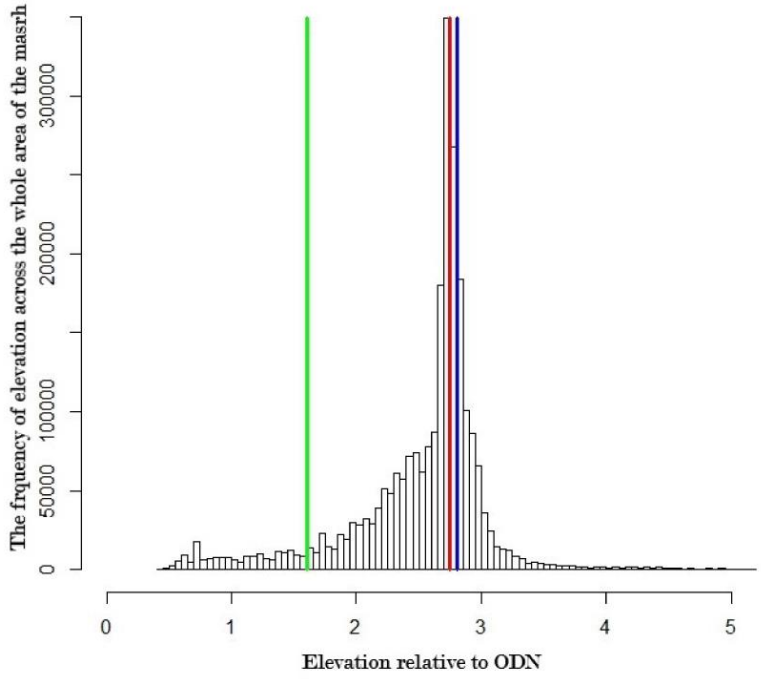


Figure 3.1: a red vertical line indicates the modal elevation at Stiffkey, green line represents MHWN, blue line represents MHWS.

At Stiffkey the marsh platform is represented by a sharp peak on the histogram (Figure 3.1) at 2.75m ODN, an elevation of 0.94 relative to MHWS and MHWN (Table 3.1). Areas below MHWN are almost all along creeks (Fig 3.3) and areas above MHWS (Fig 3.2) occur as levees

along creek banks; adjacent to the shingle ridge known as Stiffkey Meals, and at the landward edge of the marsh where land slopes rapidly upwards (Figure 2.11a see chapter 2).

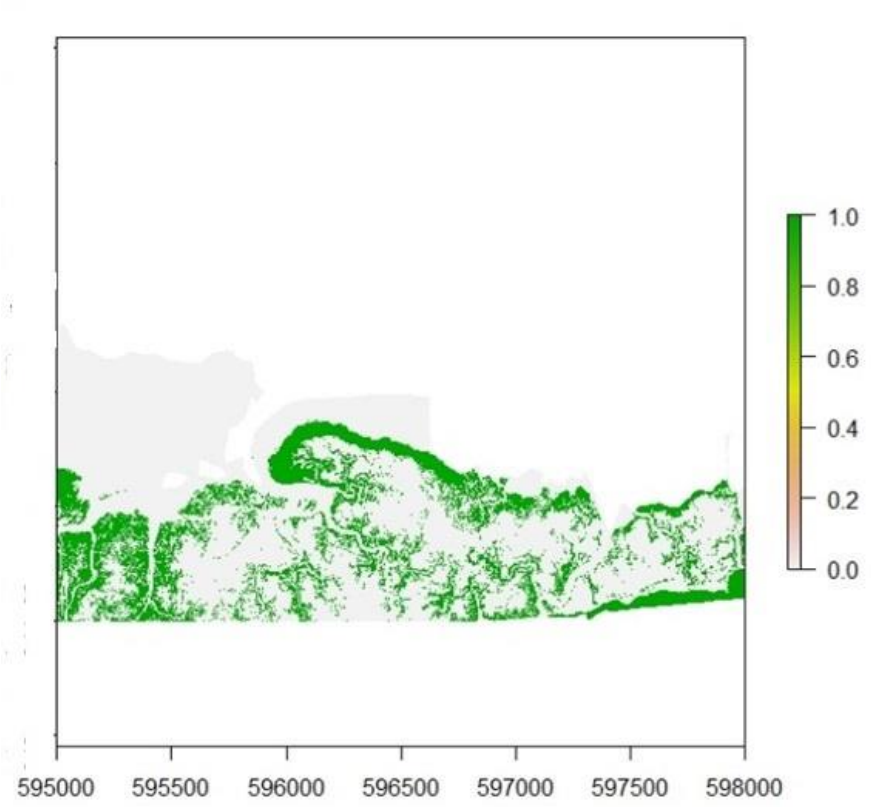


Figure 3.2 : green areas represent marsh above the level of MHWS at Stiffkey, the grey shaded area shows the extent of the saltmarsh polygons.

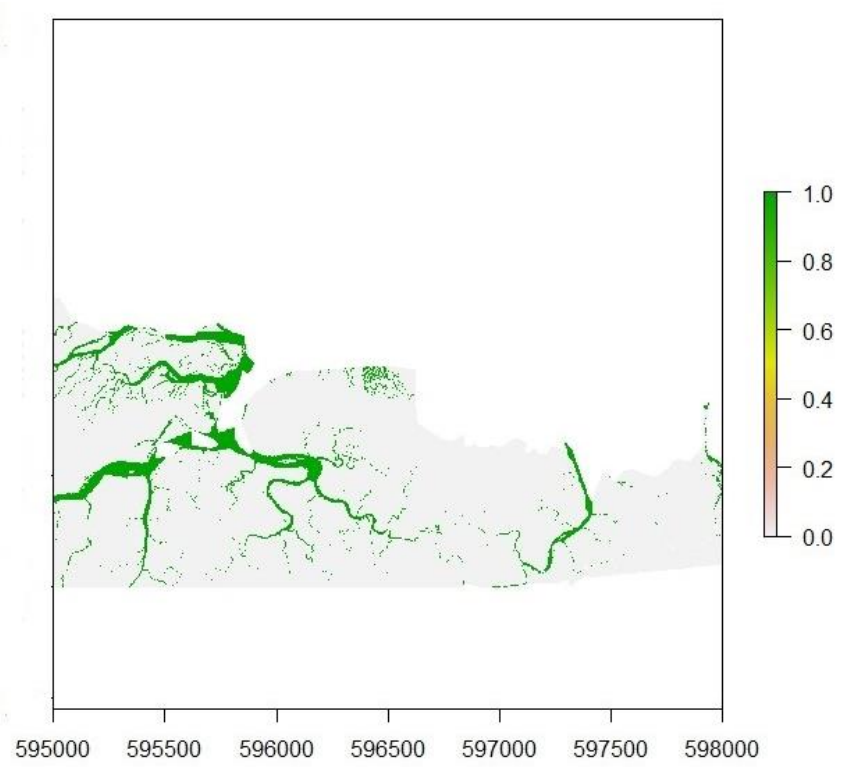


Figure 3.3 green areas represent marsh below the level of MHWN at Stiffkey, the grey shaded area shows the extent of the saltmarsh polygons.

### 3.3.1.2 Dengie Marsh

Much of the surface at Dengie consists of a sub-horizonal platform lying just below the height of MHWS (Figure 2.11c, see chapter 2). A histogram of elevations across the whole Dengie marsh is shown in figure 3.4 below.

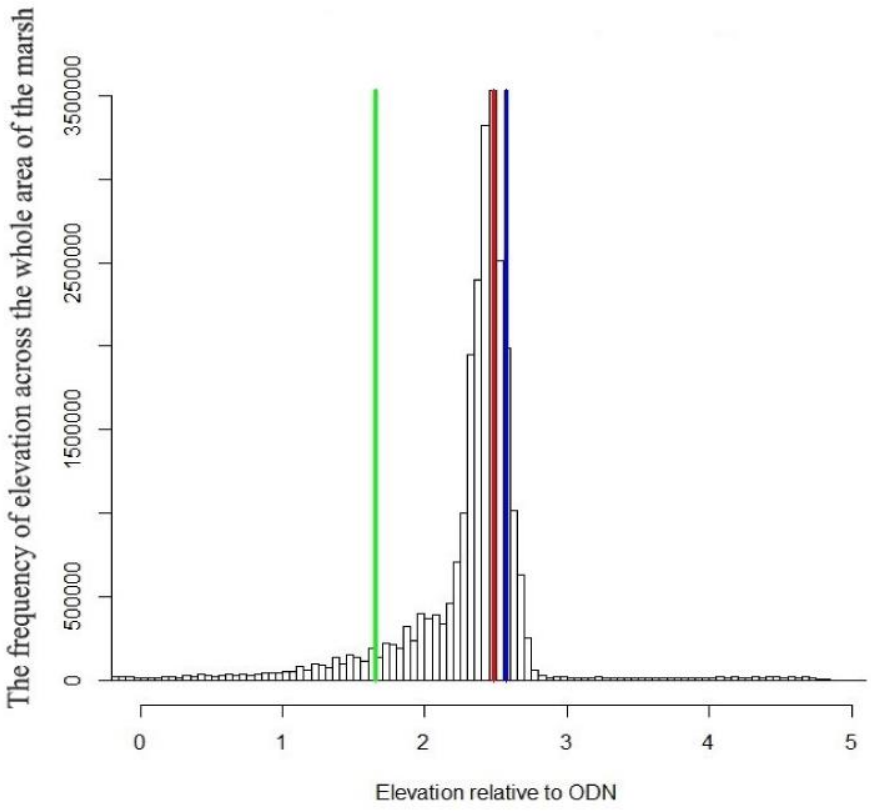


Figure 3-4 a red vertical line indicates the modal elevation at Dengie, green line represents MHWN, blue line represents MHWS.

A sharp peak of the saltmarsh elevation is observed as detailed by the red line (Fig. 3.4). The modal elevation of the marsh at Dengie is at 2.48 m (ODN), an elevation of 0.90 relative to MHWS and MHWN (Table 3.1). Areas above MHWS are along sea wall (Fig. 3.5), while areas below MHWN occur as levees along creek banks (Fig. 3.6), and the areas behind the sea wall are lower elevation than the main marsh (Fig. 2.11c see chapter 2).

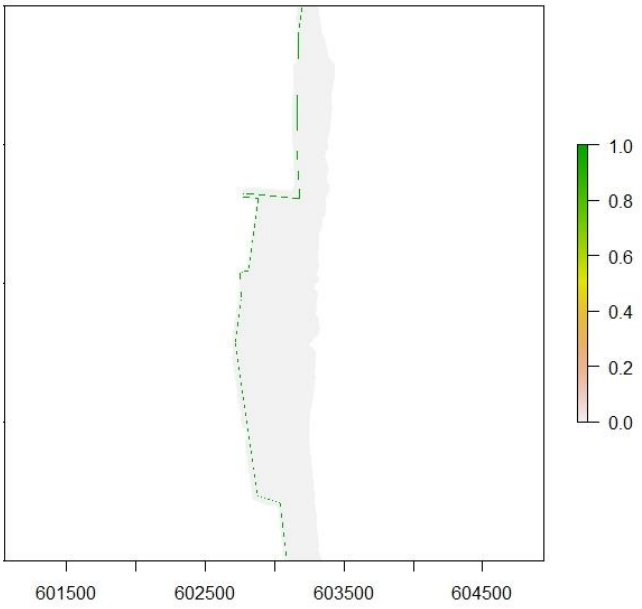


Figure 3.5 : green areas represent marsh above the level of MHWS at Dengie, the grey shaded area shows the extent of the saltmarsh polygons.

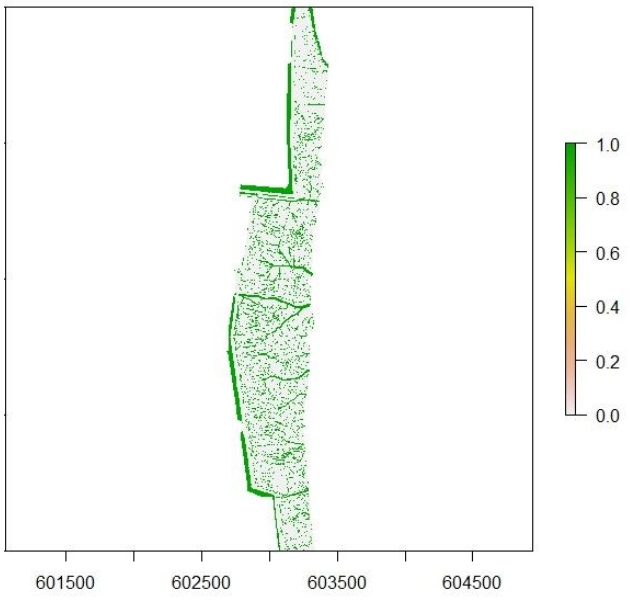


Figure 3.6 : green areas represent marsh below the level of MHWN at Dengie, the grey shaded area shows the extent of the saltmarsh polygons.

### 3.3.1.3 Morecambe Bay Marsh

Much of the surface at Morecambe Bay consists of a sub-horizonal platform lying above the height of MHWS (Fig. 3.8). A histogram of elevations across the whole Morecambe Bay marsh is shown in figure 3.7 below.

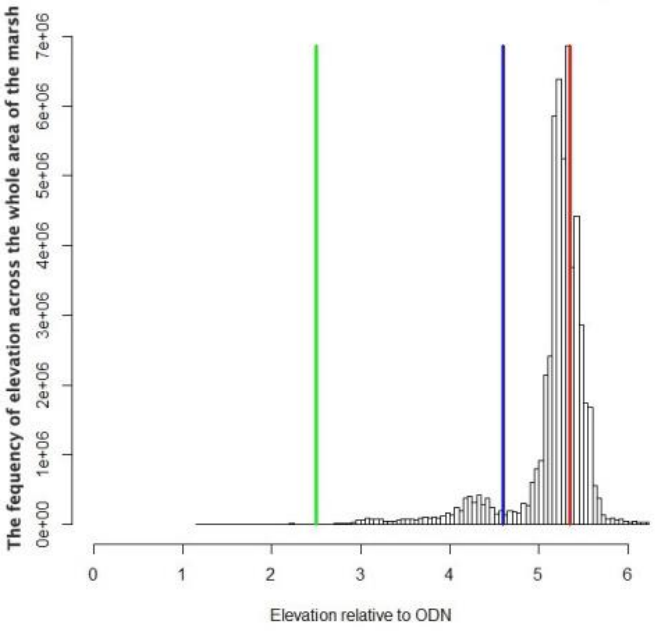


Figure 3-7 : a red vertical line indicates the modal elevation at Morecambe Bay, green line represents MHWN, blue line represents MHWS.

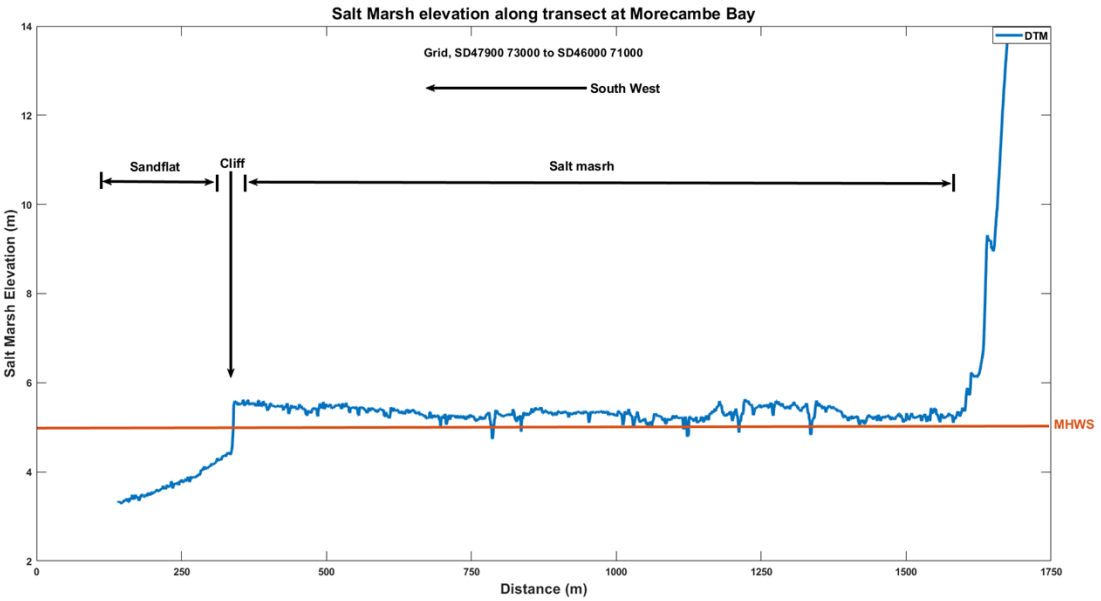


Figure 3.8: elevation of the DTM along transect across salt marsh at Morecambe Bay.

The marsh platform is represented by a sharp peak on the histogram (Figure 3.7) at 5.33m ODN, an elevation of 1.18 relative to MHWS and MHWN (Table 3.1). The whole areas almost are above MHWS (Fig 3.9), while very small areas are below MHWN through creeks (Figure 3.10).

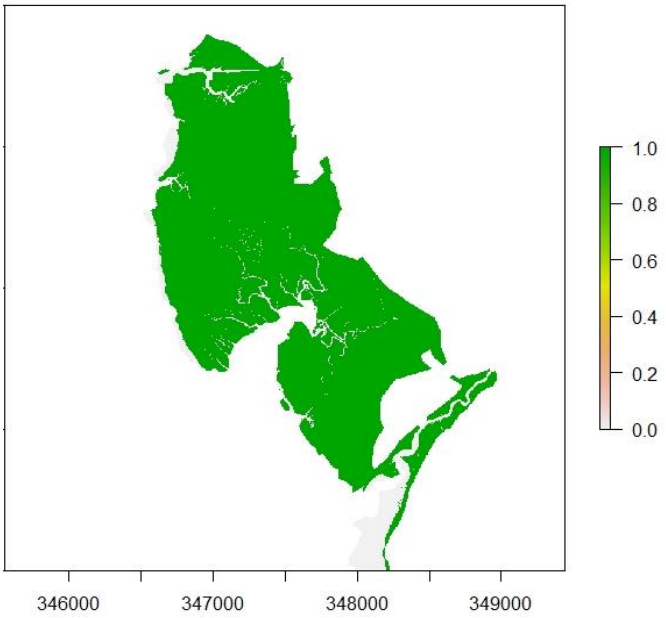


Figure 3.9 : green areas represent marsh above the level of MHWS at Morecambe Bay, the grey shaded area shows the extent of the saltmarsh polygons.

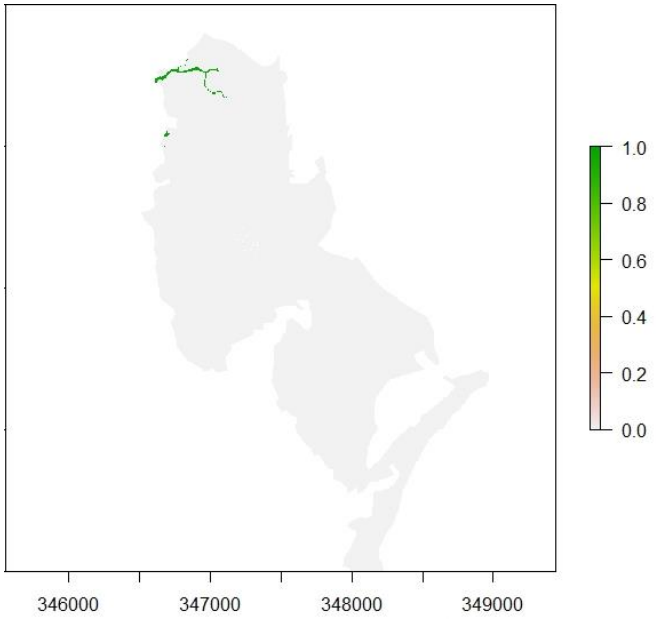


Figure 3.10 : green areas represent marsh below the level of MHWN at Morecambe Bay, the grey shaded area shows the extent of the saltmarsh polygons.

#### 3.3.1.4 Llanrhidian Marsh

Much of the surface at Llanrhidian platform lying above the height of MHWS. A histogram of elevations across the whole Llanrhidian marsh is shown in figure 3.11 below.

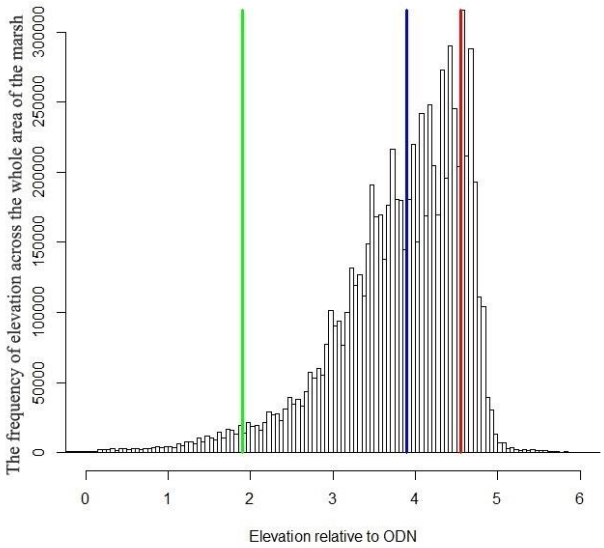


Figure 3-11 a red vertical line indicates the modal elevation at Lianrhidian, green line represents MHWN, blue line represents MHWS.

In this particular marsh the platform is not represented by a sharp peak on the histogram (Figure 3.11) at 4.6 m ODN, an elevation of 1.35 relative to MHWS and MHWN (Table 3.1). The whole areas almost are above MHWS (Fig 3.12), while areas below MHWN are along creeks and channels (Figure 3.13).

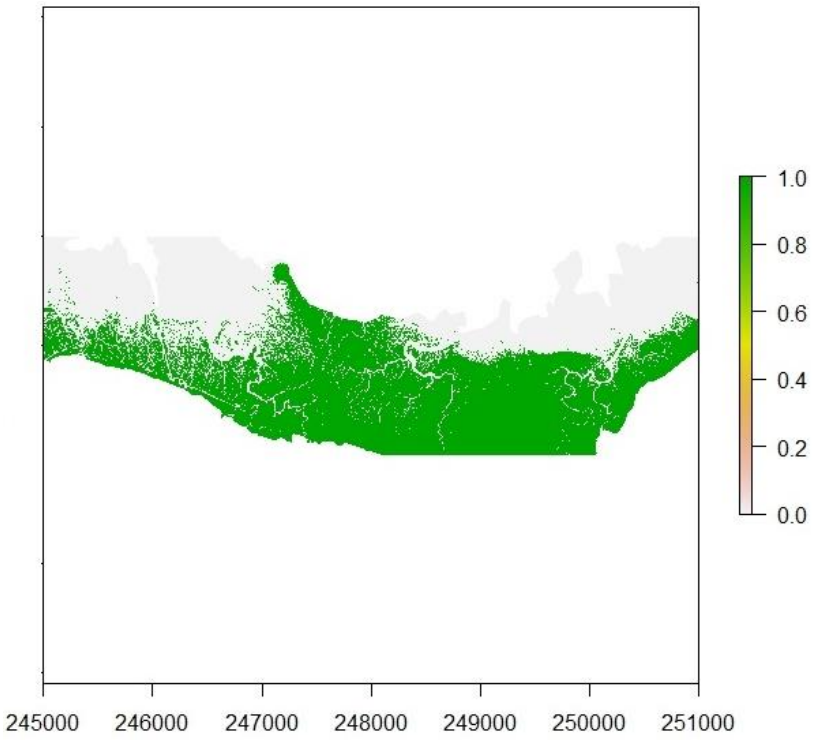


Figure 3.12 green areas represent marsh above the level of MHWS at Llanrhidian, the grey shaded area shows the extent of the saltmarsh polygons.

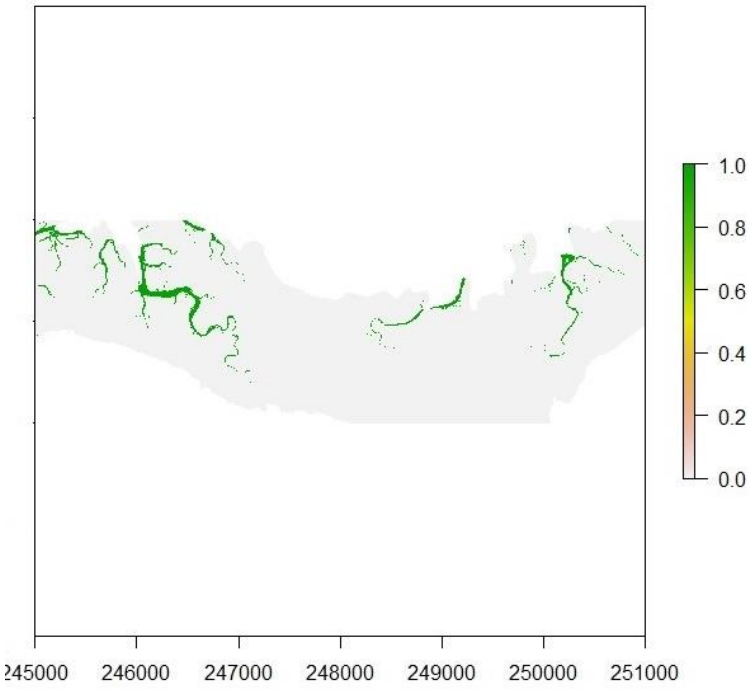


Figure 3.13 green areas represent marsh below the level of MHWN at Llanrhidian, the grey shaded area shows the extent of the saltmarsh polygons.

### 3.3.1.5 Dovey Marsh

Much of the surface at Dovey consists of a sub-horizonal platform lying between the height of MHWS and MHWN. A histogram of elevations across the whole Dovey marsh is shown in figure 3.14 below.

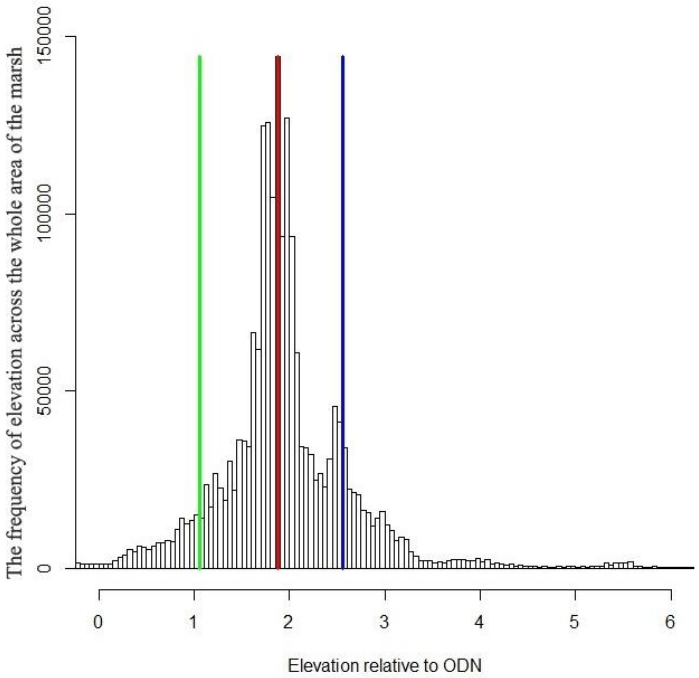


Figure 3-14 a red vertical line indicates the modal elevation at Dovey, green line represents MHWN, blue line represents MHWS.

The marsh platform is represented by a sharp peak on the histogram (Figure 3.14) at 1.82 m ODN, an elevation of 0.51 relative to MHWS and MHWN (Table 3.1). Areas above MHWS are in the landward of the marsh where land slopes upwards (Fig 3.15), and as levees along creek banks. Areas below MHWN are along creeks (Figure 3.16).

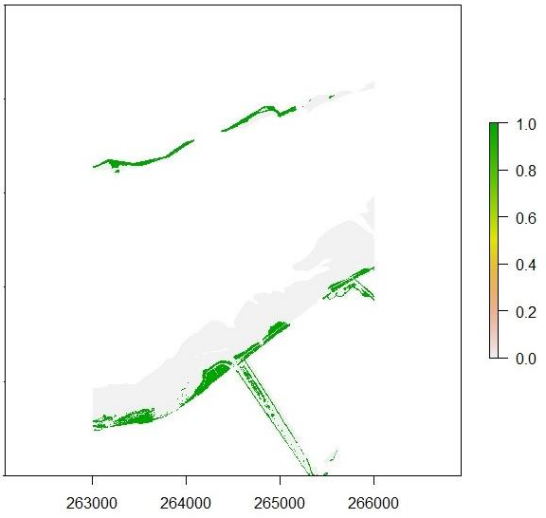


Figure 3.15 green areas represent marsh above the level of MHWS at Dovey, the grey shaded area shows the extent of the saltmarsh polygons.

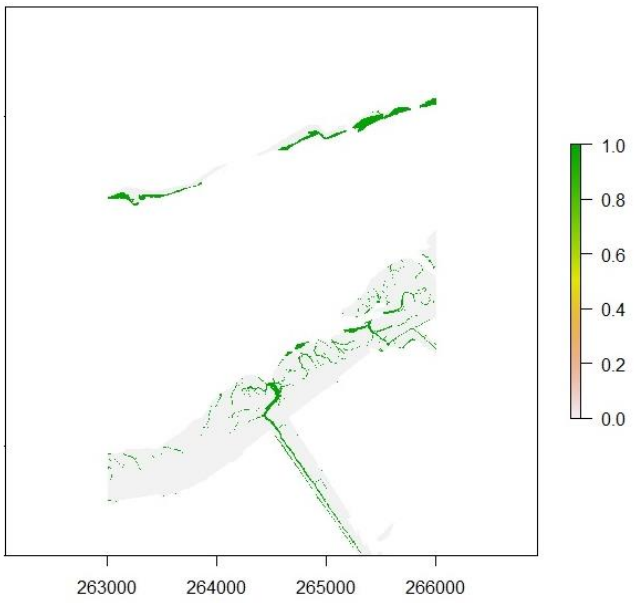


Figure 3.16 green areas represent marsh below the level of MHWN at Dovey, the grey shaded area shows the extent of the saltmarsh polygons.

### 3.3.1.6 Steart Marsh

Much of the surface at Steart platform is lying around the height of MHWS. A histogram of elevations across the whole Steart marsh is shown in figure 3.17 below.

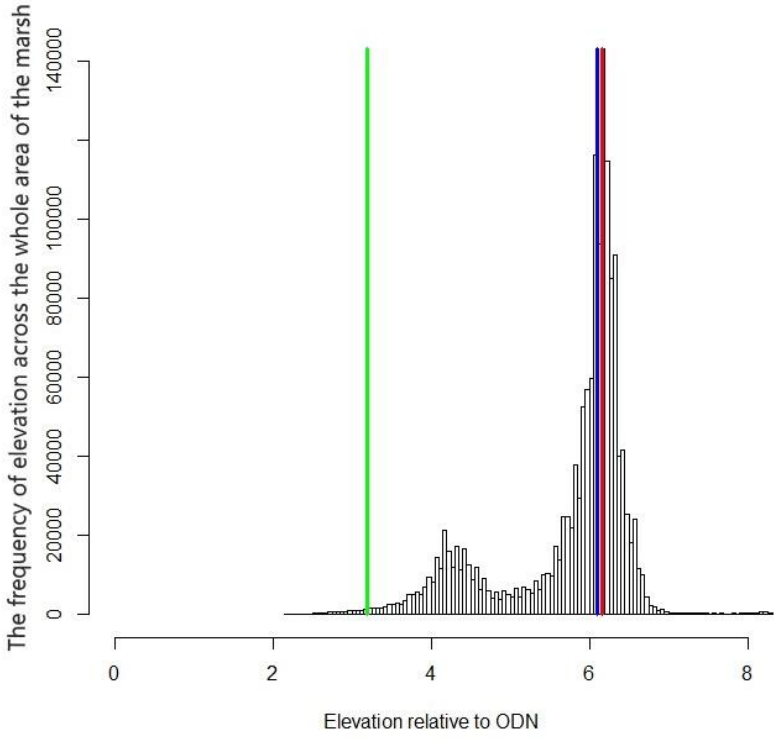


Figure 3-17 a red vertical line indicates the modal elevation at Steart, green line represents MHWN, blue line represents MHWS.

The marsh platform is represented by a sharp peak on the histogram (Figure 3.17) at 6.89 m ODN, an elevation of 1.27 relative to MHWS and MHWN (Table 3.1). Areas above MHWS are in the whole upper marsh and in the landward of the marsh (Fig 3.18), while very small areas below MHWN along creeks (Figure 3.19).

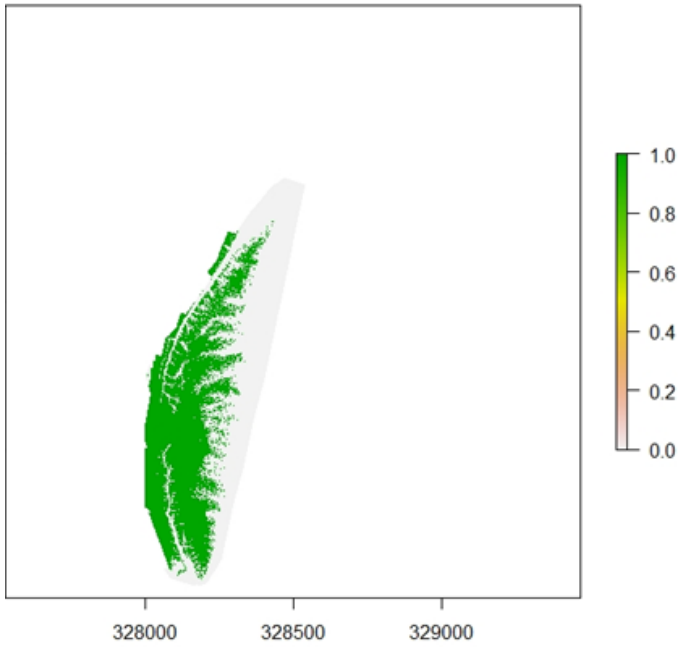


Figure 3.18 green areas represent marsh above the level of MHWS at Steart, the grey shaded area shows the extent of the saltmarsh polygons.

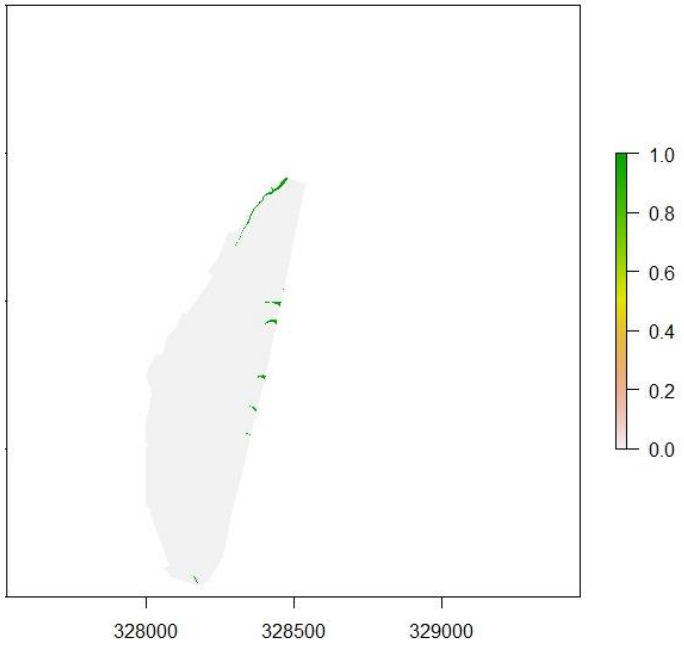


Figure 3.19 green areas represent marsh below the level of MHWN at Steart, the grey shaded area shows the extent of the saltmarsh polygons.

### 3.3.2 The distribution of marsh elevations relative to tidal height over different marshes in the UK.

Marshes in the six case studies above (section 3.3.1) have quite extensive platforms that are close to horizontal, except (Lianrhidian) which is not illustrated a sharp peak on the histogram. Four out of six marshes illustrated that marsh areas are below or around MHWS. By looking at (Fig 3.20) which shows 35 sites around the UK, elevations of these marshes often have a frequency distribution which displays a fairly sharp peak, corresponding to the presence of sub-horizontal platforms on the upper marsh. Most of these marshes (Twenty five out of thirty-five) are below or around MHWS (Fig 3.21, table 3.1).

Marsh platforms in North Norfolk including Stiffkey, Warham and Scolt Head Island lie between 2.75 and 3.075 m ODN. These platforms occur at approximately the level of MHWS (Table 3.1, Fig 3.21). In Humber Estuary marsh, their platforms occur at around MHWS in Welwick and Crably Creek at approximately 3.37 and 4.33 m (ODN) respectively, while marsh platform at Donna Nook is lower than the level of MHWS and the whole marsh lies between MHWS and MHWN (Table 3.1, Fig 3.21).

Marsh platforms in the Severn Estuary including Steart, Brean Down and Sand point occur slightly above the level of MHWS (Fig 3. 21). While at Undy marsh, the platform lies at around the level of MHWS (Figs 3.21). The marshes including Llanelli, Dovey (Dyfi) and Llarnhidian, have variable platforms corresponding to MHWS. Llanelli marsh platforms occur at approximately the level of MHWS, although there is still a large area above the level of MHWS over the marsh. At Dovey (Dyfi) almost the whole marsh lies between MHWS and MHWN, But Llarnhidian marsh platform occurs above the level of MHWS (Figs 3.20 and 21). All marsh platforms in the Solway and some marshes in Scotland here are above the level of MHWS and tidal inundation occurs only at the highest of spring tides.

For example, at Morecambe Bay, this marsh is wider than other marshes in the UK, 87.8 % of marsh is higher than MHWS (Fig. 3.9 and Table 3.1).

Additionally, eight of the marshes (9 if tidal data for St Germans is used for the Erth Island marsh) are at elevations greater than 1.1 on this relative tidal height scale, and these have a substantial fraction of the marsh (sometimes almost the whole area) higher than MHWS (Fig 3.21, Fig 3.22 and Table 3.1). These include marshes in Scotland (Holy Loch and Tay Estuary) and North-West England (Neston, Morecambe Bay, Skinburness and Longburgh), where isostatic uplift of the land surface is occurring. They also include marshes in the Severn Estuary (Steart and Brean Down) which have a combination of very high tidal ranges and high suspended sediment concentrations (Kirby and Parker, 1982). These processes are examined in more detail in the discussion alongside possible reasons for the high tidal elevation of marshes at Erth Island, Llanrhidian and Llanelli (which has substantial areas above MHWS, even though the modal elevation is below this).

Table 3.1. Details of study sites, including location; modal elevation of marsh; estimates of level of MHWS and MHWN at indicated location. Where now otherwise indicate, locations for tidal elevations are based on UK standard ports (NDL, 2017). Erth Island and Neston lie midway between two secondary ports, so tidal data for both are given. In the former cases the two secondary ports differ substantially in the tidal levels. Those indicated by * use elevations of MHWS and MHWN from Mossman et al (2012b). Orford Ness tidal data (indicated by [l]) are based on UK Environment Agency data (see methods for details).

| Site name | Late/long | Modal Elevation (m. ODN) | Location used for MHWS and MHWN | MHWS (m ODN) | MHWN (m ODN) | Elevation relative to MHWS & MHWN | Saltmarsh below MHWN (%) | Saltmarsh above MHWS (%) |
|---|---|---|---|---|---|---|---|---|
| Crably Creek | 53°43'48.0"N 0°37'08.0"W | 4.33 | Blacktoft | 4.2 | 2.5 | 1.07 | NA | 7.7 |
| Welwick | 53°38'58.9"N 0°01'21.5"E | 3.37 | Immingham | 3.4 | 1.9 | 0.98 | 1.7 | 22.3 |
| Donna Nook | 53°28'43.9"N 0°07'32.3"E | 2.82 | Immingham | 3.4 | 1.9 | 0.6 | 4 | 1.4 |
| Frampton (The Wash) | 52°55'11.1"N 0°02'42.8"E | 3.58 | Boston | 3.93 | 2.83 | 0.68 | 4.8 | 8.89 |
| Scolt Head Island | 52°58'55.9"N 0°41'37.5"E | 3.075 | Burnham* | 3.17 | 1.87 | 0.93 | 14.2 | 17 |
| Warham | 52°57'49.8"N 0°52'52.0"E | 2.82 | Warham* | 2.81 | 1.72 | 1 | 8.84 | 44.4 |
| Stiffkey | 52°57'43.1"N 0°55'42.6"E | 2.75 | Stiffkey* | 2.81 | 1.72 | 0.94 | 8.62 | 23.6 |
| Orford Ness | 52°05'13.9"N 1°33'20.7"E | 1.44 | Orford Quay[↑] | 1.45 | 0.7 | 0.99 | 0.1 | 38.8 |

| Site name | Late/long | Modal Elevation (m. ODN) | Location used for MHWS and MHWN | MHWS (m ODN) | MHWN (m ODN) | Elevation relative to MHWS & MHWN | Saltmarsh below MHWN (%) | Saltmarsh above MHWS (%) |
|---|---|---|---|---|---|---|---|---|
| Hemley | 52°02'14.5"N 1°20'24.8"E | 1.77 | Woodbridge Haven | 2.07 | 1.17 | 0.67 | 58.4 | 5.52 |
| Hamford Water | 51°54'56.5"N 1°15'10.7"E | 2.02 | Foulton Hall* | 2.04 | 1.28 | 0.97 | 32.3 | 17.8 |
| Tollesbury | 51°45'53.3"N 0°50'58.8"E | 2.43 | Tollesbury (natural)* | 2.72 | 1.69 | 0.72 | 78 | 2.1 |
| Dengie | 51°40'43.1"N 0°56'18.4"E | 2.48 | Dengie* | 2.57 | 1.65 | 0.90 | 9.4 | 10.6 |
| Fambridge | 51°37'59.7"N 0°39'07.3"E | 2.73 | North Fambridge | 2.95 | 1.85 | 0.8 | 62 | 10.6 |
| Witteringham | 50°47'03.3"N 0°54'37.5"W | 1.44 | Portsmouth | 1.97 | 1.07 | 0.4 | 53 | 6.1 |
| River Hamble | 50°52'29.4"N 1°18'42.1"W | 1.77 | Bursledon | 1.86 | 1.06 | 0.89 | 68.6 | 3.5 |
| Erth Island (Lynher River, Plymouth) * | 50°23'02.8"N 4°17'01.9"W | 2.36 | St. Germans | 1.98 | 1.08 | 1.4 | ----- | ----- |
| | | | Jupiter | 2.28 | 1.18 | 1.07 | 7.5 | 60.8 |
| Steart(Severn Estuary) * | 51°12'22.7"N 3°01'48.7"W | 6.89 | Waterbridge | 6.1 | 3.2 | 1.27 | 0.69 | 46.95 |

| Site name | Late/long | Modal Elevation (m. ODN) | Location used for MHWS and MHWN | MHWS (m ODN) | MHWN (m ODN) | Elevation relative to MHWS & MHWN | Saltmarsh below MHWN (%) | Saltmarsh above MHWS (%) |
|---|---|---|---|---|---|---|---|---|
| Brean Down (Severn Estuary)* | 51°19'15.7"N 2°59'53.2"W | 6.32 | Weston-super-Mare | 6 | 2.8 | 1.1 | 1.2 | 65.3 |
| Sand Point (Severn Estuary)* | 51°23'12.8"N 2°57'58.4"W | 6.59 | Clevedon | 6.3 | 3.1 | 1.09 | 10.8 | 37.9 |
| Undy (Severn Estuary) | 51°33'56.7"N 2°47'45.5"W | 6.66 | Avonmouth | 6.7 | 3.3 | 0.99 | 0.13 | 33.9 |
| Llanelli | 51°39'05.8"N 4°05'21.8"W | 4.12 | Llanelli | 4.14 | 2.14 | 0.99 | 5.2 | 50 |
| Llanrhidian | 51°37'12.1"N 4°11'26.4"W | 4.6 | Burry Port | 3.9 | 1.9 | 1.35 | 3.1 | 53.2 |
| Dovey (Dyfi) Estuary | 52°32'32.8"N 3°58'54.5"W | 1.82 | Dovey Estuary | 2.56 | 1.06 | 0.51 | 16.6 | 11.4 |
| Neston Dee Estuary | 53°17'06.2"N 3°05'27.8"W | 4.4 | Mostyn Docks | 4 | 2.2 | 1.2 | 2.48 | 82 |
| | 53°18'27.6"N 3°15'30.1"W | 4.4 | Connah's Quay | 3.95 | 2.25 | 1.26 | ----- | ------ |
| Morecambe Bay | 54°08'33.2"N 2°48'28.1"W | 5.33 | Arnside | 4.9 | 2.5 | 1.18 | 0.3 | 87.8 |
| Skinburness (Solway) | 54°53'09.8"N 3°19'00.6"W | 5.04 | Silloth | 4.8 | 2.7 | 1.11 | 2.9 | 72.2 |
| Longburgh(Solway) | 54°55'59.8"N 3°05'03.4"W | 5.9 | Annan Waterfoot | 5 | 2.7 | 1.4 | 1.1 | 87.3 |

| Site name | Late/long | Elevation (m. ODN) | Location used for MHWS and MHWN | MHWS | MHWN | Elevation relative to MHWS & MHWN | Saltmarsh below MHWN (%) | Saltmarsh above MHWS (%) |
|---|---|---|---|---|---|---|---|---|
| Holy Loch | 55°59'42.2"N 4°57'28.0"W | 1.88 | Greenock | 1.78 | 1.18 | 1.16 | 3.14 | 71.46 |
| River Wick | 58°26'47.8"N 3°06'43.5"W | 1.73 | Wick | 1.79 | 1.09 | 0.91 | 0.6 | 43.9 |
| Cromarty Firth | 57°44'00.2"N 4°02'43.6"W | 2.15 | Invergordon | 2.08 | 1.08 | 1.07 | 0.003 | 65.5 |
| River Ythan | 57°19'59.3"N 1°58'01.9"W | 2.2 | Newburgh | 2.8 | 1.7 | 0.45 | 5.1 | 1.6 |
| Tay Estuary | 56°24'50.4"N 3°06'48.3"W | 3 | Newburgh | 2.8 | 1.7 | 1.18 | 37.6 | 39.1 |
| Beal | 55°39'23.5"N 1°50'26.5"W | 1.89 | Holy Island | 2.4 | 1.3 | 0.55 | 0.26 | 23.2 |
| Budle Bay | 55°36'36.6"N 1°46'07.7"W | 2.23 | Holy Island | 2.4 | 1.3 | 0.85 | NA | 59.7 |
| Alnmouth | 55°23'16.6"N 1°37'05.6"W | 2.31 | Amble | 2.35 | 1.25 | 0.96 | 8.3 | 39.2 |

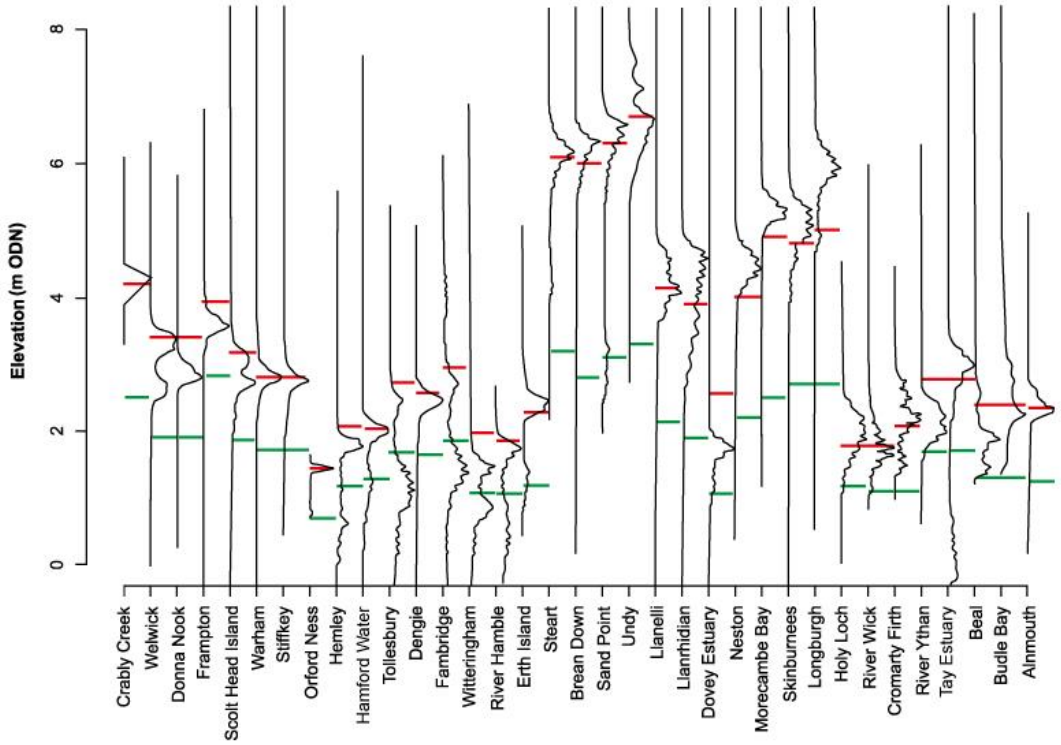


Fig 3-20: Variation of saltmarshes elevation at thirty-five sites around the UK coast. Sites are arranged in a sequence that moves clockwise around the coast, starting at the Humber Estuary. Green line represents MHWN and blue line represents MHWS.

For 15 more marshes, there is a peak on the histogram of elevations at between 0.9 and 1.1, while 11 show a peak at an elevation below 0.9, with the lowest marshes (Witteringham, River Ythan and Dovey Estuary), having modal elevations approximately midway between MHWN and MHWS (relative elevations between 0.4 and 0.51) (Fig 3.21, Table 3,1).

The great majority of saltmarsh area at the sites examined in this study lies around, or below, the elevation of MHWS. This is the case in South-East England (our sites between Frampton and Fambridge), the part of the UK that is most vulnerable to flooding during storm surges because the land is low-lying, a local isostatic sea level rise is occurring (Shennan *et al.*, 2009), and there are large areas where coastal or freshwater wetlands have been drained for agricultural use.

Histograms of elevations of all saltmarsh sites are shown in (Figs 3. 21), arranged in a sequence that runs in a clockwise direction around the UK, beginning at the Humber Estuary. Our choice of this arrangement reflects the fact that the coast of the Southern UK, from the Tees Estuary on the East coast to a point somewhere between Neston and the Dovey Estuary on the West coast is experiencing isostatic sea level rise, while the coast to the north of these points, including the whole coast of Scotland is experiencing isostatic sea level fall (Shennan, Milne *et al.*, 2009).

Comparing our findings with the subsidence/uplift values (Shennan, Milne *et al.*, 2009) concluded that the correlation is significant at 0.01 between saltmarsh platforms around the UK and the subsidence/uplift values (Fig 3.22). There are a number of sites on rising coasts with relative elevation > 1. The other sites with a modal elevation > 1 (Fig 3.22) are in the Severn and Humber which are very high turbidity, and in the Erth Island marsh, which is on pre-existing topography, while in Llanrhidian marsh might be due to peat formation.

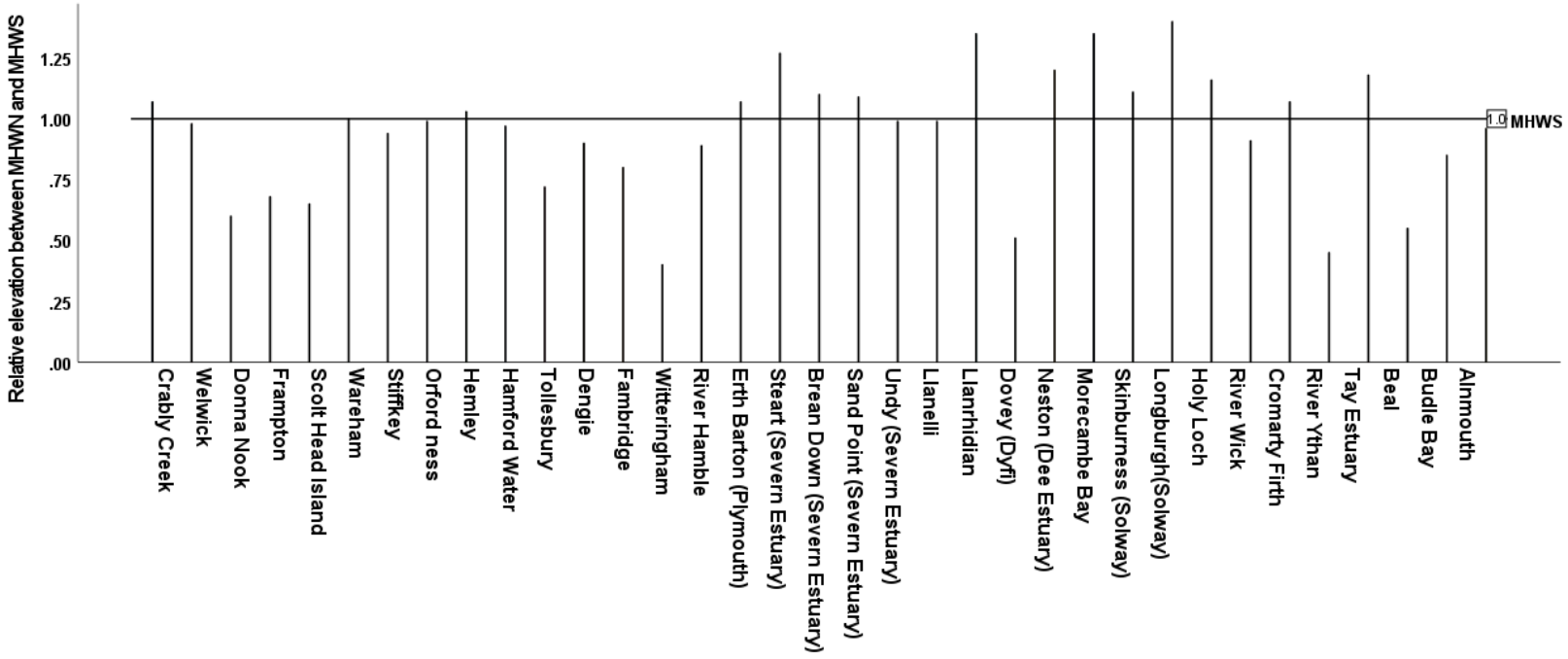


Fig 3-21: Elevation of saltmarsh platforms at 35 sites around the UK coast as indicated by modal elevation. MHWS = 1 and MHWN = 0, as they were standrised in the method . Sites are arranged in a sequence that moves clockwise around the coast, starting at the Humber Estuary

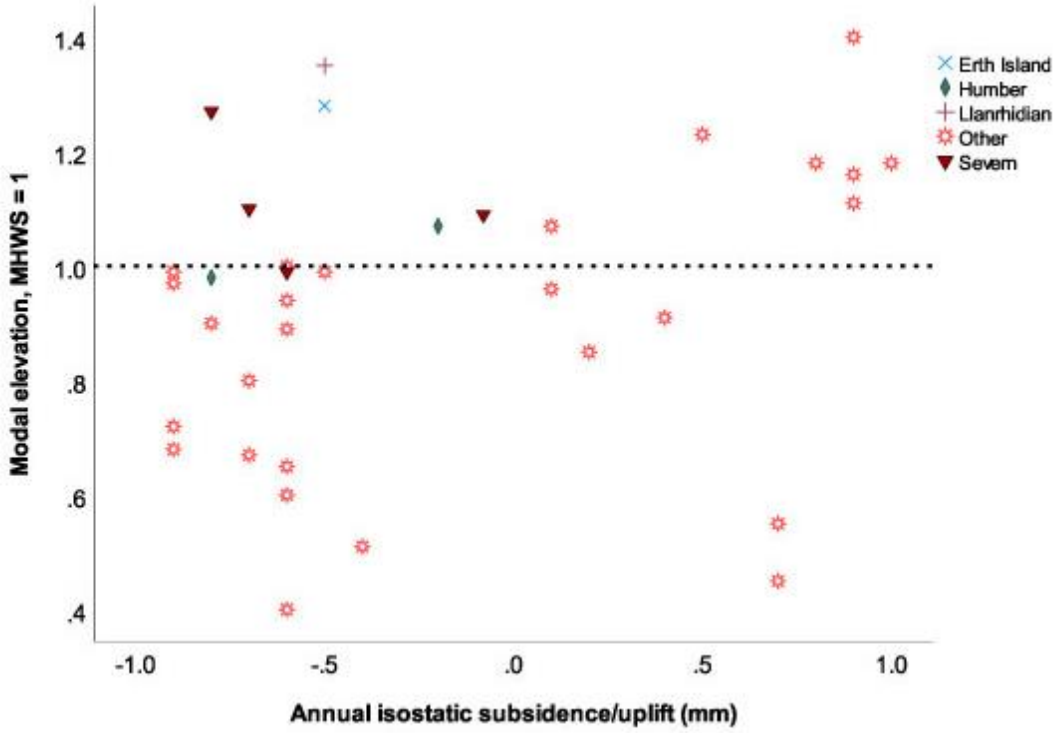


Fig 3-22: modal elevations for 35 marshes around the UK against the subsidence/uplift values by (Shennan, Milne *et al.*, 2009).

### 3.3.4 What implications does this have for water depths over saltmarshes during high tides?

During normal tidal conditions, a saltmarsh located at MHWS will be submerged on approximately 100 of the tides that occur each year, and during roughly half of the periods of spring tides the water level will remain below the marsh platform. Some literature distinguishes on this basis between bank-full and over marsh tides (Bayliss-Smith *et al.*, 1979). But even during the times of year when spring tides are at their greatest amplitude, the depth of water above the marsh will be relatively shallow. For standard ports in the UK, for which very detailed tidal data are available, the highest predicted astronomical tides are between 0.4 and 0.7m above MHWS (UK tide tables, Table V part 1). As a result, the great majority of measurements of wave dissipation across saltmarshes have been in water depths of less than 1 m. The main part of the UK where normal spring tides will flood marshes to a greater depth than this is the Severn Estuary, where the very high tidal range means that HAT is 1.33m above MHWS at Avonmouth, 1.22m above at Newport, 1.19m at Hinckley Point, 0.97m at Mumbles, 0.99m at Ilfracombe and 0.81m at Milford Haven (NTSLF, 2020). Coastal flooding normally occurs during storm surges, when tidal heights are increased substantially above their predicted level by low pressure and/or wind driven water movement, often exacerbated by relatively large waves. Coastal defences are built at a height that is sufficient to protect against these relatively rare events.

### 3.3.5 How deeply submerged would we expect marshes to be during a storm surge?

At the 39 NTSLF tide gauge sites around the UK, (NTSLF, 2020) report that seven have extreme high water values that are more than 1.5m above MHWS, with a maximum value of 1.68m for both Millport and Heysham. However, as noted in the methods section, these

data do not include the two largest recent surges on the English coast of the North Sea. Spencer, Brooks *et al.*, (2015) report values for observed water levels during the 1953 and 2013 surges and expresses them relative to MHWS at the same locations. Observed water levels at Blakeney were much higher than at adjacent sites during both surges, and water level recorded at Stiffkey was rather low during the 1953 event. But apart from this, there is a consistent pattern of water levels during surges that are 2.5m above MHWS along the whole coastline from North Norfolk to Lowestoft. A more localised surge in 1978 led to a water level of 4.91m ODN at Wells in Norfolk, 2.16m above MHWS (Steers *et al.*, 1979). So, in South-East England, surges that reach 2m above the level of MHWS occur with a return time of approximately 30 years, and 2.5m surges have a return time of about 60 years. Water levels during storm surges on the Eastern side of the North Sea can be even higher, with water levels of 10.09m and 9.93m above tide gauge datum occurring at Cuxhaven on 3rd January 1976 and 16th February 1962 (UHSCL, 2020), representing 3.29m and 3.13m above estimated MHWS respectively.

### 3.4 Discussion

Elevations of many UK saltmarshes, particularly on the South and East coasts of England, have a frequency distribution that displays a relatively tight peak corresponding to these platforms (Fig 2.20). These often lie below the level of MHWS and in many cases the proportion of marsh above MHWS is rather small. The existence of these platforms has been recognised in the geomorphological literature. Early models of saltmarsh development noted that accretion decreased asymptotically as elevation increased (Kestner, 1975; Pethick, 1981), leading to a maximum marsh elevation that is markedly lower than the height of the highest tide. This change in accretion rates over time implies that uninterrupted marsh development should lead to the formation of extensive platforms lying just below the tidal height at which accretion rate declines to zero, although neither author explicitly makes this link. Allen, (1990) and (French, 1993) present more elaborate models of accretion rates, which again show sedimentation reducing asymptotically with elevation, except where peat formation allows the upward growth of the marsh even in the absence of inputs of clastic material.

These works again focus on changes of marsh surface elevation over time, rather than on the shape of the upper marsh surface, but in a number of figures, the high marsh is drawn as a sub-horizontal surface. Allen (2000) talks explicitly about marsh platforms; the numerical models of Mariotti and Fagherazzi (2010) and Fagherazzi et al. (2012) lead to the development of a sub-horizontal high marsh platform, often separated from tidal flats by a scarp. Wang and Temmerman (2013) have argued that mudflat and high marsh platforms represent alternative stable states, and a recent review (French, 2019) presents a sketch of a “tidal salt marsh landform” in which there is a marsh platform with a wide area of high marsh and a narrow area of low marsh, separated from a tidal flat by a cliff. Indeed, some

recent work has relied on the existence of sub-horizontal marsh platforms with a small cliff at their seaward edge to automatically delimit saltmarsh extent using remotely sensed elevation data alone (Goodwin et al., 2018). But extent to which these platforms dominate many UK marshes is not widely recognised and only in a few locations do we have good information about their heights in relation to tidal elevations. Our methods provide a straightforward method of obtaining this and we provide this information for 35 marshes around the UK, although in one case (Erth Island) rapid changes of tidal levels around the site increase the uncertainty of our estimate, and in six cases our estimates rely on tidal data that we have collected ourselves.

Three marshes lying on the Severn Estuary (Steart, Brean Down and Sand Point), have platforms lying above MHWS. Relatively high elevation of marshes in the Severn Estuary, reflecting continued accretion up to an elevation of 0.6-0.8m above MHWS, has been described previously. It has been attributed to the combination of a very large tidal range and high suspended sediment concentrations (Allen, 1990; 2000; Allen and Rae, 1986). A similar explanation is likely for Crably Creek on the Humber Estuary (relative elevation of 1.07), (Table 3.1). The Humber also has a relatively high tidal range, ranging from 6.4m at Immingham to 5.9m at Blacktoft and suspended sediment concentrations that can be up to 10 g $l^{-1}$ in the vicinity of Crably Creek (site UW in Uncles et al, 2006).

There are two other individual sites that are relatively high in the tidal frame. At Llanrhidian in the Burry Estuary, South Wales, there is a less clearly defined marsh platform, and in this case the peak on the histogram of elevations occurs at 4.6 m (Fig. 3.11), substantially above the level of MHWS, which is at about 3.9m ODN here. The Llanrhidian marsh is markedly higher in the tidal frame than the nearby Llanelli marsh, even though the level of MHWS is slightly higher at Llanelli. Both are in the Burry Estuary, with Llanelli nearer the mouth. The

area of relatively high marshes extends for an area of several km along the estuary, and may result from organic matter accumulation, as sediments on the upper marsh here show high values of loss on ignition and overlie peat (Goodwin, 1983). The Erth Island marsh surrounds a tidal island, which has a maximum elevation of 6m ODN (MHWS is at around 2m ODN, see table 3.1), so at least some of this marsh has developed on pre-existing topography. Platforms can also occur at lower elevations, with 8 out of the 35 marshes examined having modal elevation lying appreciably below the level of MHWS (at elevations between 0.4 and 0.75). An example of this pattern is the Dovey Estuary (Fig. 3.14). However, the agricultural land behind the sea wall lies just below MHWS. This is an area of alluvial sediments (Shi and Lamb, 1991) which were presumably occupied by saltmarsh before the sea wall was built.

So, there are some parts of the UK where marshes extend above MHWS, and a number of presumably young marshes which are relatively low on the shore. But, particularly in the South and South-East of England, the characteristic pattern is of the formation of a marsh platform that is at or below the level of MHWS, with only relatively small areas above this. Our methods allow us to be both more precise and accurate than some previous studies. Goodwin and Mudd (2019) state that marsh platforms are located between “Mean High Tide MHT and the Observed Highest High Tide OHHT”, where OHHT is the mean of the highest tide in each month calculated over a full year. This is a rather broad range and requires a full year of tidal records, so can only be calculated for a very limited number of locations where such data are available. In addition, it will be more strongly influenced by the occurrence of storm surges within a data set than will be MHWS obtained from tide tables or as the 13.9th percentile of a number of measured high tides. For Cromer in 2013, OHHT is 2.75m ODN, as compared with MHWS of 2.32m, and only about 2.5% of tides are

higher than OHHT. Goodwin and Mudd (2019) conclude that their Mersey Estuary and Morecambe Bay marshes lie close to the level of OHHT, which they estimate as approximately 5 and 5.3m ODN respectively. On this basis, they argue that deposition during storm events plays an important role in determining marsh elevation. However, the data used to calculate these tidal levels come from gauges that are some distance away from the marshes being studied. For the Morecambe Bay marsh, they used tidal data from Heysham, and for the Mersey estuary, the marsh was located at Ellsmere Port while the tide data came from Liverpool Gladstone Pier. In both cases the marshes are approximately 15 km away from the tidal gauge used. As we have shown elsewhere, the elevations corresponding to a particular tide datum, like MHWS or OHHT, can change quite rapidly over short distances (Mossman et al., 2012b). At Heysham, MHWS is located at 3.3 ODN, while at Arnside (much closer to the marsh studied) it is at 4.9m ODN (UK Hydrographic Office, 2014), a figure that agrees closely with estimates based on a year of tide gauge data for Morecambe Bay reported by Gray (1972). In the Mersey, MHWS at Gladstone Pier is at 4.47m ODN, while at Hale Head (much closer to the marsh studied) it is 4.9m ODN. So, the Ellsmere Port marsh is actually located close to MHWS, and there is no need to invoke deposition during storm events as an explanation for its elevation. Elsewhere, Wang and Temmerman (2013) report a modal elevation of vegetated areas in the Western Scheldt at around the mean level of high tides. This relatively low elevation is likely to reflect the relatively recent development of these marshes, perhaps following the extensive reclamation of older marshes that has occurred here (Huiskes, 1988).

Marsh platforms around the elevations of MHWS will normally be effective at dissipating wave energy during normal conditions, as in the UK, highest astronomic tide is between 0.4 and 0.7m higher than MHWS (UK tide tables, Table V part 1). The main exception to this

is the Severn Estuary, where difference between MHWS and the level of the highest tides is between 0.81 and 1.33m. However, these platforms will be rather ineffective during storm surge conditions where water levels can be considerably higher. The 2013 storm surge occurred on predicted tides that were higher than MHWS (MHWS was 3.4m ODN at Immingham and 2.4m at North Shields; while predicted high tides were 3.69m and 2.97m from table 1 of (Spencer, Brooks *et al.*, 2015). The surge peaked at 2.26m higher than this, giving water levels around 2.5m higher than MHWS. The implications of this are examined in more detail in the prediction of wave dissipation chapter 4.

Some marshes do have extensive areas at higher elevation than MHWS, but these are typically in areas where land reclamation has not taken place, and the land area vulnerable to coastal flooding is small. This is implicit in (Gedan, Kirwan *et al.*, 2011), who show much flooding attenuation during surges from storms than on average (compare their Fig 6A with their 6b). However, their value for the effectiveness of saltmarshes in reducing flooding during storm surges is based on three studies examining water level, rather than wave energy (King and Lester, 1995, Krauss, Doyle *et al.*, 2009, Lovelace, 1994, Wamsley, Cialone *et al.*, 2010) analysis has been very influential, despite the fact that the claimed association between the width of marshes and seawall height that is required is based on a citation of an information leaflet targeted at the general public (National Rivers Authority, 1992 [East Anglia Saltmarshes]).

So, while saltmarshes may play an important role in protecting sea walls from wave action during normal conditions, their contribution in reducing risks of flooding during storm surge events is much less important. In contrast, a much greater part of the area of saltmarshes lies above MHWS in the northwest of England and Scotland (Fig 3.21). Saltmarshes could be more effective in reducing flooding during storm surge events in these areas, and those

parts of the UK are not vulnerable to flooding during storm surge events compared to the South and East of England.

### 3.5 Conclusion

In this chapter, the results show that many of marsh platforms particularly on the East and South England have a frequency distribution that displays a relatively tight peak corresponding to these platforms which occur at or below the level of MHWS (Fig 2.21). As such, these marshes can be effective against flooding during normal condition with their contribution in reducing risks of flooding being less important during storm surge events. In contrast in the North-West England and Scotland (Fig 3.21), This part of the UK is experiencing isostatic sea level fall (Shennan, Milne *et al.*, 2009). Most of marsh platforms occur above MHWS, and they might not be vulnerable to flooding during storm surge events.

Based on the findings from this chapter, several important questions are formulated which will be addressed in subsequent chapters. Different elevation appears to be effective of delivering ecosystem services by marshes. Additionally, High / low marsh and their influence on the effectiveness of the saltmarsh in dissipating wave energy (Chapter 4); and sediment deposition rates being low or zero on high marsh which provide question that to what extent elevation and sedimentation rates influence the carbon burial and emission of GHGs in the marsh? (Chapter 5).

## Chapter four

## Modelling Wave dissipation across four UK salt marshes

### 4.1 Introduction

Globally, satellite altimetry has shown that global mean sea level has been rising at a rate of ∼3 ± 0.4 mm/y since 1993., and this rate is accelerating at 0.084 ± 0.025 mm/y (Nerem et al. 2018). The average sea level rise rate is expected to continue to accelerate in future (Horton *et al.*, 2014, Slangen *et al.*, 2016). In some parts of the world, such as in coastal areas along the Mediterranean African coast, at the Gulf of Lion in France and along Egyptian coasts Large storm events are increasing in frequency (Cid *et al.*, 2016, Marcos *et al.*, 2009). These changes, including the ferocity of storms surges are threatening growing coastal populations (Knutson *et al.*, 2010). The UK coast has been damaged by storm surges in the eighteenth, nineteenth and twentieth centuries (ABI, 2006; Lewis and Kelman, 2009; Bankoff, 2013). The two biggest surge events in the UK also occurred in the East Coast of the UK, one in 2013 that damaged 2,800 properties and one in 1953 that damaged 24,000 properties (Wadey *et al.*, 2015).

Previous studies (Gedan, Kirwan *et al.*, 2011, Shepard, Crain *et al.*, 2011, Spalding *et al.*, 2014a, Sutton-Grier *et al.*, 2015) indicate that coastal vegetation, including coastal marshes, provide a system of defence that is resilient against flooding risks and has the ability to protect and stabilise shorelines through enhancing deposition of sediments and minimising erosion (Shepard, Crain *et al.*, 2011). Moreover, vegetation growth and marsh accretion might be sustainable protection under accelerated sea level rise (Kirwan et al., 2016), and marshes also have the capacity to attenuate large waves that are frequent, thereby, reducing flood peaks.

Saltmarshes can be highly effective in reducing potential of waves to exceeds seawall (Möller and Spencer, 2002). So, this reduces the likelihood of wave action thereby, damaging coastal defences and the extent to which overtopping of the sea defences occurs as a consequence of wave runup (Ruggiero et al. 2001). But the degree of overflow of the seawall depends on type of structural material and environmental conditions such as wave height and wave period (Owen, 1980).

Saltmarsh environments can significantly attenuate incident waves as compared to unvegetated sand/mudflats (Brampton, 1992, Möller and Spencer, 2002). These environments are, therefore, fundamental to sustainable shoreline protection (Narayan *et al.*, 2016a, Narayan *et al.*, 2016b, Spalding, McIvor *et al.*, 2014a, Spalding *et al.*, 2014b, Vuik *et al.*, 2016), and contribute to the attenuation of energy from waves during large storms (Gedan, Kirwan *et al.*, 2011, Möller, Kudella *et al.*, 2014). But (Leonardi *et al*. 2018) concluded that although large marshes are able to be effectively dissipate wave energy even under extreme water level conditions, their contribution to dissipate wave energy might be limited when the marshes are smaller or and intersected by large channels or open water areas. Moreover, (Temmerman *et al.*, 2023) indicated that the contribution of marsh vegetation during storm surge is much less effective or not effective at all, and (Shepard, C.C., 2010; Temmerman, Horstman *et al.*, 2023) concluded that marsh vegetation can be effective during storm surge if there are several thousand to tens of thousands of meters wide such as Louisiana wetlands.

Some studies have conducted in laboratory settings to investigate the value of saltmarshes in attenuating waves during storm surge events. (Anderson and Smith, 2014) used a wave flume to investigate irregular wave dissipation, and they reported that wave attenuation increases on the marsh but it can be varied based upon stem density and the length of

vegetation, the submergence ratio and emergent conditions. Möller, *et al.*, (2014) investigated wave attenuation on saltmarsh vegetation during a storm surge in a large flume and concluded that wave dissipation is less than 20% over a 40m distance even in water that is 0.9 m deep. Indeed, both studies (Anderson and Smith 2014; Möller et al. 2014) confirmed that there is a strong relationship between water depth and wave dissipation. Rupprecht *et al*. (2017) report that water depth plays an important role in the interaction between vegetation and waves during storm surge. From these studies we need to understand how we can predict wave dissipation across saltmarsh using water depth as a function of wave dissipation. We have good data of elevations across saltmarsh for many sites as we generated transects in Chapter 2. We also have data of elevation relative to tidal heights for many sites as displayed in chapter 3. So, we then generated simple model using these data to predict wave dissipation across marsh in some sites (see Method).

### 4.1.1 Aims of the study

The aims of this study are:

i. To predict wave dissipation across four saltmarshes for a range of water depths.

ii. To determine characteristics of these marshes that increase wave dissipation.

iii. To evaluate the ability of saltmarshes of reducing waves during storm surge events.

The objectives of this study are:

i. Use elevation data (DTM) for saltmarshes and heights of normal and storm surge tidal heights which were generated in chapter 3.

ii. Calculate water depths along transects across saltmarshes starting from shallow water and running to the landward limit of the marsh for a range of tidal conditions.

iii. Combine these water depths with empirical data from the literature on the relationship between wave energy dissipation and water depth to predict wave dissipation along these transects.

## 4.2 Method

### 4.2.1 Generating wave dissipation model

In the line of the previous studies the reduction of wave attenuation occurred when the water depth increased (Fonseca and Cahalan, 1992 Möller *et al*. 2014; Möller and Spencer 2002), and water depths are critical significance to the wave dissipation process. Water depth and plant density play a role of increasing wave dissipation (Augustin et al., 2009), and (Fonseca and Cahalan, 1992) found that the average reduction of wave dissipation across four species was about 40% for each species when leaf length was equal to water depth. Indeed, plant flexibility determines to what extent plants move and hence the magnitude of drag forces experienced (Luhar and Nepf, 2016, Mullarney and Henderson, 2010, Paul *et al*., 2016).

Wave height is another factor influence wave dissipation, but the reduction of wave height might be variable upon to distance across the salt marsh. For example, the reduction of wave heights across 200 m of salt marsh is an average of 63% (Moeller *et al*, 1999), and 92% over 310m (Möller and Spencer 2002). These percentages are smaller than expected based on extrapolations of (Brampton's, 1992) modelling results. Brampton's (1992) model indicates that the reduction of wave height over an 80-metre-wide salt marsh was 40%. This paradox is due to the lack of various linearly of wave attenuation according to distance across the salt marsh; rather, over the first 10 to 50 metres of the salt-marsh surface, most wave energy is dissipated and reflected (Moeller *et al*., 1999).

To model dissipation from vegetation four main assumptions were facilitated of the early wave attenuation models: (1) uniform emergent vegetation, (2) linear wave theory, (3) regular waves, and (4) rigid plants (WU and Cox, 2015; Pinsky *et al.*, 2013). These early wave

attenuation models have been investigations in terms of the flexibility of vegetation assumed that plants are flexible structures which dynamically are affected by the waves passing over them, and vice-versa. Most of experimental data were analysed to define the wave height decay equations developed by Dalrymple et al. (1984) who utilized the maintenance of energy equation and regular waves to measure decay through an array of rigid cylinders.

The wave height decay equations developed by Dalrymple et al. (1984) is that:

$$\frac{Hs(x)}{Hs} = \frac{1}{1+\alpha x} \qquad (1)$$

Where H(x) = wave height at a distance x through the start of the vegetation field; and Hs = significant wave height measured at the start of the vegetation field using Hs=4.004$\sqrt{mo}$ where mo = variance of the free surface elevation time series; and α = damping factor.

We applied this equation to data wave height reductions reported by Moller (2006) to determine the relationship between damping factor and water depth.

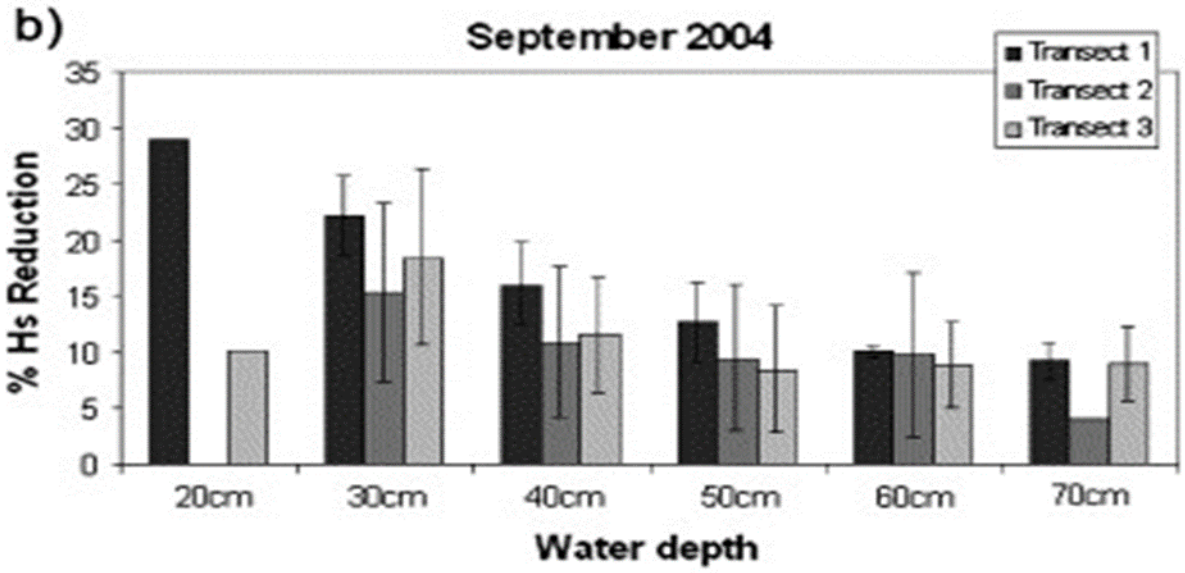


Fig 4.1. Average significant wave height (Hs) across transects in September 2004 over three 10m transect, disaggregated into 10cm water depth histogram intervals (Moller et al., 2006).

The Figure above illustrates data about Hs reduction % in different water depth over 10 m. we have selected transect 1 due to the existence values of the average significant wave height.

For finding damping factor for 30% value in 20 cm water depth over 10m in transect 1:

$$\frac{Hs(x)}{Hs} = \frac{1}{1+\alpha x}$$

$$\frac{Hs(x)}{Hs} = (1-0.3) = \frac{1}{1+\alpha x}$$

$$1 + \alpha * 10 = \frac{1}{0.7}$$

$$\alpha = 0.0428$$

For finding damping factor for 20% value in 30 cm water depth over 10m transect 1:

$$\frac{Hs(x)}{Hs} = \frac{1}{1+\alpha x}$$

$$\frac{Hs(x)}{Hs} = (1-0.2) = \frac{1}{1+\alpha x}$$

$$1 + \alpha * 10 = \frac{1}{0.8}$$

$$\alpha = 0.025$$

For finding damping factor for 15% value in 40 cm water depth over 10m transect 1:

$$\frac{Hs(x)}{Hs} = \frac{1}{1+\alpha x}$$

$$\frac{Hs(x)}{Hs} = (1-0.15) = \frac{1}{1+\alpha x}$$

$$1 + \alpha * 10 = \frac{1}{0.85}$$

$$\alpha = 0.017$$

For finding damping factor for 12% value in 50 cm water depth over 10m transect 1:

$$\frac{Hs(x)}{Hs} = \frac{1}{1+\alpha x}$$

$$\frac{Hs(x)}{Hs} = (1-0.12) = \frac{1}{1+\alpha x}$$

$$1 + \alpha * 10 = \frac{1}{0.88}$$

$$\alpha = 0.013$$

For finding damping factor for 10% value in 60 cm water depth over 10m transect 1:

$$\frac{Hs(x)}{Hs} = \frac{1}{1+\alpha x}$$

$$\frac{Hs(x)}{Hs} = (1-0.1) = \frac{1}{1+\alpha x}$$

$$1 + \alpha * 10 = \frac{1}{0.90}$$

$$\alpha = 0.011$$

For finding damping factor for 9% value in 70 cm water depth over 10m transect 1:

$$\frac{Hs(x)}{Hs} = \frac{1}{1+\alpha x}$$

$$\frac{Hs(x)}{Hs} = (1-0.09) = \frac{1}{1+\alpha x}$$

$$1 + \alpha * 10 = \frac{1}{0.91}$$

$$\alpha = 0.009$$

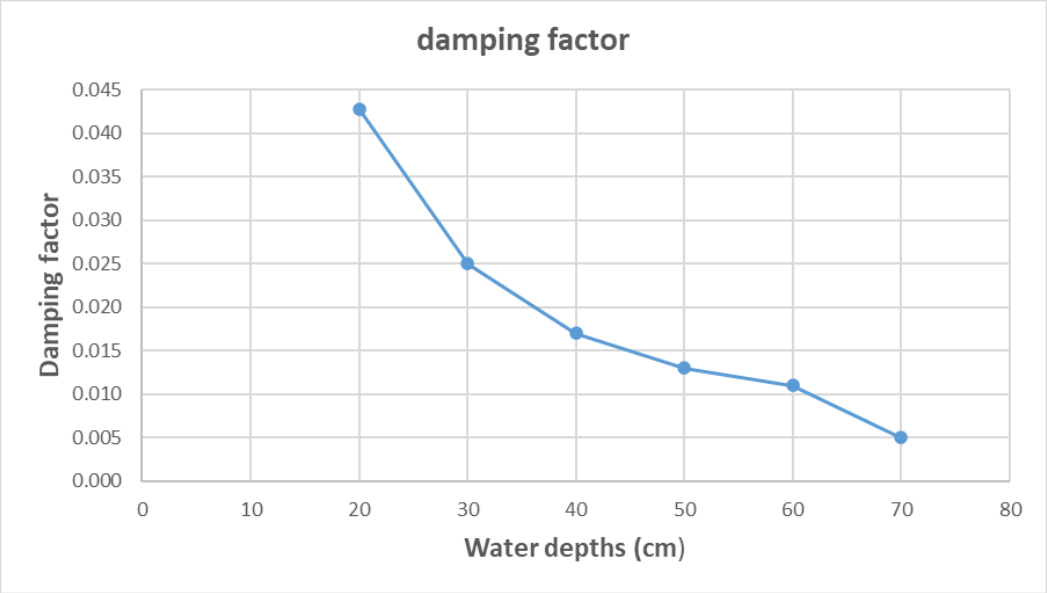


Fig 4.2. the relationship between damping factor and water depths across transect in September 2004 at Dengie saltmarsh based on analysis of data from Moller et al., (2006).

Indeed, the increase in wave height due to the decrease in water depth (Dean and Dalrymple, 1991), and (Kobayashi et al. 1993) generated linearly model of the force acting on the vegetation presenting the change in wave height can be approximated as an exponential decay (K). This model was used by (Foster-Martinez *et al.*, 2018) to estimate values of k as a Decay from a number of different studies, so for small values of k:

$$e^{-k\tilde{}}=1-k \qquad (2)$$

where: $e^{-k\tilde{}}$= wave energy remaining; and K = a Decay as a function of water depth.

Based on this approach we generated our model to estimate K value as a function of water depth across saltmarsh. In details, we assumed two points in this case depths of 0.15 m and 2.0 m, which refer to the lowest and the highest depths of the water across saltmarsh and calculating the K values corresponding to depths of 0.15m and 2.0m using equation (2).

The K value of water depth at 0.15 m is 0.143 (Morgan et al., 2009; Pinsky et al., 2013), while we assumed the wave energy remaining $e^{-k}$ = 0.999 when water depth at 2.0 m as a start point of seaward end, so the K value is 0.001.

Moreover, calculating (a) and (b) as coefficient numbers which determine the shape of the curve and fit the relationship between water depths and K values using the equation:

$$K = \mathrm{a}(\frac{1}{\mathrm{depth}}) + b(\frac{1}{\mathrm{depth}^2}) \qquad (3)$$

Where:

k = Decay (K) as a function of depth; and a & b = coefficient numbers; and depth = depth of water at 0.15 m and 2.0 m. K values = 0.143 and 0.001 at 0.15 m and 2.0 m of water depth respectively. So, the calculation of coefficient numbers (a) and (b) was that:

$$K = \mathrm{a}(\frac{1}{\mathrm{depth}}) + b(\frac{1}{\mathrm{depth}^2})$$

$$0.143 = \frac{\mathrm{a}}{(0.15)} + \frac{\mathrm{b}}{(0.15)^2}$$

$$0.143 = \frac{0.15\mathrm{a} + \mathrm{b}}{(0.15)^2}$$

$$0.143 * (0.15)^2 = 0.15a + b$$

$$b = 0.0032175 - 0.15a$$

$$0.0032175 - 0.15a = 0.004 - 2a$$

$$0.004 - 0.0032175 = 2\mathrm{a} - 0.15\mathrm{a}$$

$$0.0007825 = 1.85a$$

a = 0.00042297

$$K = \mathrm{a}(\frac{1}{\mathrm{depth}}) + b(\frac{1}{\mathrm{depth}^2})$$

$$0.001 = \frac{\mathrm{a}}{(2)} + \frac{\mathrm{b}}{(2)^2}$$

$$0.001 = \frac{2\mathrm{a} + \mathrm{b}}{(2)^2}$$

$$0.001 * (2)^2 = 2a + b$$

$$b = 0.004 - 2a$$

$$b = 0.004 - 2a$$

$$b = 0.004 - (2 * 0.00042297)$$

$$b = 0.004 - 0.00084595$$

b = 0.00315405

The values of constants of a and b were also calculated to fit the relationship between water depths and K values using Mathematica software (algebra) which the parameter values were provided (Fig 4.3). The figure 4.3 fitting a reciprocal quadratic relationship between wave attenuation and water depth, in comparing to figure 4.2, this gives a simple curve that make the relationship more flexible through the values of 0.15 and 2m.

# Fitting second order reciprocal function

## Define two points to fir - in this case depths of 0.15m and 2.0m, and K = 0.143 and 0.001

```
In[11]:= k1 = 0.143; x1 = 0.15; k2 = 0.001; x2 = 2.0;
```

## Fit second order reciprocal to go through points - parameters are aa and bb

```
In[14]:= sol = Solve[{k1 == aa/x1 + bb/x1^2, k2 == aa/x2 + bb/x2^2}, {aa, bb}]

Out[14]= {{aa → 0.000422973, bb → 0.00315405}}

In[19]:= a = First[aa/. Sol]

Out[19]= 0.000422973

In[20]:= b = First[bb/. Sol]

Out[20]= 0.00315405
```

Plot K as a function of depth

```
Plot [a/x+b/x^2,{x, 0.1, 3}]
```

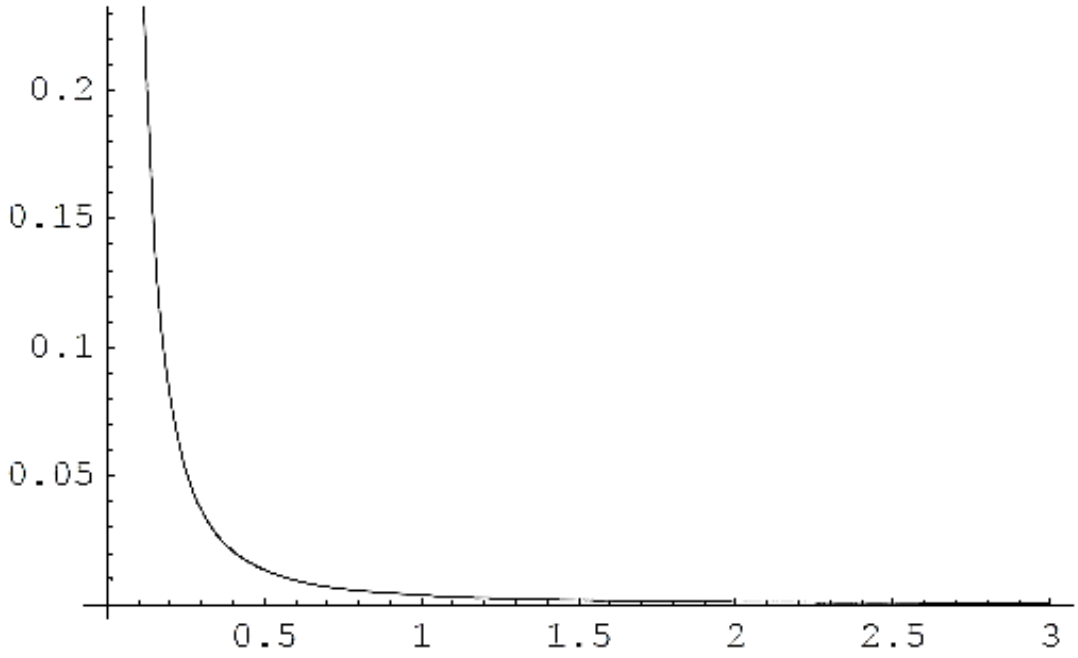


*Out[23]=* -Graphics-

Plot log (to base 10) K as a function of depth

*In[32]:=* **Plot [Log[10, (a / x + b /x^2)], {x, 0.1, 3}]**

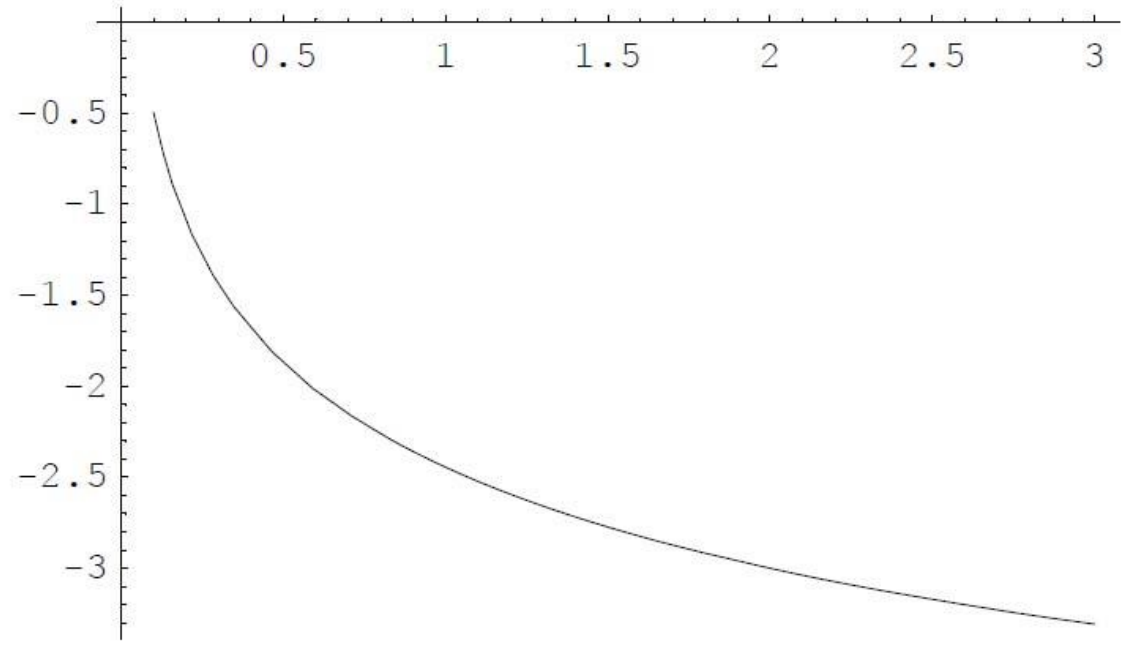


*Out[32]=* -Graphics-

Plot e^K as a function of depth

```
In[28]:= Plot[Exp[-(a / x + b / x^2)], {x, 0., 3}, Plot Range → All]
```

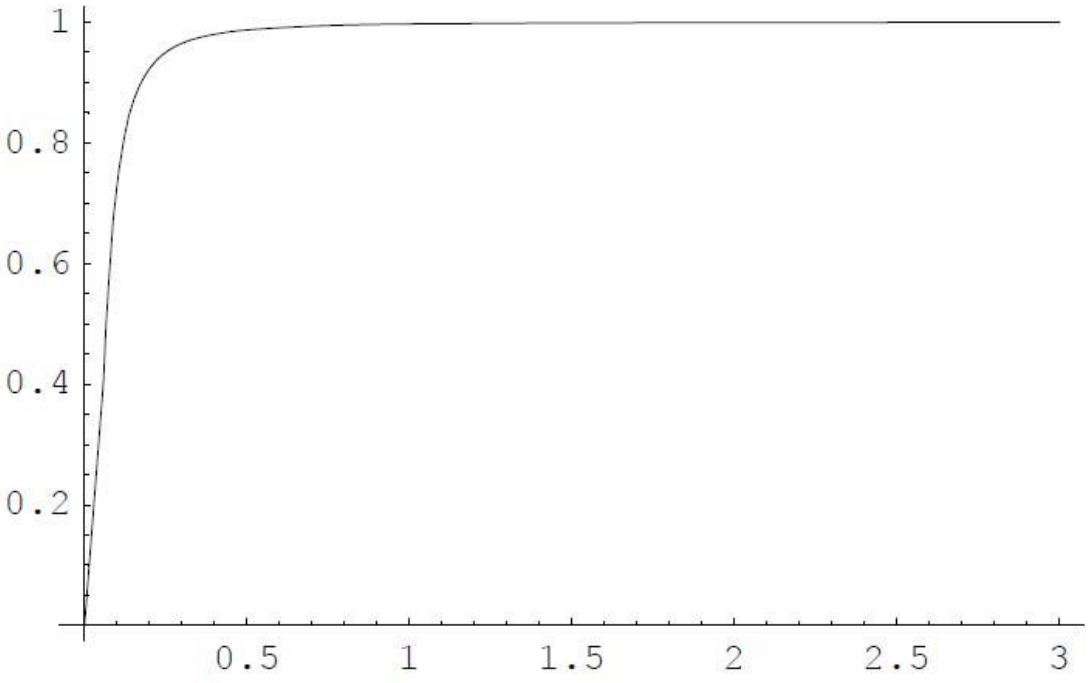


```
Out[28]= -Graphics-
```

Plot 1-(e^K)^100 (i.e. the reduction in wave energy) as a function of depth

```
In[38]:= Plot[1.-Exp[-(a/x+ b/x^2)]^100,{x, 0., 3},PlotRange→All, AxesOrigin→ {0., 0.}]
```

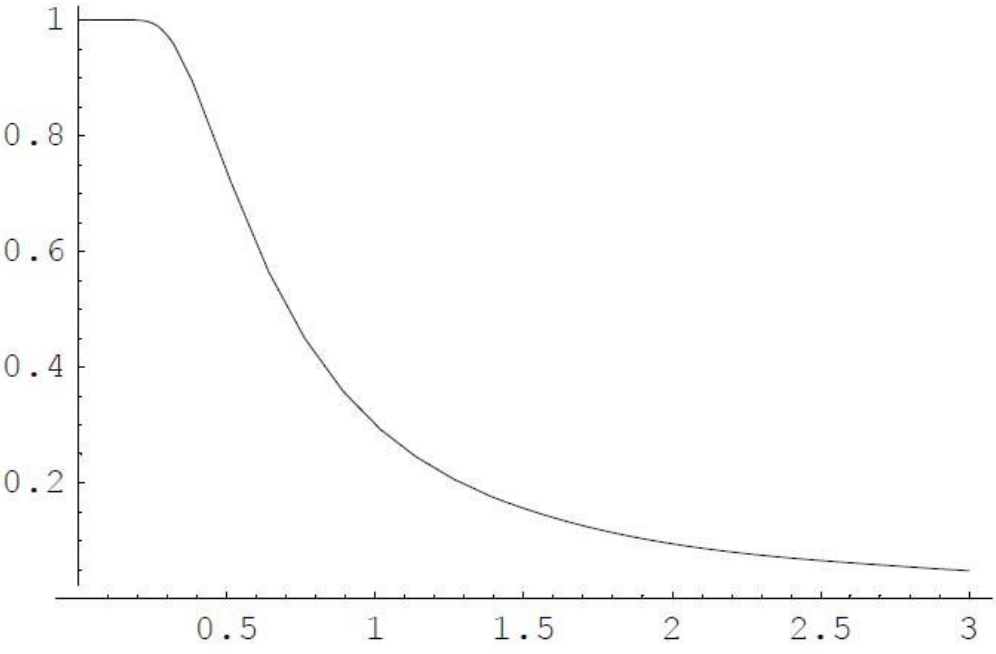


```
Out[38]= -Graphics-
```

Fig 4.3. Fitting second reciprocal function to go through points parameter are a and b.

Once we calculated the value of (a) and (b) we used different value of water depth to calculate a value of K and multiply wave height by ($e^{-k}$) for 1 m section and used this prosses along transect to get a series of K values in each 1 m along transect by using the equation Number (3) above.

4.2.2 The validation of wave dissipation model

The model of wave dissipation was validated using transect data conducted by Moller et al., (1999), including water depths and distance along transect in the Outer, Middle and Inner stations (Fig 4.4). The data was obtained from Moller et al., (1999) including the highest and lowest water depths; and the distance across sandflat and low marsh (Table 4.1).

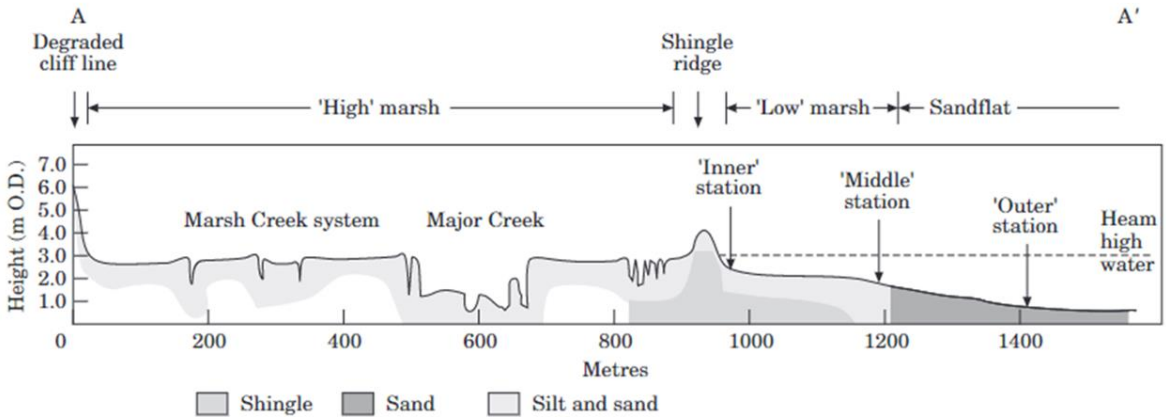


Fig 4.4 Transect conducted by Moller including three station Outer, Middle and Inner station, Moller et al., (1999).

Moller et al., (1999) data in figure 4.8 were used in (Tables 4.1; 4.1), obtain from their figure (Fig. 6, Moller et al., (1999) and were quoted in our above-mentioned tables, our data were compared as a range of water depths in Moller with a single wave energy dissipation from our model, presumably based on a single water depth. We assumed there is a linear gradient across the sandflat for 197 m, and that there is a constant gradient across the low marsh for 180 m.

The model is assuming the seabed is straight line (slopping) from Inner to Middle station across low marsh and from Middle to Outer station across sandflat. Using the Model to predict wave dissipation across low marsh from Inner to Middle station through the highest and lowest water depths. Similarly, using the Model to predict wave dissipation across

sandflat from Middle to Outer station through the highest and lowest water depths (Table 4.1).

The finding shows that wave energy dissipation reduces through the highest water depths across sandflat by around 18 %, and 67 % across low marsh, while through the lowest water depths across sandflat by around 47 %, and 99 % across low marsh (Figs 4.5 and 4.6).

Table 4.1 Transect conducted in this study using Moller et al., (1999), including location, length, habitats, tidal height, and the range of water depths throughout the whole transect at Outer, Middle and Inner station.

| | | | | | The range of water depths (m) | | | |
|---|---|---|---|---|---|---|---|---|
| | Location | Length (m) | Habitats | Tidal height m (ODN) | | Outer station | Middle station | Inner Station |
| Data in this study using Moller et al., (1999) | Stiffkey saltmarsh | 197 | Sandflat | (3) in the Outer station | The highest water depth | 1.75 | 1.4 | 0.9 |
| | | 180 | Saltmarsh (low marsh and stopping at shingle ridge) | | The lowest water depth | 0.91 | 0.6 | 0.2 |

Comparing our prediction of wave energy dissipation (Figs. 4.5 and 4.6) with Moller measurements (Fig 4.8) indicated that our model underestimates wave energy dissipation

across sandflat, and overestimates wave energy dissipation on low marsh (Table 4.2).

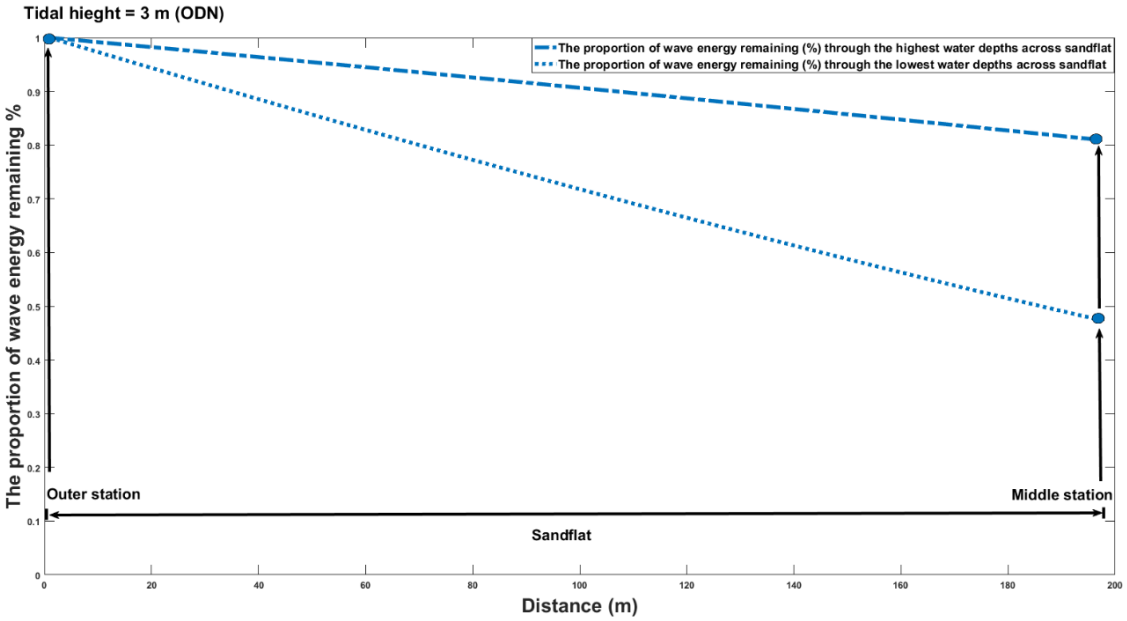


Fig 4.5 The two lines are the wave energy remaning from Moller corresponding to water depths 1.75 m in the Outer station and 1.4 m in the Middle station, and in the lowest tide corresponding to water depths 0.91 m in the Outer station and 0.6 m in the Middle station.

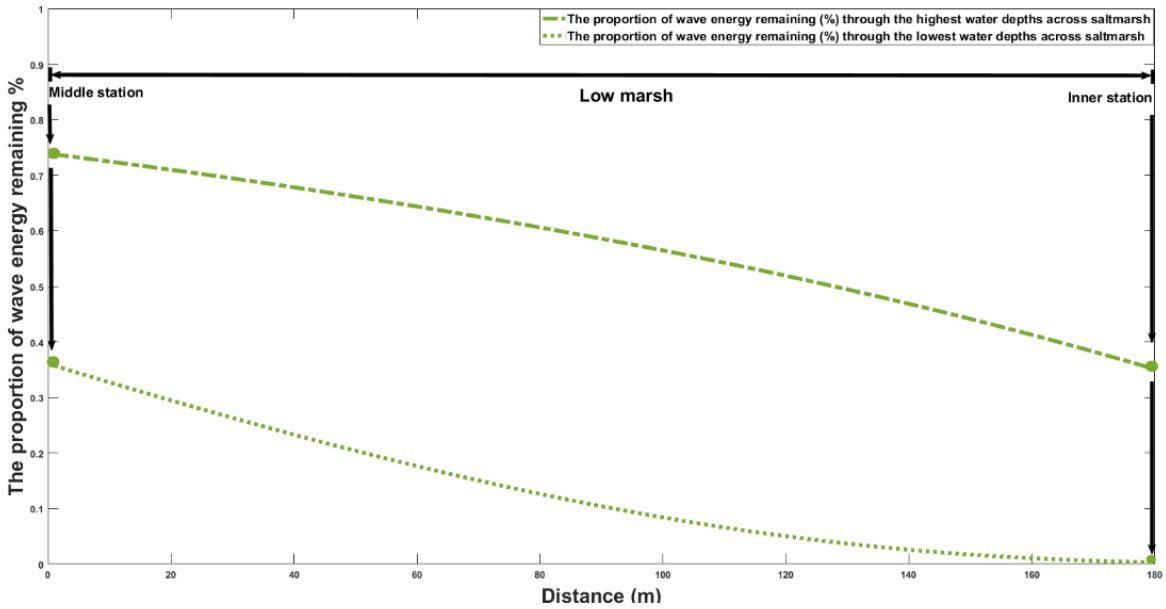


Fig 4.6 The two lines are the wave energy remaining from Moller corresponding to water depths 1.4 m in the Middle station and 0.9 m in the Inner station, and in the lowest tide corresponding to water depths 0.6 m in the Middle station and 0.2 m in the Inner station.

However, as we assuming that the seabed is straight line (sloping) between three stations, the actual shape of the seabed is different which is convex across sandflat and concave across low marsh (Figs 4.8 and 4.10). The depth of water would show an exponential decline, as a fixe proportion of the energy is dissipated every metre, the water is getting gradually shallower, and the rate of dissipation increases so the lines could be linear, concave or convex, depending upon the slope of the seabed. This shape of the seabed appears to make differences between our prediction and Moller measurements. So, in Moller measurements, there is more dissipation of wave energy across sandflat than our prediction. Across low marsh, the wave energy dissipation is less than our prediction,

In terms of elevations across sandflat and low marsh, Moller et al., (1999) does not give the exact elevations a long transect for three stations in her study which cause difficulties to replicate exact elevations in the Outer, Middle and Inner stations. So, we have done some works at Stiffkey by plotting transect with real elevations across sandflat and low marsh (Fig 4.9) showing that the elevation at outer station appears to be around 1.5 m OD (Fig 4.10). This indicted that the transect might be a reasonable approximation than Moller's transect because it starts with right elevation around 1.5 m OD in the outer station.

At Stiffkey, marsh platform is at 2.75 m OD (Table 3.1, chapter 3), and the tidal heights are between 2.6 and 3 m OD and the maximum is 3.3 m OD, so that will be corresponding to the maximum 60 cm of water depth across saltmarsh platform which indicated that the water is very shallow on the saltmarsh even in the highest tide measured by Moller. Contrary to this situation, during storm surge event at Stiffkey the tidal heights were between 4.76 to 5.34m OD with 2.59 m maximum of water depth across saltmarsh platform (Spencer et al., 2015). Using the model to predict wave energy dissipation in real elevations (Fig 4.10) showing that wave energy reduces by around 38 % across sandflat, and 86 %

across saltmarsh (Fig 4.11), but the wave energy dissipation in real elevations is substantially different comparing with wave energy dissipation when the seabed seen to be straight line (sloping).

Comparing wave energy dissipation between the seabed to be straight line and (real elevations conducted in (Fig. 4.10 and 4.11) and Moller's transect . In the case of vegetation presence, the wave energy dissipation will be different, but if we look at the effective of water depth on wave energy dissipation where water depth goes from a maximum of 60 cm in lower study (Moller el at., 1999), to 2m above saltmarsh platform in deep flume (Moller et al,. 2014). The differences between vegetation and non-vegetation are going to be very small when water depth reaches 2 m above marsh platform (Moller et al., 2014; Forysinski, K., 2019; Temmerman, *et al.*, 2023). So, the model appears to be a reasonable approximation of the relationship between water depth and wave energy dissipation across sandflat and saltmarsh.

Table 4.2 Comparison of wave energy dissipation across sandflat and across saltmarsh on the highest and lowest water depths between our Model assuming seabed straight line (slopping) between Outer, Middle and Inner stations; and Moller study (Moller et al., 1999).

| | Zone | Water depths (m) | | Moller study, Fig 6, Moller et al (1999). | Wave dissipation Model in this study assuming seabed straight line (sloping) between three stations. |
|---|---|---|---|---|---|
| The wave energy dissipation % | Sandflat | The highest water depths | 1.75 – 1.4 | 20 – 30 % | 18 % |
| | | The lowest water depths | 0.91 – 0.6 | 40 – 60 % | 47 % |
| | Low marsh | The highest water depths | 1.4 – 0.9 | 50 – 60 % | 67 % |
| | | The lowest water depths | 0.6 – 0.2 | 99 % | 99 % |

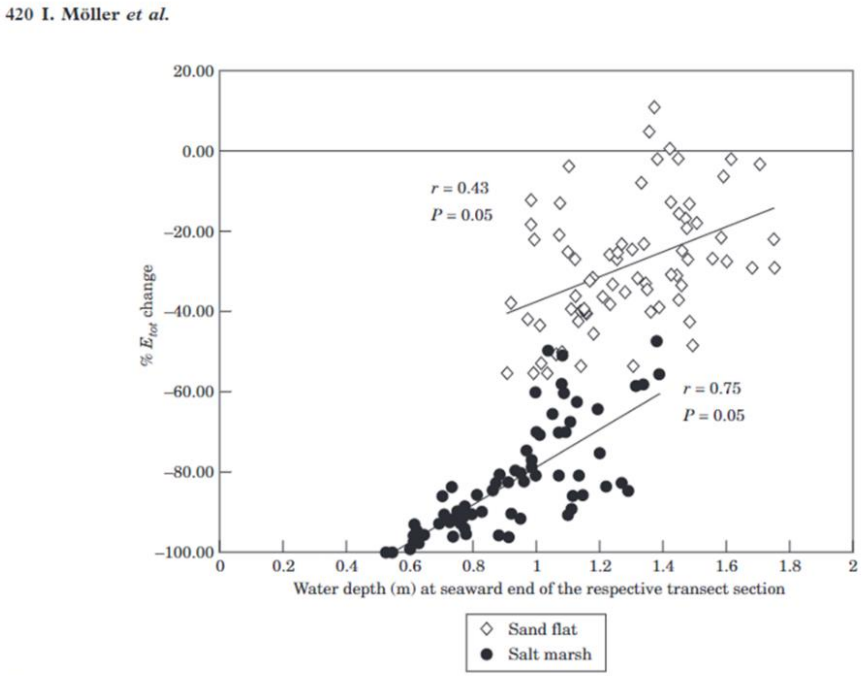


FIGURE 6. Relationship between wave energy attenuation and water depth for the sand flat (over transect section between outer and middle station) and salt marsh (middle to inner station).

Fig 4.7 The reduction of wave energy across sandflat (from outer to middle station), and low marsh (from middle to inner station) obtained from Moller et al., (1999), Fig 6 in their study.

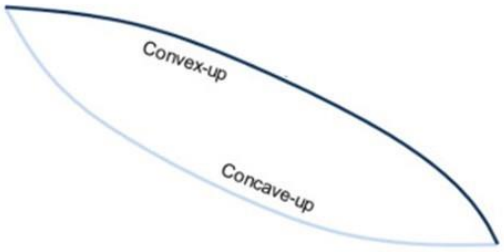


Fig 4.8 The shape of the serface for both convex and concave .


Fig 4. 9 Locations of transects across sandflat and low marsh. Blue line a transect conducted in this study from North to South with grid reference TF96457 45231 to TF95487 43934, and red line

a transect from Northeast to Southwest conducted by Moller et al., (1999).

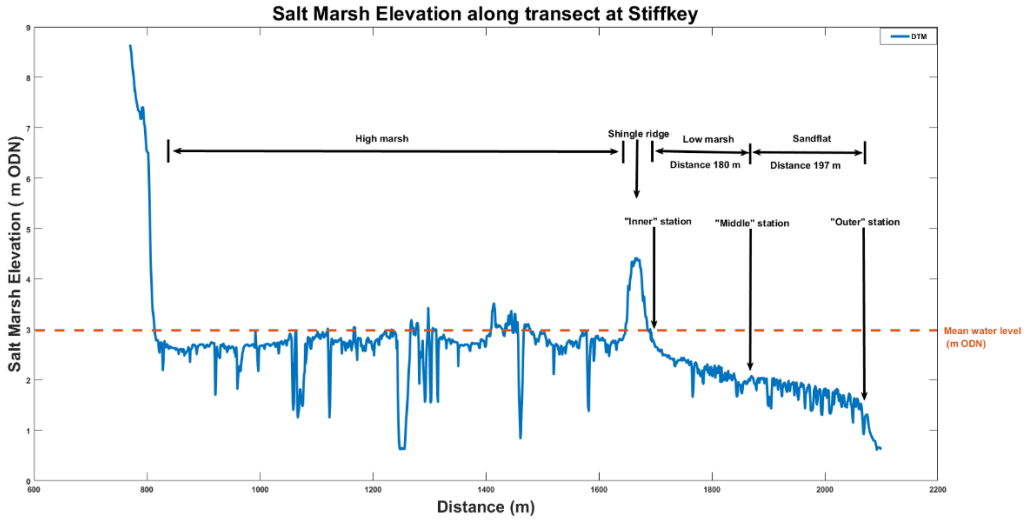


Fig 4.10 Elevation along transect across sandflat and low marsh and stopping at shingle ridge at Stiffkey.

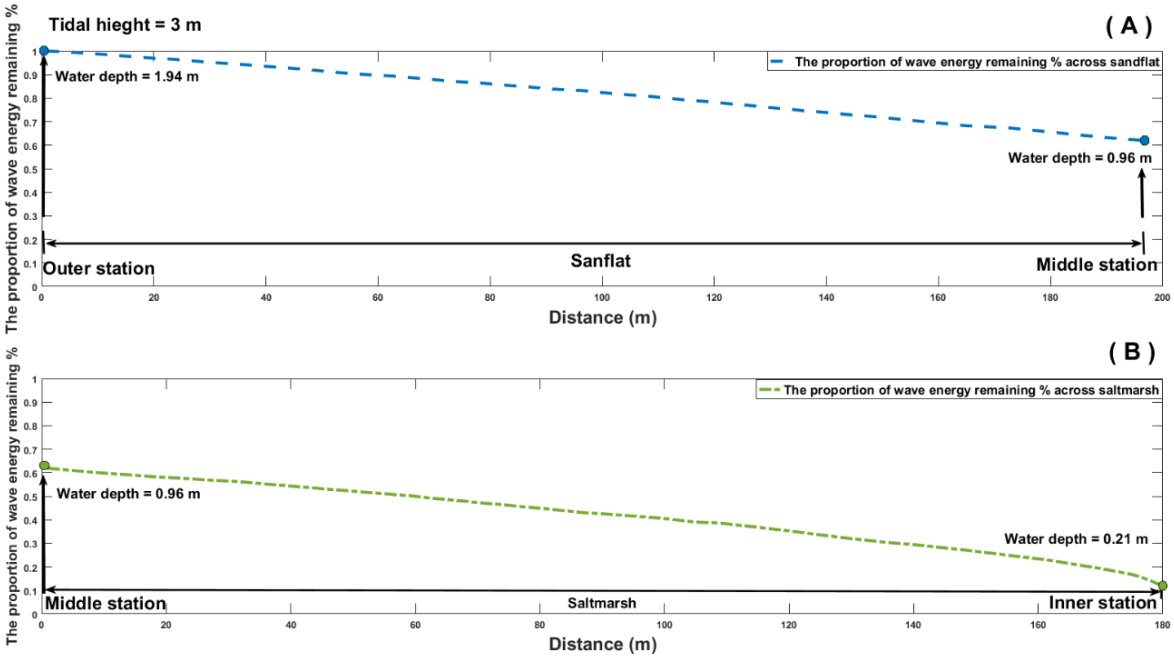


Fig 4.11 wave energy remaining in the real elevations; (A) wave energy remaining across sandflat corresponding to water depth at 1.94 m in the outer station and 0.96 m in the middle satation. (B) wave energy remaining across saltmarsh corresponding to water depth at 0.96 m in the middle station and 0.21 m in the inner station.

### 4.2.3 Using the model for four sites around the UK

Four sites were chosen based on elevation details and relative tidal heights of saltmarshes (see Table 3.1 and Fig 3.29 in chapter 3), most of saltmarshes in South and East England at or below MHWS, and these marshes appear to be in the part of the UK where the flooding is the biggest concerned (see result in chapter 3), while saltmarshes in the North and North West of England are above MHWS which indicated that these marshes may not be vulnerable to flooding during storm surge events. From this conclusion, the marshes were chosen to span the range of the marsh in order to predict wave dissipation from typical mature marshes in South and East England to rather high marshes at Llanrhidian and Morecambe Bay with high cliff and with a shingle ridge at Morecambe Bay and Stiffkey respectively thrown in for additional interest. (Fig 4.12).

Elevation for these saltmarsh sites was derived from DTM data using the techniques described in chapter 2 and 3. Transects were located at each site to run from the intertidal mud/sandflat across the saltmarsh to the landward marsh edge or the seawall if this formed the landward limit of the marsh. Spatial resolutions ranged from 25 cm to 1 m depending on the availability of data (see method in chapter 2, Table 2.1). Spatial resolutions for Stiffkey, Dengie and Llanrhidian was 1m, whereas it was 25 cm for Morecambe Bay. Each transect was set up to be across saltmarsh, mudflat and the edge of marsh (embankment) with single direction, and upon the tidal height direction. The Stiffkey and Llanrhidian transects ran from the north to south the Dengie transect ran from East to West. In Morecambe Bay transect ran from southwest to northeast.


Fig 4.12 a map of four saltmarshes were undertaken in this study including Stiffkey, Dengie, Llanrhidian and Morecambe Bay marshes. (The UK Digimap, https://digimap.edina.ac.uk/ ). They are at different scales but the grid squares are 1km in all cases.

### 4.2.4 The prediction of wave energy dissipation for four saltmarshes

We have used water depth as a function of wave dissipation a long transects to simplify measurements of wave dissipation. Water depths along transect were calculated by subtracting marsh surface elevations along transect from the water level elevation during storm surges. Water level during surges in storms was based on the two largest surge storm events that have occurred in the UK in recent history (1953 and 2013, see table 4.1). Water height was set for each transect to be at MHWS, 1 m above MHWS, 2 m above MHWS and at the elevation observed during storm surge events at that site if this was available. The water depths were identified each point of elevation as we mentioned in previous section (4.2.3). The transect at Stiffkey was 1200 m long, running from north to south, from grid reference TF96500 44000 to TF96500 45200 (Fig 4.5a). At Dengie, the transect ran from east to west for 600 m from grid reference TM02000 03000 to TM02000 03600 (Fig 4.3a). At Llanrhidian the transect ran from south to north for 1300 m from grid reference SS49500 93000 to SS49500 94300 (Fig 4.4a). At Morecambe Bay, the transect was running from northeast to southwest for 1500 m from grid reference SD47900 73000 to SD46000 71000 (Fig 4.5a).

From previous details, wave dissipation was predicted in each point from sea edge moving steeply with different elevation to mid/high marsh including marsh vegetation, shingle ridge, creeks, ponds, embankment and (sea wall/levee if is occurred). We used an equation to predict wave dissipation based on elevation for each pixel along transect by using water depth as a function of wave dissipation, using equation number (3).

Table 4.3: Water height above mean high water spring in the 1953 and 2013 North Sea storm surges. Water levels during these surges are taken from Spencer et al (2014). Estimates of MHWS at these sites are based on UK tide tables (NDL, 2017), except those indicated by an asterisk (*) where elevations of MHWS are obtained from Mossman et al (2011).

| Location | 2013 max (m ODN) | 1953 max (m ODN) | MHWS (m ODN) | Water height above MHWS 2013 (m) | Water height above MHWS 1953 (m) |
|---|---|---|---|---|---|
| Stiffkey | 5.34 | 4.57 | 2.81* | 2.53 | 1.76 |
| Blakeney | 6.30 | 6.07 | 2.82* | 3.48 | 3.25 |
| Great Yarmouth | 3.32 | 3.30 | 0.9 | 2.42 | 2.4 |
| Lowestoft | 3.26 | 3.44 | 0.9 | 2.36 | 2.54 |
| Southend-On-Sea | 4.10 | 4.60 | 2.7 | 1.4 | 1.9 |

### 4.3 Results

At Stiffkey, there is an inactive shingle ridge with a height of about 4m ODN (Fig 4.13a) which separates an outer lower marsh that lies between MHWN and MHWS from a high marsh platform that lies at around MHWS (Table 3.1, see chapter 3). When the water level is at MHWS, there is considerable wave energy dissipation across the outer marsh. When water level is at 1m above MHWS there is some wave energy dissipation across the outer marsh, but as the water level is still below the crest of the shingle ridge, no wave energy propagates beyond this. For water level 2m above MHWS and during storm surges, the crest of the shingle ridge is submerged, and propagation of waves occurs across the whole marsh, although some wave energy dissipation does occur across the marsh platform (Fig 4.13b). Although wave energy was dissipated through the shingle ridge at around a distance of 250 m wave dissipation decreased considerably when water height at its peak (5.34 m ODN) during storm surge (Fig 4.13a, b; table 4.1). Additionally, wave energy is slightly affected through shingle ridge when water height is at 2 m above MHWS and during storm surge. During storm surge even the waves seems to be dissipated much lower through saltmarsh at Stiffkey.

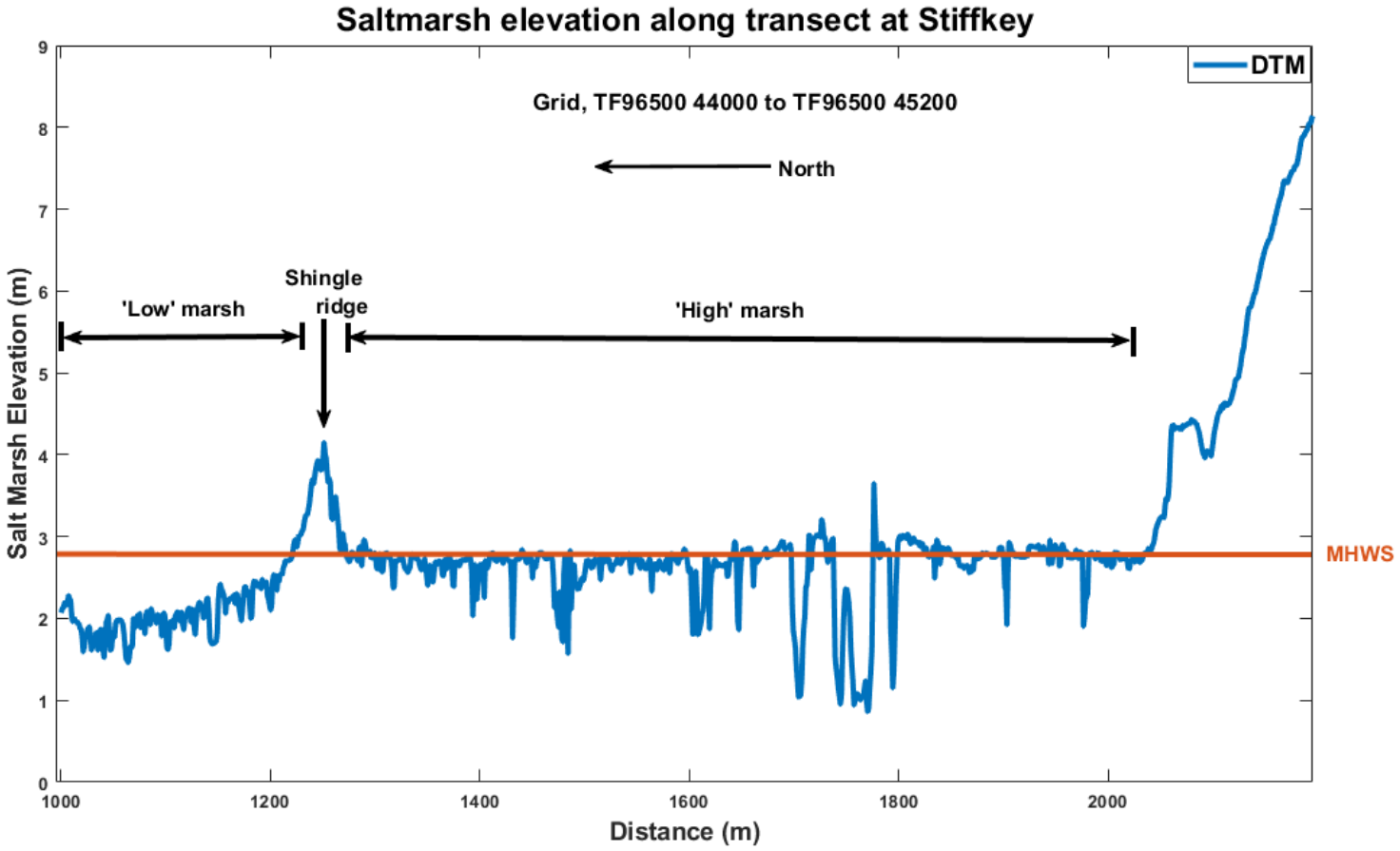


Fig 4.13a Elevation of the DTM along transect across salt marsh at Stiffkey used to predict wave energy dissipation. Red line indicates the level of MHWS.

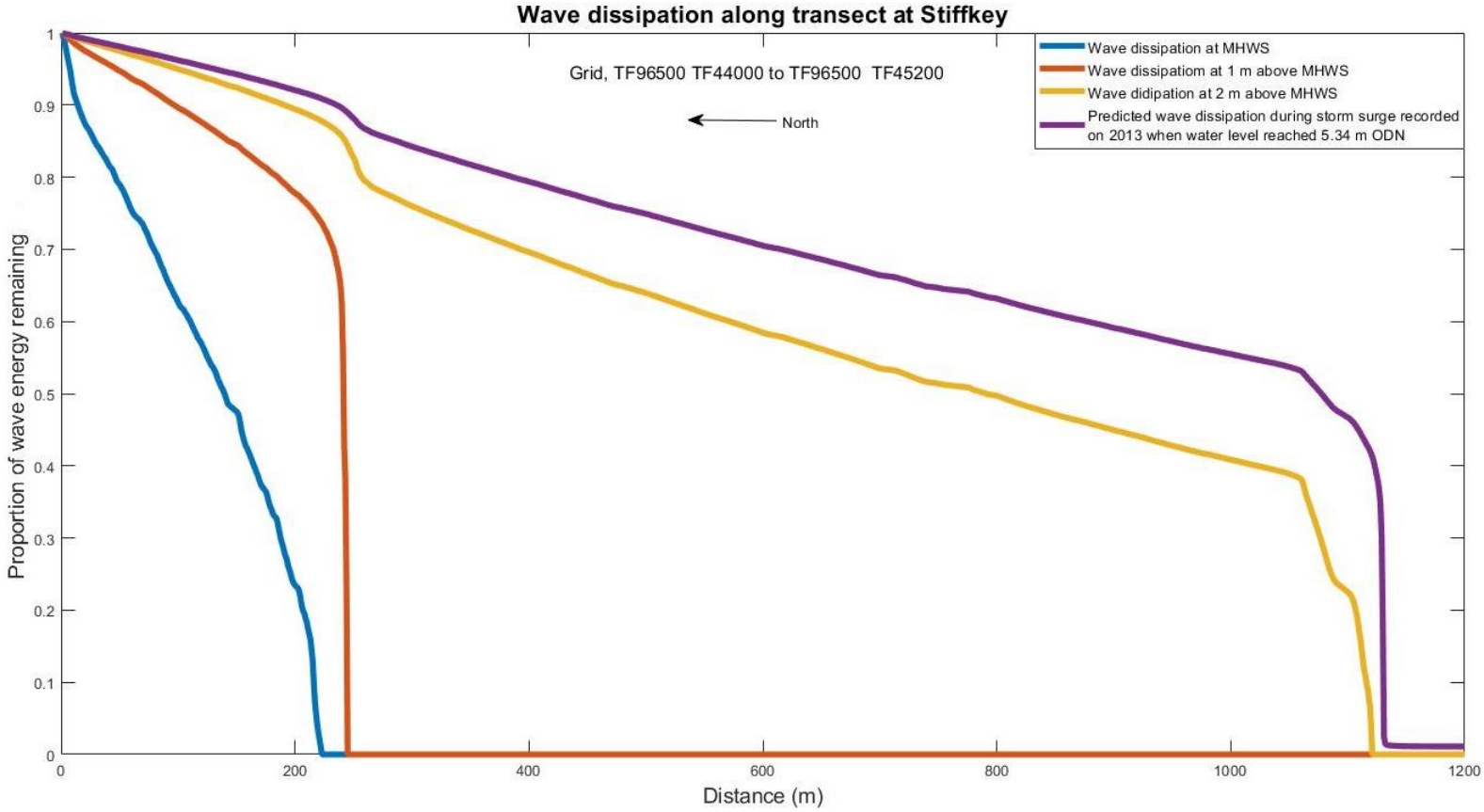


Fig 4.13b Wave energy dissipation across the saltmarsh at Dengie for water levels corresponding to MHWS, and 1 and 2m above MHWS, and during storm surge event in 2013 when water level reached at 5.34m ODN.

At Dengie, the level of water at MHWS is 2.57 m ODN, which is just above the marsh platform at an elevation of 2.48 m ODN (Table 3. 1, see Chapter 3). So, when the water level is at MHWS, wave energy dissipation occurs on the outer marsh (Fig 4.14a, b). Once the water level is at 1m above MHWS, waves are able to propagate across the marsh. Once water level is at 2m above MHWS, which corresponds approximately to the level of the 1953 storm surge in this area (Table 4.3), only limited dissipation of wave energy occurs on the marsh platform, and the majority of wave energy reaches the seawall the landward edge of the marsh, which is at about 5m ODN, 2.32m ODN above the level of MHWS. In our simple model, there is no propagation of waves beyond the seawall (Fig 4.14a, b). However, if wave height was substantial during a storm surge that was at 2m above MHWS, it is likely that waves could overtop the sea wall which would be approximately 30 cm above the still water level.

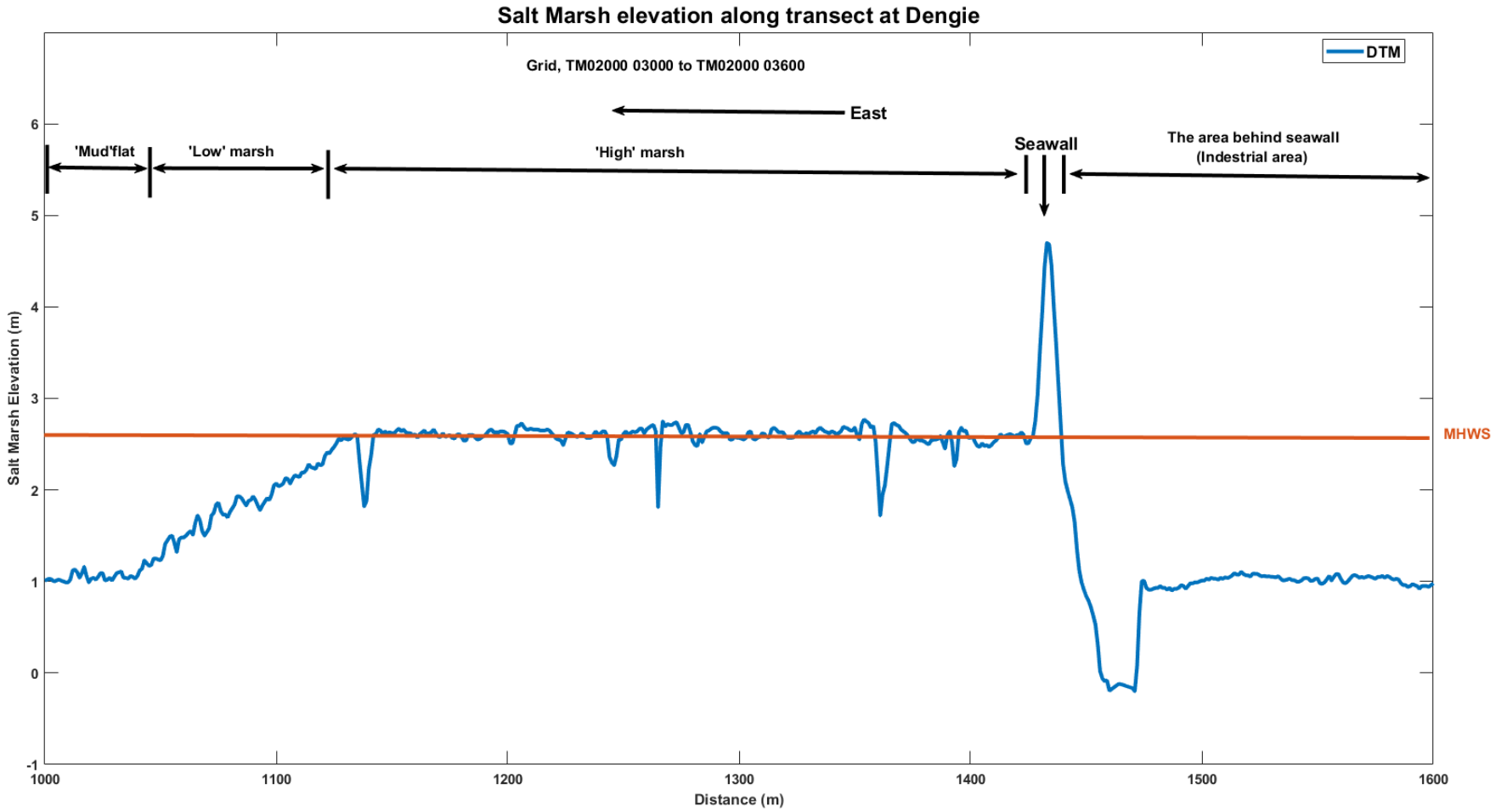


Fig 4.14a Elevation of the DTM along transect across salt marsh at Dengie used to predict wave energy dissipation. Red line indicates the level of MHWS.

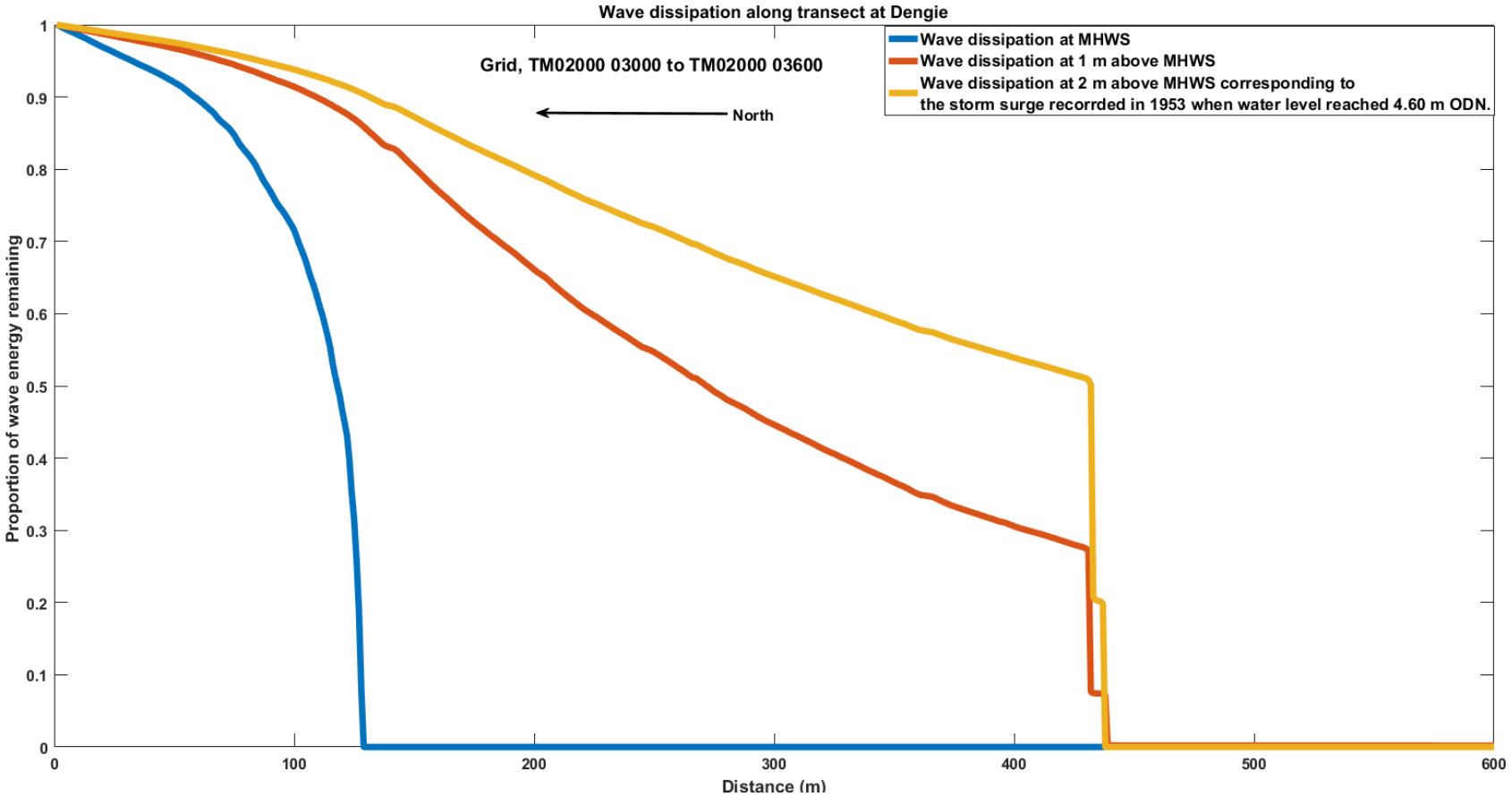


Fig 4.14b Wave energy dissipation across the saltmarsh at Dengie for water levels corresponding to MHWS, and 1 and 2m above MHWS.

At Llanrhidian, marsh platform elevation is at 4.6 m ODN, which is 0.7 m higher than MHWS at 3.9 m ODN, meaning that the marsh is very effective in reducing wave energy (Table 3.15, see chapter 3). There is a cliff that rises to a height of about 5.3m ODN (Fig 4.15a) which lies at 1.4 m above MHWS and separates an outer lower marsh that lies slightly above MHWN. In the first few meter's wave dissipation increases significantly when water level is at MHWS along transect. When water level is at 1m above MHWS there is much wave energy dissipates across the outer marsh, as the water level is still below the crest of the cliff. Once the level of water is at 2m above MHWS, the crest of the cliff and ridge is submerged, and waves are able to propagate across the whole marsh, and some wave energy is dissipated across the marsh platform (Fig 4.15a, b). As waves are propagated across the whole marsh when water level is at 2 m above MHWS, wave energy reduces gradually along the transect.

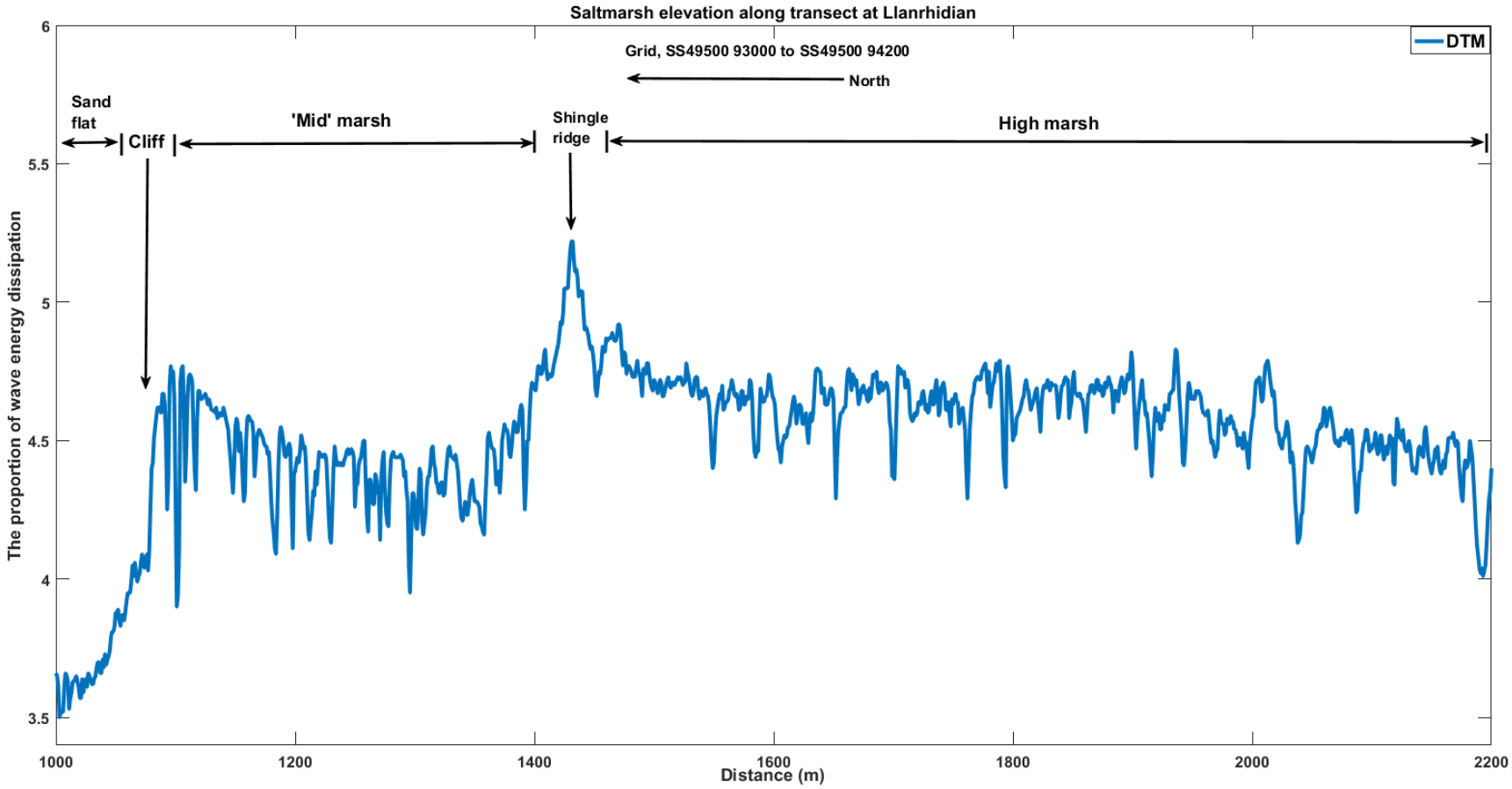


Fig 4.15a Elevation of the DTM along transect across salt marsh at Llanrhidian used to predict wave energy dissipation. Red line indicates the level of MHWS.

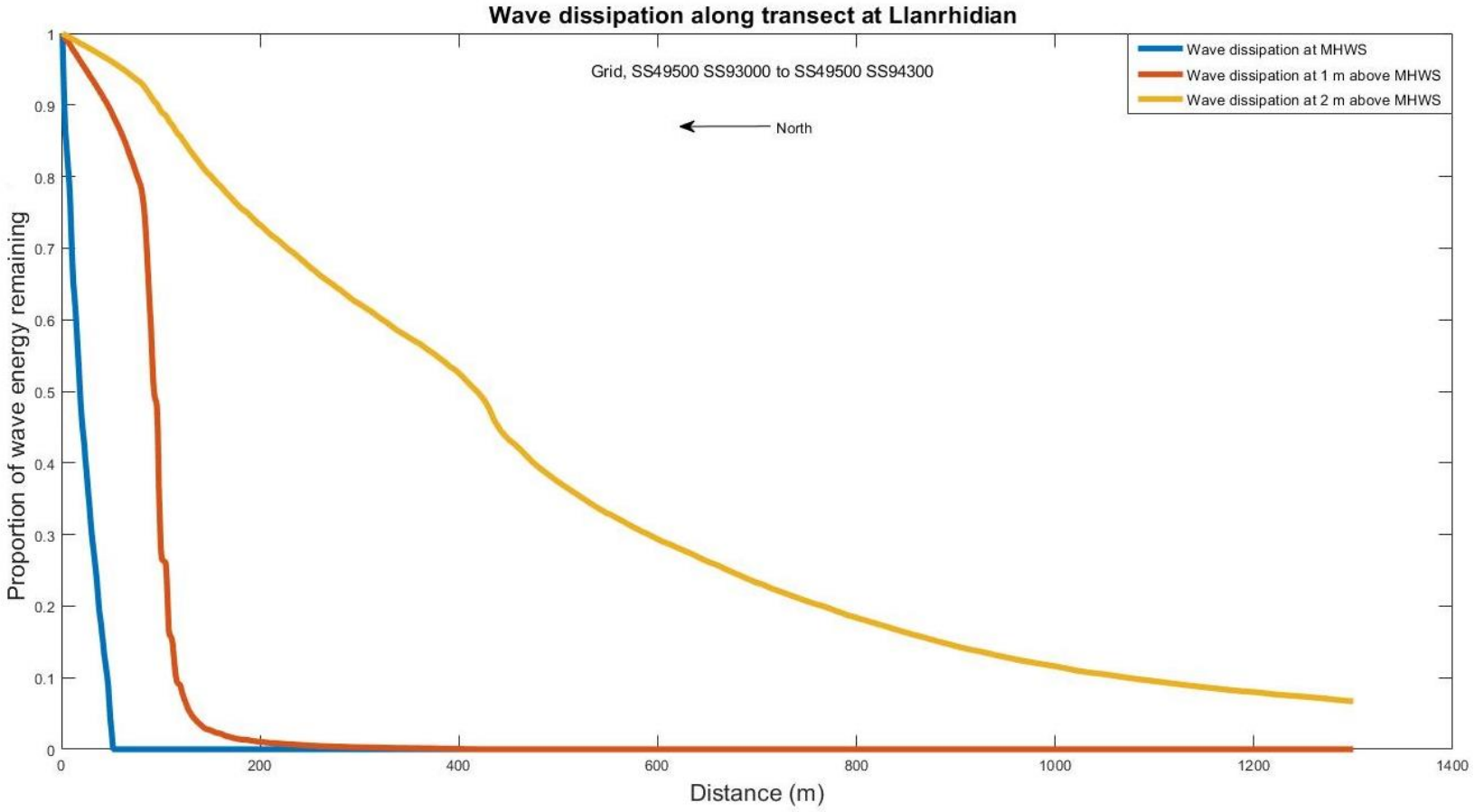


Fig 4.15b Wave energy dissipation across the saltmarsh at Llanrhidian for water levels corresponding to MHWS, and 1 and 2m above MHWS.

At Morecambe Bay, there is a large cliff in the front of the marsh separating sandflat from pioneer zone with a height of about 5.8 m ODN which is 1.2 m above MHWS and 0.47 m above marsh platform (Fig 4.16a). The marsh platform in Morecambe Bay is at 5.33 m ODN, which is 0.73 m higher than MHWS at 4.6 m ODN (Table 3.1, see chapter 3). Once water level is at MHWS there is considerable wave energy dissipation close to the cliff in the front of the marsh. When water level is at 1m above MHWS, there is much waves dissipation occurred as water level is still below the crest of the cliff (Fig 4.16a, b). Once the level of water is 2m above MHWS, the crest of the cliff is submerged, and waves are able to propagate, but does not exceed the low marsh and most of wave energy dissipates across the mid and high marsh (Fig4.16b).

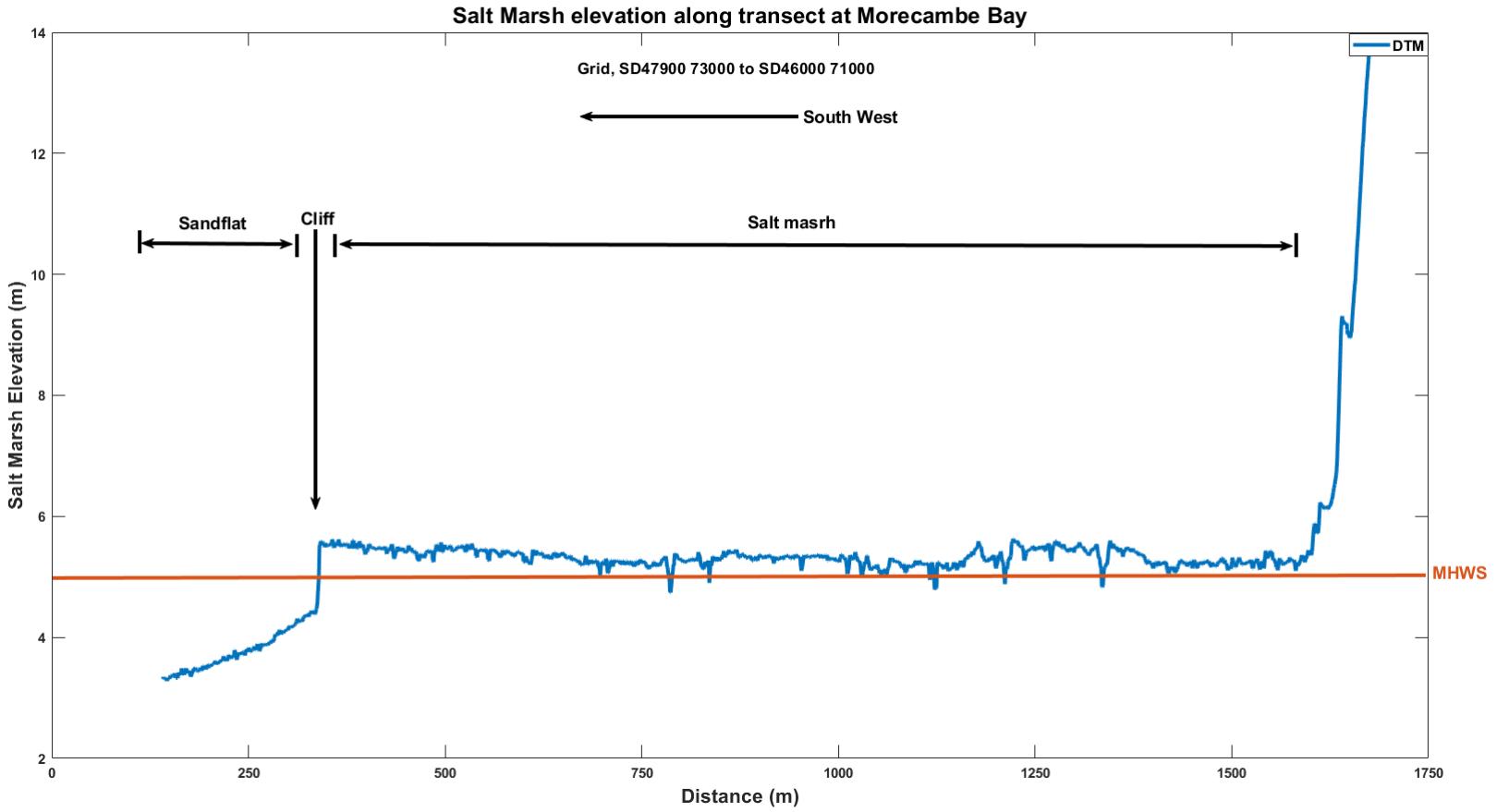


Fig 4.16a Elevation of the DTM along transect across salt marsh at Morecambe Bay used to predict wave energy dissipation. Red line indicates the level of MHWS.

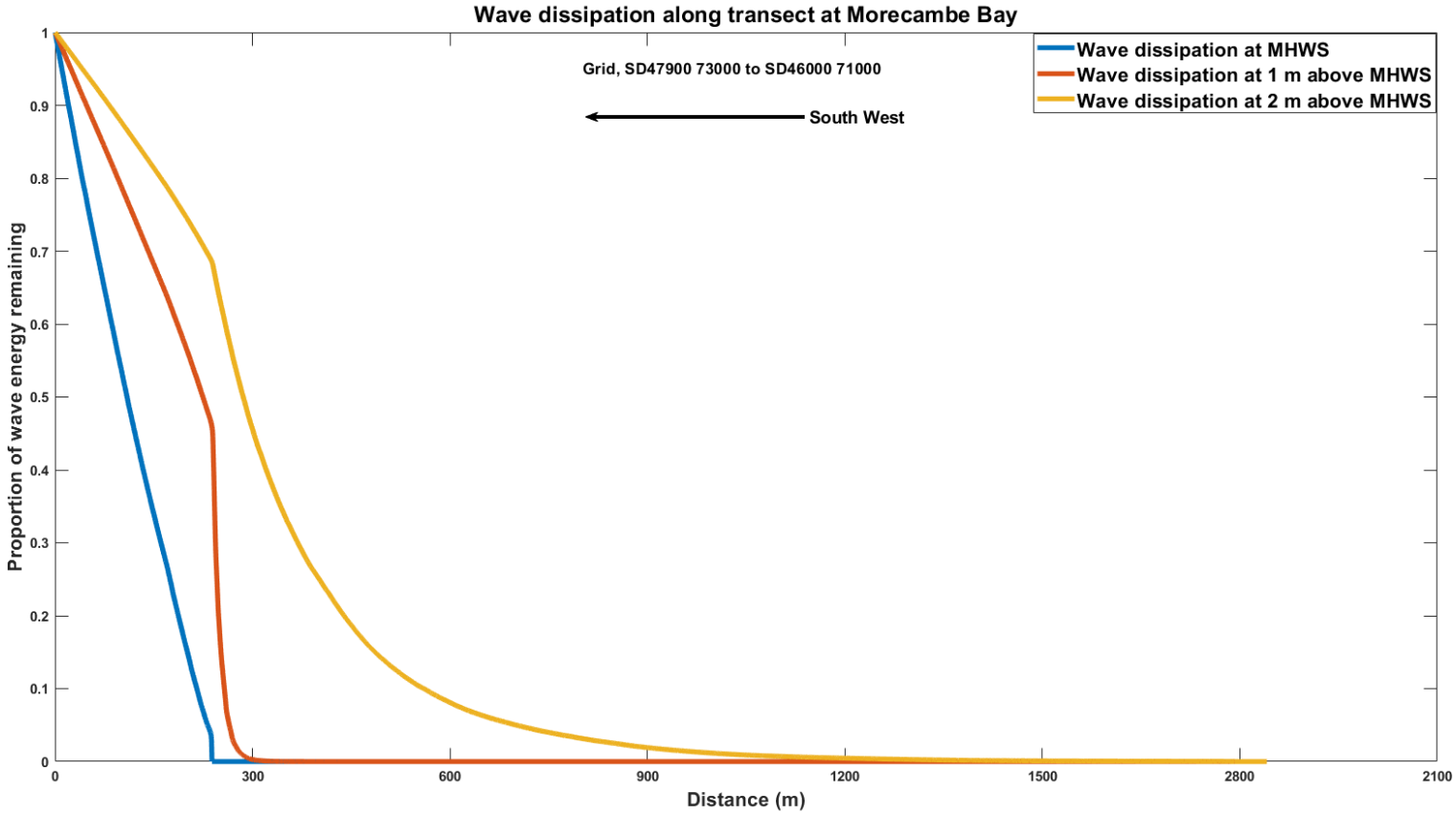


Fig 4.16b Wave energy dissipation across the saltmarsh at Morecambe Bay for water levels corresponding to MHWS, and 1 and 2m above MHWS.

## 4.4 Discussion

The wave energy dissipation is much greater over a short distance at the front of the marsh during normal condition when water level at MHWS. This occurs because all four of these marshes lie around and above MHWS, with marsh platform at Stiffkey and Dengie lying around the level of MHWS, while at Llanrhidian and Morecambe Bay they lie above MHWS. Therefore, wave dissipation greatly affected by the elevation of water over the marsh when water level at MHWS.

At Stiffkey, when water level reaches 1m above MHWS, waves energy dissipation occurs largely at the shingle ridge because the height of the water is lower than its crest. But some dissipation does occur across the outer lower marsh between shingle ridge and mudflat of about a few tens of meter. The highest of water depth appears to be at 1.06 m ODN above the marsh and then deceases across the lower marsh until the shingle ridge is reached. So, the reduction of wave energy is attributed to the depth of water (Fonseca and Cahalan, 1992). In the marsh pioneer zone, steep gradient can reduce wave energy but is not effective during the highest high of spring tides. During storm surges, the greatest water depth reached is about 2.06 m ODN above the marsh and this then decreases across the whole marsh. Although the waves are propagated across the whole marsh, some dissipation does occurs, but as water depth decreases the wave energy reduces across the marsh (Möller and Spencer, 2002, Yang *et al.*, 2012).

At Dengie, when the level of water reaches 1m above the level of MHWS, although waves are propagated across the whole marsh, wave dissipation still occurs even though there are no obstacles through salt marsh surface as a cliff or a shingle ridge (Figs. 4.14a, b), and the greatest water depth is at 1.09 m ODN above the marsh and it then decreases across

the whole marsh which confirms that the reverse association between attenuation of waves and the depth of water is more significant across the salt marsh (Möller, *et al.*, 2014). During storm surge events, the level of water overtops the whole marsh, and most of the energy reduced largely by the seawall with no propagation beyond the seawall. This may be due to the height of the seawall, which is 0.52 m ODN higher than the water level during a storm. However, the seawall could be broken or damaged by waves (Owen, 1980) when the water level is overtopping the crest of the seawall (Möller *et al.*, 2014).

At Morecambe Bay, the greatest water depth is 1.27 m ODN above the marsh when the level of water is at 1 m ODN above the level of MHWS. The wave energy dissipates considerably, but this is clearly due to the presence of a large cliff at the front of the marsh (Möller and Christie, 2019, Möller, Kudella *et al.*, 2014) with a height of about 5.8 m ODN. The waves do not propagate across the marsh because the water level does not reach the crest of the cliff and most of the wave energy reduces before reaching the cliff. However, during storm surge when the greatest depth of water is at 1.57m ODN, the water level reaches the crest of the cliff and waves propagate on the lower marsh and a part of the middle marsh. Across the rest of the marsh there is no water to be dissipated.

Wave dissipation at Llanrhidian, occurs similarly to waves dissipation at Morecambe Bay when the level of water reaches 1m above the MHWS level. However, at Llanrhidian, during a storm surge, wave dissipation occurs across the outer marsh before the cliff when the greatest of water depth is 1.3 above the marsh platform, and the cliff does not reduce wave energy because the water overtops the crest of the cliff (Loder *et al.*, 2009). Moreover, although waves are propagated the dissipation of waves are occurred across the whole marsh, but as water level decreases wave energy reduces.

Although, the cliff is effectively reducing wave energy significantly when the water level is at 1 m above MHWS, its contribution is much less during storm surge, and waves are propagated across the whole marsh. Additionally, saltmarsh elevations increase steeply from the outer lower marsh to the top of the marsh regardless if there are morphological features across the marsh surface. Therefore, during the waves, the water level decreases as elevation increases from the lower marsh to the marsh top level and as levels of water decrease the wave energy reduces. During storm surge, saltmarshes are not effective particularly when water level reaches more than 2 m above MHWS such as Stiffkey and Dengie in the South-East England. This confirmed what was observed that most of the marsh in the South-East England are vulnerable against flooding risks during storm events (See more in Chapter 3). By contrast, saltmarshes are effective during storm event such as Morecambe Bay in Solway, since this marsh platform lie above MHWS and the North coast is experiencing isostatic sea level fall (Shennan, Milne *et al.*, 2009).

Concerning vegetation and its impact on wave attenuation, (Sutton-Grier, Wowk *et al.*, 2015) indicate that the vegetation in the coastal region, including marshes in the coast have an ability of reducing the risk of flooding. (Temmerman, Horstman *et al.*, 2023)indicated that the contribution of marsh vegetation during storm surge is much less effective or not effective at all, (Shepard, C.C., 2010; Temmerman, *et al.*, 2023) concluded that marsh vegetation can be effective during storm surge if there are several thousand to tens of thousands of meters wide such as Louisiana wetlands, But this is not a case in the Uk marshes as it's marsh a hundred meters maximum. So, marsh vegetation of reducing the risk of flooding might be effective during normal condition but their contribution during storm surge is less important. So, in the line of previous studies (Gedan, *et al.*, 2011, Möller,

*et al.*, 2014, Möller and Spencer, 2002) indicated that saltmarshes play a key role in coastal protection, is overstated.

## 4.5 Conclusion

In this chapter, the results show that the relationship between wave dissipation and depth of water was more apparent over the salt marsh. The changes of saltmarsh elevation are partly effective of decrease the water depth across saltmarsh leading to reducing wave energy. The water level during storm surge in this study is about 2 m above MHWS, but in some events such as storm surge in 2013 at Blakeney in the UK (Table 4.1) water level reached 3.48 m above MHWS with high wave velocity which might damages the seawall. Saltmarshes play a useful role during normal conditions, but their contribution is much less effective during storm surges.

## Chapter five

## The contribution of elevation relative to tidal height of estimating Carbon burial and greenhouse gases (GHG) emissions in the UK saltmarsh.

### 5.1 Introduction

Saltmarsh environments store carbon, as plants and photosynthetic microorganisms absorb carbon dioxide from the atmosphere (Mcleod *et al.*, 2011), and deposit some of the resulting organic carbon into the marsh sediment. In addition, some organic matter produced elsewhere gets deposited onto marshes in sediment. Much of this carbon will be oxidised and converted back to $CO_2$, but some will be buried long term, representing net removal of carbon from the atmosphere (Adams, 2008). Where sediments are anoxic, some of this carbon may get converted by methanogenic microorganisms to methane (Dalal *et al.*, 2008). Some nitrogen compounds may be converted by denitrification or nitrification to $N_2O$, and fluxes of $N_2O$ are also often higher from anoxic sediments (Capooci *et al.*, 2019). Both of these are potent greenhouse gases (Livesley and Andrusiak, 2012). Global Warming Potential (GWP) expresses the impact of $CH_4$ and $N_2O$ emission as the mass of $CO_2$ that would have an equivalent effect on global warming by integrating their effects over a time horizon, usually 100-years. This allows the combined effect on global warming of carbon burial and production or removal of $CH_4$ and $N_2O$ to be calculated. The GWP for $CH_4$ and $N_2O$ are 25 and 298 $gCO_2/m^2/yr$ respectively (Marten and Newbold, 2012).

$CO_2$ is produced by the respiration of plants and microbial life in the soil, but microbial respiration is most efficient in aerobic conditions (Yiqi and Zhou, 2010). Where soils are anoxic, aerobic respiration is reduced, which usually leads to an increase in carbon burial ((Adams, 2008). However, this may be partially counterbalanced by increased production of $CH_4$ and $N_2O$ in anoxic conditions (Kelleway *et al.*, 2017). At the landward margin of

saltmarshes, *Phragmites* colonisation/invasion can be associated with the development of peat, leading to very high rates of carbon burial (Baugh, 2019). However, *Phragmites* is only abundant when salinity of the upper marsh is reduced and in these conditions $CH_4$ production may be very high (Baugh, 2019).

Diverse researchers have further undertaken studies to measure the emission levels of $CH_4$ and $N_2O$ in wetlands including saltmarshes, seagrass meadows and mangroves. A study by (Rosentreter, *et al.*, 2021) summarized the magnitude and variability of $CH_4$ and $N_2O$ flux for blue carbon ecosystems which included saltmarshes, mangroves and seagrass. The maximum and minimum measurements for $CH_4$ and $N_2O$ reported in their literature review are displayed in Fig 5.1 below.

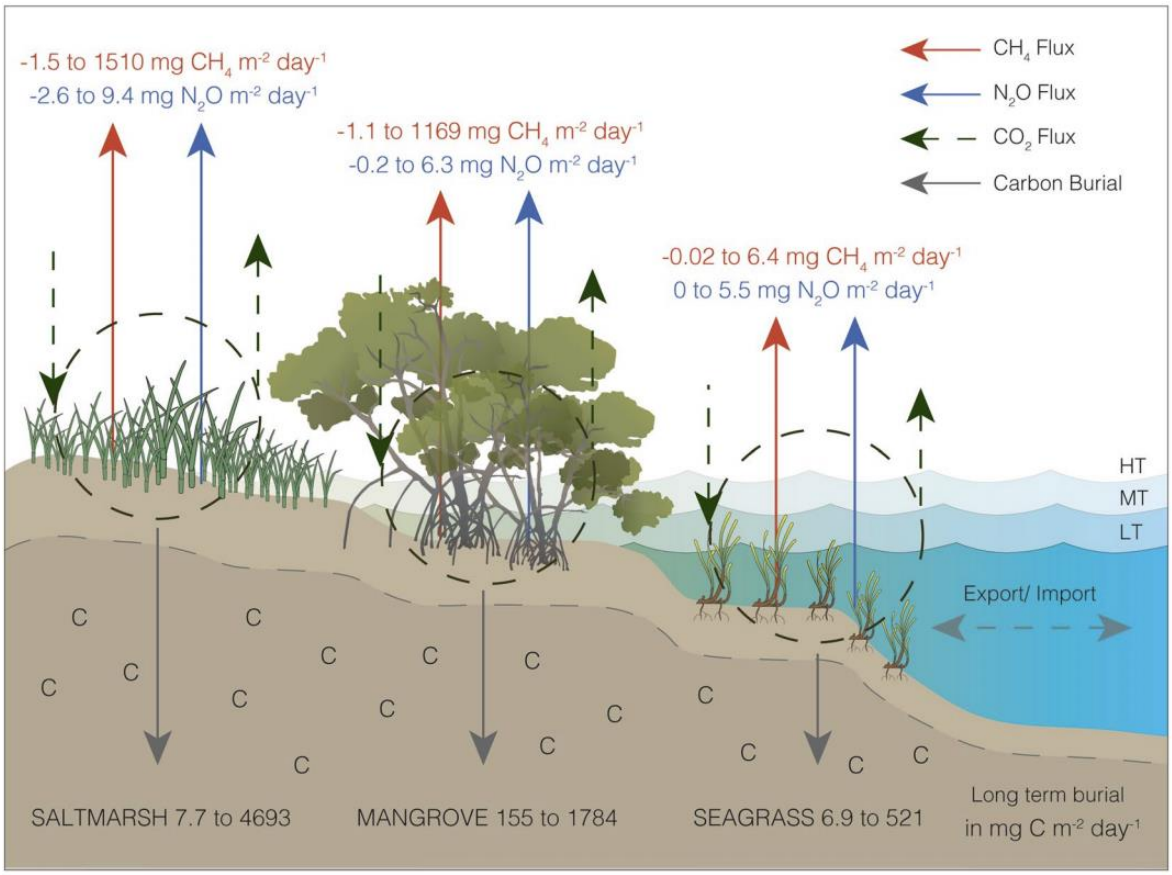


Fig 5.1 Summary of $CH_4$ and $N_2O$ fluxes for coastal ecosystems (Rosentreter, *et al.*, 2021)

The findings from (Rosentreter, *et al.*, 2021) are in line with those of (Wang, 2010) who also found that the saltmarshes contributed the highest levels of $CH_4$ and $N_2O$. In addition, the saltmarshes were recorded as generating the highest carbon burial level around 4693 mg C/$m^2$/yr as compared with mangroves at 1784mg C/$m^2$/yr and seagrass at 520 mg C/$m^2$/yr (Rosentreter, *et al.*, 2021). In a study of (Wang *et al.*, 2010) revealed that the salt marsh generated lower $N_2O$ flux in comparison to the grassland and meadow.Other researchers (Bartlett *et al.*, 1985, King and Wiebe, 1978) reported that $CH_4$ emissions from saltmarshes are lower in the more saline parts of salt marshes (Sanders-DeMott *et al*., 2022), because the high dissolved sulphate inputs to interstitial water of salt marsh sediments can inhibit methanogenesis (DeLaune et al., 1983), and increase $CH_4$ oxidation in the soil (Martens and Berner, 1977) which suggests that freshwater marshes should have higher emissions.

However, one of the striking features of the synthesis by Rosentreter et al (2021) is the very wide range of values for carbon burial, methane and nitrous oxide emissions. If we are to develop an overall picture of the extent to which saltmarshes contribute to global carbon budgets, a deeper understanding of the factors that influence these fluxes is vital. Can we use our data on elevation to predict the range of redox potentials likely to be found on the saltmarshes that we have studied? If so, we can predict how important contributions of $CH_4$ and $N_2O$ emissions to the net GHG flux are likely to be and identify the proportion of marsh area over which anoxia will enhance carbon burial.

The redox status of sediments will have a substantial impact on carbon burial, with this being greater in sections of the marsh where soils are anoxic (Adams, 2008). Redox potential is also very important in investigating saltmarsh elevation in term of GHG emissions (Capooci, Barba *et al.*, 2019). Moreover, redox potential increases from low to

high marshes and depend on the sediment properties (Chapman, 1960, Davy *et al.*, 2011). (Lawrence, 2018; Mossman *et al*., 2020) investigated the relationship between redox potential and topography and indicated that redox potential varies substantially across individual marshes and is significantly higher on natural sites than managed realignment sites. (Mossman, 2007) measured redox potential in different sites of saltmarshes around the UK including Severn Estuary, North Devon, South Devon, South Coast, Essex, Suffolk, North Norfolk, the Wash and Humber Estuary, and indicated that redox potential had significant effects on the distribution of plant species and communities. Although redox and elevation are correlated with each other, redox has effects on plant distributions that are independent of the effects of elevation, demonstrated both by statistical analysis of distribution data (Sullivan et al., 2018; Davy et al, 2011) and by experimental manipulation of local elevation (Mossman, Grant *et al.*, 2020).

In oxic conditions, bacteria can use oxygen as an electron acceptor. When oxygen is depleted, other electron acceptors are used, including reducing sulphate to sulphide, nitrate, iron and manganese reduction. Only when all these electron acceptors are depleted the carbon dioxide reduced to methane (Ponnamperuma, 1972). Therefore, bacteria can reduce carbon dioxide to methane when sulphate and oxygen are used up (Dalal et al., 2008). Poffenbarger et al. (2011) indicated that $CH_4$ and $N_2O$ emissions will be reduced at high salinity, and therefore that GHG emissions, including $CH_4$ and $N_2O$, decrease as salinity increases (Canfield et al., 2005; Capooci et al., 2019).

The average carbon burial on British saltmarshes, has been estimated as 140 $gCO_2$ $m^{-2}$ $yr^{-1}$, varying from 64 $gCO_2$ $m^{-1}$ $yr^{-1}$ in North Norfolk to 219 $gCO_2$ $m^{-1}$ $yr^{-1}$ at the Solent in Portsmouth (Cannell *et al.*, 1999). They stated that, in all cases these calculations assume that sedimentation rates is equal to the local sea level rise of 0.1 mm/yr to estimate the

average carbon burial by multiply carbon content and sedimentation rate. (Ouyang and Lee, 2014) estimated average rates of the accumulation of carbon in salt marsh sediments to be 242.2 $gCO_2\ m^{-2}\ yr^{-1}$ using sedimentation rates obtained from measurements for different marshes around the world in the literature and multiplying with carbon contents. (Chmura *et al.*, 2003) calculated the mean carbon burial rate at 218 g C $m^2\ yr^{-1}$ using carbon content and accretion rate obtained from different studies conducted in 96 saltmarshes around the world. the carbon burial rate is calculated by multiplying sedimentation rate by sediment carbon content measured some distance below the surface (after labile organic matter has been broken down).

Previous studies have been conducted to calculate carbon burial, redox potential, and sedimentation rates in attempts to estimate GHG emissions, including $CO_2$ flux, $CH_4$ flux, and $N_2O$. (Adams, Andrews *et al.*, 2012) assumed that sedimentation rate was in equilibrium with sea-level rise at 5.4 mm/yr to calculate carbon burial and GHG emissions in marsh realigment and natural marsh sites in the Blackwater estuary. Contrary, (Shennan and Horton, 2002) give overview of how sea level has changed mentioning that the maximum values of sea level rise are between 1.22 mm/year at Southend and 1.81 mm/year at Lowestoft. (Howes *et al.*, 1985) estimated carbon burial and GHG emissions based on measurements of sediment adjacent *Spartina alterniflora* at low tide in the low marsh. (Chmura, Anisfeld *et al.*, 2003) estimated carbon burial and GHG emissions based on measurements of sediment in only low marsh for four marshes with a simillar zones of elevations. These studies calculate ecosystem services delivered by saltmarshes as a homogeneous object and assumed a square metre of saltmarsh is the same. However, ecological characteristics of saltmarshes vary substantially with elevation and there are important differences in biogeochemical functioning between low shore and high shore of

saltmarshes (Chapman, 1960, Davy, Brown *et al.*, 2011, Mossman, Grant *et al.*, 2020). Therefore, recognising elevations and relative tidal heights across saltmarshes seem to be important when estimating sedimentation rates, and carbon burial is as essential characteristic of marshes that must be considered when evaluating GHG emissions.

The (Mason *et al.*, 2012) report notes the importance of reporting elevation amongst the metadata for work on GHG production and carbon burial and they mention that most studies give only the vaguest of information about tidal levels., in addition, (Mason, *et al.*, 2012)don't even mention redox, and the individual studies of GHG emissions do so, even though it is a key determinant of biogeochemical functions.

The overarching objective of this chapter is to evaluate the degree to which saltmarsh elevations relative to tidal height alter the amount of GHG emissions ($N_2O$ and $CH_4$ fluxes) and carbon burial due to variations from low to high elevations. This work goes beyond what is currently known in previous researchers by clarifying the role of elevation of saltmarshes, and providing a framework that identifies areas where sedimentation rate will be zero; areas where sedimentation rate is likely to be set by sea level rise and areas where it could be higher than this.

### 5.1.1 Aims of the study

The aims of this study are:

i. To evaluate to what extent saltmarsh elevations, alter the amount of carbon burial and the likely magnitude of GHG emissions.

The objectives of this study are:

i. To use saltmarsh elevations, data on heights of tides (see Chapter 2 & 3) and Pethick's equation (Pethick, 1981) to predict sedimentation rates across saltmarshes and comparing this approach with other approaches in terms of marsh morphology of estimating sedimentation rates across saltmarsh.

ii. To use these sedimentation rates to calculate likely carbon burial across saltmarsh.

iii. To use the data on the relationship between redox potential and tidal heights (Mossman, 2007, Mossman, Davy *et al.*, 2012a) to predict the distribution of redox potential across saltmarsh elevations for each marsh in this study, and thus evaluate the extent to which methane and nitrous oxide emissions are likely to counterbalance $CO_2$ removal and thus reduce the net GHG removal by saltmarshes.

## 5.2 Method

### 5.2.1 Data from previous studies

Many studies have estimated GHG emissions including $CH_4$ and $N_2O$ (Table 5.1). These studies were conducted in different parts of saltmarsh including intertidal mudflat, Natural saltmarsh, marsh realignment, brackish, creek marsh and freshwater marsh. These studies provided the ranges of $CH_4$ and $N_2O$ expressed as equivalents of $gCO_2$ $m^2$/ yr. These values of GHG emissions were used in this study toward evaluating the status of GHG emissions across saltmarshes. This research does not seek to estimate GHG emissions. Instead, the focus is to evaluate GHG emissions based on elevation implications that are relative to tidal height, and to what extent saltmarsh elevation relative to tidal height alter the amount of carbon burial and GHG emissions.

Table 5.1. Published values for $CH_4$ and $N_2O$ emissions on saltmarshes, intertidal mudflat, managed realignment sites, brackish and freshwater marshes.

| site | | $CH_4$ –$CO_2$ equivalents (g $m^{-2}$ $yr^{-1}$) | $N_2O$ –$CO_2$ equivalents (g $m^{-2}$ $yr^{-1}$) | Reference |
|---|---|---|---|---|
| Blackwater estuary (Essex) North Norfolk coast, UK, | Intertidal mudflat | 2.0 | 52 | (Adams, Andrews *et al.*, 2012) |
| | Managed realignment saltmarsh | 3.0 | 116 | |
| | | 3.0 | 116 | |
| | Natural saltmarsh | 4.4 | 10 | |
| East Coast USA, | Saltmarsh | 4.3 | - | (DeLaune, Smith *et al.*, 1983) |
| | Brackish | 73 | - | |
| | Freshwater marsh | 160 | - | |
| East Coast USA | Saltmarsh | 1.3 | - | (Bartlett, Harriss *et al.*, 1985) |
| East Coast USA | Saltmarsh | 5.6 | - | (Bartlett et al., 1987) |
| | Brackish | 22.4 | - | |
| | Freshwater marsh | 18.2 | - | |
| East Coast USA | Saltmarsh | 4.22 | - | (Howes, Dacey *et al.*, 1985) |
| Eastern England marsh | Pan marsh | 11.7 | - | (Senior et al., 1982) |
| | Creek marsh | 4.95 | - | |
| South-west England, | marsh realignment | - | 8.94 | (Blackwell et al., 2010) |
| | Nature- saltmarsh | - | 3.72 | |
| Dibbour Harbour USA | Saltmarsh | 7.008 | - | (Magenheimer et al., 1996) |

| site | | $CH_4$ –$CO_2$ equivalents (g $m^{-2}$ $yr^{-1}$) | $N_2O$ –$CO_2$ equivalents (g $m^{-2}$ $yr^{-1}$) | Reference |
|---|---|---|---|---|
| The Jiulong River Estuary Mangrove Reserve (117°54'E, 24°23'N) in the monsoonal subtropics of Southeast Chin, | Kandelia forest | 10.64 | 44.37 | (Chen et al., 2015) |
| | Sonneratia forest | 21.6 | 56.15 | |
| | Cyperus marsh | 12.75 | 63.4 | |
| | Spartina marsh | 22.2 | 95.6 | |
| Eastern Canada along the Atlantic coasts of New Brunswick and Nova Scotia, | Dipper Harbour | 8.7 | -2.05 | (Chmura et al., 2011) |
| | Kouchibouguacis marsh | 4.7 | 13.9 | |
| Northwest Devon, the UK. | Managed realignment saltmarsh | | 10.7 | (Blackwell, Yamulki *et al.*, 2010) |
| The Ribble estuary North-West England | Grazed marsh | 5.6 | | (Ford, Garbutt *et al.*, 2012) |
| | Un-grazed marsh | 1.22 | | |
| **Average** | | **17.93** | **45.28** | |

### 5.2.2 Redox potential

The redox potential is influenced by elevation and local drainage of marshes within the tidal frame (Mossman, Davy *et al.*, 2012a), and both redox potential and elevation influence the distributions of plants (Mossman, Grant *et al.*, 2020). (Davy, Brown *et al.*, 2011, Mossman, 2007) reported that redox potential increased significantly from −200 mV at the lowest elevations to +400 mV at the elevation which was highest in their study across the marsh at the Brancaster managed realignment (MR) site on the North Norfolk coast, UK. Variability of redox is greater on the low marsh than on the high marsh (Mossman, Davy *et al.*, 2012a). Based on this approach we predicted the distribution of redox potential related to elevation and relative tidal height.

To begin with, elevation data was extracted for each of the selected marsh (refer to chapter 2 & 3 method which details this data as we generated transects and histograms). The data were expressed as relative tidal heights, whereby, a value of 0 corresponded to MHWN and 1 corresponded to MHWS.

The regression line equation was fitted using (Mossman, 2007, Mossman, Davy *et al.*, 2012a) data and used to predict redox from our data using tidal height to calculate the standard deviation of redox values. The regression equation was that:

Predicted redox = (226.29*relative tidal heights) +117.21

To predict variability of redox, relative to tidal heights were further divided into three categories (0-0.5; 0.5-1.0 and 1.0-1.5). For each category the standard deviation (SD) of the residuals of individual redox values from the regression line were calculated using:

Predicted SD = (138-(62.53* elevation relative to Tidal height))

The procedure of predicting redox potential from elevation in this study involved the following steps.

i. We identified MHWS and MHWN for each marsh (Table 3.1, see Chapter 3 for more details) to enable calculation of relative tidal heights.

ii. We extracted the number of pixels falling into every 5cm category of elevation on a marsh and calculated the relative tidal height of the midpoint of the category.

iii. (Mossman, 2007) measured redox potential in different marsh sites around the UK and indicated that redox potential increased significantly from −200 mV at the lowest elevations to +400 mV at the elevation. Most of these sites are similar to marsh sites in this study. So, we set upper and lower limits to predicted redox values of < + 400 mV and > - 200 mV.

iv. For each 5 cm elevation category, predicted mean redox and predicted standard deviation were calculated using the equations below.

Predicted mean redox = ((226.29*elevation relative to tidal height) +117.21)

v. Assuming that redox data were normally distributed within a 5 cm elevation category, we calculated the probability of a location at this elevation having a particular redox value, rounded to the nearest integer and truncated at -200 and +400 mV.

vi. Finally, we multiplied these probabilities by the number of pixels in each elevation band and the area of a single pixel to give estimates of the distribution of redox values over each marsh.

vii. Analyses of this data were carried out in R 3.5.0 version using the raster, rgdal, rgeos, magick, imager and ggplot2 packages (Barthelme, 2017, Bivand, Keitt *et al.*, 2015, Bivand and Rundel, 2017, Hadley, 2016, Hijmans, van Etten *et al.*, 2017, Jeroen, 2018).

### 5.2.3 Sedimentation rate and carbon burial calculations

Sedimentation rates appear to be variable spatially or temporarily across saltmarshes, and there is a strong relationship has also been observed between rates of sedimentation and changes in elevation which result in the variation of sedimentation rates between low and high saltmarsh platforms (Carling, 1982; Wilson et al., 2014). For most marshes, sediment is transported to the marsh in suspension, so the sediment that is added to the marsh will be dependent up number of inundations and/or time inundated. (Pethick, 1981) formulated a model of the relationship between surface elevation and marsh age as a function of the marsh accretion rate using equation:

$$h = a - be^{-ct}$$

where: h = height of marsh surface, t = age of marsh a, b, c are constants, a= the equilibrium marsh elevation (equal to the current marsh platform elevation for marshes where the platform is an active geomorphological structure rather than a relic of previously higher sea levels), b= the distance that the marsh is currently below that elevation, and c = indicates how fast the marsh grows towards equilibrium. This implies that sedimentation rate declines with increasing elevation on the marsh (see below).

In many previous studies, sedimentation rates have been assumed as being equal to the rise in sea level, with an implicit assumption that every square meter of the marsh is the same (Adams, Andrews *et al.*, 2012, Cannell, Milne *et al.*, 1999). In other studies, sedimentation rates were estimated just in the low marsh and assumed all marsh areas are similar (Chmura, Kellman *et al.*, 2011, Howes, Dacey *et al.*, 1985). Our approach to predict sedimentation rates differed from previous research studies in three ways;

First, predicted sedimentation rates was calculated using a re-arranged version of Pethick's equation (Pethick, 1981) based on the average of changes in elevation across marsh ranging

from low to high levels as a function of sedimentation rate. The calculations were carried out at 5 cm elevation intervals from low to high across saltmarsh and calculate the average sedimentation for all these points. These calculations were made for 35 marshes around the UK. The equation to predict sedimentation rates as a function of elevation was re-arranged to:

$$S = c(a - b)$$

Where: S = Sedimentation rate (cm/yr); c= equal to the sedimentation rate when (a-b =1), a = elevation of marsh platform; b = elevation of each point across the marsh.

By adding relative sea level rise the equation to predict sedimentation rates is:

$$S = c(a - b + SLR)$$

Where: SLR= the local relative sea level rise for each part corresponding with marsh around the UK (Figure 5.12), obtained from (Shennan and Horton, 2002).

Secondly, in our approach, sedimentation above MHWS was assumed to be zero because most of the marsh here at or above MHWS, and areas above MHWS are not inundated, and sedimentation will not occur except during storm event or the highest of high spring tide. However, in the Severn Estuary, as marsh platforms are above MHWS, we have taken into account the area above MHWS in sedimentation rate calculations.

Thirdly, we also assumed that sedimentation rates below MHWN is zero because in most marshes the small areas below MHWN (See marsh area below MHWN and above MHWS maps in chapter 3, table 3.1) are normally creeks in which no sedimentation will occur. In a small number of sites there are more substantial areas of marsh below MHWN, such as at Tollesbury, Fambridge and Hemley. We assumed sedimentation in these areas was zero because these marshes are badly eroding, and sedimentation is not stable due to cycle of erosion and deposition.

Previous studies (Adams, Andrews *et al.*, 2012, Adams, 2008, Andrews *et al.*, 2008, Cannell, Milne *et al.*, 1999, Ford, Garbutt *et al.*, 2012, Howes, Dacey *et al.*, 1985, Marion, Anthony *et al.*, 2009) have assumed that sedimentation occurs at a rate equivalent to the sea level rise across the whole marsh which can be an issue for predicting sedimentation rate. Other literature studies adopted a different approach to estimate regional sea level rise although the marshes considered the same estuary (Chini *et al.*, 2010, Gehrels and Long, 2008, NRA, 1994, Pethick, 1981).

Therefore, in our approach, we used rise in sea level as reported by (Shennan and Horton, 2002) and added this to the sedimentation rate (Figure 5.5). Shennan and Horton, (2002) provide uplift (sea level fall) and subsidence (sea level rise) which provides a clear statement of sea level for all parts around the UK. Some marshes lie in the part of the UK where sea level fall such as Solway and Scotland marshes. The sea level is observed to fall in these parts of the UK and most of the marshes are also observed to be above sea level. Therefore, all negative values in the part of the UK where sea level fall were not added to the sedimentation rate calculation.

Predicted carbon burial for each individual elevation was calculated by multiplying sedimentation rates, carbon content and the area of marsh in that elevation category. The elevation and area for each marsh was obtained from results from chapter 2 & 3 (See chapter 2 and 3 for more details). In terms of carbon content, previous studies reported that there are no significant changes in soil carbon content in saltmarsh habitat (Perry and Mendelssohn, 2009, Raw *et al.*, 2019, Yando *et al.*, 2018). Serrano *et al.*, (2016) concluded that the carbon content in soils from estuarine and coastal habitats were similar. Additionally, there were several studies calculated carbon content in the UK saltmarsh particularly natural saltmarsh (NSM). For example, (Andrews, Samways *et al.*, 2008)

calculated carbon content to be from 0.057 g C $cm^3$ at the Humber estuary. (Callaway *et al.*, 1996) calculated carbon content in North Norfolk marshes to be 0.041 g C $cm^3$ at both Stiffkey, and Hut marsh. These values in different studies indicated that there is just a small different in carbon content between different places of saltmarshes. So, we assumed that sedimentation might be more important than sediment of carbon content and using soil carbon content of natural saltmarsh (NSM) 0.023 g/$cm^3$, based on (Adams, *et al.*, 2012).

The total carbon burial was calculated using the average of sedimentation rates converted to g $CO_2m^{-2}$ $yr^{-1}$, and this calculation was made for each site:

$$Carbon\ burial\ (g/m2/yr) = (\frac{total\ carbon\ burial}{total\ area})10000$$

Analyses of elevation data and relative tidal heights were carried out in R 3.5.0 version (R Core Team, 2018) using the raster, rgdal, rgeos, magick, imager and ggplot2 packages (Barthelme, 2017, Bivand, Keitt *et al.*, 2015, Bivand and Rundel, 2017, Hadley, 2016, Hijmans, van Etten *et al.*, 2017, Jeroen, 2018). The calculations were carried out in Excel (Microsoft Corporation. 2018).

## 5.3 Results

### 5.3.1 Redox potential

In our approach, the predicted redox values indicated that small areas in the low marsh have low redox approximately -100mV to 100 mV (Fig. 5.3; Stiffkey site used as an example, see more in appendix to chapter 5). In contrary, predicted redox across much of the marsh were in the range 250 - 400 mV, corresponding to oxic conditions. This occurs on those parts of the marsh where elevations are high (Fig.5.3; Stiffkey site used as an example, see more in appendix to chapter 5). In a large number of marshes, such as in the Solway, Scotland, the high marsh areas are not inundated by tides except during the highest high spring tide which indicated that these areas are not receiving much amount of sediment. In these marsh areas, biogeochemical processes (methanogenesis and denitrification) appear to be an inactive, representing the lack of methane and nitrous oxide production.

In some marshes, where parts of the areas of marshes are very high, there can be organic matter left due to the highest high spring tide where the high shore is colonised by *Phragmites* such as the marsh at Cley Next-the-Sea, Norfolk (52◦ 57’ 51’’N,1◦ 02’ 34’’E), close to Stiffkey. This occurs in areas of the high marsh where there is a substantial flow of freshwater, leading to a reduction in their salinity. Reduced salinity leads to lower sulphate concentrations. This leads to bacteria reducing carbon dioxide to methane where soils are anoxic at depth.

The predicted redox values (Figs 5.4a, b) indicate that most of the areas of each marsh have notably high redox values in the range 250-400 mV. This reflects the presence of marsh platforms lying at or above the level of MHWS (Figs 5.2; 5.3; which use the Stiffkey site as an example, see more in appendix to chapter 3 and 5). So, the soils of most of the area of

the marshes that we have studied are predicted to be oxic. In these circumstances, it is unlikely that substantial quantities of methanogenesis to produce $CH_4$ and denitrification or nitrification to produce $N_2O$ will occur. So $CH_4$ and $N_2O$ emissions are predicted to be negligible for most of marshes here.

This prediction of the distribution of redox potentials across marshes can provide information about the places where GHG emissions may be important. Average redox potential is lowest at Tollesbury, so this is the site at which $N_2O$ and $CH_4$ production might be expected to be most important. This site includes a managed realignment site and some eroding saltmarshes which have sections at relatively low elevations. Adams et al. (2012) measured fluxes of $N_2O$ and $CH_4$ at the Tollesbury managed realignment site and other locations within the Blackwater estuary. We would expect sediment characteristics and other environmental conditions to be similar throughout this estuary. $N_2O$ and $CH_4$ fluxes reduced net carbon sequestration on mudflats and managed realignment saltmarsh by between 20 and 49%, with $N_2O$ contributing most of this reduction. By contrast, GHG production reduced next carbon sequestration by only 2% on natural saltmarsh sites (their table 6). The vegetation at their natural saltmarsh sites was characterised by "higher saltmarsh species" including *Atriplex portulacoides*, *Limonium vulgare*, *Armeria maritima* and *Triglochin maritimum* (their table 1), species which are characteristic of oxic sediments at relatively high elevations (Davy *et al.*, 2012).

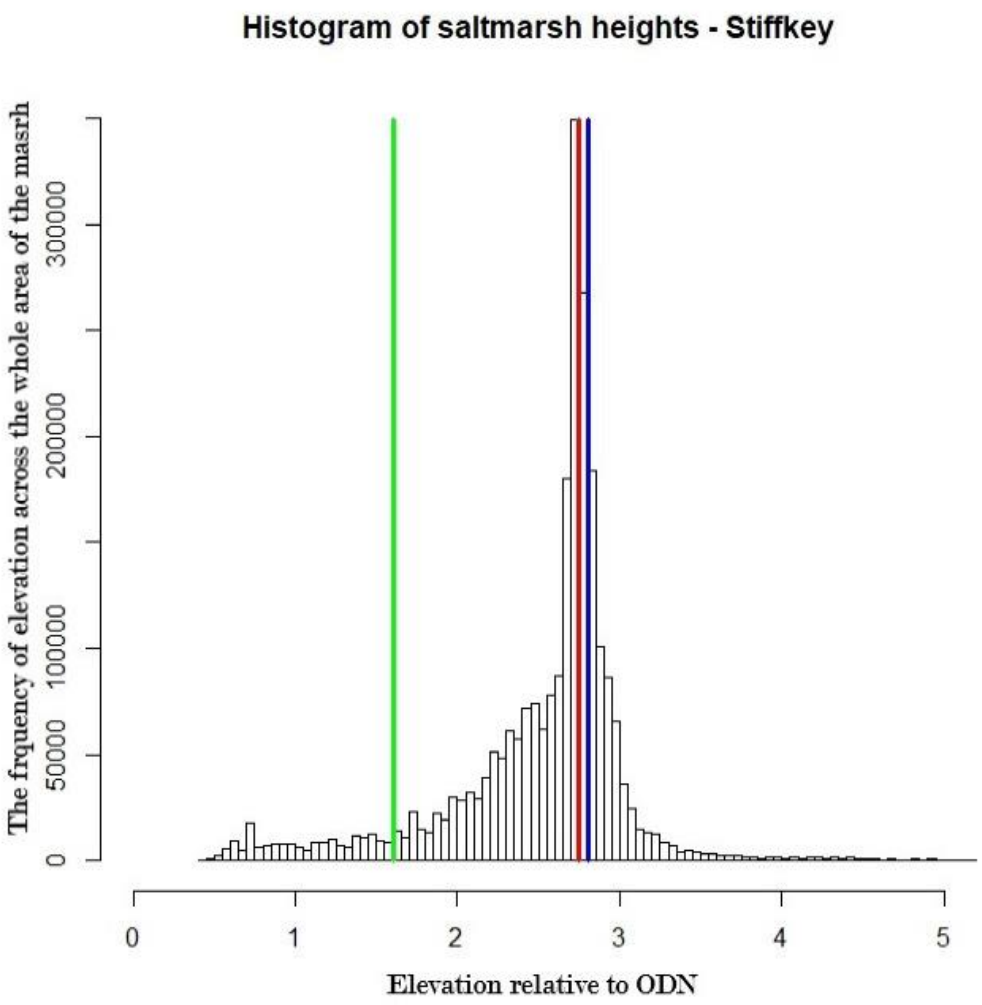


Figure 5-2 Saltmarsh elevation relative to ODN at Stiffkey, green line represents MHWN, blue line represents MHWS and red line represents saltmarsh platform.

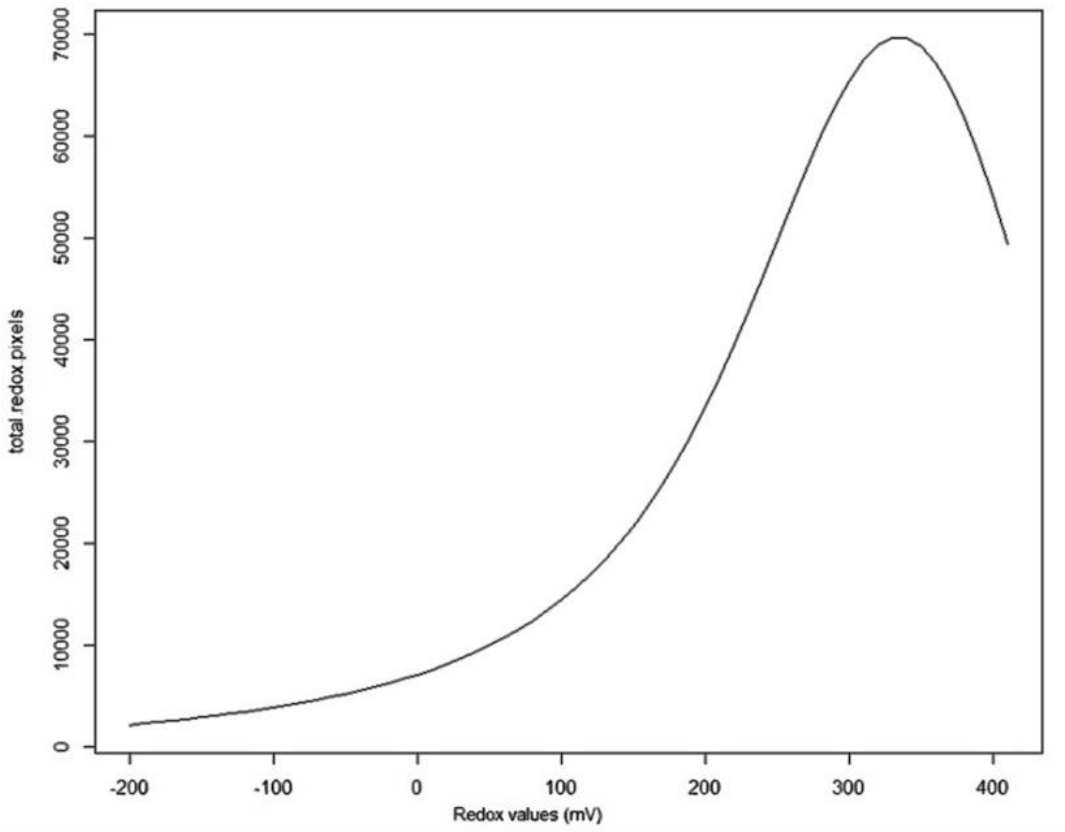


Figure 5-3 Predicted distribution of redox values averaged across the whole area of the marsh at Stiffkey.

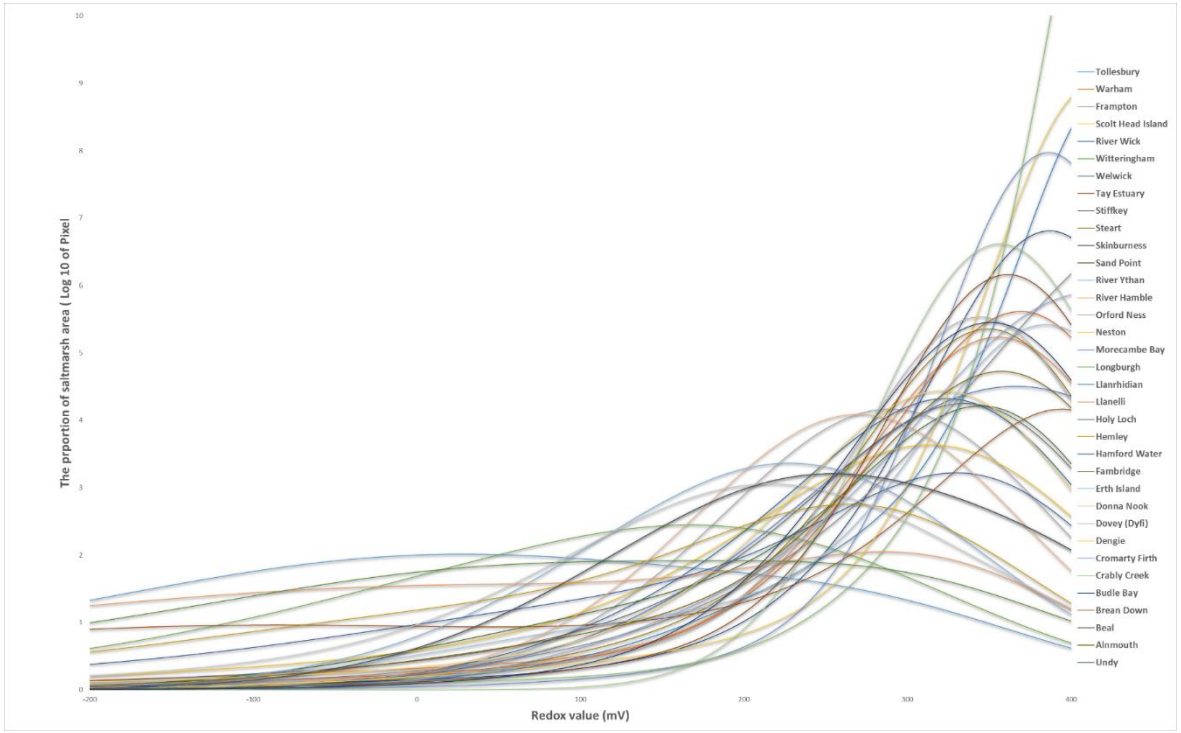


Figure 5-4a Predicted distribution of redox values across the whole area of the marsh at each individual marsh.

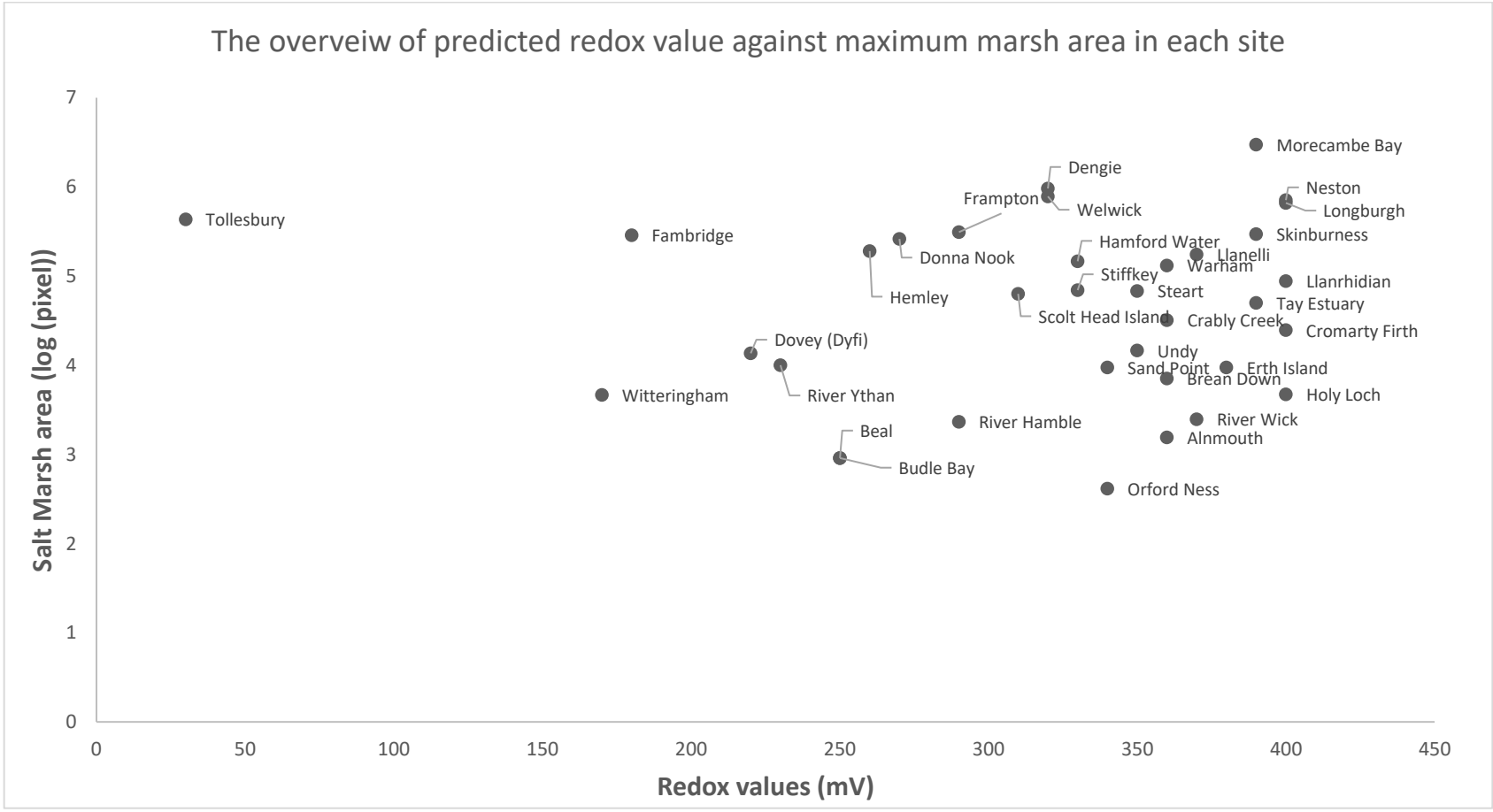


Figure 5-4b Predicted redox values on the saltmarsh platform at each individual site, each point represents redox values of maximum area of saltmarsh elevation.

### 5.3.2 Sedimentation rates and carbon burial.

#### 5.3.2.1 prediction of sedimentation using Pethick's equation

Our approach of predicting sedimentation rates using Pethick's equation an individual marsh is taken as the average across the whole elevation range from low to high marsh. Predicting sedimentation rates indicated that there is very low sedimentation occurring in the marsh platform, but it increases as we move down to the low shore, where there are very high sedimentation rates (Figures 5.5; Stiffkey used as example). Our approach, using Pethick's equation predicted that the average of sedimentation rate varies from 0.18 cm/yr in North Norfolk to 1.45 cm/yr at Sand Point in the Severn Estuary (Table 5.2). In the Humber Estuary, the highest sedimentation rate is around 0.42 cm/yr, at Welwick marsh, while the lowest is 0.23 cm/yr at Donna Nook marsh. Additionally, in the east south of England in Essex marshes, the average of sedimentation rates is around 0.58 cm/yr, whereas it is around 1.41 cm/yr in the Severn Estuary marshes in the West of England (Table 5.2). At Solway marshes in the northwest of England, the average of sedimentation rate is 0.17 cm/yr, while it is 0.09 cm/yr in Scotland marshes (Table 5.2).

Most of the active sedimentation occurs in the low shore in all marshes here (Figure 5.5, Stiffkey used as example ), and the area of low marsh is significantly smaller than the high marsh area ((CCP), 2021). As such, the relative contributions of higher and lower marshes to overall sedimentation and carbon burial are influenced by the balance between these two factors. Sedimentation occurs in the low elevation areas of the marsh, particularly in the mudflat and pioneer zones. Moreover, the pioneer zone area is kept open to water moving and is frequently submerged by tides which allows much sediment to enter. A large amount of sediment might return to the sea/estuary depending on the duration of tidal flooding. In contrast, sedimentation is very low (Figure 5.5, Stiffkey used as example) in the

high marsh, and as many marshes here lie at around MHWS, this area of the marsh is not received much sediment.

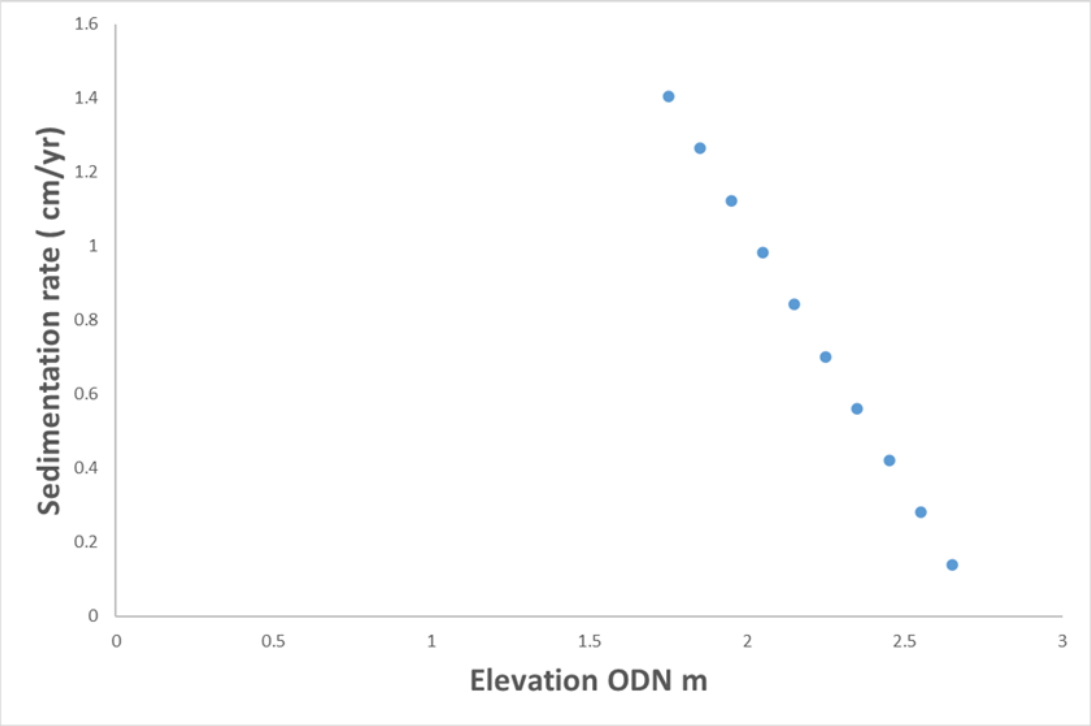


Figure 5.5 The relationship between predicted sedimentation rate and elevation for the Stiffkey saltmarsh.

#### 5.3.2.2 The prediction of carbon burial

The finding shows that carbon burial can be variable across marsh based on sedimentation rates. This indicated that sedimentation rate might be the dominant factor for Carbon burial calculation. Carbon burial is active in the low shore in all marshes here (Figs 5.6; 5.7, Stiffkey and Tollesbury used as example).

Our approach to predicting carbon burial is that the average carbon burial for all marshes here is approximately 239.7 g $CO_2/m^2/yr$ (Table 5.2). This value is close to that reported by (Ouyang and Lee, 2014), who estimated average rates of the accumulation of carbon in salt marsh sediments to be 242.2 gC $m^{-2}$ $yr^{-1}$, using extensive data of sedimentation rates and carbon contents in the sediment across different marshes of the world, while (Chmura, *et al.*, 2003) calculated the mean carbon burial rate at 218 g C $m^2$ $yr^{-1}$ using carbon content and accretion rate obtained from different studies conducted in 96 saltmarshes around the world. Cannell *et al.* (1999) estimated an average carbon burial of 140 g $m^{-2}$ $yr^{-1}$ in British saltmarshes by assuming sedimentation rates equal to the local sea level rise of 0.1 mm/yr.

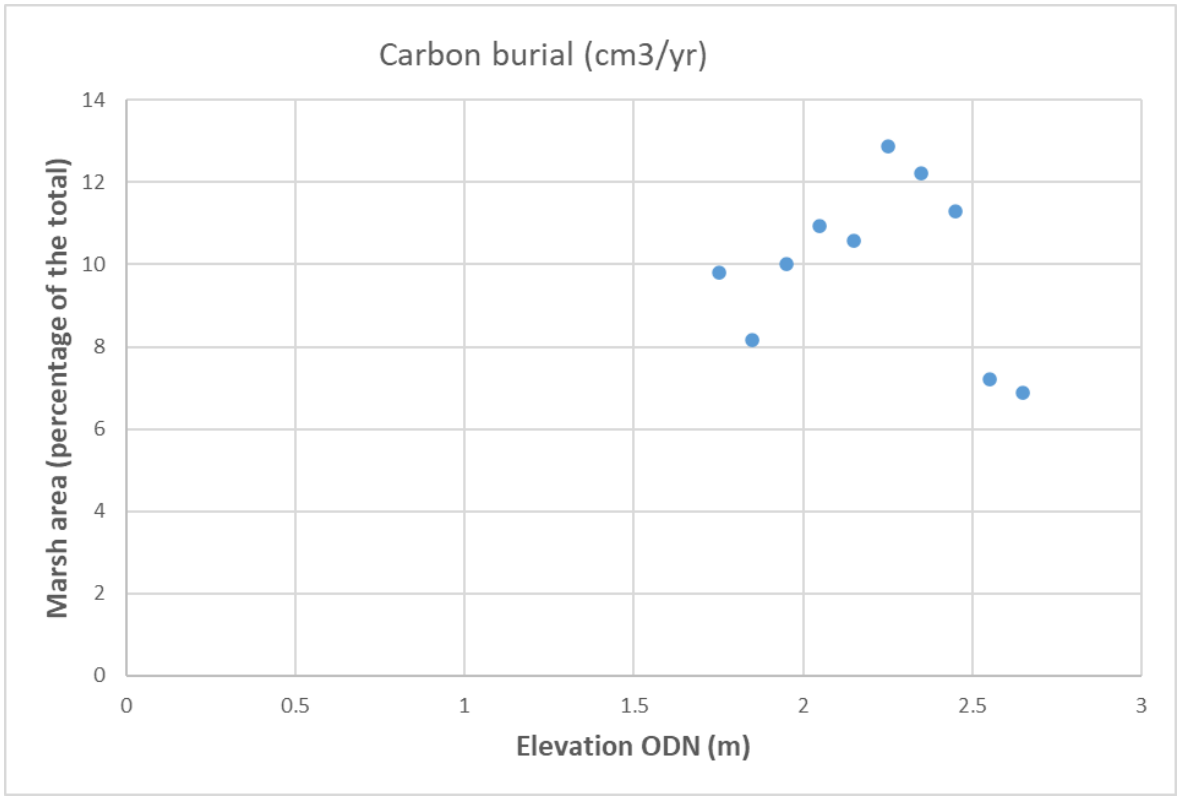


Figure 5.6 The percentage of carbon burial at each individual elevation across the whole marsh at Stiffkey.

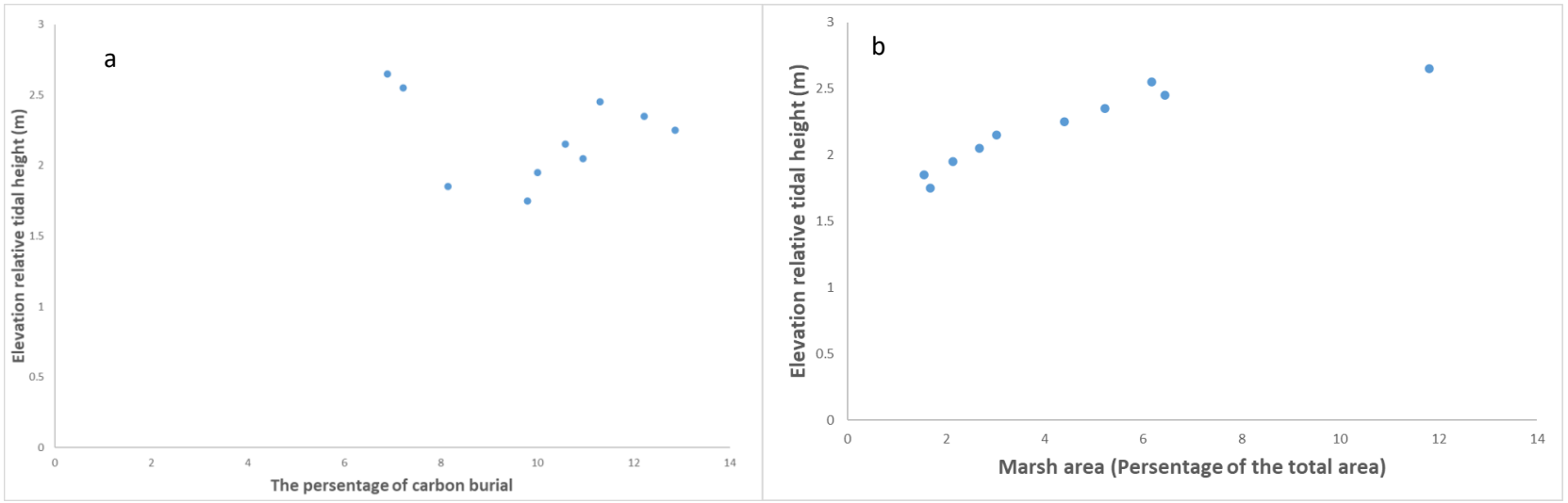


Figure 5.7 a The percentage of carbon burial at each individual elevation across the whole marsh at Tollesbury; b. The percentage of marsh area at each individual elevation across the whole marsh at Tollesbury

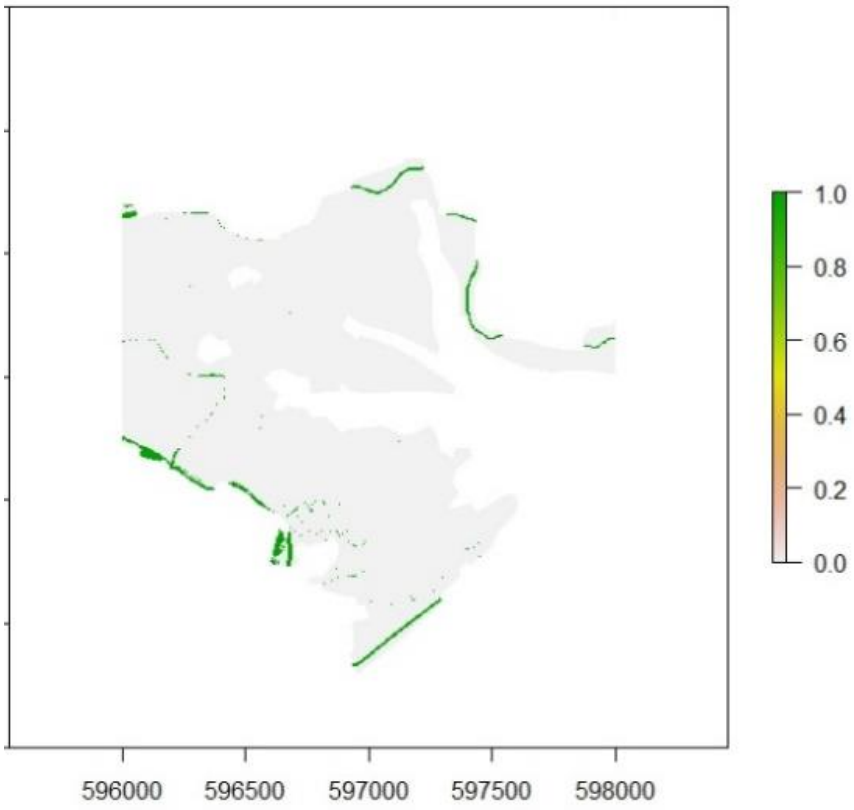


Figure (5.8) marsh area above the level of MHWS at Tollesbury

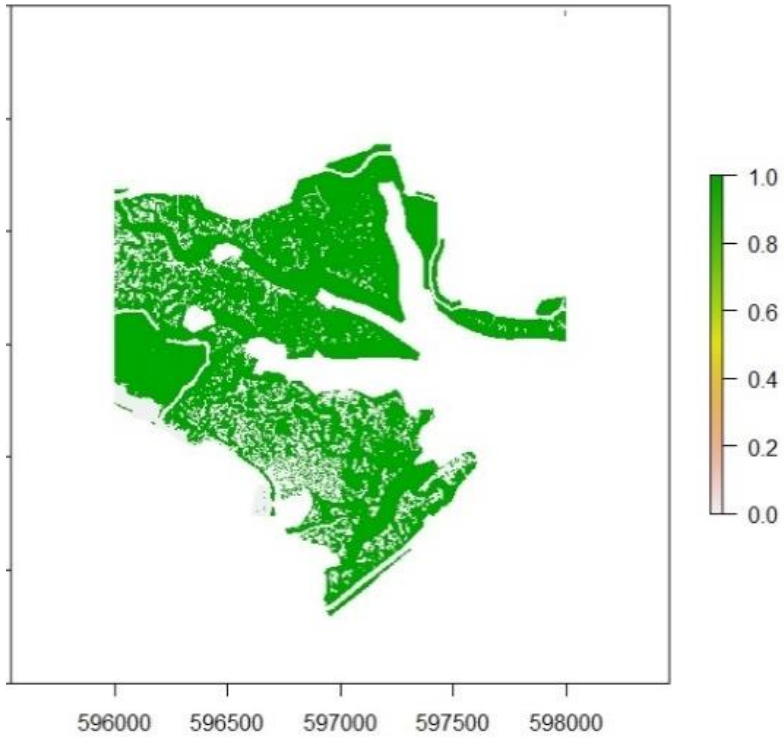


Figure (5.9) marsh area below the level of MHWN at Tollesbury

Figure (5.10) Photograph of saltmarsh area at Tollesbury

Table 5.2 The average of sedimentation rates (cm/ yr), The average predicted sedimentation rate (cm/ yr) + sea level range, carbon burial equivalent $CO_2$ (g $C/m^2/yr$), the proportion of the marsh above MHWS across the whole saltmarsh in 35 sites around the UK.

| Site name | Predicted sedimentation rate using Pethick's equation (cm/yr) | Sea level rise/fall around the UK, (Shennan and Horton, 2002), (mm) | The average predicted sedimentation rate (cm/ yr) + sea level range | Area of the marsh above MHWS (%) | Carbon burial g Eq $CO_2/m^2/yr$ |
|---|---|---|---|---|---|
| Crably Creek | 0.28 | 0.8 | 0.37 | 7.7 | 89.15 |
| Welwick | 0.34 | 0.8 | 0.42 | 22.3 | 411.9 |
| Donna Nook | 0.15 | 0.8 | 0.23 | 1.4 | 59.1 |
| Frampton (The Wash) | 0.24 | 0.7 | 0.31 | 8.89 | 100.2 |
| Scolt Head Island | 0.1 | 0.8 | 0.18 | 17 | 336.7 |
| Warham | 0.096 | 0.8 | 0.176 | 44.4 | 304 |
| Stiffkey | 0.099 | 0.8 | 0.179 | 23.6 | 203 |
| Orford ness | 0.39 | 0.9 | 0.47 | 38.8 | 109.7 |
| Hemley | 0.44 | 0.9 | 0.53 | 5.52 | 292.2 |
| Hamford water | 0.7 | 0.9 | 0.79 | 17.8 | 373.8 |
| Tollesbury | 0.56 | 0.8 | 0.64 | 2.1 | 218 |
| Dengie | 0.63 | 0.7 | 0.7 | 10.6 | 221.9 |
| Fambridge | 0.6 | 0.8 | 0.68 | 10.6 | 243.8 |
| Witteringham | 0.21 | 0.6 | 0.27 | 6.1 | 486.5 |
| River Hamble | 0.48 | 0.6 | 0.54 | 3.5 | 407.9 |
| Erth Island (Lynher River, Plymouth) | 0.24 | 0.2 | 0.36 | 60.8 | 240 |
| Steart (Severn Estuary) | 1.3 | 0.8 | 1.38 | 46.95 | 498.6 |
| Brean Down (SevernEstuary) | 1.32 | 0.8 | 1.4 | 65.3 | 482.1 |

| Site name | Predicted sedimentation rate using Pethick's equation (cm/yr) | Sea level rise/fall around the UK, (Shennan and Horton, 2002), (mm) | The average predicted sedimentation rate (cm/ yr) + sea level range | Area of the marsh above MHWS (%) | Carbon burial g Eq $CO_2/m^2/yr$ |
|---|---|---|---|---|---|
| Sand Point (Severn Estuary) | 1.37 | 0.8 | 1.45 | 37.9 | 1132.4 |
| Undy (Severn Estuary) | 1.23 | 0.8 | 1.31 | 33.9 | 458.9 |
| Llanelli | 0.22 | 0.5 | 0.27 | 50 | 218.8 |
| Llanrhidian | 0.36 | 0.5 | 0.41 | 53.2 | 223.6 |
| Dovey (Dyfi) Estuary | 0.55 | 0.3 | 0.58 | 11.4 | 205.9 |
| Neston (Dee Estuary) | 0.39 | 0 | 0.39 | 82 | 96.6 |
| Morecambe Bay | 0.16 | - 0.9 | 0.16 | 87.8 | 80.9 |
| Skinburness (Solway) | 0.17 | - 0.9 | 0.17 | 72.2 | 105 |
| Longburgh (Solway) | 0.19 | - 0.9 | 0.19 | 87.3 | 58 |
| Holy Loch | 0.07 | - 2 | 0.07 | 71.46 | 53.9 |
| River Wick | 0.07 | - 0.6 | 0.07 | 43.9 | 106.8 |
| Cromarty Firth | 0.19 | - 0.7 | 0.19 | 65.5 | 141 |
| River Ythan | 0.05 | - 1.4 | 0.05 | 1.6 | 133.6 |
| Tay Estuary | 0.09 | - 1.2 | 0.09 | 39.1 | 139.8 |
| Beal | 0.04 | 0.5 | 0.09 | 23.1 | 147.9 |
| Budle Bay | 0.07 | 0.5 | 0.12 | 59.7 | 100 |
| Alnmouth | 0.19 | 0.5 | 0.24 | 39.2 | 185 |
| **Average** | - | | - | | **239.7** |

### 5.3.2.2 Contribution to sedimentation due to sea level rise

Many marshes are equivalent to sea level rise (Table 5.2) particularly in the East South of England such as Donna Nook, Stiffkey, Hemley and Tullesbury which indicated that these marshes keep pace with sea level rise. In most of the marshes here, there is a steep gradient at the pioneer zone, which might raise the amount of sediment to be deposited. There are also morphological features that might influence sediment deposition in the low marsh area. At Stiffkey, there is a shingle ridge with elevation reach 4 m (ODN) that lies above MHWS, which might keep much sediment in the pioneer zone, but the stability of this amount of sediment depends on tidal duration and movement and erosion (Figure 5.11).

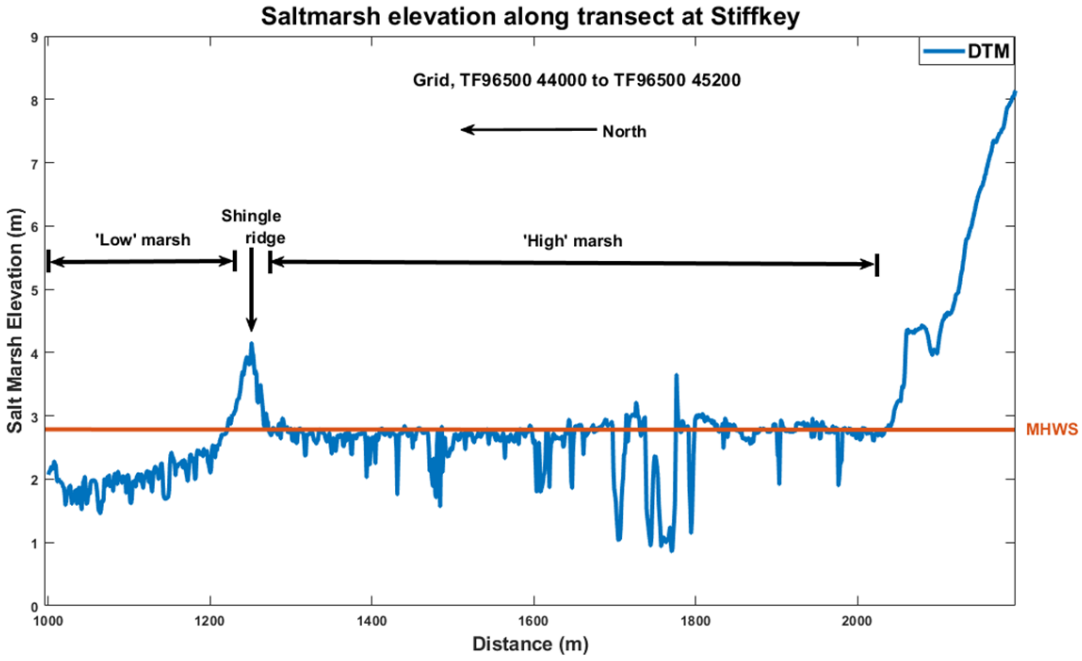


Fig 5.11 Elevation of the DTM along transect across salt marsh at Stiffkey.

In some marshes here, there is a tall cliff in the front of the marsh with high elevation reaches 6 m (ODN), (Fig. 5.12). There may be periods of erosion, where the marsh edge has a cliff, and deposition isn't occurring alternating with periods when pioneer marsh development occurs to the seaward of the cliff, such as Morecambe Bay marsh and no

amount of sediment may occur in the mudflat rather than in the pioneer zone (Figure 5.11, Morecambe Bay used as example).

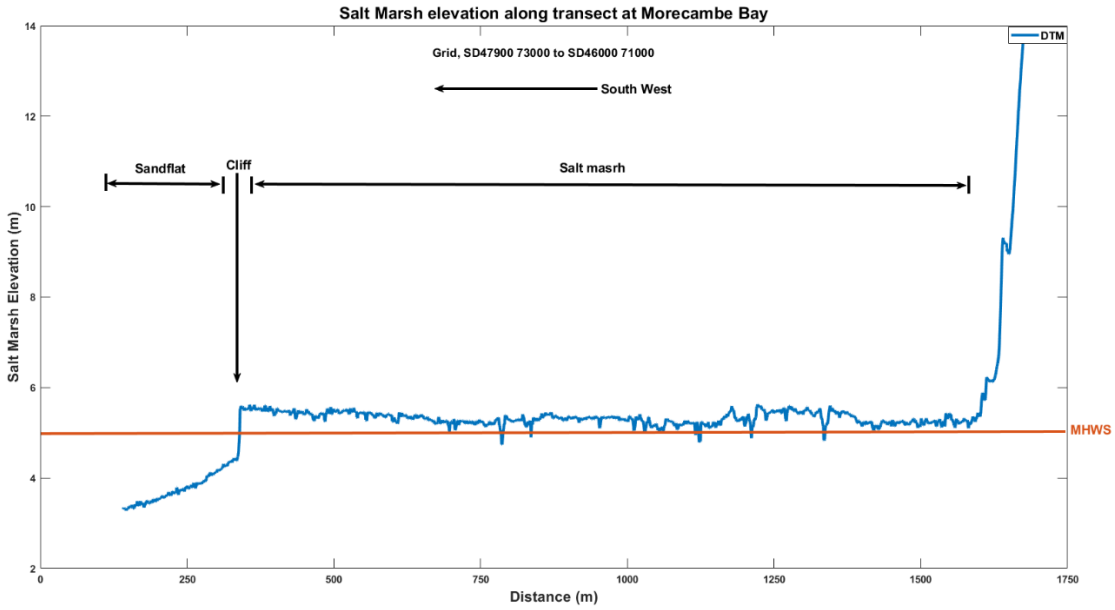


Fig 5.12 Elevation of the DTM along a transect across the salt marsh at Morecambe Bay.

There are fluctuations of elevation (badly eroding marsh areas dissected by creeks and channels) in the pioneer zone in some marshes, such as Tollesbury and Fambridge. These marshes are undergoing severe erosion (Figs 5.8; 5.9; 5.10, Tollesbury used as example) and are heavily dissected by creeks. This pattern of the marsh indicated that although sediment is deposited in the creek margins in the pioneer zone of these marshes, the sedimentation might not stable, and a large amount of sediment might return to the estuary rather than be deposited in the pioneer zone.

Many marsh platforms here lie at or above MHWS, and are inundated during relatively high spring tides, limiting the number of occasions during the year when sedimentation occurs. In some marshes, the platform lies above MHWS and can be submerged only during the highest spring tides such as Morecambe Bay marsh. The sedimentation rate over most of the area of these marshes will be close to zero, even in the face of rising sea level.

In different parts of the UK, some marshes have one of the world's largest ranges of tidal activity such as the Severn Estuary marshes (Xia *et al.*, 2010). These marshes can be inundated by a substantial depth of water on high spring tides, even when their platforms are above MHWS. As suspended sediment concentrations in the Severn Estuary are high, sediment deposition occurs up to a higher relative tidal height than elsewhere (Allen, 1990; 1991, Allen and Rae, 1986). There is also a transition area landward of the marsh that can be submerged, and some amount of sedimentation can occur. The sedimentation can also occur much higher in the marshes, such as Dovey (Dyfi). These marshes are inundated frequently by spring tide and might receive amount of sediment across the whole area of the marsh. The accretions can be also distributed unevenly though different parts of marsh (Kelleway, Saintilan *et al.*, 2017), but much accretion might be in the levees along the creek bank which was confirmed by (Carling, 1982).

### 5.3.3 Discussion

In this section, a discussion on the influence of saltmarsh elevation and sedimentation on generated redox values is undertaken. Various important findings regarding the impact of saltmarsh conditions on sedimentation and redox potentials are detailed. To begin with, it is important to highlight that the predicted redox values are high at approximately 250-400 mV across the majority of the area of most of the marshes considered in this study. Our approach to predicting redox values is based on natural saltmarshes, and redox is lower on realignment sites that are managed than on marshes that are natural (Mossman, Davy *et al.*, 2012a). Therefore, $CH_4$ and $N_2O$ emissions will be higher on managed realignment sites. Most of these platforms lie around MHWS (see more in Chapter 3, Table. 3.1, and Fig 3.29). The high redox values for these marshes are attributed to their relative tidal height across the marsh (Castillo *et al.*, 2000, Davy, Brown *et al.*, 2011). This indicates that GHG emissions are likely to be low across most of the marshes here. (Poffenbarger *et al.*, 2011) indicated that $CH_4$ and $N_2O$ emissions will be reduced at high salinity, and therefore that GHG emissions, including $CH_4$ and $N_2O$, decrease as salinity increases (Canfield *et al.*, 2005, Capooci, Barba *et al.*, 2019). This is due to saline water increasing sulphate reduction, which is more favourable than methanogenesis, which results in lower $CH_4$ emissions (Capone and Kiene, 1988). As such, redox potential is likely to be more important than salinity across saltmarshes, since increases in sediment redox lower sediment and GHG emissions are reduced.

An additional finding observed was that the average sedimentation rates varied between the studied 35 groups of marshes around the UK. Pethick's model can be appropriate for estimating sedimentation rates in North Norfolk marshes, because, suspended sediment concentrations in these marshes are relatively low (French and Spencer, 1993). Allen,

(1990) presents more elaborate models of accretion rates focus on changes of marsh surface elevation over time, rather than on the shape of the upper marsh surface, but in a number of figures, the high marsh is drawn as a sub-horizontal surface. Pethick generated his model by looking at the time taken for North Norfolk marshes to reach equilibrium. Therefore, sedimentation can be very high in the low shore and decreases once elevation increases across the marsh. This development can begin when there are changes in shingle or sand dune ridges that allow initiation of the development of a new marsh. After that, rapid deposition of sediment occurs on low marshes such as at Stiffkey. However, the position and extent of marshes may remain constant, because, in some areas of the marshes, deposition on low marshes in one place is balanced by erosion elsewhere, such as Tollesbury, Fambridge, and Dengie marshes, and a low marsh does not necessarily have the highest rates of sedimentation (Koppel *et al.*, 2005, Randerson, 1979, Richards, 1934). Many marshes here appear to be in equilibrium with sea level rise based on uplift (sea level fall) and subsidence (sea level rise) reported by (Shennan and Horton, 2002) (Figure 5.13). However, some studies have estimated different ranges of sea level rise, even in the same region. Both Pethick (1981) and NRA (1994) reported a regional sea level rise at 4 mm yr and 6 mm yr respectively in the Blackwater estuary. (Cundy and Croudace, 1996) estimated the sea level rise at around 4 mm/yr in Southern England, and others (Chini, Stansby *et al.*, 2010, Gehrels and Long, 2008) estimated the range of sea level rise as between 2.5 and 4 mm/yr around the UK.

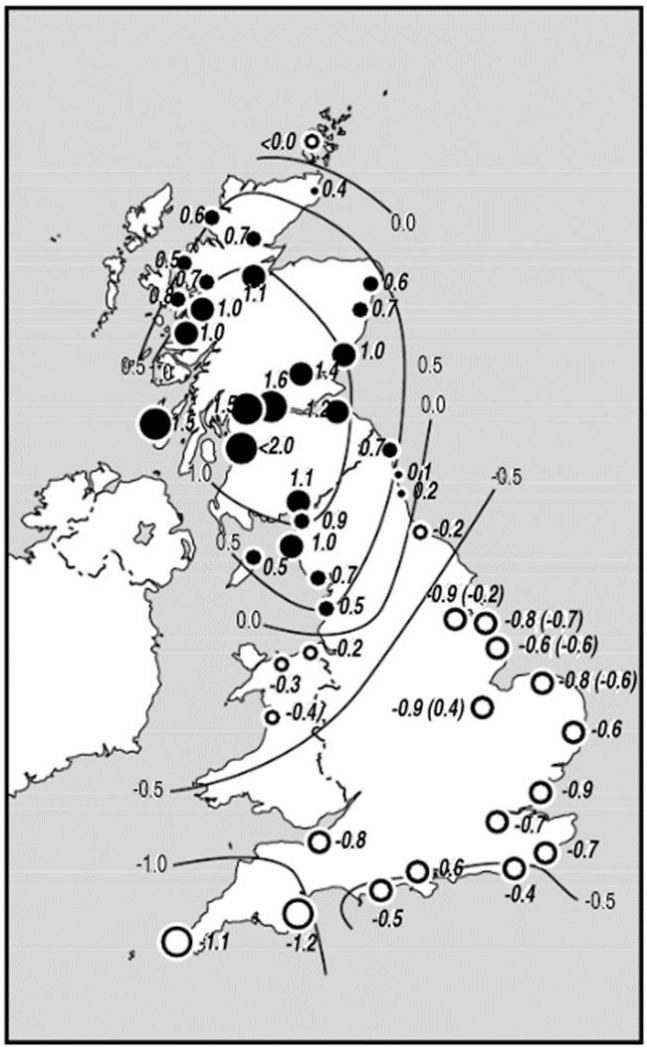


Figure 5-13 relative land-/ sea-level changes (mm $yr^{-1}$) in Great Britain, positive values indicate relative land uplift or sea-level fall, negative values are relative land subsidence or sea-level rise, (Shennan and Horton, 2002).

Our approach using Pethick's equation for estimating carbon burial is based on sedimentation of each point of elevation across marshes from low to high marsh, and carbon content. While (Cannell, *et al.*, 1999) assumed that sedimentation across the whole area of every marsh maintains its pace with local level in sea rise regardless of the position of the sedimentation. However, there are notable variations in sedimentation positions across marshes from low to high. The low marsh area is frequently inundated and receives a large amount of sediment by tides. Although, a large amount of sediment occurs in the

low marsh, sedimentation can be zero in the marsh which is much higher than MHWS such as Morecambe Bay in Solway. Therefore, this part of the marsh will not receive sediment until submerged during storm events. Additionally, in eroding mashes, sedimentation cannot be stable in one position of the low marsh and will be variable depending on duration of inundation such as Tollesbury and Fambridge (Figure 5.10, Tollesbury as example). So, variations of sedimentation are linked to the position of the site on the marsh and the accretion is identified in the marshes' back at a lower rate as compared to the rest of the marsh (Cundy and Croudace, 1995; 1996).

Allen (1990) reported that the major source of organogenic sediment is where there is a high shore transition in the back of the marsh. As well as the transitions to *Phragmites* marshes discussed above. (Kelleway, Saintilan *et al.*, 2017) measured deposition rates between different species of marsh vegetation and indicated that *Juncus kraussii* was the dominant contributor of matter to soils in the high marsh areas. This may lie behind the accumulation of organic rich sediments at a relatively high level on the Llanridian marsh, where the vegetation is dominated by *Juncus maritimus* (Goodwin, 1983).

50 studies measuring carbon burial in saltmarshes were summarised by (Ouyang and Lee, 2014). Of these, 64 % used radionuclide markers ($^{137}Cs$, $^{210}Pb$) to measure sediment accumulation rates, whereas 27 % used marker horizons. Although there are different models for estimating sedimentation rates across saltmarsh (Allen, 1990, Pethick, 1981, Temmerman *et al.*, 2004), mechanisms of sedimentation might be variable across marshes. Sedimentation rates across marshes are temporally and spatially variable, even within a small area (Carling 1982), and depending on the elevational impact on inundation frequency, and suspended sediment can occur in pathways of water movement (French, 1993).

The role of vegetation colonisation on the rate of sedimentation was also explored, whereby, it was suggested that it could increase the sedimentation rate of different parts of the marsh. At Welwick marsh, on a smaller scale, there are some observations of the way in which vegetation colonisation at the marsh edge increases the sedimentation rate leading to raised vegetated bumps separated by unvegetated areas (Brown, Warman *et al.*, 1999). (Alizai and McManus, 1980) observed that up to 2.6 kg $m^2$ of sediment can be stored in different parts across a marsh within reed stems that are broken *(Phragmites)* in Scotland's Tay Estuary. Stumpf (1983) revealed that the retention of sediment by *Spartina alterniflora* extended to 50% of the lost material from suspension in a small Delaware marsh. (Kelleway, Saintilan *et al.*, 2017) found different rates of sediments between vegetations in different parts across saltmarshes.

A further finding was that, rates of sedimentation could also be affected by the extent of closed vegetation (Adam, 1993). In some cases, the low areas are where marshes are eroding, such as the natural marsh at Tollesbury (Figure 5.10). However, assuming that these low areas are accreting may not align with reality, since erosion can influence sedimentation rates across the whole marsh or specific areas of the marsh. The marsh platform occurs in the same position, and there are alternating phases of erosion and deposition (Harmsworth and Long, 1986) that can occur at the marsh edge. This can be due to accretion occurring on the outer edge, leading to a relatively steep gradient, and wave energy that is concentrated on this gradient leading to erosion, developing into a cliff. Hence, a pioneer marsh may then develop at the foot of the cliff, leading to a terrace on the marsh that continues to move in a landwards direction. This cycle of erosion and deposition can occur when the main channel lies close to that bank, and deposition occurs when the channel moves over to be closer to the opposite bank. (Harmsworth and Long,

1986) observed that an identified variation in the erosion cycle and deposition occurs across the marsh. As such, at Dengie saltmarsh, the rate of erosion was notable between 1978 and 1981, and from 1960 to 1970 when there occurred a period of slow marsh building. Nevertheless, various qualitative differences in the deposition and erosion cycles can also be identified (Harmsworth and Long, 1986). Sediment measurements in short intervals can be variable in terms of the rate of accretion in the lower marsh areas due to phases of erosion by the incidence of storms (Adam, 1993, Harrison and Bloom, 1977).

The influence of wind-borne sand on mechanisms of sedimentation on the high marsh areas was further examined where it was observed to exert an influence. This might pose an issue due to the transport of coarser material during storm surges such as Morecambe Bay and river Mersey marshes (Goodwin and Mudd, 2019). Marshall, (1962) observed higher fractional percentages of silt and clay and almost all of the saltmarsh material comes from eroding zones at Morecambe Bay. In regions with macro- or meso- tidal regimes, wind-borne sand may settle in the upper marsh zone due to strong winds particularly through extensive sand flats in the low shore areas (Adam, 1993). Morecambe Bay marsh area is considered to be the biggest marsh in the UK (Adam, 1993). Although, the area of this marsh is vast, the predicted of the average carbon burial is notably low at 80 g $CO_2/m^2/yr$ (Table 5.2).

Although, the range of $CH_4$ and $N_2O$ emissions from saltmarshes might be negligible compared to the range of carbon burial (Callaway *et al.*, 2012, Connor *et al.*, 2001, Livesley and Andrusiak, 2012), $CH_4$ emissions can be produced much higher in freshwater marshes, such as those dominated by *Phragmites* (DeLaune, Smith *et al.*, 1983). In landward sections of saltmarshes, transition to freshwater marshes can occur where there is freshwater run-off in ground water or where the area of wetland that develops is so extensive that

freshwater does not completely drain off at low tide. Therefore, saline influence gradually becomes limited to the areas adjacent to the tidal channels and as sulphate concentrations are low, large quantities of methane ($CH_4$) can be produced. These transitions from saltmarsh to freshwater marsh and fen used to cover extensive areas in eastern England from the Humber to the Thames and around the Severn Estuary, but most of the area of these freshwater wetland have been reclaimed for agriculture. An extensive transition from a high salinity saltmarsh to a *Phragmites* marsh does occur at Cley in North Norfolk. In this marsh, there is a project to recreate large areas of *Phragmites* marsh, although at the moment none of this is adjacent to salt marshes (https://www.norfolkwildlifetrust.org.uk). For some time after *Phragmites* marsh is created, the benefits of carbon burial are likely to be outweighed by methane emissions. However, from decades to centuries the increased $CH_4$ emissions might be outweighed by carbon burial, as the lifetime of methane in the atmosphere is finite while carbon burial is essentially permanent.

Ecologically, sediment can be deposited by vegetation across saltmarshes leading to a rise in the surface of marshes. Hence, the inundation frequency and the influence of saline water will be reduced, and sediment redox is increased, which then allows ecological succession to take place. However, researchers have failed to find evidence that succession occurs on saltmarshes, particularly the type that represents a temporal succession of vegetation (Olff *et al.*, 1997, Wolters *et al.*, 2005). The transitional communities between saltmarsh and terrestrial vegetation are rarely on land reclamation. This might occur in very low lying areas where land claims an extensive impact on the transition to *Phragmites,* such as the Severn Estuary marsh. However, where there is significant gradient of the terrestrial land surface, such as at Stiffkey and Warham, the transition zone will always have been

over the space of a few metres horizontally, and as such, there is a narrow band of *Sueada vera* and *Elytrigia* on the top edge of the marsh at Stiffkey.

Overall, the elevations across saltmarsh present variable in sedimentation from low to high marshes, which result in variations in the rates of the accumulation from low to high marshes (Ouyang and Lee, 2014). Carbon burial rates can be changed depending on the area extent and elevation changes in habitats such as saltmarsh (Duarte *et al.*, 2005). The distinguished elevation distribution can indicate carbon accumulation rates, which was confirmed by (Wang *et al.* 2019). The marsh area and elevation are significant in terms of estimating overall sedimentation and carbon burial. Most of the marshes discussed here have high sedimentation rates in the low marsh areas. However, low marsh areas are small compared to the high marsh areas in the same marshes ((CCP), 2021). There are also morphodynamical factores such as tidal flcutuations leading to cycle of erosion and deposition that might make a difference in sedimentation across saltmarsh elevations, leading to variations in estimated carbon burial and GHG emissions. Mechanisms of sedimentation and vegetation succession appear to be variable and unstable, whether across the whole saltmarsh or of different parts in an individual marsh.

### 5.3.4 Conclusion

In this chapter, the findings ahow that most of the marshes examined have high redox which point that GHG emissions reduced. the bulk of UK saltmarsh area is likely to be relatively well oxygenated, so $N_2O$ and methane production will be relatively unimportant.The range of $CH_4$ and $N_2O$ emissions from saltmarshes appears to be negligible compared to the range of carbon burial for all marshes here. The variation of elevations across marsh play a crucial role of determining the amount of sediment which can be deposited within tidal duration. there will be limited sedimentation across substantial areas of marsh, particularly in the northern half of the UK. For marsh platforms that are at or below the level of MHWS, sedimentation will keep pace with sea level rise. There are small areas of low marsh where sedimentation rates may be higher than this, but these are, almost by definition, transitory in their occurrence such as Welwick and unless something has led to the development of a new marsh, they probably often undergo cyclical erosion and redeposition. This morphodynamical process might alter the amount of carbon burial which result in variations of GHG emissions across marsh. Due to the variations of sedimentation mechanisms which can be morphodinamically occurred across marshes, there will be difficulties of considering that saltmarsh is uniform gradients of gradually reducing sedimentation rates.

# Chapter six

## General discussion

### 6.1 General discussion

Saltmarshes deliver diverse and important ecosystem services, encompassing coastal protection, carbon sequestration, tourism, and nurseries for fish, crabs and other animals (Costanza, Pérez-Maqueo *et al.*, 2008). The assessment of ecosystem services provided by saltmarshes in the literature (Adams, Andrews *et al.*, 2012, Ford, Garbutt *et al.*, 2012, King and Lester, 1995, Möller, 2006, Möller and Spencer, 2002, Möller, Spencer *et al.*, 1999), have usually calculated ecosystem services delivered by saltmarshes on the assumption that they can be treated as a homogeneous object. They do not consider the substantial heterogeneity of their ecology and biogeochemical functioning, particularly that driven by their elevation in the tidal frame. Therefore, the overarching aim of this research regarded the assessment of the extent to which considering saltmarsh elevations altered estimates of the ecosystem services that were provided in the UK saltmarshes. The premise of this study was to determine the elevation and relative tidal height characteristics of 35 saltmarshes around the UK and the consequences of this for ecosystem service delivery.

The 35 saltmarshes were chosen to cover all the areas of the UK where there are substantial areas of saltmarsh (Table 2.1, Chapter 2). LIDAR data has been widely used to examine saltmarsh environments (Hladik and Alber, 2012; Schmid et al., 2011; Wang et al., 2009), and this thesis confirms that saltmarsh topography can be successfully characterised by LiDAR data. However, there are two types of elevation data DTMs and DSMs need to be investigated to identify which one is reliable to estimate elevations of the surface of the sediment on the marsh. The DSMs fails to estimate surface elevation in creeks and sets the elevation to NaN (plotted in white on the DSMs) (Fig. 2.5, Chapter 2), while the DTMs

algorithm makes reasonable estimates of the elevations of the bottoms of the creeks. Additionally, the DTMs can also successfully remove trees and shrubs such as gorse (*Ulex europeaus*) in areas adjacent to the saltmarsh and removes some of the herbaceous vegetation on the saltmarsh itself (Chapter 2).

Comparisons between GPS estimates and DTM of elevation on the salt marsh surface showed that in most cases the DTM estimated elevations of the surface of the sediment on the marsh with an accuracy better than 20 cm (Fig 2.11, Chapter 2). The great majority of saltmarsh areas were correctly identified using the UK landcover map (Rowland, Morton *et al.*, 2017), with only a small number of polygons needing to be removed manually, and no areas needing to be added in (Table 2.1, Chapter 2). Elevations of pixels occupied by saltmarsh could then be extracted from LIDAR data (Chapter 2 and 3) rather than relying on unsupervised classification of LIDAR data alone (Goodwin et al, 2018).

The ecological literature on saltmarshes focusses on succession and usually represents them as showing an approximately constant gradient from pioneer communities at an elevation just above MHWN to high marsh and transitional communities at elevations around those reached by the highest tides(Prahalad, et al. 2019; Doody, 2008; Boorman, 2003b; Adnitt 2007). By contrast, the elevations of the UK saltmarshes studied here often have a frequency distribution which displays a relatively tight peak, corresponding to the presence of sub-horizontal platforms on the upper marsh (Goodwin et al., 2018, Möller, 2006). Data on the elevations corresponding to mean high water of spring and neap tides (MHWS and MHWN) from (Mossman et al. 2012 a) and (UK Hydrographic Office, 2014) show that most of these marsh platforms from the Humber Estuary on the East coast moving in clockwise to the Dovey Estuary on the West coast occur at or below the level of MHWS (Fig. 3.15, Chapter 3). This is consistent with models of marsh development in the

geomorphological literature which note that limited sediment deposition is possible on the high marsh as the number of annual inundations is low (Pethick, 1981). If isostatic sea level rise is occurring, then these models predict the development of a marsh platform at the elevation where sediment deposition is equal to the rise in sea level. Furthermore, where there are high suspended concentrations of sediment, such as the Severn Estuary, the amount of sediment deposited per tidal inundation is greater and marsh platforms develop at slightly higher elevations than in areas where suspended sediment concentrations are lower (Allen, 1991; Allen, 1990; Kirby and Parker, 1982).

In these parts of the UK, the area of marsh that is above the level of MHWS is usually small, although on some marshes (such as Stiffkey, Fig. 3.2 and 3.3, Chapter 3) levees along creek banks lie just above the level of MHWS. Other areas above MHWS such as Erth Island result from isostatic lift, deposition of organogenic sediments, high input of fluvial sediments (Ranwell and Rosalind, 1986), transportation of sediments during storm surges or pre-existing topography. In the past a number of marshes in the South and East England would have undergone transition to *Phragmites* fen at their landward boundaries and deposition of peat would have led to sediment accumulation above the level of MHWS. However, almost all these areas have been claimed for agricultural use (Hughes and Paramor, 2004). An exception where organogenic sediment accumulation may be occurring is the Llanrihidian marsh in south Wales where there is a relatively large area above the level of MHWS. Soils here are high in organic matter and the vegetation is dominated by *Juncus maritimus* (Goodwin, 1983) a species associated with organogenic sediments elsewhere. By contrast, in Northwest England and Scotland a number of marshes have substantial areas that lie above MHWS. This is likely to be a consequence of isostatic sea level fall. In almost all areas, low marshes make up only a small proportion of the total saltmarsh area.

The implication of the variation in the elevation of the saltmarshes is that, it influences sedimentation rates and the effectiveness of the marshes in dissipating wave energy as well as protecting or preserving the coastal ecosystems. In most cases, however, the saltmarshes lie at or just below the MHWS. In addition, there are only limited areas where the pioneer marsh can continue to extend outwards over a long period of time, as has been observed at Welwick on the Humber estuary. This marsh is unique in comparison to the other examined marsh profiles since in most instances, marshes are part of an equilibrium with the estuarine channel and cannot extend further out into the estuary because the need to dissipate tidal energy. In turn, this makes them increasingly vulnerable to erosion as they extend outwards and can lead to steep gradients in the pioneer zones at the seaward edge of marshes, such as at Stiffkey and Warham, and in other cases the formation of a vertical cliff at the seaward edge. Steep gradients are, however, not invariably present and the seaward edge of the marsh. At Frampton and Welwick, for example, there is only a slight change in elevation at the seaward edge of the marsh.

The badly eroding marshes such as Tollesbury in the Blackwater Estuary and North Fambridge marshes (Crooks, Schutten *et al.*, 2002) were reclaimed for long period ago. Reclaim marsh platform lie between MHWS and MHWN, which considered to be low marsh, but in this particular marsh, accretion rates can be changed significantly during long periods (Shi, 1993). Some marshes lie above the level of MHWS due to the deposition of substantial amounts of sediment that is concentrated in areas such as the Severn Estuary marshes.

The understanding of the distribution of elevations for ecosystem service delivery leads to implications in this research. First, some marshes have extended to a considerable size. The second implication is that some of the marshes also have extensive areas at higher

elevation than MHWS, particularly where land reclamation has not occurred and the land area vulnerable to coastal flooding is small. The high elevation of saltmarshes at these sites mean that these saltmarshes are able to reduce flooding during storm surges.

There are significant relationships between wave dissipation and water depth over the salt marsh. As water depth decreases wave dissipation decreases across saltmarsh (Möller and Spencer, 2002, Yang, Shi *et al.*, 2012), (Table 4). This will reduce the vulnerability of the seawall to wave action during normal high tides. However, saltmarshes are less effective against flooding during storm surge events, such as when water height overtops the crest of the seawall at the peak of 3.48 above MHWS such as Blakeney in the UK during 2013 storm (Table 4.1) the seawall could be broken or damaged by waves, when the water level overtops the seawall's crest (Masselink *et al.*, 2016),(Chapter 4).

The role of saltmarshes in reducing risks of coastal flooding by dissipating wave energy has played a prominent role in argument in favour of managed realignment and more formal assessment of the ecosystem services that they deliver. Saltmarsh environments can significantly attenuate incident waves as compared to unvegetated sand/mudflats (Brampton, 1992, Möller and Spencer, 2002). These environments are, therefore, fundamental to sustainable shoreline protection and contribute to wave energy attenuation during large storms (Gedan, Kirwan *et al.*, 2011, Möller, Kudella *et al.*, 2014). Marshes also have the ability to attenuate large frequent waves and reduce flood peaks.

The areas that are most vulnerable to coastal flooding are in South and East England where the construction of seawalls has led to extensive land claims (Hughes and Paramor, , 2004). This thesis shows that the presence of saltmarshes to seawards of this will help to protect sea walls from wave action during normal tidal conditions. However, most of the saltmarsh area is at elevations at or below the level of MHWS, which is approximately 2.5m lower

than the water level during storm surges that occurred in the two recent biggest storm surge events in 1953 and 2013 (Table 4.1, Chapter 4). Saltmarshes can't be effective in reducing potential seawall overtopping, and 71 wave events through saltmarsh that overtopped a seawall with 0.4m (ODN) at Dengie (Möller and Spencer, 2002). Some dissipation of wave energy will occur in this depth of water, but waves will still reach the sea wall so their contribution in reducing risks of flooding during storm surge events is much less important (Chapter 3 and 4). By contrast, saltmarsh elevations are above (MHWS) in the Northern west of England and Scotland (Figure 3.29). These marshes will be more effective in dissipating wave energy during storm surge events, but rather few of the saltmarshes in these areas are observed to be low-lying in nature, thereby, being vulnerable to flooding (Chapter 3 and 4).

Blue carbon ecosystems, including saltmarshes, play a greater role in the global carbon cycle due to their storage of organic carbon in saltmarsh soils. The origin of organic carbon stored in saltmarsh soils, which may be allochthonous or autochthonous. The origin of organic carbon is either in the form of freshly deposited sediment (allochthonous source), or aboveground and belowground biomass of vegetation (autochthonous sources). There are some factors their sedimentation such as surface elevation and distance to a sediment source, which have been found to determine the spatial patterns of sediment deposition, are also important factors determining the relative contribution of allochthonous to topsoil organic carbon stocks of saltmarshes (Mueller et al.,2019). Saltmarsh environments fix more $CO_2$ from the atmosphere annually than most other natural ecosystems. Organic carbon gets deposited onto marshes in sediment with much of the carbon being oxidised and converted back to $CO_2$. However, some of the carbon is buried in long-term leading to its subsequent elimination from the atmosphere. GHG emissions are also observed in cases

where sediments are anoxic as some of the carbon is converted by methanogenic microorganisms to methane and some nitrogen compounds are converted by denitrification or nitrification to $N_2O$.

Previous researchers have attempted to investigate the redox potential of saltmarshes in different parts of the globe including in the UK. Much of the findings reported have focused on identifying the association between carbon burial and salinity of the saltmarshes as well as the influence of sea levels. Our work goes beyond what is currently known in previous research studies by considering the levels of sedimentation and elevation of the marshes as influential factors in calculating carbon burial for elevated saltmarshes. The importance of reporting elevation amongst the metadata for work on GHG production and carbon burial mentioning that most studies give only the vaguest of information about tidal levels., in addition, (Mason, Choi *et al.*, 2012) don't even mention redox, and the individual studies of GHG emissions do so, even though it is a key determinant of biogeochemical functions.

The redox potential increases when elevation increases across saltmarshes (Davy et al., 2011), and the predicted of redox potential of most of the marsh areas here have high redox which provide a clear indication of GHG level. Therefore, redox potential can be more important than salinity of providing information regarding places where GHG emissions occur across saltmarshes. Most of These marshes' platforms lie at or above MHWS which indicated that lower sediment occurred and GHG emissions reduced. The range of values of $CH_4$ and $N_2O$ emissions from saltmarshes (Fig. 5.1, Chapter 5) appears to be negligible compared to the range of carbon burial (Callaway et al., 2012; Connor et al., 2001; Livesley and Andrusiak, 2012), however, $N_2O$ emission is a little higher. This might be due to the process conditions of both Methanogenic and denitrification in saltmarsh sediment (Chapter 5).

The changes in elevations across marsh can determine the amount of sediment which can be deposited within tidal duration. This will influence the amount of carbon burial in the sediment which result in variations of GHG emissions across marsh. Most of the marshes discussed here are predictably to have high sedimentation rates in the low marsh areas. However, low marsh areas are small compared to the high marsh areas in the same marshes (((CCP), 2021) Fig.5.6, Chapter 5). There are also morphodynamical factors might make a difference in sedimentation across saltmarshes, which may result in variations of estimating carbon burial and GHG emission. Mechanisms of sedimentation and vegetation succession appears to be variable and unstable, whether across the whole saltmarsh or in different parts in an individual marsh (Chapter 5). Therefore, it will be informative in the future work to examine sedimentation in each small scale of elevation of different positions of the marsh.

**6.2 Suggestions for future research**

Despite the novel findings identified in this research, most of the tests, experiments and adaptations should be completed in future. Understanding sedimentation across saltmarsh elevation needs to be considerable. Previous studies estimated higher sedimentation rates in low marshes and lower sedimentation rates in high marshes using different models (Allen, 1990; Pethick, 1981; Temmerman et al., 2004). Our observations that the area of the high marsh is much greater than that of low marsh, and sedimentation can occur extensively in small scale of elevation, and different positions across saltmarsh whether in low or high marsh (Cundy and Croudace, 1996; Cundy and Croudace, 1995). In the low marshes a cycle of erosion and deposition can occurs (Harmsworth and Long, 1986), which leads to little permeant sedimentation. In the high marsh, sedimentation might occur rather than low marsh (Goodwin and Mudd, 2019). It is also relevant that big chunks of

marsh in NW England and Scotland are very high in the tidal frame so will not accumulate any additional carbon due to the rise in sea levels. This is indicative that it will be informative to extend field work measurements considering the high and low marsh area which fall into small scale of elevations across saltmarsh. This will determine sedimentation positions across saltmarsh in the reality and how carbon burial can be variable across marsh elevations. In addition, it is recommended that in future studies, fieldwork focuses on the biggest uncertainties regarding suspended sediment concentrations and soil organic matter content.

## 6.3 Conclusion

This research reveals that although saltmarshes play an integral role in the delivery of diverse ecosystems services ranging from coastal protection to carbon sequestration and provision of habitats for birds and other animals, there is need to assess their services from a heterogenous perspective rather than a position of homogeneity. This work has extended previous research regarding delivery of ecosystem services in saltmarshes by considering the influence of substantial differences in their ecology, particularly driven by elevation and sedimentation rates. Most of the marshes examined have high redox which point that GHG emissions reduced. The findings emphasise that elevation of the saltmarshes and deposition of sediments accounts for significant performance in services such as wave dissipation and redox potential. As a result, the insights from this research on how elevation and sedimentation affect wave dissipation and GHG emissions as well as carbon burial serve as an important input for policy and practice on the reclamation of saltmarshes.

## 7. References


Abril, G., Nogueira, M., Etcheber, H., Cabeçadas, G., Lemaire, E. and Brogueira, M. 2002. Behaviour of organic carbon in nine contrasting European estuaries. *Estuarine, Coastal and Shelf Science* 54(2) 241-262.

Adam, P. 1978. Geographical variation in British saltmarsh vegetation. *The Journal of Ecology* 339-366.

Adam, P. 1993. *Saltmarsh ecology*: Cambridge University Press.

Adam, P. 2002. Saltmarshes in a time of change. *Environmental conservation* 29(1) 39-61.

Adams, C., Andrews, J. and Jickells, T. 2012. Nitrous oxide and methane fluxes vs. carbon, nitrogen and phosphorous burial in new intertidal and saltmarsh sediments. *Science of the Total Environment* 434 240-251.

Adams, C.A. 2008. Carbon burial and greenhouse gas fluxes of new intertidal and saltmarsh sediments. University of East Anglia.

Adnitt, C. 2007. Saltmarsh management manual.

Alizai, S. and McManus, J. 1980. The significance of reed beds on siltation in the Tay Estuary. *Proceedings of the Royal Society of Edinburgh, Section B: Biological Sciences* 78(3-4) s1-s13.

Allen, J. 1990. Salt-marsh growth and stratification: a numerical model with special reference to the Severn Estuary, southwest Britain. *Marine Geology* 95(2) 77-96.

Allen, J. 1991. Fine sediment and its sources, Severn Estuary and inner Bristol Channel, southwest Britain. *Sedimentary geology* 75(1-2) 57-65.

Allen, J. and Rae, J. 1986. Time sequence of metal pollution, Severn Estuary, southwestern UK. *Marine Pollution Bulletin* 17(9) 427-431.

ALLEN, J. R. 2000. Morphodynamics of Holocene salt marshes: a review sketch from the Atlantic and Southern North Sea coasts of Europe. Quaternary Science Reviews, 19, 1155-1231.

Alongi, D.M. 1998. *Coastal ecosystem processes*.

Anders, N., Valente, J., Masselink, R. and Keesstra, S. 2019. Comparing Filtering Techniques for Removing Vegetation from UAV-Based Photogrammetric Point Clouds. *Drones* 3(3) 61.

Anderson, M.E. and Smith, J. 2014. Wave attenuation by flexible, idealized salt marsh vegetation. *Coastal Engineering* 83 82-92.

Andrew, M.E. and Ustin, S.L. 2009. Habitat suitability modelling of an invasive plant with advanced remote sensing data. *Diversity and Distributions* 15(4) 627-640.

Andrews, J., Burgess, D., Cave, R., Coombes, E., Jickells, T., Parkes, D. and Turner, R. 2006. Biogeochemical value of managed realignment, Humber estuary, UK. *Science of the total environment* 371(1) 19-30.

Andrews, J., Samways, G., Dennis, P. and Maher, B. 2000. Origin, abundance and storage of organic carbon and sulphur in the Holocene Humber Estuary: emphasizing human impact on storage changes. *Geological Society, London, Special Publications* 166(1) 145-170.

Andrews, J., Samways, G. and Shimmield, G. 2008. Historical storage budgets of organic carbon, nutrient and contaminant elements in saltmarsh sediments: Biogeochemical context for managed realignment, Humber Estuary, UK. *Science of the total environment* 405(1) 1-13.

Arzandeh, S. and Wang, J. 2003. Monitoring the change of Phragmites distribution using satellite data. *Canadian Journal of Remote Sensing* 29(1) 24-35.

Assessment, M.E. 2005. Ecosystems and human well-being: wetlands and water. *World resources institute, Washington, DC* 5.

Association of British Insurers (ABI) 2005, Financial Risks of Climate Change, Summary Report, ABI,London, England

Barbier, E.B., Hacker, S.D., Kennedy, C., Koch, E.W., Stier, A.C. and Silliman, B.R. 2011. The value of estuarine and coastal ecosystem services. *Ecological monographs* 81(2) 169-193.

Barthelme, S. 2017. imager: image processing library based on 'CImg'. *R package version 0.40* 2 357.

Bartlett, K.B., Bartlett, D.S., Harriss, R.C. and Sebacher, D.I. 1987. Methane emissions along a salt marsh salinity gradient. *Biogeochemistry* 4(3) 183-202.

Bartlett, K.B., Harriss, R.C. and Sebacher, D.I. 1985. Methane flux from coastal salt marshes. *Journal of Geophysical Research: Atmospheres* 90(D3) 5710-5720.

Bankoff, G., 2013. The'English Lowlands' and the North Sea basin system: A history of shared risk. Environment and History, 19(1), pp.3-37.

Baugh, L., 2019. Spatial analysis of blue carbon in a UK saltmarsh: Implications of carbon distribution (Doctoral dissertation, Liverpool John Moores University (United Kingdom)). Bayliss-Smith, T., Healey, R., Lailey, R., Spencer, T. and Stoddart, D. 1979. Tidal flows in salt marsh creeks. *Estuarine and Coastal Marine Science* 9(3) 235-255.

Bertness, M.D. 1991. Interspecific interactions among high marsh perennials in a New England salt marsh. *Ecology* 72(1) 125-137.

Bertness, M.D. and Ellison, A.M. 1987. Determinants of pattern in a New England salt marsh plant community. *Ecological monographs* 57(2) 129-147.

Beumier, C. 2008. Building verification from disparity of contour points. 2008 First Workshops on Image Processing Theory, Tools and Applications, IEEE.

Bhuvaneswari, K., Dhamotharan, R. and Radhakrishnan, N. 2011. Remote sensing satellite data for Coastal Ecosystem and Human Interaction-A Case study in Tamilnadu, India. *International Journal of Computer Information Systems* 2(4) 77-81.

Bivand, R., Keitt, T., Rowlingson, B., Pebesma, E., Sumner, M., Hijmans, R., Rouault, E. and Bivand, M.R. 2015. Package 'rgdal'. *Bindings for the Geospatial Data Abstraction Library. Available online: https://cran. r-project. org/web/packages/rgdal/index. html (accessed on 15 October 2017)*.

Bivand, R. and Rundel, C. 2017. rgeos: interface to geometry engine-open source (GEOS). *R package version 0.3-26*.

Blackwell, M.S., Yamulki, S. and Bol, R. 2010. Nitrous oxide production and denitrification rates in estuarine intertidal saltmarsh and managed realignment zones. *Estuarine, Coastal and Shelf Science* 87(4) 591-600.

Bockelmann, A.-C., Bakker, J.P., Neuhaus, R. and Lage, J. 2002. The relation between vegetation zonation, elevation and inundation frequency in a Wadden Sea salt marsh. *Aquatic botany* 73(3) 211-221.

Boorman, L. 2003a. Saltmarsh review. *An overview of coastal saltmarshes, their*.

Boorman, L. 2003b. SALTMARSH REVIEW An overview of coastal saltmarshes, their dynamic and sensitivity characteristics for conservation and management. *REPORT-JOINT NATURE CONSERVATION COMMITTEE*(334).

Boorman, L., Hazelden, J. and Boorman, M. 2002. New salt marshes for old-salt marsh creation and management. Littoral.

Boorman, L., Pakeman, R., Garbutt, R. and Barratt, D. 1996. *Effect of Environmental Change on European Salt Marshes: Structure, Functioning and Exchange Potentialities with Marine Coastal Waters. Vol. 5: Results of the Institute of Terrestrial Ecology, England*.

Boorman, L.A. 1999. Salt marshes–present functioning and future change. *Mangroves and Salt Marshes* 3(4) 227-241.

Brampton, A. 1992. Engineering significance of British saltmarshes. *Saltmarshes: Morphodynamics, conservation and engineering significance* 115-122.

Brovelli, M.A., Cannata, M. and Longoni, U.M. 2004. LIDAR data filtering and DTM interpolation within GRASS. *Transactions in GIS* 8(2) 155-174.

Brown, S., Warman, E., McGrorty, S., Yates, M., Pakeman, R., Boorman, L., Goss-Custard, J. and Gray, A. 1999. Sediment fluxes in intertidal biotopes: BIOTA II. *Marine Pollution Bulletin* 37(3-7) 173-181.

Burd, F. 1989. *Saltmarsh survey of Great Britain: an inventory of British Saltmarshes*.

Burger, M., Van Vuren, J., De Wet, L. and Nel, A. 2019. A comparison of water quality and macroinvertebrate community structure in endorheic depression wetlands and a salt pan in the Gauteng province, South Africa. *Environmental monitoring and assessment* 191(1) 1-21.

Byrd, K.B. and Kelly, M. 2006. Salt marsh vegetation response to edaphic and topographic changes from upland sedimentation in a Pacific estuary. *Wetlands* 26(3) 813-829.

Cahoon, D.R. and Lynch, J.C. 1997. Vertical accretion and shallow subsidence in a mangrove forest of southwestern Florida, USA. *Mangroves and Salt Marshes* 1(3) 173-186.

Cahoon, D.R. and Reed, D.J. 1995. Relationships among marsh surface topography, hydroperiod, and soil accretion in a deteriorating Louisiana salt marsh. *Journal of Coastal Research* 357-369.

Callaway, J., DeLaune, R. and Patrick Jr, W. 1996. Chernobyl 137Cs used to determine sediment accretion rates at selected northern European coastal wetlands. *Limnology and Oceanography* 41(3) 444-450.

Callaway, J.C., Borgnis, E.L., Turner, R.E. and Milan, C.S. 2012. Carbon sequestration and sediment accretion in San Francisco Bay tidal wetlands. *Estuaries and Coasts* 35(5) 1163-1181.

Canfield, D.E., Kristensen, E. and Thamdrup, B. 2005. The methane cycle. *Advances in Marine Biology*. Elsevier. pp. 383-418.

Cannell, M., Milne, R., Hargreaves, K., Brown, T., Cruickshank, M., Bradley, R., Spencer, T., Hope, D., Billett, M. and Adger, W. 1999. National inventories of terrestrial carbon sources and sinks: the UK experience. *Climatic Change* 42(3) 505-530.

Capone, D.G. and Kiene, R.P. 1988. Comparison of microbial dynamics in marine and freshwater sediments: Contrasts in anaerobic carbon catabolism 1. *Limnology and oceanography* 33(4part2) 725-749.

Capooci, M., Barba, J., Seyfferth, A.L. and Vargas, R. 2019. Experimental influence of storm-surge salinity on soil greenhouse gas emissions from a tidal salt marsh. *Science of the total environment* 686 1164-1172.

Carling, P. 1982. Temporal and spatial variation in intertidal sedimentation rates. *Sedimentology* 29(1) 17-23.

Castillo, J., Fernández-Baco, L., Castellanos, E., Luque, C., Figueroa, M. and Davy, A. 2000. Lower limits of Spartina densiflora and S. maritima in a Mediterranean salt marsh determined by different ecophysiological tolerances. *Journal of Ecology* 88(5) 801-812.

Cawkwell, F.G., Dwyer, N., Bartlett, D., Ameztoy, I., O'Connor, B., O'Dea, L., Hills, J., Brown, A., Cross, N. and O'Donnell, M. 2007. Saltmarsh habitat classification from satellite imagery. Bolzano, Italy.

C.C.P. 2021. Global Mean Sea Level Rise (GMSLR) [online]: Centre for Climate Adaptation [Accessed 20.2.2021 2021].

Chapman, V.J. 1960. Salt marshes and salt deserts of the world.

Chassereau, J.E., Bell, J.M. and Torres, R. 2011. A comparison of GPS and lidar salt marsh DEMs. *Earth Surface Processes and Landforms* 36(13) 1770-1775.

Chen, G., Ye, Z., Jin, R., He, J., Wu, J. and Gu, J. 2021. Spatial-temporal Distribution of Salt Marshes in Intertidal Zone of China during 1985-2019.

Chen, Y., Chen, G. and Ye, Y. 2015. Coastal vegetation invasion increases greenhouse gas emission from wetland soils but also increases soil carbon accumulation. *Science of the Total Environment* 526 19-28.

Chini, N., Stansby, P., Leake, J., Wolf, J., Roberts-Jones, J. and Lowe, J. 2010. The impact of sea level rise and climate change on inshore wave climate: A case study for East Anglia (UK). *Coastal Engineering* 57(11-12) 973-984.

Chmura, G.L., Anisfeld, S.C., Cahoon, D.R. and Lynch, J.C. 2003. Global carbon sequestration in tidal, saline wetland soils. *Global biogeochemical cycles* 17(4).

Chmura, G.L., Kellman, L. and Guntenspergen, G.R. 2011. The greenhouse gas flux and potential global warming feedbacks of a northern macrotidal and microtidal salt marsh. *Environmental Research Letters* 6(4) 044016.

Chust, G., Galparsoro, I., Borja, A., Franco, J. and Uriarte, A. 2008. Coastal and estuarine habitat mapping, using LIDAR height and intensity and multi-spectral imagery. *Estuarine, Coastal and Shelf Science* 78(4) 633-643.

Cid, A., Menéndez, M., Castanedo, S., Abascal, A.J., Méndez, F.J. and Medina, R. 2016. Long-term changes in the frequency, intensity and duration of extreme storm surge events in southern Europe. *Climate Dynamics* 46(5-6) 1503-1516.

Collin, A., Long, B. and Archambault, P. 2010. Salt-marsh characterization, zonation assessment and mapping through a dual-wavelength LiDAR. *Remote Sensing of Environment* 114(3) 520-530.

Connor, R.F., Chmura, G.L. and Beecher, C.B. 2001. Carbon accumulation in Bay of Fundy salt marshes: implications for restoration of reclaimed marshes. *Global Biogeochemical Cycles* 15(4) 943-954.

Costanza, R., Pérez-Maqueo, O., Martinez, M.L., Sutton, P., Anderson, S.J. and Mulder, K. 2008. The value of coastal wetlands for hurricane protection. *AMBIO: A Journal of the Human Environment* 37(4) 241-248.

Craft, C., Megonigal, P., Broome, S., Stevenson, J., Freese, R., Cornell, J., Zheng, L. and Sacco, J. 2003. The pace of ecosystem development of constructed Spartina alterniflora marshes. *Ecological Applications* 13(5) 1417-1432.

Crooks, S., Schutten, J., Sheern, G.D., Pye, K. and Davy, A.J. 2002. Drainage and elevation as factors in the restoration of salt marsh in Britain. *Restoration Ecology* 10(3) 591-602.

Cundy, A.B. and Croudace, I.W. 1995. Sedimentary and geochemical variations in a salt marsh/mud flat environment from the mesotidal Hamble estuary, southern England. *Marine chemistry* 51(2) 115-132.

Cundy, A.B. and Croudace, I.W. 1996. Sediment accretion and recent sea-level rise in the Solent, southern England: inferences from radiometric and geochemical studies. *Estuarine, Coastal and Shelf Science* 43(4) 449-467.

Dahdouh-Guebas, F. 2002. The use of remote sensing and GIS in the sustainable management of tropical coastal ecosystems. *Environment, development and sustainability* 4(2) 93-112.

Dai, Y., Zeng, X., Dickinson, R.E., Baker, I., Bonan, G.B., Bosilovich, M.G., Denning, A.S., Dirmeyer, P.A., Houser, P.R. and Niu, G. 2003. The common land model. *Bulletin of the American Meteorological Society* 84(8) 1013-1023.

Dalal, R., Allen, D., Livesley, S. and Richards, G. 2008. Magnitude and biophysical regulators of methane emission and consumption in the Australian agricultural, forest, and submerged landscapes: a review. *Plant and Soil* 309(1) 43-76.

Dalrymple, R.A., Kirby, J.T. and Hwang, P.A., 1984. Wave diffraction due to areas of energy dissipation. Journal of waterway, port, coastal, and ocean engineering, 110(1), pp.67-79.

Davy, A.J., Brown, M.J., Mossman, H.L. and Grant, A. 2011. Colonization of a newly developing salt marsh: disentangling independent effects of elevation and redox potential on halophytes. *Journal of Ecology* 99(6) 1350-1357.

Dawe, N., Bradfield, G., Boyd, W.S., Trethewey, D.E. and Zolbrod, A.N. 2000. Marsh creation in a northern Pacific estuary: is thirteen years of monitoring vegetation dynamics enough? *Conservation Ecology* 4(2).

Dawson, T.P., Berry, P.M. and Kampa, E. 2003. Climate change impacts on freshwater wetland habitats. *Journal for Nature Conservation* 11(1) 25-30.

DeLaune, R., Smith, C. and Patrick Jr, W. 1983. Relationship of marsh elevation, redox potential, and sulfide to Spartina alterniflora productivity. *Soil Science Society of America Journal* 47(5) 930-935.

Dixon, A.M. Leggett, D.J. & Weight, R.C. (1998).Habitat creation opportunities for landwardcoastal re-alignment: Essex case studies.Journal of the Chartered Institute of Water andEnvironmental Management; 12: 102-112.

DIGIACOMO, A. E., BIRD, C. N., PAN, V. G., DOBROSKI, K., ATKINS-DAVIS, C., JOHNSTON, D. W. & RIDGE, J. T. 2020. Modeling salt marsh vegetation height using unoccupied aircraft systems and structure from motion. Remote Sensing, 12, 2333.

Dean, R.G. and Dalrymple, R.A., 1991. Water wave mechanics for engineers and scientists (Vol. 2). world scientific publishing company.

Doody, J.P. 2008. *Saltmarsh conservation, management and restoration*: Springer Science & Business Media.

Duarte, C.M., Middelburg, J.J. and Caraco, N. 2005. Major role of marine vegetation on the oceanic carbon cycle. *Biogeosciences* 2(1) 1-8.

El-Sheimy, N., Valeo, C. and Habib, A. 2005. *Digital terrain modeling: acquisition, manipulation, and applications*: Artech House.

EKBERG, M. L. C., RAPOSA, K. B., FERGUSON, W. S., RUDDOCK, K. & WATSON, E. B. 2017. Development and application of a method to identify salt marsh vulnerability to sea level rise. Estuaries and coasts, 40, 694-710.

Esselink, P., Dijkema, K.S., Reents, S. and Hageman, G. 1998. Vertical accretion and profile changes in abandoned man-made tidal marshes in the Dollard estuary, the Netherlands. *Journal of Coastal Research* 570-582.

Fagherazzi, S., Kirwan, M.L., Mudd, S.M., Guntenspergen, G.R., Temmerman, S., D'Alpaos, A., Van De Koppel, J., Rybczyk, J.M., Reyes, E., Craft, C. and Clough, J., 2012. Numerical models of salt marsh evolution: Ecological, geomorphic, and climatic factors. Reviews of Geophysics, 50(1).

Farris, A.S., Defne, Z. and Ganju, N.K. 2019. Identifying Salt Marsh Shorelines from Remotely Sensed Elevation Data and Imagery. *Remote Sensing* 11(15) 1795.

Fernandez-Nunez, M., Burningham, H. and Ojeda Zujar, J. 2017. Improving accuracy of LiDAR-derived digital terrain models for saltmarsh management. *Journal of Coastal Conservation* 21(1) 209-222.

Foley, J.A., Levis, S., Prentice, I.C., Pollard, D. and Thompson, S.L. 1998. Coupling dynamic models of climate and vegetation. *Global change biology* 4(5) 561-579.

Fonseca, M.S. and Cahalan, J.A. 1992. A preliminary evaluation of wave attenuation by four species of seagrass. *Estuarine, Coastal and Shelf Science* 35(6) 565-576.

Ford, H., Garbutt, A., Jones, L. and Jones, D.L. 2012. Methane, carbon dioxide and nitrous oxide fluxes from a temperate salt marsh: Grazing management does not alter Global Warming Potential. *Estuarine, Coastal and Shelf Science* 113 182-191.

Forysinski, K., 2019. Nature-based flood protection: the contribution of tidal marsh vegetation to wave attenuation at Sturgeon Bank (Doctoral dissertation, University of British Columbia).

Foster-Martinez, M.R., Lacy, J.R., Ferner, M.C. and Variano, E.A. 2018. Wave attenuation across a tidal marsh in San Francisco Bay. *Coastal Engineering* 136 26-40.

Foster NM, Hudson MD, Bray S, Nicholls RJ (2013) Intertidal mudflat and saltmarsh conservation, and sustainable use in the UK: a review. J Environ Manage 126:96–100

French, J.R. 1993. Numerical simulation of vertical marsh growth and adjustment to accelerated sea-level rise, North Norfolk, UK. *Earth Surface Processes and Landforms* 18(1) 63-81.

French, J.R. and Spencer, T. 1993. Dynamics of sedimentation in a tide-dominated backbarrier salt marsh, Norfolk, UK. *Marine Geology* 110(3-4) 315-331.

French, J., 2019. Tidal Salt Marshes: Sedimentology and Geomorphology. In Coastal wetlands (pp. 479-517). Elsevier.

GANJU, N. K., DEFNE, Z. & FAGHERAZZI, S. 2020. Are elevation and open-water conversion of salt marshes connected? Geophysical Research Letters, 47, e2019GL086703.

Gao, Z. and Zhang, L. 2006. Measuring and analyzing of the multi-seasonal spectral characteristics for saltmarsh vegetation in Shanghai. *Acta Ecologica Sinica* 26(3) 793-800.

Garzon, J.L., Maza, M., Ferreira, C., Lara, J. and Losada, I. 2019. Wave attenuation by Spartina saltmarshes in the Chesapeake Bay under storm surge conditions. *Journal of Geophysical Research: Oceans* 124(7) 5220-5243.

Gedan, K.B., Kirwan, M.L., Wolanski, E., Barbier, E.B. and Silliman, B.R. 2011. The present and future role of coastal wetland vegetation in protecting shorelines: answering recent challenges to the paradigm. *Climatic change* 106(1) 7-29.

Gehrels, R. and Long, A. 2008. Sea level is not level: the case for a new approach to predicting UK sea-level rise. *Geography* 93(1) 11-16.

Genç, L., Dewitt, B. and Smith, S. 2004. Determination of wetland vegetation height with LIDAR. *Turkish Journal of agriculture and forestry* 28(1) 63-71.

Glennie, C., Brooks, B., Ericksen, T., Hauser, D., Hudnut, K., Foster, J. and Avery, J. 2013. Compact multipurpose mobile laser scanning system—Initial tests and results. *Remote Sensing* 5(2) 521-538.

Goetz, S.J., Steinberg, D., Betts, M.G., Holmes, R.T., Doran, P.J., Dubayah, R. and Hofton, M. 2010. Lidar remote sensing variables predict breeding habitat of a Neotropical migrant bird. *Ecology* 91(6) 1569-1576.

Gong, P. 2012. Remote sensing of environmental change over China: A review. *Chinese science bulletin* 57(22) 2793-2801.

Goodwin 1983. S oils and Vegetation o f the North GowerSaltmarshes, South Wales, A thesis submitted to the University o f Wales incandidature fo r the degree o f Philosophiae Doctor. *University o f Wales*.

Goodwin, G.C. and Mudd, S.M. 2019. High platform elevations highlight the role of storms and spring tides in salt marsh evolution. *Frontiers in Environmental Science* 7 62.

GOODWIN, G. C., MUDD, S. M. & CLUBB, F. J. 2018. Unsupervised detection of salt marsh platforms: a topographic method. Earth Surface Dynamics, 6, 239-255.

Gray, A. and Bunce, R. 1972a. Ecology of Morecambe Bay. 6. Soils and Vegetation of Salt Marshes-Multivariate Approach. *Journal of Applied Ecology* 9(1) 221-&.

Gray, A. and Bunce, R. 1972b. The ecology of Morecambe Bay. VI. Soils and vegetation of the salt marshes: a multivariate approach. *Journal of applied Ecology* 221-234.

Gray, A. and Scott, R. 1977. The ecology of Morecambe Bay. VII. The distribution of Puccinellia maritima, Festuca rubra and Agrostis stolonifera in the salt marshes. *Journal of Applied Ecology* 229-241.

Gray, A.J., 1972. The ecology of Morecambe Bay. v. The salt marshes of Morecambe Bay. Journal of Applied Ecology, pp.207-220.

Griffin, P.J., Theodose, T. and Dionne, M. 2011. Landscape patterns of forb pannes across a northern New England salt marsh. *Wetlands* 31(1) 25-33.

GROUP, U.B. 1999. *UK Biodiversity Group Tranche 2 action plans. Volume V-Maritime species and habitats*: English Nature.

Gu, J., Jin, R., Chen, G., Ye, Z., Li, Q., Wang, H., Li, D., Christakos, G., Agusti, S. and Duarte, C.M. 2021. Areal extent, species composition, and spatial distribution of coastal saltmarshes in China. *IEEE Journal of Selected Topics in Applied Earth Observations and Remote Sensing* 14 7085-7094.

Hacker, S.D. and Bertness, M.D. 1999. Experimental evidence for factors maintaining plant species diversity in a New England salt marsh. *Ecology* 80(6) 2064-2073.

Hadley, W. 2016. *Ggplot2: Elegrant graphics for data analysis*: Springer.

Harmsworth, G. and Long, S. 1986. An assessment of saltmarsh erosion in Essex, England, with reference to the Dengie Peninsula. *Biological Conservation* 35(4) 377-387.

Harrison, E.Z. and Bloom, A.L. 1977. Sedimentation rates on tidal salt marshes in Connecticut. *Journal of Sedimentary Research* 47(4) 1484-1490.

Healey, R., Pye, K., Stoddart, D. and Bayliss-Smith, T. 1981. Velocity variations in salt marsh creeks, Norfolk, England. *Estuarine, Coastal and Shelf Science* 13(5) 535-545.

Hijmans, R., van Etten, J., Cheng, J., Mattiuzzi, M., Sumner, M., Greenberg, J., Lamigueiro, O., Bevan, A., Racine, E. and Shortridge, A. 2017. raster: Geographic Data Analysis and Modeling. R package version 2.6–7. 2017.

Hladik, C. and Alber, M. 2012. Accuracy assessment and correction of a LIDAR-derived salt marsh digital elevation model. *Remote Sensing of Environment* 121 224-235.

Hladik, C. and Alber, M. 2014. Classification of salt marsh vegetation using edaphic and remote sensing-derived variables. *Estuarine, Coastal and Shelf Science* 141 47-57.

Hladik, C., Schalles, J. and Alber, M., 2013. Salt marsh elevation and habitat mapping using hyperspectral and LIDAR data. Remote Sensing of Environment, 139, pp.318-330.

Hopkinson, C., Chasmer, L., Zsigovics, G., Creed, I., Sitar, M., Treitz, P. and Maher, R. 2004. Errors in LiDAR ground elevation and wetland vegetation height estimates. *International Archives of Photogrammetry, Remote Sensing, and Spatial Information Sciences* 36(8) 108-113.

Horton, B.P., Rahmstorf, S., Engelhart, S.E. and Kemp, A.C. 2014. Expert assessment of sea-level rise by AD 2100 and AD 2300. *Quaternary Science Reviews* 84 1-6.

Howes, B.L., Dacey, J.W. and Teal, J.M. 1985. Annual carbon mineralization and belowground production of Spartina alterniflora in a New England salt marsh. *Ecology* 66(2) 595-605.

Huiskes, H.L., 1988. The salt marshes of the Westerschelde and their role in the estuarine ecosystem. Hydrobiological Bulletin, 22, pp.57-63.

Hughes, R.G. and Paramor, O.A.L., 2004. On the loss of saltmarshes in south-east England and methods for their restoration. Journal of applied ecology, 41(3), pp.440-448.

Jacobsen, K. and Lohmann, P. 2003. Segmented filtering of laser scanner DSMs. *International Archives of Photogrammetry and Remote Sensing* 34(3/W13).

James, T.D., Murray, T., Barrand, N.E. and Barr, S.L. 2006. Extracting photogrammetric ground control from lidar DEMs for change detection. *The Photogrammetric Record* 21(116) 312-328.

Jeroen, O. 2018. cld2: Google's Compact Language Detector 2. *R package version* 1.

GEDAN, K. B., KIRWAN, M. L., WOLANSKI, E., BARBIER, E. B. & SILLIMAN, B. R. 2011. The present and future role of coastal wetland vegetation in protecting shorelines: answering recent challenges to the paradigm. Climatic change, 106, 7-29.

Jickells, T., Andrews, J., Samways, G., Sanders, R., Malcolm, S., Sivyer, D., Parker, R., Nedwell, D., Trimmer, M. and Ridgway, J. 2000. Nutrient fluxes through the Humber estuary—past, present and future. *AMBIO: A Journal of the Human Environment* 29(3) 130-135.

Jones, L., Angus, S., Cooper, A., Doody, J., Everard, M., Garbutt, A., Gilchrist, P., Hansom, J., Nicholls, R.J., Pye, K., Ravenscroft, N., Rees, S., Rhind, P. and Whitehouse, A. 2011a. Coastal margins.

Jones, L., Angus, S., Cooper, A., Doody, P., Everard, M., Garbutt, A., Gilchrist, P., Hansom, J., Nicholls, R. and Pye, K. 2011b. Coastal margins.

Jung, M., Henkel, K., Herold, M. and Churkina, G. 2006. Exploiting synergies of global land cover products for carbon cycle modeling. *Remote Sensing of Environment* 101(4) 534-553.

Kelleway, J.J., Saintilan, N., Macreadie, P.I., Baldock, J.A. and Ralph, P.J. 2017. Sediment and carbon deposition vary among vegetation assemblages in a coastal salt marsh. *Biogeosciences* 14(16) 3763-3779.

Kestner, F.J.T., 1975. The loose-boundary regime of the Wash. Geographical Journal, pp.388-414.

Kirby, R. and Parker, W.R., 1983. Distribution and behavior of fine sediment in the Severn Estuary and Inner Bristol Channel, UK. Canadian Journal of Fisheries and Aquatic Sciences, 40(S1), pp.s83-s95.

King, G.M. and Wiebe, W. 1978. Methane release from soils of a Georgia salt marsh. *Geochimica et Cosmochimica Acta* 42(4) 343-348.

King, S.E. and Lester, J.N. 1995. The value of salt marsh as a sea defence. *Marine Pollution Bulletin* 30(3) 180-189.

Kirby, R. and Parker, W. 1982. A suspended sediment front in the Severn Estuary. *Nature* 295(5848) 396-399.

Kirwan, M.L., Walters, D.C., Reay, W.G. and Carr, J.A., 2016. Sea level driven marsh expansion in a coupled model of marsh erosion and migration. Geophysical Research Letters, 43(9), pp.4366-4373.

Kobayashi, N., Raichle, A.W. and Asano, T., 1993. Wave attenuation by vegetation. Journal of waterway, port, coastal, and ocean engineering, 119(1), pp.30-48.

Knutson, T.R., McBride, J.L., Chan, J., Emanuel, K., Holland, G., Landsea, C., Held, I., Kossin, J.P., Srivastava, A. and Sugi, M. 2010. Tropical cyclones and climate change. *Nature Geoscience* 3(3) 157-163.

Koppel, J.v.d., Wal, D.v.d., Bakker, J.P. and Herman, P.M. 2005. Self-organization and vegetation collapse in salt marsh ecosystems. *The American Naturalist* 165(1) E1-E12.

Kumar, L. and Sinha, P., 2014. Mapping salt-marsh land-cover vegetation using high-spatial and hyperspectral satellite data to assist wetland inventory. *GIScience & Remote Sensing*, *51*(5), pp.483-497.

Krauss, K.W., Doyle, T.W. and Howard, R.J. 2009. Is there evidence of adaptation to tidal flooding in saplings of baldcypress subjected to different salinity regimes? *Environmental and experimental botany* 67(1) 118-126.

Krolik-Root, C., Stansbury, D.L. and Burnside, N.G. 2015. Effective LiDAR-based modelling and visualisation of managed retreat scenarios for coastal planning: An example from the southern UK. *Ocean & Coastal Management* 114 164-174.

Laba, M., Downs, R., Smith, S., Welsh, S., Neider, C., White, S., Richmond, M., Philpot, W. and Baveye, P. 2008. Mapping invasive wetland plants in the Hudson River National Estuarine Research Reserve using quickbird satellite imagery. *Remote Sensing of Environment* 112(1) 286-300.

LaFontaine, J.H., Hay, L.E., Viger, R.J., Regan, R.S. and Markstrom, S.L. 2015. Effects of climate and land cover on hydrology in the southeastern US: Potential impacts on watershed planning. *JAWRA Journal of the American Water Resources Association* 51(5) 1235-1261.

Lang, F., von der Lippe, M., Schimpel, S., Scozzafava-Jaeger, T. and Straub, W. 2010. Topsoil morphology indicates bio-effective redox conditions in Venice salt marshes. *Estuarine, Coastal and Shelf Science* 87(1) 11-20.

Laporte-Fauret, Q., Lubac, B., Castelle, B., Michalet, R., Marieu, V., Bombrun, L., Launeau, P., Giraud, M., Normandin, C. and Rosebery, D. 2020. Classification of atlantic coastal sand dune vegetation using in situ, uav, and airborne hyperspectral data. *Remote Sensing* 12(14) 2222.

Lawrence, P.J. 2018. How to create a saltmarsh: understanding the roles of topography, redox and nutrient dynamics. Manchester Metropolitan University.

Leonard, P. 1997. *Postmodern welfare: Reconstructing an emancipatory project*: Sage.

Leonardi, N., Carnacina, I., Donatelli, C., Ganju, N.K., Plater, A.J., Schuerch, M. and Temmerman, S., 2018. Dynamic interactions between coastal storms and salt marshes: A review. Geomorphology, 301, pp.92-107.

Lewis, J. and Kelman, I., 2009. Housinq Flooding, And Risk-Ecology: Thames Estuary South-Shoreland And North Kent. Journal of architectural and planning research, pp.14-29.

Li, Z., Zhu, C. and Gold, C. 2004. *Digital terrain modeling: principles and methodology*: CRC press.

Liang, L., Xu, B., Chen, Y., Liu, Y., Cao, W., Fang, L., Feng, L., Goodchild, M.F. and Gong, P. 2010. Combining spatial-temporal and phylogenetic analysis approaches for improved understanding on global H5N1 transmission. *PLoS One* 5(10) e13575.

Lim, K., Treitz, P., Wulder, M., St-Onge, B. and Flood, M. 2003. LiDAR remote sensing of forest structure. *Progress in physical geography* 27(1) 88-106.

Liu, J., Chen, J., Cihlar, J. and Park, W. 1997. A process-based boreal ecosystem productivity simulator using remote sensing inputs. *Remote sensing of environment* 62(2) 158-175.

Livesley, S.J. and Andrusiak, S.M. 2012. Temperate mangrove and salt marsh sediments are a small methane and nitrous oxide source but important carbon store. *Estuarine, Coastal and Shelf Science* 97 19-27.

Loder, N., Irish, J.L., Cialone, M. and Wamsley, T. 2009. Sensitivity of hurricane surge to morphological parameters of coastal wetlands. *Estuarine, Coastal and Shelf Science* 84(4) 625-636.

Lohani, B. and Mason, D.C. 2001. Application of airborne scanning laser altimetry to the study of tidal channel geomorphology. *ISPRS Journal of Photogrammetry and Remote Sensing* 56(2) 100-120.

Lovelace, J.K. 1994. Storm-tide elevations produced by Hurricane Andrew along the Louisiana Coast, August 25-27, 1992. US Geological Survey; USGS Earth Science Information Center, Open-File ….

Luhar, M. and Nepf, H.M., 2016. Wave-induced dynamics of flexible blades. Journal of Fluids and Structures, 61, pp.20-41.

Magenheimer, J., Moore, T., Chmura, G. and Daoust, R. 1996. Methane and carbon dioxide flux from a macrotidal salt marsh, Bay of Fundy, New Brunswick. *Estuaries* 19(1) 139-145.

Mani, S. and Parthasarathy, N. 2006. Tree diversity and stand structure in inland and coastal tropical dry evergreen forests of peninsular India. *Current Science* 1238-1246.

Marcos, M., Tsimplis, M.N. and Shaw, A.G. 2009. Sea level extremes in southern Europe. *Journal of Geophysical Research: Oceans* 114(C1).

Marion, C., Anthony, E.J. and Trentesaux, A. 2009. Short-term (≤ 2 yrs) estuarine mudflat and saltmarsh sedimentation: High-resolution data from ultrasonic altimetery, rod surface-elevation table, and filter traps. *Estuarine, Coastal and Shelf Science* 83(4) 475-484.

Mariotti, G. and Fagherazzi, S., 2010. A numerical model for the coupled long-term evolution of salt marshes and tidal flats. Journal of Geophysical Research: Earth Surface, 115(F1).

Marten, A.L. and Newbold, S.C., 2012. Estimating the social cost of non-CO2 GHG emissions: Methane and nitrous oxide. Energy Policy, 51, pp.957-972.

Marshall, J.R. 1962. The morphology of the upper Solway salt marshes. *Scottish Geographical Magazine* 78(2) 81-99.

Martens, C.S. and Berner, R.A. 1977. Interstitial water chemistry of anoxic Long Island Sound sediments. 1. Dissolved gases 1. *Limnology and Oceanography* 22(1) 10-25.

Martin, J.F., Roy, E.D., Diemont, S.A. and Ferguson, B.G. 2010. Traditional Ecological Knowledge (TEK): Ideas, inspiration, and designs for ecological engineering. *Ecological Engineering* 36(7) 839-849.

Mason, R.P., Choi, A.L., Fitzgerald, W.F., Hammerschmidt, C.R., Lamborg, C.H., Soerensen, A.L. and Sunderland, E.M. 2012. Mercury biogeochemical cycling in the ocean and policy implications. *Environmental research* 119 101-117.

Masselink, G., Scott, T., Poate, T., Russell, P., Davidson, M. and Conley, D. 2016. The extreme 2013/2014 winter storms: hydrodynamic forcing and coastal response along the southwest coast of England. *Earth Surface Processes and Landforms* 41(3) 378-391.

Matso, K., Barker, S. and Kiedrowski, C. 2019. Great Bay Estuary Submerged Aquatic Vegetation (SAV) Monitoring Program for 2019-2023 Quality Assurance Project Plan.

May, V. and Hansom, J.D. 2003. *Coastal Geomorphology of Great Britain*: Joint Nature Conservation Committee.

Mckee, K.L. and Patrick, W. 1988. The relationship of smooth cordgrass (Spartina alterniflora) to tidal datums: a review. *Estuaries* 11(3) 143-151.

Mcleod, E., Chmura, G.L., Bouillon, S., Salm, R., Björk, M., Duarte, C.M., Lovelock, C.E., Schlesinger, W.H. and Silliman, B.R. 2011. A blueprint for blue carbon: toward an improved understanding of the role of vegetated coastal habitats in sequestering CO2. *Frontiers in Ecology and the Environment* 9(10) 552-560.

Miller, P., Mills, J., Edwards, S., Bryan, P., Marsh, S., Hobbs, P. and Mitchell, H. 2007. A robust surface matching technique for integrated monitoring of coastal geohazards. *Marine Geodesy* 30(1-2) 109-123.

Millette, T.L., Argow, B.A., Marcano, E., Hayward, C., Hopkinson, C.S. and Valentine, V. 2010. Salt marsh geomorphological analyses via integration of multitemporal multispectral remote sensing with LIDAR and GIS. *Journal of Coastal Research* 809-816.

Mitasova, H., Hardin, E., Overton, M.F. and Kurum, M.O. 2010. Geospatial analysis of vulnerable beach-foredune systems from decadal time series of lidar data. *Journal of Coastal Conservation* 14(3) 161-172.

Mitsch, W.J. and Gosselink, J.G. 2007 Wetlands 4th edn (New York: Van Nostrand Reinhold) p 571.

MILLARD, K., REDDEN, A., WEBSTER, T. & STEWART, H. 2013. Use of GIS and high resolution LiDAR in salt marsh restoration site suitability assessments in the upper Bay of Fundy, Canada. Wetlands ecology and management, 21, 243-262.

Möller, I. 2006. Quantifying saltmarsh vegetation and its effect on wave height dissipation: Results from a UK East coast saltmarsh. *Estuarine, Coastal and Shelf Science* 69(3) 337-351.

Möller, I. and Christie, E. 2019. Hydrodynamics and modeling of water flow in coastal wetlands. *Coastal wetlands*. Elsevier. pp. 289-323.

Möller, I., Kudella, M., Rupprecht, F., Spencer, T., Paul, M., Van Wesenbeeck, B.K., Wolters, G., Jensen, K., Bouma, T.J. and Miranda-Lange, M. 2014. Wave attenuation over coastal salt marshes under storm surge conditions. *Nature Geoscience* 7(10) 727-731.

Möller, I. and Spencer, T. 2002. Wave dissipation over macro-tidal saltmarshes: Effects of marsh edge typology and vegetation change. *Journal of Coastal Research*(36) 506-521.

Möller, I., Spencer, T., French, J.R., Leggett, D. and Dixon, M. 1999. Wave transformation over salt marshes: a field and numerical modelling study from North Norfolk, England. *Estuarine, Coastal and Shelf Science* 49(3) 411-426.

Montané, J.M. and Torres, R. 2006. Accuracy assessment of lidar saltmarsh topographic data using RTK GPS. *Photogrammetric Engineering & Remote Sensing* 72(8) 961-967.

Morgan, P.A., Burdick, D.M. and Short, F.T. 2009. The functions and values of fringing salt marshes in northern New England, USA. *Estuaries and Coasts* 32(3) 483-495.

Morris, J.T., Sundareshwar, P., Nietch, C.T., Kjerfve, B. and Cahoon, D.R. 2002. Responses of coastal wetlands to rising sea level. *Ecology* 83(10) 2869-2877.

Morris, R.K., Reach, I., Duffy, M., Collins, T. and Leafe, R. 2004. On the loss of saltmarshes in south-east England and the relationship with Nereis diversicolor. *Journal of Applied Ecology* 41(4) 787-791.

Mossman, H.L. 2007. Development of saltmarsh vegetation in response to coastal realignment. University of East Anglia.

Mossman, H.L., Davy, A.J. and Grant, A. 2012a. Does managed coastal realignment create saltmarshes with 'equivalent biological characteristics' to natural reference sites? *Journal of Applied Ecology* 49(6) 1446-1456.

Mossman, H.L., Davy, A.J. and Grant, A. 2012b. Quantifying local variation in tidal regime using depth-logging fish tags. *Estuarine, Coastal and Shelf Science* 96 122-128.

Mossman, H.L., Grant, A. and Davy, A.J. 2020. Manipulating saltmarsh microtopography modulates the effects of elevation on sediment redox potential and halophyte distribution. *Journal of Ecology* 108(1) 94-106.

Mount, R., Prahalad, V., Sharples, C., Tilden, J., Morrison, B., Lacey, M., Ellison, J., Helman, M. and Newton, J. 2010. Circular Head region coastal foreshore habitats: sea level rise vulnerability assessment.(Boullanger Bay-Robbins Passage-Big Bay-Duck Bay).

Mueller, P., Ladiges, N., Jack, A., Schmiedl, G., Kutzbach, L., Jensen, K. and Nolte, S., 2019. Assessing the long-term carbon-sequestration potential of the semi-natural salt marshes in the European Wadden Sea. Ecosphere, 10(1), p.e02556.

Mullarney, J.C. and Henderson, S.M., 2018. Flows within marine vegetation canopies. Advances in coastal hydraulics, pp.1-46.

Narayan, S., Beck, M.W., Reguero, B.G., Losada, I.J., Van Wesenbeeck, B., Pontee, N., Sanchirico, J.N., Ingram, J.C., Lange, G.-M. and Burks-Copes, K.A. 2016a. The effectiveness, costs and coastal protection benefits of natural and nature-based defences. *PLoS One* 11(5) e0154735.

Narayan, S., Beck, M.W., Wilson, P., Thomas, C., Guerrero, A., Shephard, C., Reguero, B.G., Franco, G., Ingram, C. and Trespalacios, D. 2016b. Coastal wetlands and flood damage reduction: using risk industry-based models to assess natural defenses in the northeastern USA.

NRA, 1994 NRA Anglian Region, 1994. Blackwater Catchment Management Plan: Consultation Report.

Navarro, A., Young, M., Macreadie, P.I., Nicholson, E. and Ierodiaconou, D., 2021. Mangrove and saltmarsh distribution mapping and land cover change assessment for South-eastern Australia from 1991 to 2015. *Remote Sensing*, *13*(8), p.1450.

Nationally Data List, N. 2017. https://data.gov.uk/dataset/94633813-168d-4357-a332-803eb4450ad6. *national-dataset-list*.

NatureServe, Y. 2022. Arlington, Virginia: NatureServe Explorer [https://explorer.natureserve.org/Taxon/ELEMENT_GLOBAL.2.860269/Salt_Marsh_Formation#:~:text=Salt%20Marsh%20vegetation%20comprises%20primarily,as%20broad%2Dleaved%20emergent%20macrophytes.] [Accessed 15.05.2022.

Nayak, S., Sarangi, R. and Rajawat, A. 2001. Application of IRS-P4 OCM data to study the impact of cyclone on coastal environment of Orissa. *Current Science* 1208-1213.

Nemmaoui, A., Aguilar, F.J., Aguilar, M.A. and Qin, R. 2019. DSM and DTM generation from VHR satellite stereo imagery over plastic covered greenhouse areas. *Computers and Electronics in Agriculture* 164 104903.

Nerem, R.S., Beckley, B.D., Fasullo, J.T., Hamlington, B.D., Masters, D. and Mitchum, G.T., 2018. Climate-change–driven accelerated sea-level rise detected in the altimeter era. Proceedings of the national academy of sciences, 115(9), pp.2022-2025.

NTSLF 2020. National Tidal & Sea Level Facility (NTSLF). *https://www.ntslf.org/*.

Olff, H.D., De Leeuw, J., Bakker, J., Platerink, R. and Van Wijnen, H. 1997. Vegetation succession and herbivory in a salt marsh: changes induced by sea level rise and silt deposition along an elevational gradient. *Journal of Ecology* 799-814.

Ouyang, X. and Lee, S. 2014. Updated estimates of carbon accumulation rates in coastal marsh sediments. *Biogeosciences* 11(18) 5057-5071.

Owen, M. 1980. Design of seawalls allowing for wave overtopping. *Report Ex* 924 39.

Özesmi, U. and Mitsch, W.J. 1997. A spatial habitat model for the marsh-breeding red-winged blackbird (Agelaius phoeniceus L.) in coastal Lake Erie wetlands. *Ecological Modelling* 101(2-3) 139-152.

SAKET, A., PEIRSON, W. L., BANNER, M. L. & ALLIS, M. J. 2018. On the influence of wave breaking on the height limits of two-dimensional wave groups propagating in uniform intermediate depth water. Coastal Engineering, 133, 159-165.

Sanders-DeMott, R., Eagle, M.J., Kroeger, K.D., Wang, F., Brooks, T.W., O'Keefe Suttles, J.A., Nick, S.K., Mann, A.G. and Tang, J., 2022. Impoundment increases methane emissions in Phragmites-invaded coastal wetlands. Global Change Biology, 28(15), pp.4539-4557.

Pauleit, S. and Duhme, F. 2000. Assessing the environmental performance of land cover types for urban planning. *Landscape and urban planning* 52(1) 1-20.

Paul, M., Rupprecht, F., Möller, I., Bouma, T.J., Spencer, T., Kudella, M., Wolters, G., van Wesenbeeck, B.K., Jensen, K., Miranda-Lange, M. and Schimmels, S., 2016. Plant stiffness and biomass as drivers for drag forces under extreme wave loading: a flume study on mimics. Coastal Engineering, 117, pp.70-78.

Pearson, R.G., Dawson, T.P. and Liu, C. 2004. Modelling species distributions in Britain: a hierarchical integration of climate and land-cover data. *Ecography* 27(3) 285-298.

Pennings, S.C. and Callaway, R.M. 1992. Salt marsh plant zonation: the relative importance of competition and physical factors. *Ecology* 73(2) 681-690.

Pennings, S.C., Selig, E.R., Houser, L.T. and Bertness, M.D. 2003. Geographic variation in positive and negative interactions among salt marsh plants. *Ecology* 84(6) 1527-1538.

Pinsky, M.L., Guannel, G. and Arkema, K.K., 2013. Quantifying wave attenuation to inform coastal habitat conservation. Ecosphere, 4(8), pp.1-16.

Perry, C.L. and Mendelssohn, I.A. 2009. Ecosystem effects of expanding populations of Avicennia germinans in a Louisiana salt marsh. *Wetlands* 29(1) 396-406.

Pethick, J. 1981. Long-term accretion rates on tidal salt marshes. *Journal of Sedimentary Research* 51(2).

Pinheiro, J., Bates, D., DebRoy, S. and Sarkar, D. 2018. R Core Team. 2018. nlme: linear and nonlinear mixed effects models. R package version 3.1-137. *R Found. Stat. Comput. Retrieved from https://CRAN. R-project. org/package= nlme (accessed 19 Jul. 2018)*.

Pinsky, M.L., Guannel, G. and Arkema, K.K. 2013. Quantifying wave attenuation to inform coastal habitat conservation. *Ecosphere* 4(8) 1-16.

Poffenbarger, H.J., Needelman, B.A. and Megonigal, J.P. 2011. Salinity influence on methane emissions from tidal marshes. *Wetlands* 31(5) 831-842.

Polunin, O. and Walters, M. 1985. *Guide to the Vegetation of Britain and Europe*: Oxford University Press.

Posford, D. 1998. Review of Lincshore nourishment strategy study. *Report Prepared for the Environment Agency, Anglian Region*.

Ponnamperuma, F.N., 1972. The chemistry of submerged soils. Advances in agronomy, 24, pp.29-96.

Perillo, G.M. and Iribarne, O.O., 2003. New mechanisms studied for creek formation in tidal flats: from crabs to tidal channels. Eos, Transactions American Geophysical Union, 84(1), pp.1-5.

Prahalad, V. and Pearson, J. 2013. A Preliminary Strategic Assessment.

Prahalad, V., Whitehead, J., Latinovic, A. and Kirkpatrick, J.B. 2019. The creation and conservation effectiveness of State-wide wetlands and waterways and coastal refugia planning overlays for Tasmania, Australia. *Land Use Policy* 81 502-512.

Raji, O., Del Río, L., Gracia, F.J. and Benavente, J. 2011. The use of LIDAR data for mapping coastal flooding hazard related to storms in Cádiz Bay (SW Spain). *Journal of Coastal Research* 1881-1885.

Randerson, P. 1979. A simulation model of salt-marsh development and plant ecology. *Estuarine and coastal land reclamation and water storage* 48-67.

Ranwell, D.S. and Rosalind, B. 1986. *Coastal dune management guide*: Institute of terrestrial Ecology.

Raw, J., Julie, C. and Adams, J. 2019. A comparison of soil carbon pools across a mangrove-salt marsh ecotone at the southern African warm-temperate range limit. *South African Journal of Botany* 127 301-307.

Reed, D.J., Spencer, T., Murray, A.L., French, J.R. and Leonard, L. 1999. Marsh surface sediment deposition and the role of tidal creeks: Implications for created and managed coastal marshes. *Journal of Coastal conservation* 5(1) 81-90.

Richards, F. 1934. The salt marshes of the Dovey Estuary. IV. The rates of vertical accretion, horizontal extension and scarp erosion. *Annals of Botany* 48(189) 225-259.

Rodarmel, C., Samberg, A., Theiss, H. and Johanesen, T. 2006. A review of the ASPRS guidlines for the reporting of horizontal and vertical accuracies in LIDAR data. *International Archives of Photogrammetry and Remote Sensing spatial Information Sciences* 36 34-39.

Rooth, J. and Stevenson, J. 2000. Sediment deposition patterns in Phragmites australiscommunities: Implications for coastal areas threatened by rising sea-level. *Wetlands Ecology and Management* 8(2) 173-183.

Rosencranz, J.A., Brown, L.N., Holmquist, J.R., Sanchez, Y., MacDonald, G.M. and Ambrose, R.F. 2017. The Role of Sediment Dynamics for Inorganic Accretion Patterns in Southern California's Mediterranean-Climate Salt Marshes. *Estuaries and Coasts* 40(5) 1371-1384.

Rosentreter, J.A., Al-Haj, A.N., Fulweiler, R.W. and Williamson, P. 2021. Methane and nitrous oxide emissions complicate coastal blue carbon assessments. *Global Biogeochemical Cycles* 35(2) e2020GB006858.

Rosso, P., Ustin, S. and Hastings, A. 2006. Use of lidar to study changes associated with Spartina invasion in San Francisco Bay marshes. *Remote Sensing of environment* 100(3) 295-306.

Rowland, C.S., Morton, R.D., Carrasco, L., McShane, G., Neil, A.W. and Wood, C.M. 2017. Land Cover Map 2015 (1km percentage aggregate class, GB). NERC Environmental Information Data Centre.

Rupprecht, F., Möller, I., Paul, M., Kudella, M., Spencer, T., Van Wesenbeeck, B.K., Wolters, G., Jensen, K., Bouma, T.J., Miranda-Lange, M. and Schimmels, S., 2017. Vegetation-wave interactions in salt marshes under storm surge conditions. Ecological Engineering, 100, pp.301-315.

Ruggiero, P., Komar, P.D., McDougal, W.G., Marra, J.J. and Beach, R.A., 2001. Wave runup, extreme water levels and the erosion of properties backing beaches. Journal of coastal research, pp.407-419.

Sadr, K. 2016. A Comparison of Accuracy and Precision in Remote Sensing Stone-walled Structures with Google Earth, High Resolution Aerial Photography and LiDAR; a Case Study from the South African Iron Age. *Archaeological Prospection* 23(2) 95-104.

Sadro, S., Gastil-Buhl, M. and Melack, J. 2007. Characterizing patterns of plant distribution in a southern California salt marsh using remotely sensed topographic and hyperspectral data and local tidal fluctuations. *Remote Sensing of Environment* 110(2) 226-239.

Saket, A., Peirson, W.L., Banner, M.L. and Allis, M.J. 2018. On the influence of wave breaking on the height limits of two-dimensional wave groups propagating in uniform intermediate depth water. *Coastal Engineering* 133 159-165.

Salach, A., Bakuła, K., Pilarska, M., Ostrowski, W., Górski, K. and Kurczyński, Z. 2018. Accuracy assessment of point clouds from LidaR and dense image matching acquired using the UAV platform for DTM creation. *ISPRS International Journal of Geo-Information* 7(9) 342.

Sanderson, E.W., Foin, T.C. and Ustin, S.L. 2001. A simple empirical model of salt marsh plant spatial distributions with respect to a tidal channel network. *Ecological Modelling* 139(2) 293-307.

Santin, C., De La Rosa, J., Knicker, H., Otero, X., Alvarez, M. and González-Vila, F.J. 2009. Effects of reclamation and regeneration processes on organic matter from estuarine soils and sediments. *Organic Geochemistry* 40(9) 931-941.

Schmid, K.A., Hadley, B.C. and Wijekoon, N. 2011. Vertical accuracy and use of topographic LIDAR data in coastal marshes. *Journal of Coastal Research* 27(6A) 116-132.

Sellars, J.D. and Jolls, C.L. 2007. Habitat modeling for Amaranthus pumilus: an application of light detection and ranging (LIDAR) data. *Journal of Coastal Research* 23(5) 1193-1202.

Senior, E., Lindström, E.B., Banat, I.M. and Nedwell, D.B. 1982. Sulfate reduction and methanogenesis in the sediment of a saltmarsh on the east coast of the United Kingdom. *Applied and environmental microbiology* 43(5) 987-996.

Serrano, O., Lavery, P.S., Duarte, C.M., Kendrick, G.A., Calafat, A., York, P.H., Steven, A. and Macreadie, P.I. 2016. Can mud (silt and clay) concentration be used to predict soil organic carbon content within seagrass ecosystems? *Biogeosciences* 13(17) 4915-4926.

Sghair, A. and Goma, F. 2013. Remote sensing and GIS for wetland vegetation study. University of Glasgow.

Sheng, Y.P., Lapetina, A. and Ma, G. 2012. The reduction of storm surge by vegetation canopies: Three-dimensional simulations. *Geophysical research letters* 39(20).

Shennan, I. and Horton, B. 2002. Holocene land-and sea-level changes in Great Britain. *Journal of Quaternary Science: Published for the Quaternary Research Association* 17(5-6) 511-526.

Shennan, I., Milne, G. and Bradley, S. 2009. Late Holocene relative land-and sea-level changes: Providing information for stakeholders. *GSa today* 19(9) 52-53.

Shepard, C.C., Crain, C.M. and Beck, M.W. 2011. The protective role of coastal marshes: a systematic review and meta-analysis. *PLoS One* 6(11) e27374.

Shepherd, D., Burgess, D., Jickells, T., Andrews, J., Cave, R., Turner, R., Aldridge, J., Parker, E. and Young, E. 2007. Modelling the effects and economics of managed realignment on the cycling and storage of nutrients, carbon and sediments in the Blackwater estuary UK. *Estuarine, Coastal and Shelf Science* 73(3) 355-367.

Shi, Z. and Lamb, H.F., 1991. Post-glacial sedimentary evolution of a microtidal estuary, Dyfi Estuary, west Wales, UK. Sedimentary geology, 73(3-4), pp.227-246.

SHI, Z. 1993. Recent saltmarsh accretion and sea level fluctuations in the Dyfi Estuary, central Cardigan Bay, Wales, UK. Geo-Marine Letters, 13, 182-188.

Siemes, R.W., Borsje, B.W., Daggenvoorde, R.J. and Hulscher, S.J. 2020. Artificial structures steer morphological development of salt marshes: a model study. *Journal of marine science and engineering* 8(5) 326.

Silvestri, S., Defina, A. and Marani, M. 2005. Tidal regime, salinity and salt marsh plant zonation. *Estuarine, coastal and shelf science* 62(1) 119-130.

Silvestri, S. and Marani, M. 2004. Salt-Marsh Vegetation and Morphology: Basic Physiology, Modelling and Remote Sensing Observations. *The Ecogeomorphology of Tidal Marshes* 5-25.

Slangen, A.B., Church, J.A., Agosta, C., Fettweis, X., Marzeion, B. and Richter, K. 2016. Anthropogenic forcing dominates global mean sea-level rise since 1970. *Nature climate change* 6(7) 701-705.

Spalding, M.D., McIvor, A.L., Beck, M.W., Koch, E.W., Möller, I., Reed, D.J., Rubinoff, P., Spencer, T., Tolhurst, T.J. and Wamsley, T.V. 2014a. Coastal ecosystems: a critical element of risk reduction. *Conservation Letters* 7(3) 293-301.

Spalding, M.D., Ruffo, S., Lacambra, C., Meliane, I., Hale, L.Z., Shepard, C.C. and Beck, M.W. 2014b. The role of ecosystems in coastal protection: Adapting to climate change and coastal hazards. *Ocean & Coastal Management* 90 50-57.

Spencer, T., Brooks, S.M., Evans, B.R., Tempest, J.A. and Möller, I. 2015. Southern North Sea storm surge event of 5 December 2013: water levels, waves and coastal impacts. *Earth-Science Reviews* 146 120-145.

Steers, J., Stoddart, D., Bayliss-Smith, T., Spencer, T. and Durbidge, P. 1979. The storm surge of 11 January 1978 on the east coast of England. *Geographical Journal* 192-205.

Stumpf, R.P., 1983. The process of sedimentation on the surface of a salt marsh. Estuarine, Coastal and Shelf Science, 17(5), pp.495-508.

Sutton-Grier, A.E., Wowk, K. and Bamford, H. 2015. Future of our coasts: The potential for natural and hybrid infrastructure to enhance the resilience of our coastal communities, economies and ecosystems. *Environmental Science & Policy* 51 137-148.

Temmerman, S., Govers, G., Wartel, S. and Meire, P. 2003. Spatial and temporal factors controlling short-term sedimentation in a salt and freshwater tidal marsh, Scheldt estuary, Belgium, SW Netherlands. *Earth Surface Processes and Landforms* 28(7) 739-755.

Temmerman, S., Govers, G., Wartel, S. and Meire, P. 2004. Modelling estuarine variations in tidal marsh sedimentation: response to changing sea level and suspended sediment concentrations. *Marine Geology* 212(1-4) 1-19.

Temmerman, S., Horstman, E.M., Krauss, K.W., Mullarney, J.C., Pelckmans, I. and Schoutens, K. 2023. Marshes and mangroves as nature-based coastal storm buffers. *Annual Review of Marine Science* 15 95-118.

Thomas, L., Buckland, S.T., Rexstad, E.A., Laake, J.L., Strindberg, S., Hedley, S.L., Bishop, J.R., Marques, T.A. and Burnham, K.P. 2010. Distance software: design and analysis of distance sampling surveys for estimating population size. *Journal of Applied Ecology* 47(1) 5-14.

Titus, J.G. and Anderson, K.E. 2009. *Coastal sensitivity to sea-level rise: a focus on the mid-Atlantic region*: Government Printing Office.

UHSCL 2020. University of Hawaii, sea level center. *https://uhslc.soest.hawaii.edu/stations/*.

UK Hydrographic Office, 2014, Admiralty Tide Tables, Volume 1, United Kingdom and Ireland (including Channel ports). United Kingdom Hydrographic Office, NP201.University Press, Cambridge, pp.115-122.

UNEP, G.M.A. 2002. United Nations Environment Programme. *Chemicals, Geneva, Switzerland*.

Van der Molen, J. 1997. Tidal distortion and spatial differences in surface flooding characteristics in a salt marsh: implications for sea-level reconstruction. *Estuarine, Coastal and Shelf Science* 45(2) 221-233.

van Rooijen, A., Lowe, R., Ghisalberti, M., Conde-Frias, M. and Tan, L. 2018. Predicting current-induced drag in emergent and submerged aquatic vegetation canopies. *Frontiers in Marine Science* 5 449.

Vince, S.W. and Snow, A.A. 1984. Plant zonation in an Alaskan salt marsh: I. Distribution, abundance and environmental factors. *The Journal of Ecology* 651-667.

Vuik, V., Jonkman, S.N., Borsje, B.W. and Suzuki, T. 2016. Nature-based flood protection: The efficiency of vegetated foreshores for reducing wave loads on coastal dikes. *Coastal Engineering* 116 42-56.

Wadey, M.P., Haigh, I., Nicholls, R.J., Brown, J.M., Horsburgh, K., Carroll, B., Gallop, S.L., Mason, T. and Bradshaw, E. 2015. A comparison of the 31 January–1 February 1953 and 5–6 December 2013 coastal flood events around the UK. *Frontiers in Marine Science* 2 84.

Wamsley, T.V., Cialone, M.A., Smith, J.M., Atkinson, J.H. and Rosati, J.D. 2010. The potential of wetlands in reducing storm surge. *Ocean Engineering* 37(1) 59-68.

Wang, C., Menenti, M., Stoll, M.-P., Feola, A., Belluco, E. and Marani, M. 2009. Separation of ground and low vegetation signatures in LiDAR measurements of salt-marsh environments. *IEEE Transactions on Geoscience and Remote Sensing* 47(7) 2014-2023.

Wang, J., Wang, G., Hu, H. and Wu, Q. 2010. The influence of degradation of the swamp and alpine meadows on CH4 and CO2 fluxes on the Qinghai-Tibetan Plateau. *Environmental Earth Sciences* 60(3) 537-548.

Wang, H., 2010. Reducing GHG mitigation costs in the shipping industry using the clean development mechanism. Management of Environmental Quality: An International Journal, 21(4), pp.452-463.

Wang, C. and Temmerman, S., 2013. Does biogeomorphic feedback lead to abrupt shifts between alternative landscape states?: An empirical study on intertidal flats and marshes. Journal of Geophysical Research: Earth Surface, 118(1), pp.229-240.

Wang, F., Lu, X., Sanders, C.J. and Tang, J., 2019. Tidal wetland resilience to sea level rise increases their carbon sequestration capacity in United States. Nature Communications, 10(1), p.5434.

Williams, K., Olsen, M.J., Roe, G.V. and Glennie, C. 2013. Synthesis of transportation applications of mobile LiDAR. *Remote Sensing* 5(9) 4652-4692.

Wilson, C.A., Hughes, Z.J., FitzGerald, D.M., Hopkinson, C.S., Valentine, V. and Kolker, A.S., 2014. Saltmarsh pool and tidal creek morphodynamics: Dynamic equilibrium of northern latitude saltmarshes?. Geomorphology, 213, pp.99-115.

Wolters, M., Bakker, J.P., Bertness, M.D., Jefferies, R.L. and Möller, I. 2005. Saltmarsh erosion and restoration in south-east England: squeezing the evidence requires realignment. *Journal of Applied Ecology* 42(5) 844-851.

Woodruff, J.D., Irish, J.L. and Camargo, S.J. 2013. Coastal flooding by tropical cyclones and sea-level rise. *Nature* 504(7478) 44-52.

Wu, W.C. and Cox, D.T., 2015. Effects of wave steepness and relative water depth on wave attenuation by emergent vegetation. Estuarine, Coastal and Shelf Science, 164, pp.443-450.

Xia, J., Falconer, R.A. and Lin, B. 2010. Hydrodynamic impact of a tidal barrage in the Severn Estuary, UK. *Renewable energy* 35(7) 1455-1468.

Xie, T., Li, S., Cui, B., Bai, J., Wang, Q. and Shi, W. 2019. Rainfall variation shifts habitat suitability for seedling establishment associated with tidal inundation in salt marshes. *Ecological Indicators* 98 694-703.

Yando, E., Osland, M. and Hester, M. 2018. Microspatial ecotone dynamics at a shifting range limit: plant–soil variation across salt marsh–mangrove interfaces. *Oecologia* 187(1) 319-331.

Yang, J., Gong, P., Fu, R., Zhang, M., Chen, J., Liang, S., Xu, B., Shi, J. and Dickinson, R. 2013. The role of satellite remote sensing in climate change studies. *Nature climate change* 3(10) 875.

Yang, S., Shi, B., Bouma, T., Ysebaert, T. and Luo, X. 2012. Wave attenuation at a salt marsh margin: a case study of an exposed coast on the Yangtze Estuary. *Estuaries and Coasts* 35(1) 169-182.

Yiqi, L. and Zhou, X. 2010. *Soil respiration and the environment*: Elsevier.

Yu, L., Shi, Y. and Gong, P. 2015. Land cover mapping and data availability in critical terrestrial ecoregions: A global perspective with Landsat thematic mapper and enhanced thematic mapper plus data. *Biological Conservation* 190 34-42.

Zedler, J.B., Callaway, J.C., Desmond, J.S., Vivian-Smith, G., Williams, G.D., Sullivan, G., Brewster, A.E. and Bradshaw, B.K. 1999. Californian salt-marsh vegetation: an improved model of spatial pattern. *Ecosystems* 2(1) 19-35.

Zhong, L., Gong, P. and Biging, G.S. 2012. Phenology-based crop classification algorithm and its implications on agricultural water use assessments in California's Central Valley. *Photogrammetric Engineering & Remote Sensing* 78(8) 799-813.

## 8. Appendix

### Appendix to Chapter two

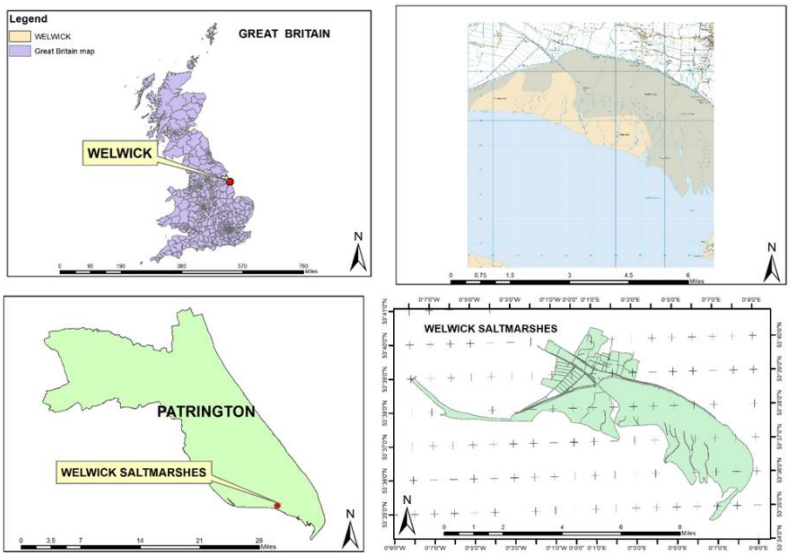


**Appendix 2.1** A map detail at Welwick Saltmarsh.

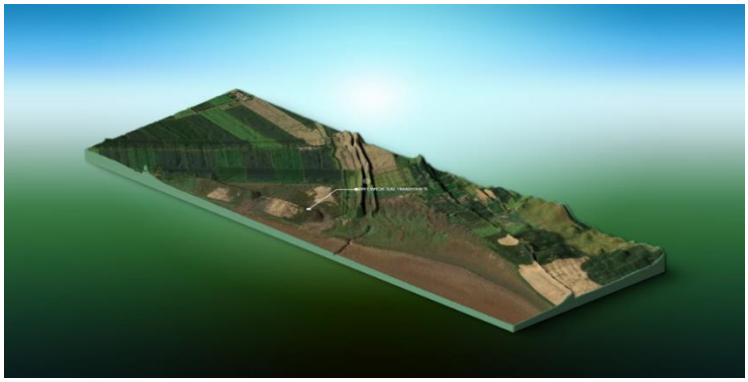

**Appendix 2.2** Welwick saltmarsh 3D terrain generator

**Appendix 2.3** Aerial photograph at Welwick saltmarsh.

**Appendix 2.4** Aerial photograph with polygons at Welwick saltmarsh.

**Appendix 2.5** Aerial photograph of polygons after removing Non marsh polygons at Welwick saltmarsh.

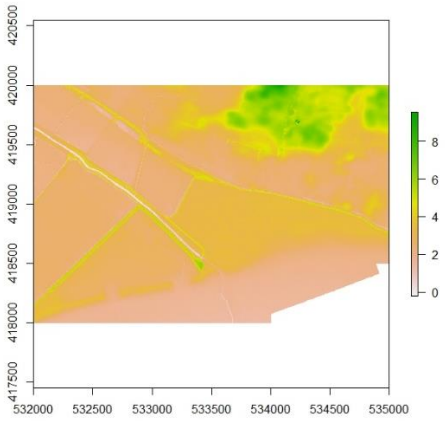


**Appendix 2.6** LIDAR image at Welwick saltmarsh.

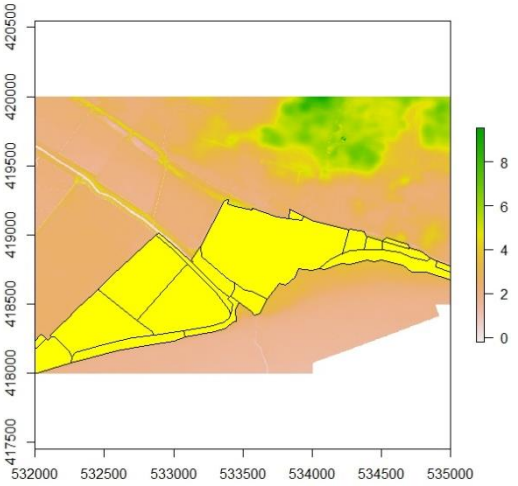


**Appendix 2.7** LIDAR image with polygons at Welwick saltmarsh.

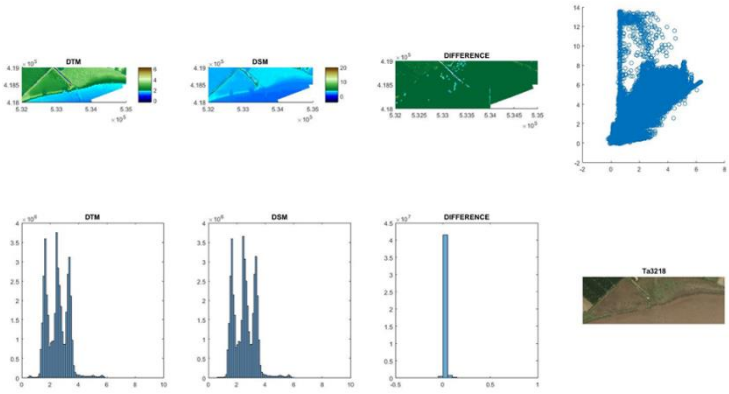


**Appendix 2.8** The differences in saltmarsh elevation between DTM and DSM at Wewick.

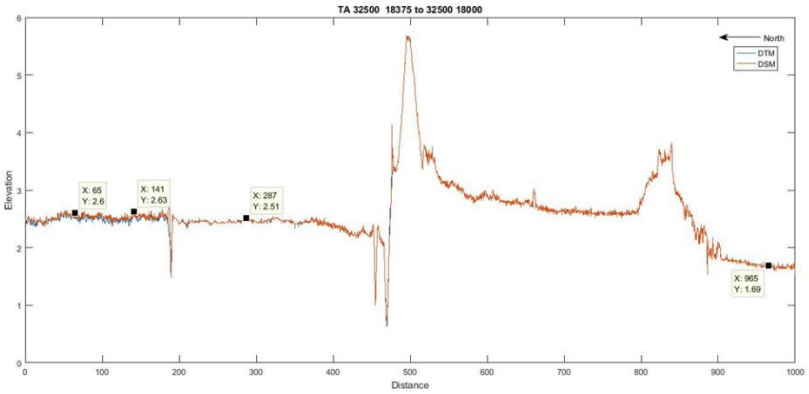


**Appendix 2.9** Salt marsh elevation (DTM &DSM) along transect across saltmarsh at Welwick.

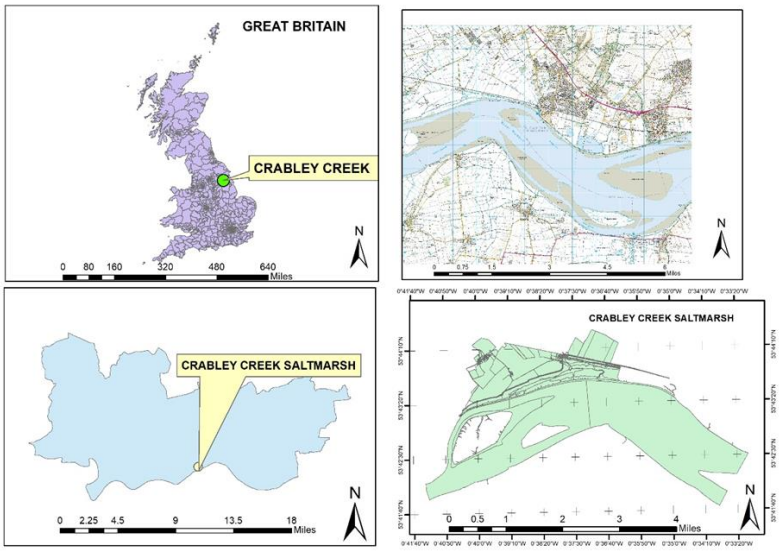


**Appendix 2.10** A map detail at Crably Creek Saltmarsh.

**Appendix 2.11** Crably Creek saltmarsh 3D terrain generator.

**Appendix 2.12** Aerial photograph at Crably Creek saltmarsh.

**Appendix 2.13** Aerial photograph with polygons at Crably Creek saltmarsh.

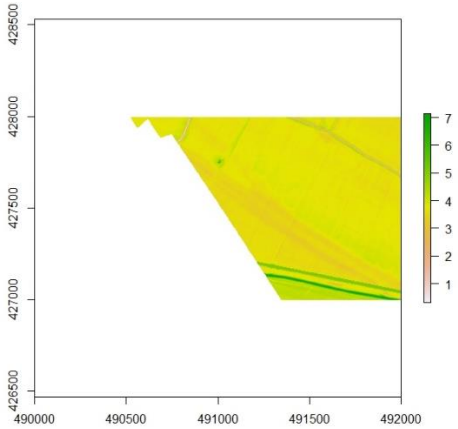


**Appendix 2.14** LIDAR image at Crably Creek saltmarsh.

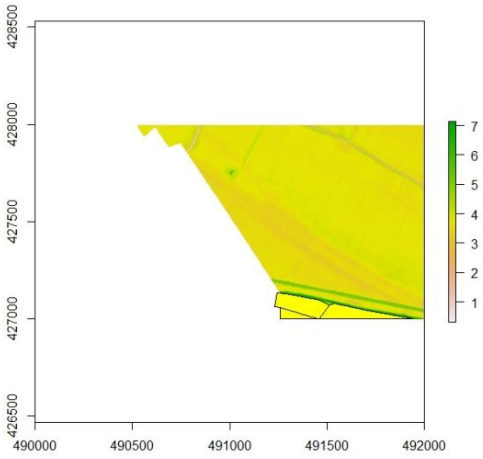


**Appendix 2.15** LIDAR image with polygons at Crably Creek saltmarsh.

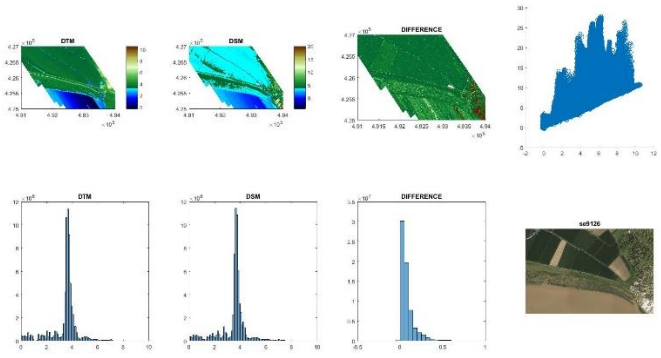


**Appendix 2.16** The differences in saltmarsh elevation between DTM and DSM at Crably Creek.

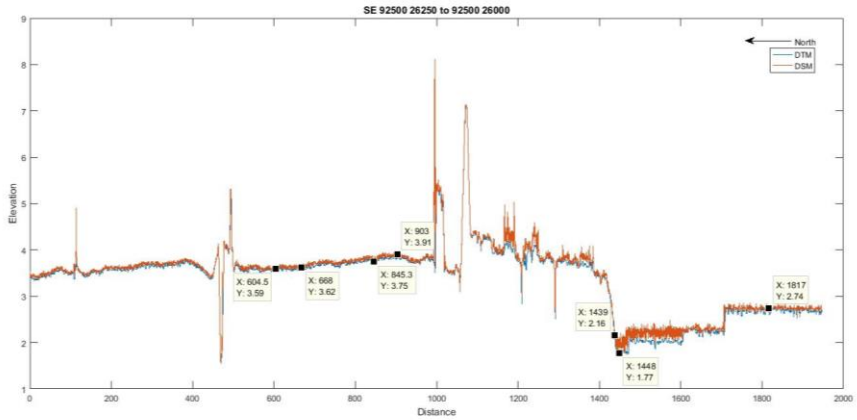


**Appendix 2.17** Salt marsh elevation (DTM &DSM) along transect across saltmarsh at Crably Creek.

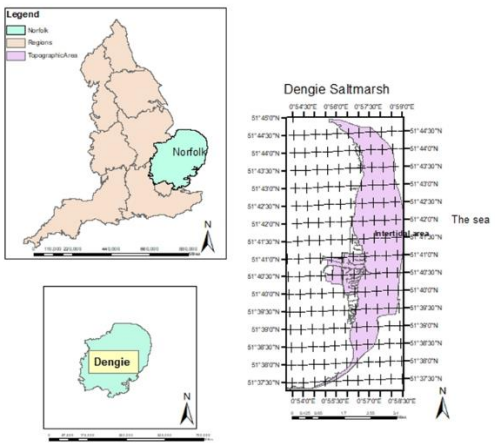

**Appendix 2.18** A map detail at Dengie Saltmarsh.

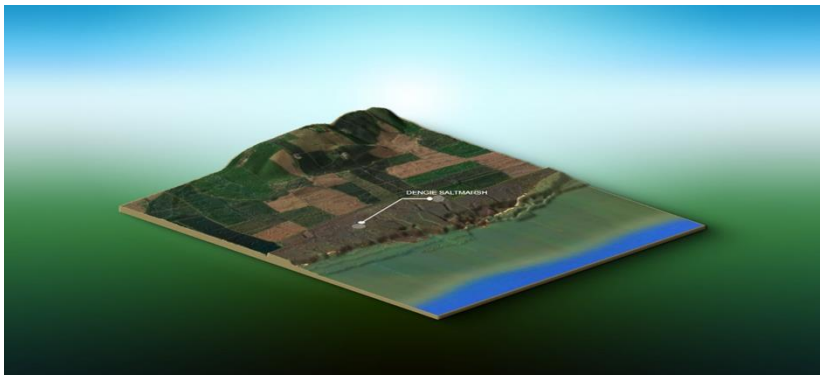


**Appendix 2.19** Welwick saltmarsh 3D terrain generator.

**Appendix 2.20** Aerial photograph at Dengie saltmarsh.

**Appendix 2.21** Aerial photograph with polygons at Dengie saltmarsh.

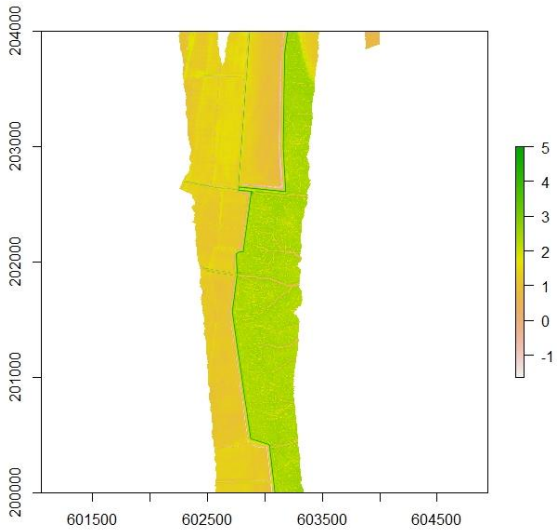


**Appendix 2.22** LIDAR image at Dengie saltmarsh.

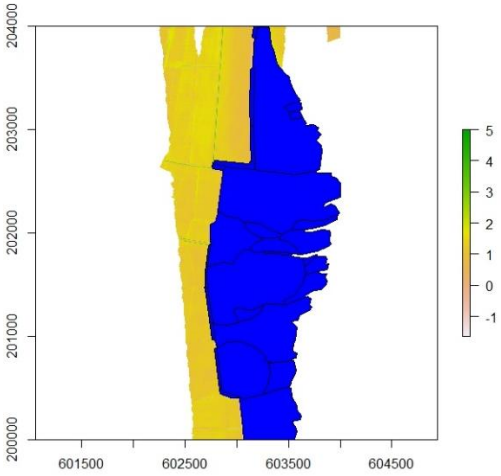


**Appendix 2.23** LIDAR image with polygons at Dengie saltmarsh.

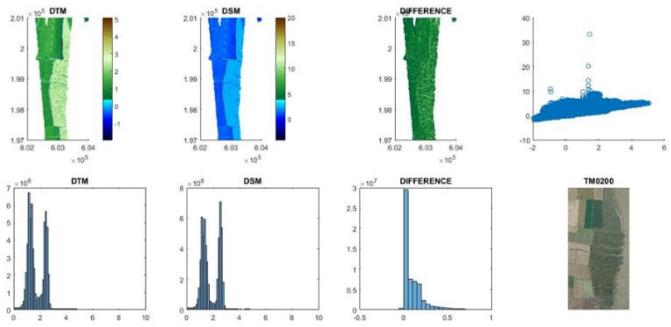


**Appendix 2.24** The differences in saltmarsh elevation between DTM and DSM at Dengie.

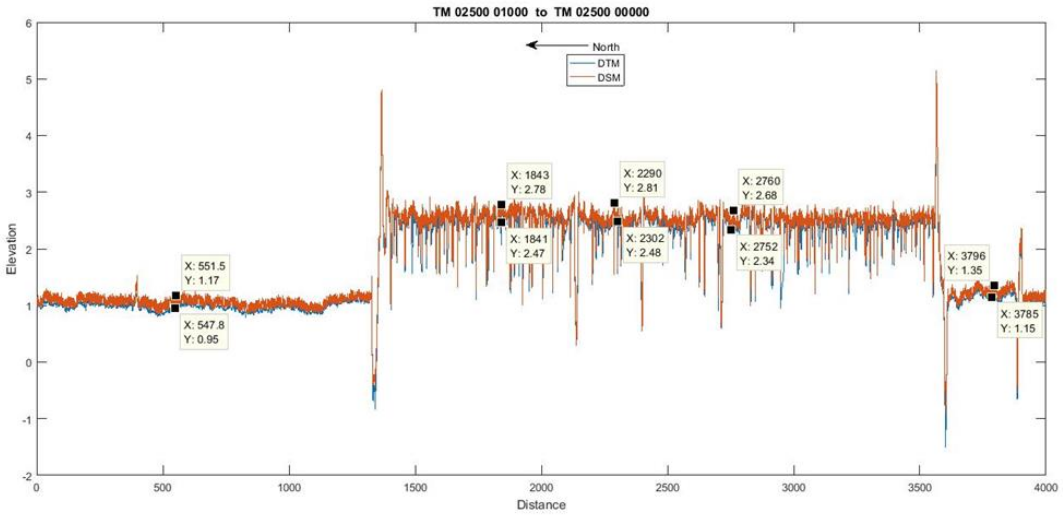


**Appendix 2.25** Salt marsh elevation (DTM &DSM) along transect across saltmarsh at Dengie.

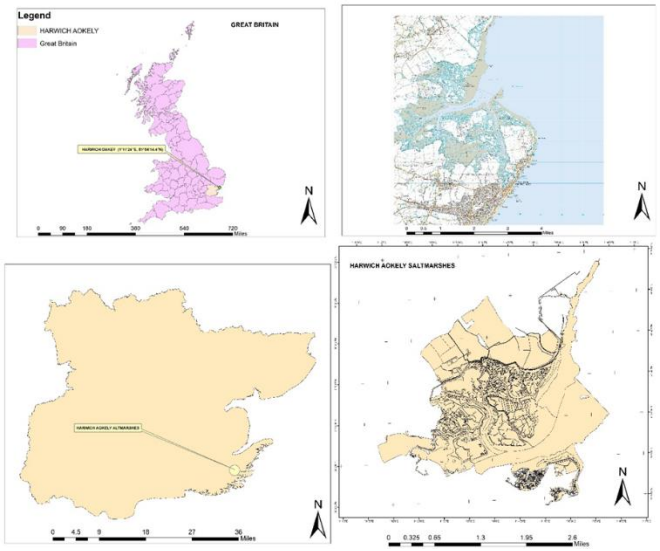


**Appendix 2.26** A map detail at Hamford Water Saltmarsh.


**Appendix 2.27** Hamford Water saltmarsh 3D terrain generator.

**Appendix 2.28** Aerial photograph at Hamford Water saltmarsh.

**Appendix 2.29** Aerial photograph with polygons at Hamford Water saltmarsh.

**Appendix 2.30**Aerial photograph of polygons after removing Non marsh polygons of Hamford Water saltmarsh.

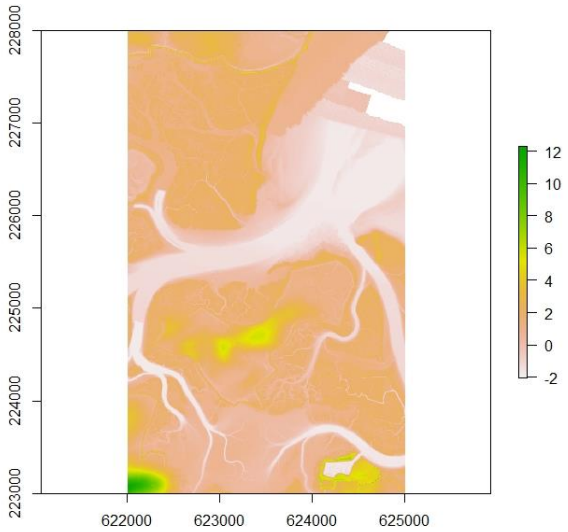


**Appendix 2.31** LIDAR image at Hamford Water saltmarsh.

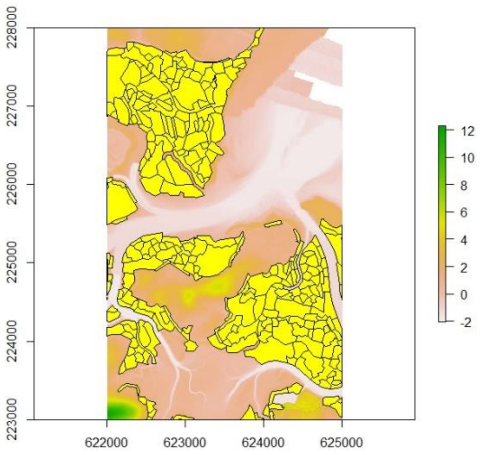


**Appendix 2.32** LIDAR image with polygons of Hamford Water saltmarsh.

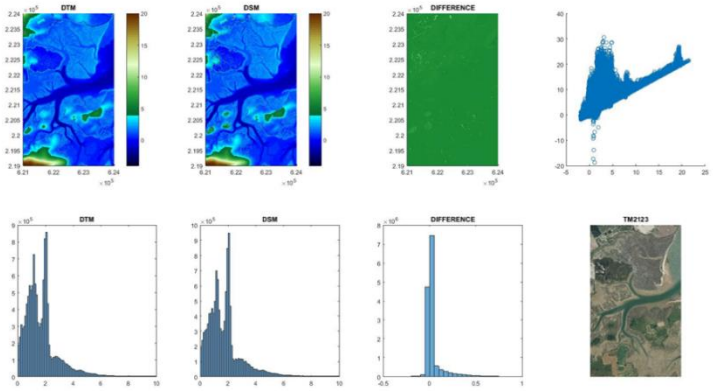


**Appendix 2.33** The differences in saltmarsh elevation between DTM and DSM at Hamford Water.

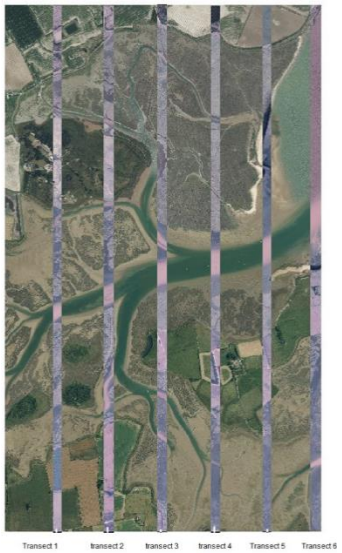

**Appendix 2.34** Transects across Hamford Water saltmarsh.

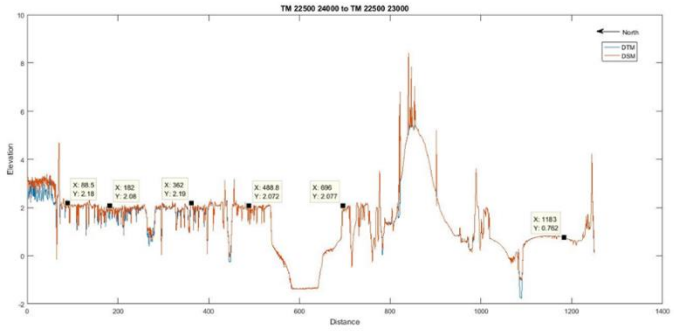


**Appendix 2.35** Salt marsh elevation (DTM &DSM) along transect across saltmarsh at Hamford Water.

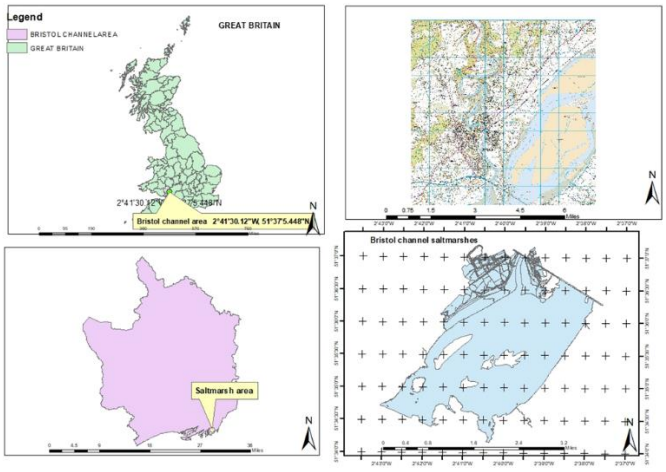


**Appendix 2.36** A map detail of Undy (Severn Estuary) Saltmarsh.

**Appendix 2.37** Aerial photograph of Undy (Severn Estuary) saltmarsh.

**Appendix 2.38** Aerial photograph with polygons of Undy (Severn Estuary) saltmarsh.

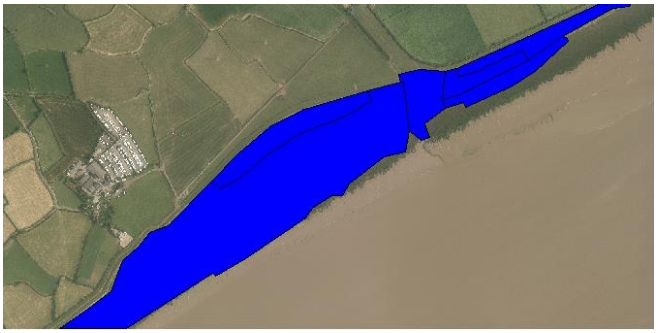

**Appendix 2.39** Aerial photograph of polygons after removing Non marsh polygons of Undy (Severn Estuary) saltmarsh.

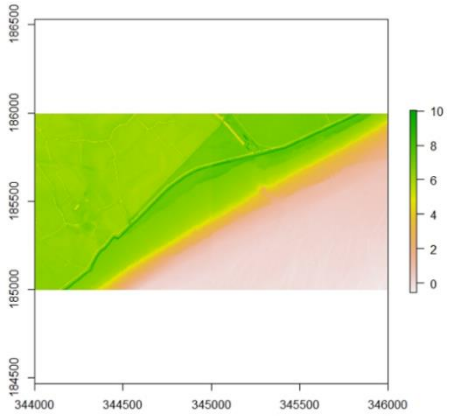


**Appendix 2.40** LIDAR image of Undy (Severn Estuary) saltmarsh.

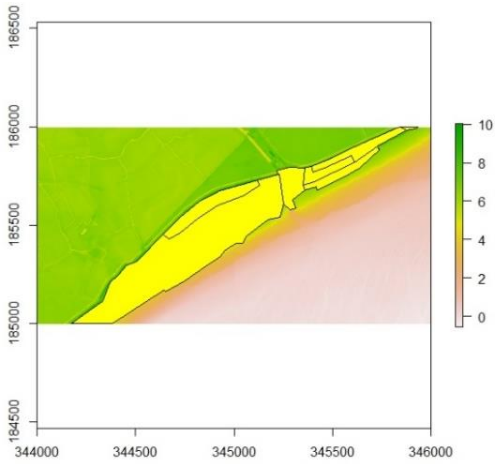


**Appendix 2.41** LIDAR image with polygons of Undy (Severn Estuary) saltmarsh.

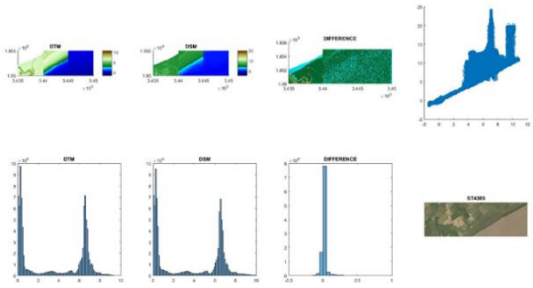

**Appendix 2.42** The differences in saltmarsh elevation between DTM and DSM at Undy (Severn Estuary).

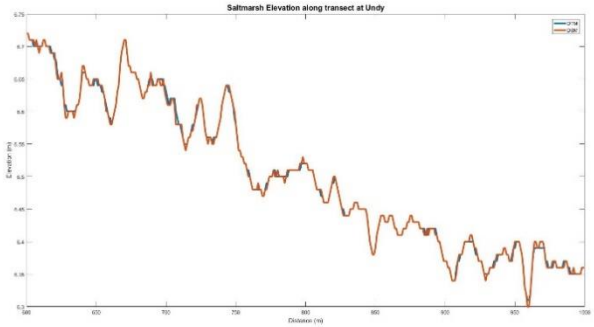


**Appendix 2.43** Salt marsh elevation (DTM &DSM) along transect across saltmarsh at Undy (Severn Estuary).

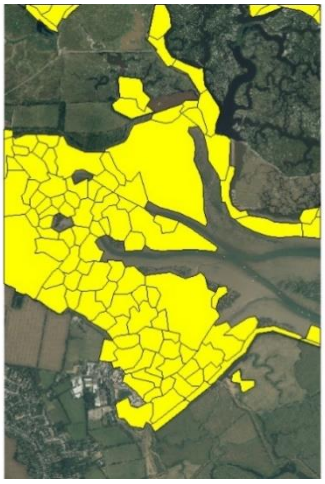

**Appendix 2.44** Aerial photograph of polygons at Tollesbury saltmarsh.

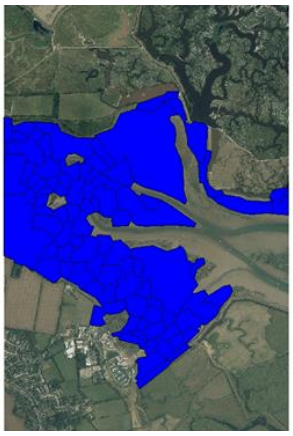

**Appendix 2.45** Aerial photograph of polygons after removing Non marsh polygons at Tollesbury saltmarsh.

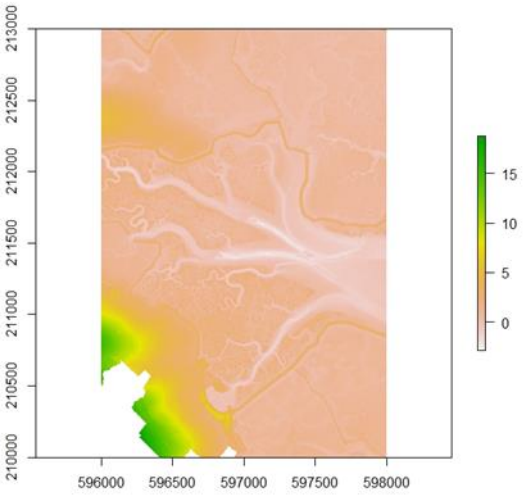

**Appendix 2.46** LIDAR image at Tollesbury saltmarsh.

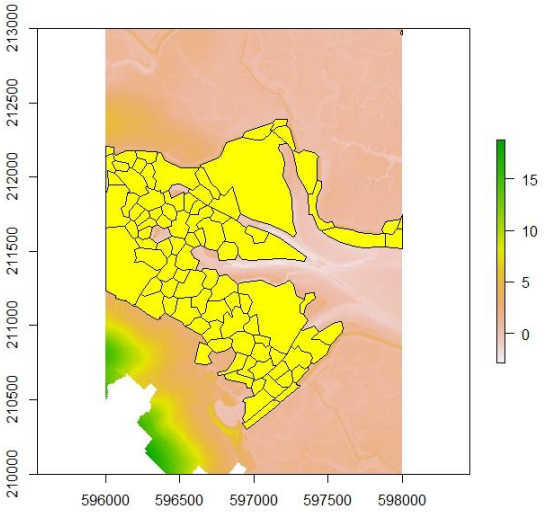


**Appendix 2.47** LIDAR image with polygons at Tollesbury saltmarsh.

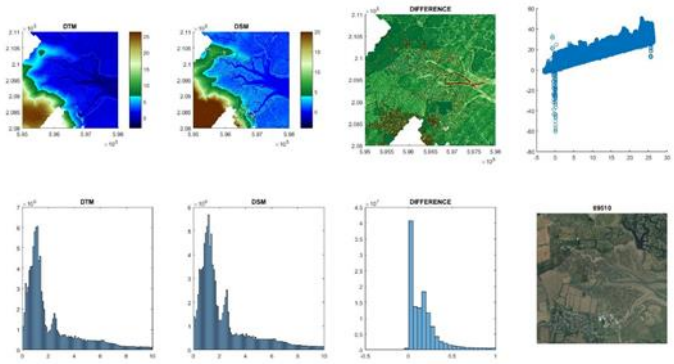


**Appendix 2.48** The differences in saltmarsh elevation between DTM and DSM at Tollesbury.

**Appendix 2.49** Aerial photograph at Tollesbury saltmarsh.

```
'OneDrive - University of East Anglia';

root1='tf9144';
letter=root1(1:2)
east=str2num(root1(3:4))
north=str2num(root1(5:6))
ix=3
iy=3
iieast=1
 for e=east:east+ix-1


    east2=e
% if easting = 100, set east2=00 and increment letter(2) to the next
letter of the alphabet

    if e >=100
        east2=0;
        letter(2)=char(single(letter(2))+1);
    end
    iinorth=1
        for n=north:north+iy-1
            estr=num2str(east2);
            nstr=num2str(n);
            if east2<10
                                estr=strcat('0',estr);
            end

                if n<10
                            nstr=strcat('0',nstr);
                end
            root=strcat(letter,estr,nstr)

            filelist=dir(strcat(root,'_12_250_03.jpg'))
            Z=imread(filelist.name);
%            imshow(Z)
%             figure
        lidar_dtm=strcat(root,'_dtm_1m.asc')
        [LZ_dtm,R]=arcgridread(lidar_dtm);
            if e==east&&n==north
                Rstart=R;
            end
        lidar_dsm=strcat(root,'_dsm_1m.asc')
        [LZ_dsm,R]=arcgridread(lidar_dsm);


%         mapshow(LZ,R,'DisplayType','surface');

        if iinorth
            ZZ=Z;
            LZZ_dtm=LZ_dtm;
            LZZ_dsm=LZ_dsm;
            iinorth=0
        else
            ZZ=[Z;ZZ];
            LZZ_dtm=[LZ_dtm;LZZ_dtm];
            LZZ_dsm=[LZ_dsm;LZZ_dsm];
        end
            end
    if iieast
            ZQ=ZZ;
            LZQ_dtm=LZZ_dtm;
            LZQ_dsm=LZZ_dsm;
            iieast=0
        else
            ZQ=[ZQ,ZZ];
            LZQ_dtm=[LZQ_dtm,LZZ_dtm];
            LZQ_dsm=[LZQ_dsm,LZZ_dsm];
        end

end
imshow(ZQ)
figure
mapshow(LZQ_dsm,Rstart,'DisplayType','surface');
caxis([-4,20])
subplot(2,4,1)
max(LZQ_dtm(:))
min(LZQ_dtm(:))
demcmap([-4 20])
mapshow(LZQ_dtm,Rstart,'DisplayType','surface');title('DTM')
demcmap([-4 20])
colorbar;
subplot(2,4,5)
edges=[0:0.1:10]
histogram(LZQ_dtm,edges);title('DTM')
max(LZQ_dsm(:))
min(LZQ_dsm(:))
subplot(2,4,2)
demcmap([-4 0;0 16])
demcmap([-4 16],64,[],[])
mapshow(LZQ_dsm,Rstart,'DisplayType','surface');title('DSM')
colorbar;
caxis([-4,20])
subplot(2,4,6)
edges=[0:0.1:10]
histogram(LZQ_dsm,edges);title('DSM')
subplot(2,4,8)
imshow(ZQ);title('TF9144 to TF9345')
difference=(LZQ_dsm-LZQ_dtm);
max(difference(:))
min(difference(:))
subplot(2,4,7)
edges2=[-0.5:0.05:1.0]
histogram(difference,edges2);title('DIFFERENCE')
subplot(2,4,3)
colorbar;
demcmap([-0.5 1.0])
mapshow(difference,Rstart,'DisplayType','surface');title('DIFFERENCE')
demcmap([-0.5 1.0])
subplot(2,4,4)
scatter(LZQ_dtm(:),LZQ_dsm(:))
figure
Distance=(1000:2200);
plot(Distance,LZQ_dtm(1000:2200,2500))
hold
plot(Distance,LZQ_dsm(1000:2200,2500))
hold off
```

**Appendix 2.50** Matlab script of analysing the differences between the DTMs and the DSM along transects across saltmarshes.

## Appendix to Chapter three

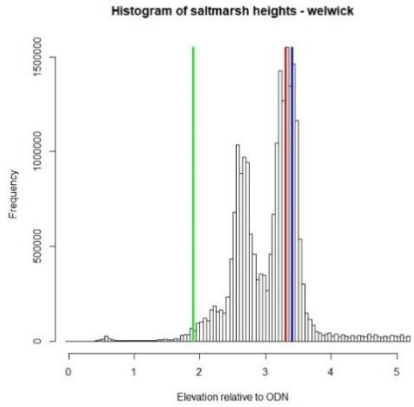


**Appendix 3.1** Elevation histogram relative to ODN at Welwick saltmarsh.

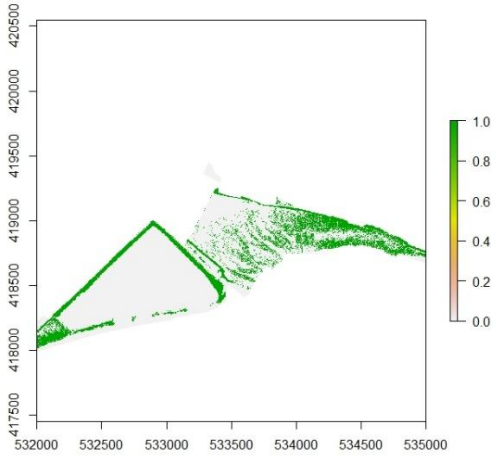


**Appendix 3.2** Saltmarsh polygons above MHWS at Welwick.

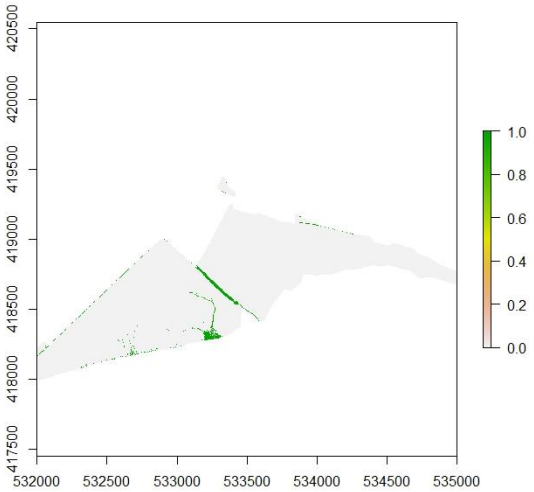


**Appendix 3.4** Saltmarsh polygons below MHWN at Welwick.

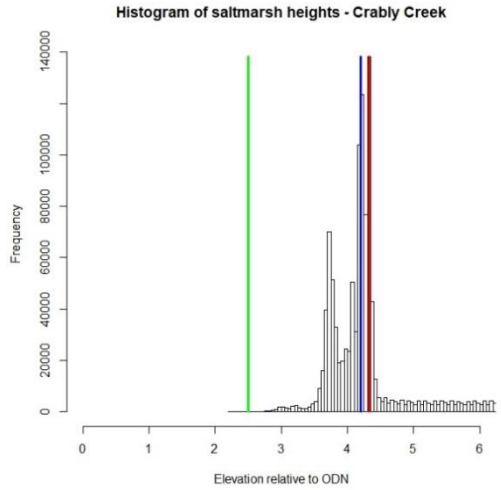


**Appendix 3.5** Elevation histogram relative to ODN at Crably Creek saltmarsh.

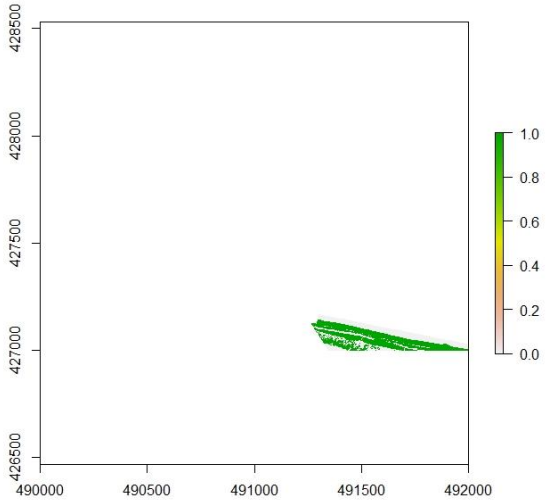


**Appendix 3.6** Saltmarsh polygons above MHWS at Crably Creek.

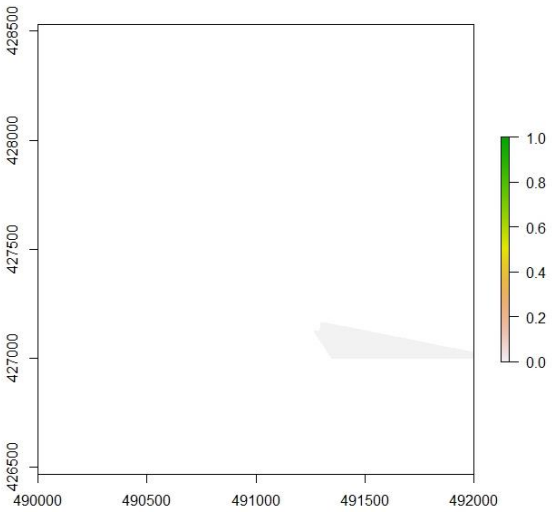

**Appendix 3.7** Saltmarsh polygons below MHWN at Crably Creek.

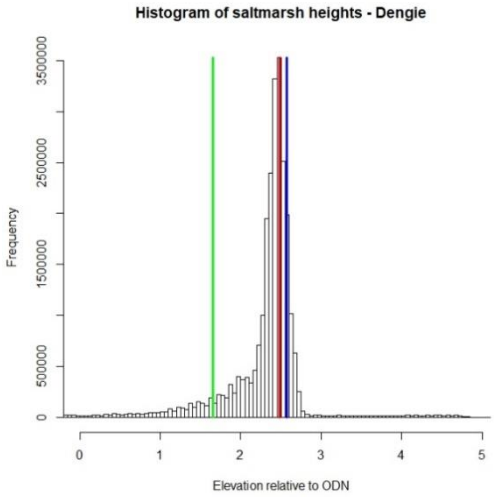


**Appendix 3.8** Elevation histogram relative to ODN at Dengie saltmarsh.

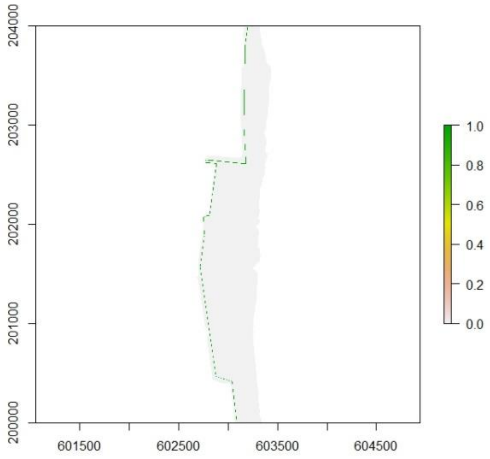


**Appendix 3.9** Saltmarsh polygons above MHWS at Dengie.

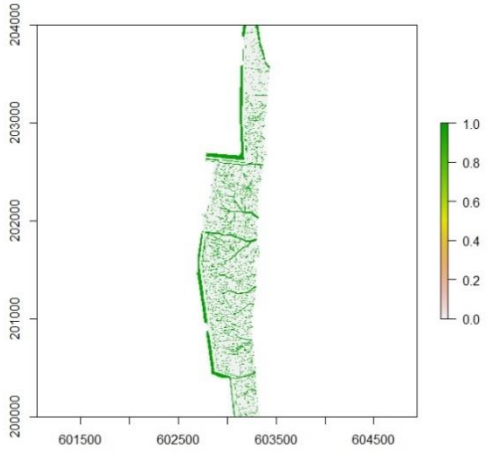


**Appendix 3.10** Saltmarsh polygons below MHWN at Dengie.

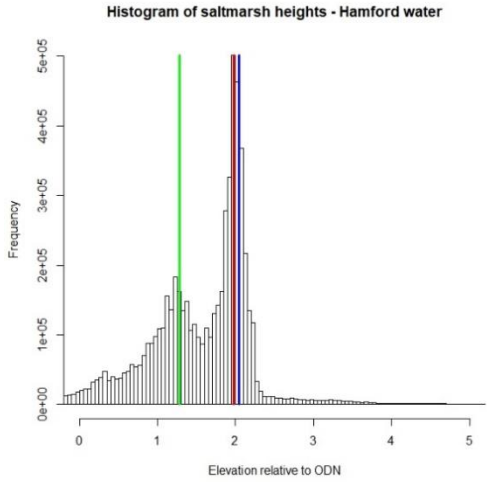


**Appendix 3.11** Elevation histogram relative to ODN at Hamford Water saltmarsh.

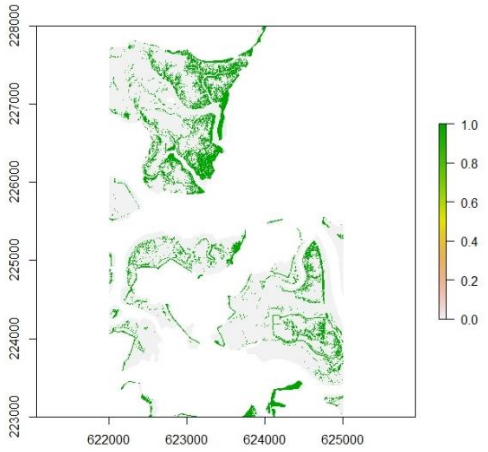

**Appendix 3.12** Saltmarsh polygons above MHWS at Hamford Water.

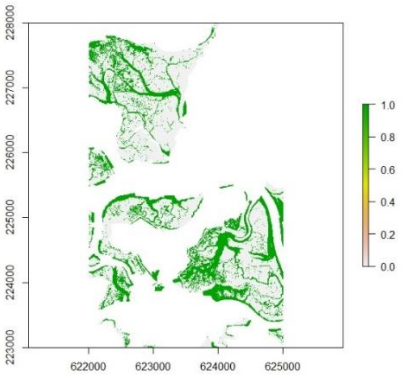


**Appendix 3.13** Saltmarsh polygons below MHWN at Hamford Water.

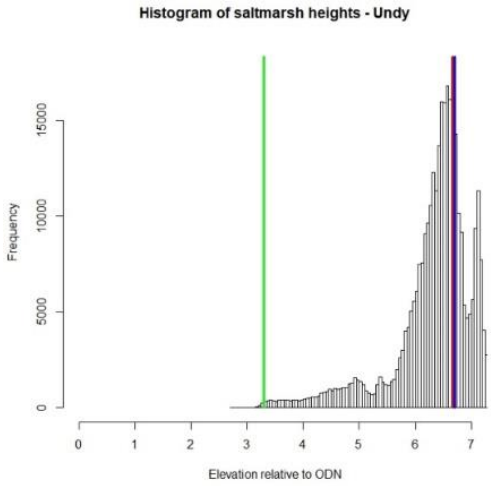


**Appendix 3.14** Elevation histogram relative to ODN at Undy (Severn Estuary) saltmarsh.

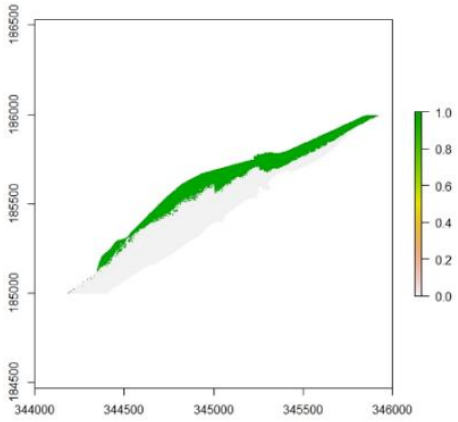


**Appendix 3.15** Saltmarsh polygons above MHWS at Undy (Severn Estuary).

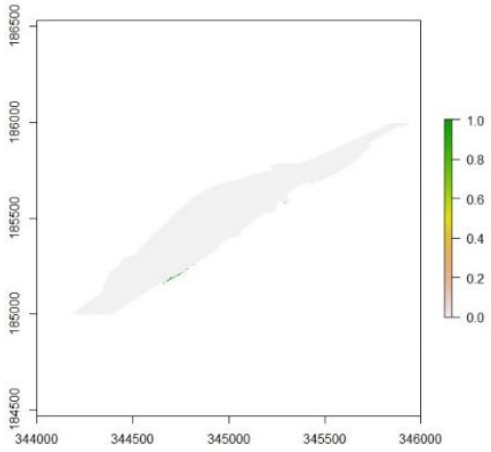


**Appendix 3.16** Saltmarsh polygons below MHWN at Undy (Severn Estuary).

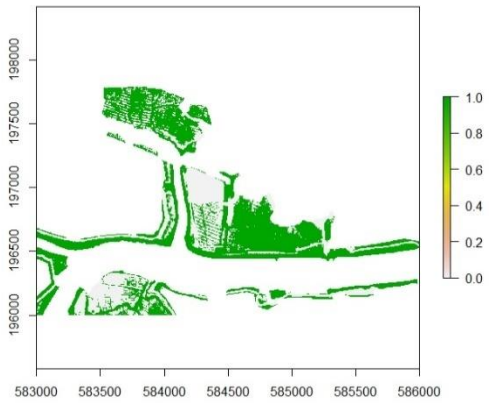


**Appendix 3.16** Saltmarsh polygons above MHWS at Fambridge.

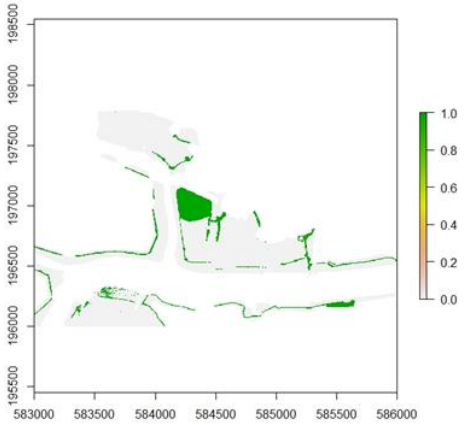


**Appendix 3.17** Saltmarsh polygons below MHWN at Fambridge.

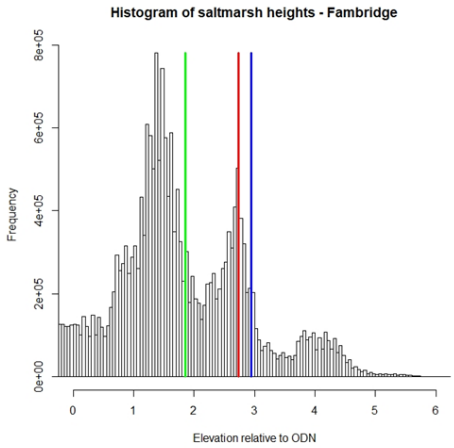


**Appendix 3.18** Elevation histogram relative to ODN at Fambridge.

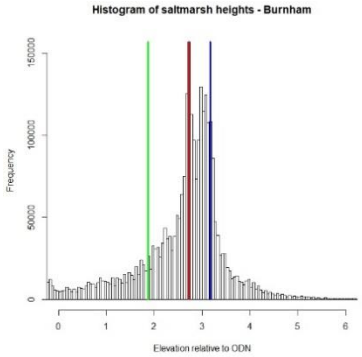


**Appendix 3.19** Elevation histogram relative to ODN at Scolt Head Island.

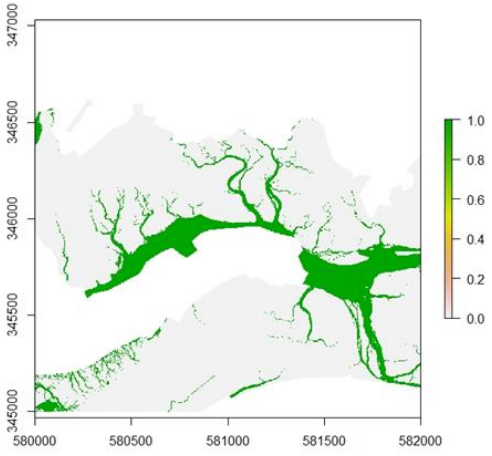


**Appendix 3.20** Saltmarsh polygons above MHWS at Scolt Head Island.

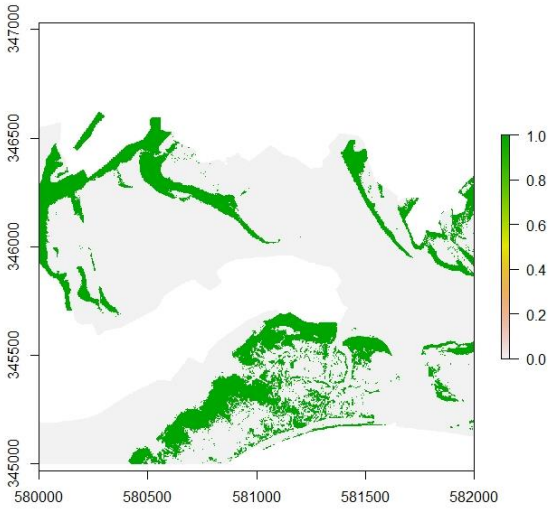


**Appendix 3.21** Saltmarsh polygons below MHWN at Scolt Head Island.

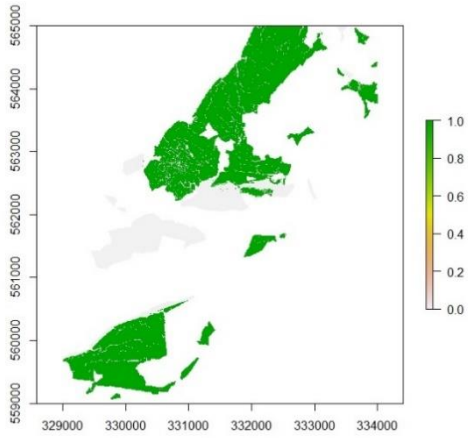


**Appendix 3.22** Saltmarsh polygons above MHWS at Longburgh.

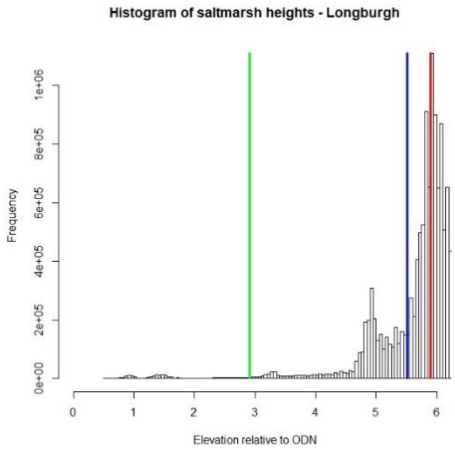


**Appendix 3.23** Elevation histogram relative to ODN at Longburgh.

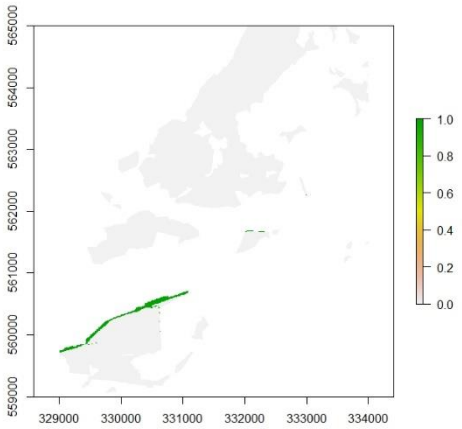


**Appendix 3.22** Saltmarsh polygons below MHWN at Longburgh.

```
#install.packages("raster")
#install.packages("rgdal")
#install.packages("rgeos")
#install.packages("magick")
#install.packages("imager")
require(rgdal)

require(rgeos)

library(raster)
library(magick)
library(imager)
library(modeest)
#mlvlibrary(raster)
library(genefilter)
getwd()
# reading data file name from keyboard not working yet
#readLines(con=stdin(),n=1)
#print("input data file name without the .txt extension     ")
#infile=readLines(con=stdin(),n=1)
setwd("C:/Users/zvs16rja/OneDrive - University of East Anglia")
infile="Burnham_clipped"
infile2=paste(infile,".txt",sep="")
outfile=paste(infile,"_clipped.txt",sep="")

inputspec <- readLines(infile2)
title=inputspec[1]
data_directory=inputspec[2]
fileroot=unlist(strsplit(inputspec[3],","))
map_limits=as.numeric(unlist(strsplit(inputspec[4],",")))
#
#Map_limits is not currently used to do any clipping
#
hist_limits=as.numeric(unlist(strsplit(inputspec[5],",")))
key_heights=as.numeric(unlist(strsplit(inputspec[6],",")))
excluded=as.numeric(unlist(strsplit(inputspec[7],",")))
remove_polygons=as.numeric(inputspec[8])

#read in the salt marsh polygons
setwd("C:/Users/zvs16rja/OneDrive - University of East Anglia")
#setwd("C:/Users/zvs16rja/OneDrive - University of East Anglia")

shape3 <- readOGR(dsn = ".", layer = "LCM2015_GB3")

#set working directory containing lidar data
```

```
#set working directory containing lidar data
setwd(data_directory)
#setwd("C:/Users/zvs16rja/OneDrive - University of East Anglia")

#set the squares that we want to use



# check first image file exists

image1=load.image(paste(fileroot[1],"_rgb_250_04.jpg",sep=""))
plot(image1)

# check first lidar file exists
lidar_test=raster(paste(fileroot[1],"_dtm_1m.asc",sep=""))

plot(lidar_test)



par(mfrow=c(2,3))

nnn=length(fileroot)
image_files=""
for (iii in 1:nnn) {
  image_files[iii]=intersect(list.files(pattern = fileroot[iii]), list.files(pattern = "jpg"))
  if (length(image_files[iii])>1){
    print("more than one image file for this square")
    image_files[iii]
    image_files[iii]=image_files[iii,1]
  }
}

image_files


lidar_all=raster(paste(fileroot[1],"_dtm_1m.asc",sep=""))
image_all=brick(paste(fileroot[1],"_rgb_250_04.jpg",sep=""))
image_all=brick(image_files[1])

extent(image_all)=extent(lidar_all)

for (iii in 2:nnn){
  lidar2=raster(paste(fileroot[iii],"_dtm_1m.asc",sep=""))
  lidar_all=merge(lidar_all,lidar2)
```

```
  lidar_all=merge(lidar_all,lidar2)
  image2=brick(paste(fileroot[iii],"_rgb_250_04.jpg",sep=""))
  image2=brick(image_files[iii])
  extent(image2)=extent(lidar2)
  image_all=merge(image_all,image2)
}
extent2=extent(lidar_all)


#next lines extend are with a 1 km buffer

extent2[1]=extent2[1]-1000;

extent2[2]=extent2[2]+1000;

extent2[3]=extent2[3]-1000;

extent2[4]=extent2[4]+1000;




#cropped_shapes2<-crop(shape3,extent(573000, 576000, 342000, 347000) )

cropped_shapes2<-crop(shape3,extent2 )



cropped_shapes<-crop(shape3,lidar_all)

cropped_shapes<-subset(cropped_shapes,OBJECTID!=excluded)



heights2=extract(lidar_all,cropped_shapes2)

dev.new()
hist(unlist(heights2,use.names=FALSE),breaks=200)

MHWN=1.87
MHWS=3.17

#Find mode
```

```
mlv(unlist(heights2),method="naive",bw=0.001)
?mlv

nHeights=length(unlist(heights2))
nHeights
below_mhwn=sum(unlist(heights2) < MHWN)
proportion_below=below_mhwn/nHeights

proportion_below

above_mhws=sum(unlist(heights2) > MHWS)

proportion_above=above_mhws/nHeights
proportion_above

dev.new()
#plot whole lidar image as normal
plot(lidar_all)
dev.new()
#plot areas in whole lidar image above MHWS
plot(lidar_all>MHWS)
dev.new()
#plot areas in whole lidar image below MHWN
plot(lidar_all<MHWN)
dev.new()
#plot areas within saltmarsh polygons above MHWS
plot(mask(lidar_all>MHWS,cropped_shapes))
dev.new()
#plot areas within saltmarsh polygons below MHWN

plot(mask(lidar_all<MHWN,cropped_shapes))


dev.new()
plotRGB(image_all,r=1,g=2,b=3)
par(new=TRUE)
dev.new()
plotRGB(image_all,r=1,g=2,b=3)
par(new=TRUE)
plot(cropped_shapes,add=TRUE,col='yellow')

###########
#
# Polygon removal - number to be removed is read from input file
```

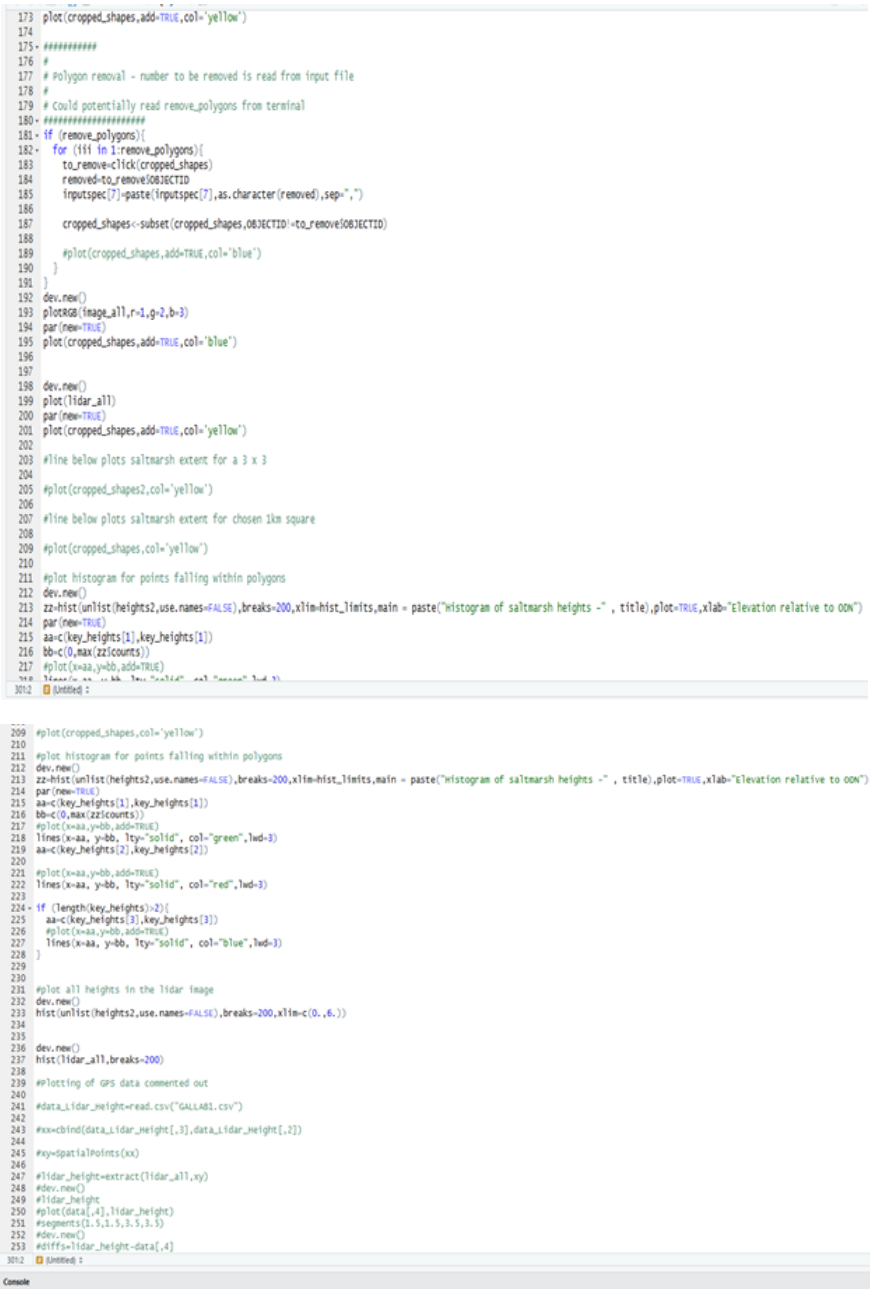

```
plot(cropped_shapes,add=TRUE,col='yellow')

##########
#
# Polygon removal - number to be removed is read from input file
#
# Could potentially read remove_polygons from terminal
####################
if (remove_polygons){
  for (iii in 1:remove_polygons){
    to_remove=click(cropped_shapes)
    removed=to_remove$OBJECTID
    inputspec[7]=paste(inputspec[7],as.character(removed),sep=",")

    cropped_shapes<-subset(cropped_shapes,OBJECTID!=to_remove$OBJECTID)

    #plot(cropped_shapes,add=TRUE,col='blue')
  }
}
dev.new()
plotRGB(image_all,r=1,g=2,b=3)
par(new=TRUE)
plot(cropped_shapes,add=TRUE,col='blue')


dev.new()
plot(lidar_all)
par(new=TRUE)
plot(cropped_shapes,add=TRUE,col='yellow')

#line below plots saltmarsh extent for a 3 x 3

#plot(cropped_shapes2,col='yellow')

#line below plots saltmarsh extent for chosen 1km square

#plot(cropped_shapes,col='yellow')

#plot histogram for points falling within polygons
dev.new()
zz=hist(unlist(heights2,use.names=FALSE),breaks=200,xlim=hist_limits,main = paste("Histogram of saltmarsh heights -" , title),plot=TRUE,xlab="Elevation relative to ODN")
par(new=TRUE)
aa=c(key_heights[1],key_heights[1])
bb=c(0,max(zz$counts))
#plot(x=aa,y=bb,add=TRUE)
```

```
#plot(cropped_shapes,col='yellow')

#plot histogram for points falling within polygons
dev.new()
zz=hist(unlist(heights2,use.names=FALSE),breaks=200,xlim=hist_limits,main = paste("Histogram of saltmarsh heights -" , title),plot=TRUE,xlab="Elevation relative to ODN")
par(new=TRUE)
aa=c(key_heights[1],key_heights[1])
bb=c(0,max(zz$counts))
#plot(x=aa,y=bb,add=TRUE)
lines(x=aa, y=bb, lty="solid", col="green",lwd=3)
aa=c(key_heights[2],key_heights[2])

#plot(x=aa,y=bb,add=TRUE)
lines(x=aa, y=bb, lty="solid", col="red",lwd=3)

if (length(key_heights)>2){
  aa=c(key_heights[3],key_heights[3])
  #plot(x=aa,y=bb,add=TRUE)
  lines(x=aa, y=bb, lty="solid", col="blue",lwd=3)
}


#plot all heights in the lidar image
dev.new()
hist(unlist(heights2,use.names=FALSE),breaks=200,xlim=c(0.,6.))


dev.new()
hist(lidar_all,breaks=200)

#Plotting of GPS data commented out

#data_Lidar_height=read.csv("GALLA01.csv")

#xx=cbind(data_Lidar_height[,3],data_Lidar_height[,2])

#xy=SpatialPoints(xx)

#lidar_height=extract(lidar_all,xy)
#dev.new()
#lidar_height
#plot(data[,4],lidar_height)
#segments(3.5,3.5,3.5,3.5)
#dev.new()
#diffs=lidar_height-data[,4]
```

Appendix 3.23 script of R program to analyse elevation data and relative tidal heights for all marsh sites undertaken in this study.

## Appendix to Chapter Four

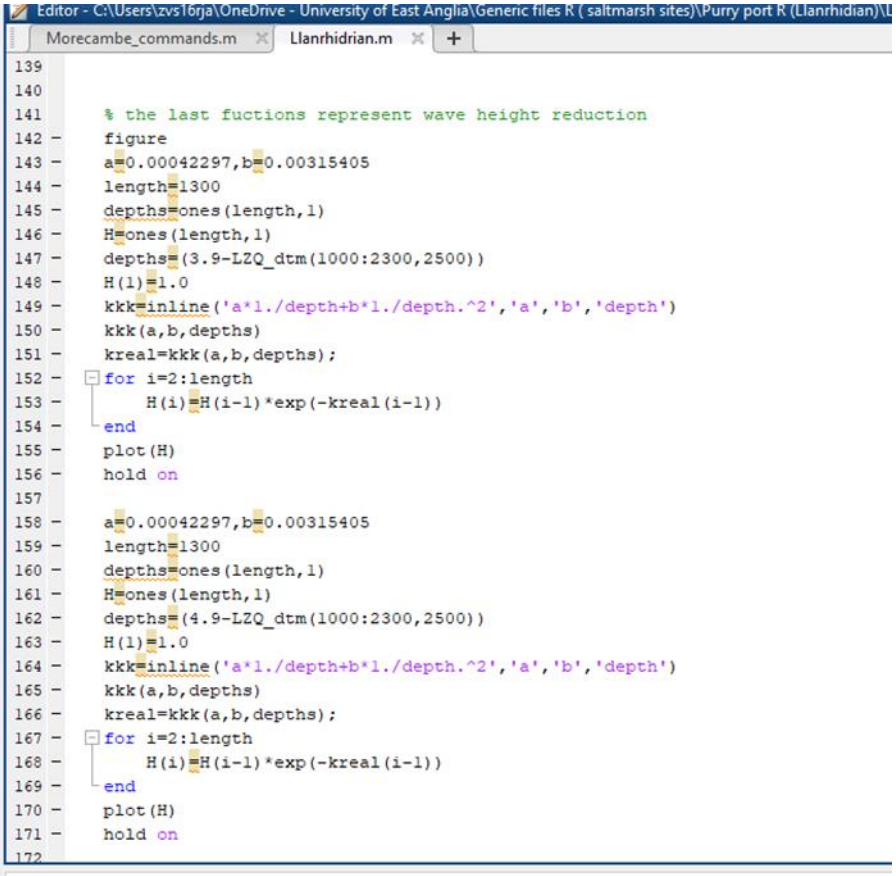


Appendix 4.1 script of R program to analyse water level as a function of wave dissipation using K (Decay) at Llanrhidian marsh.

## Appendix to Chapter five

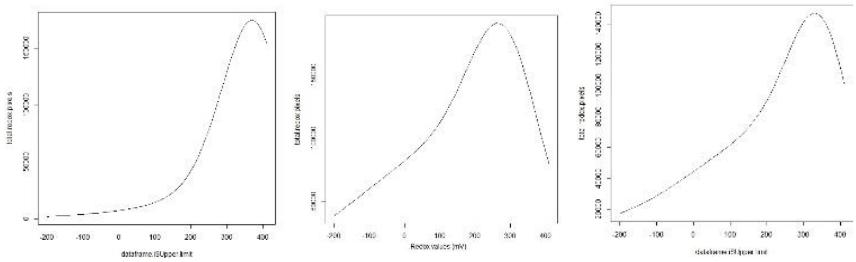

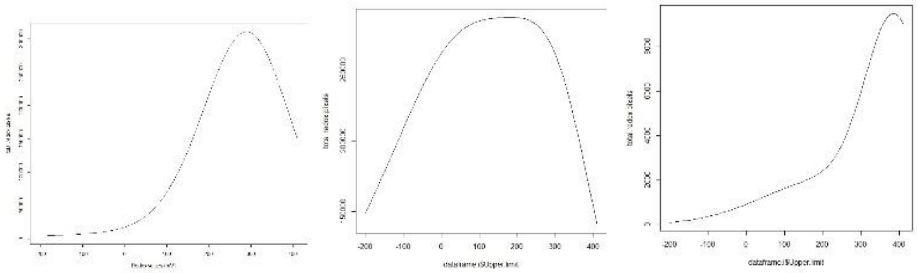

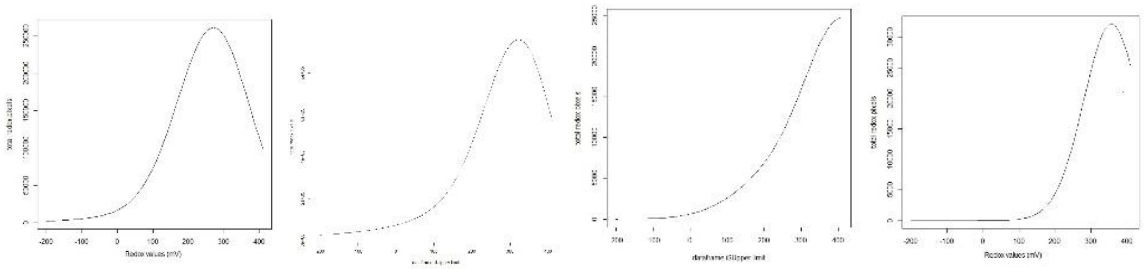

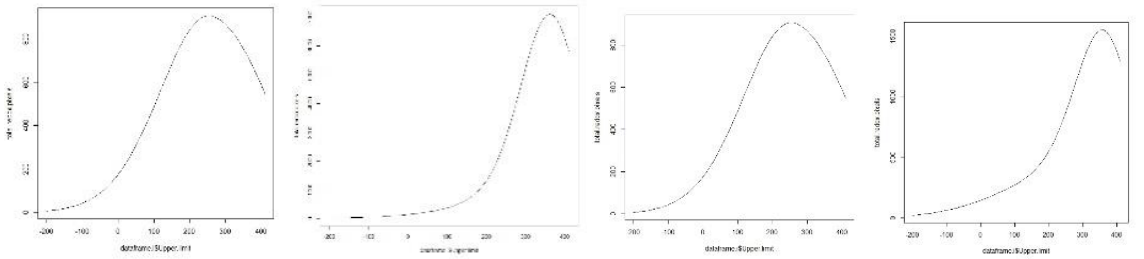

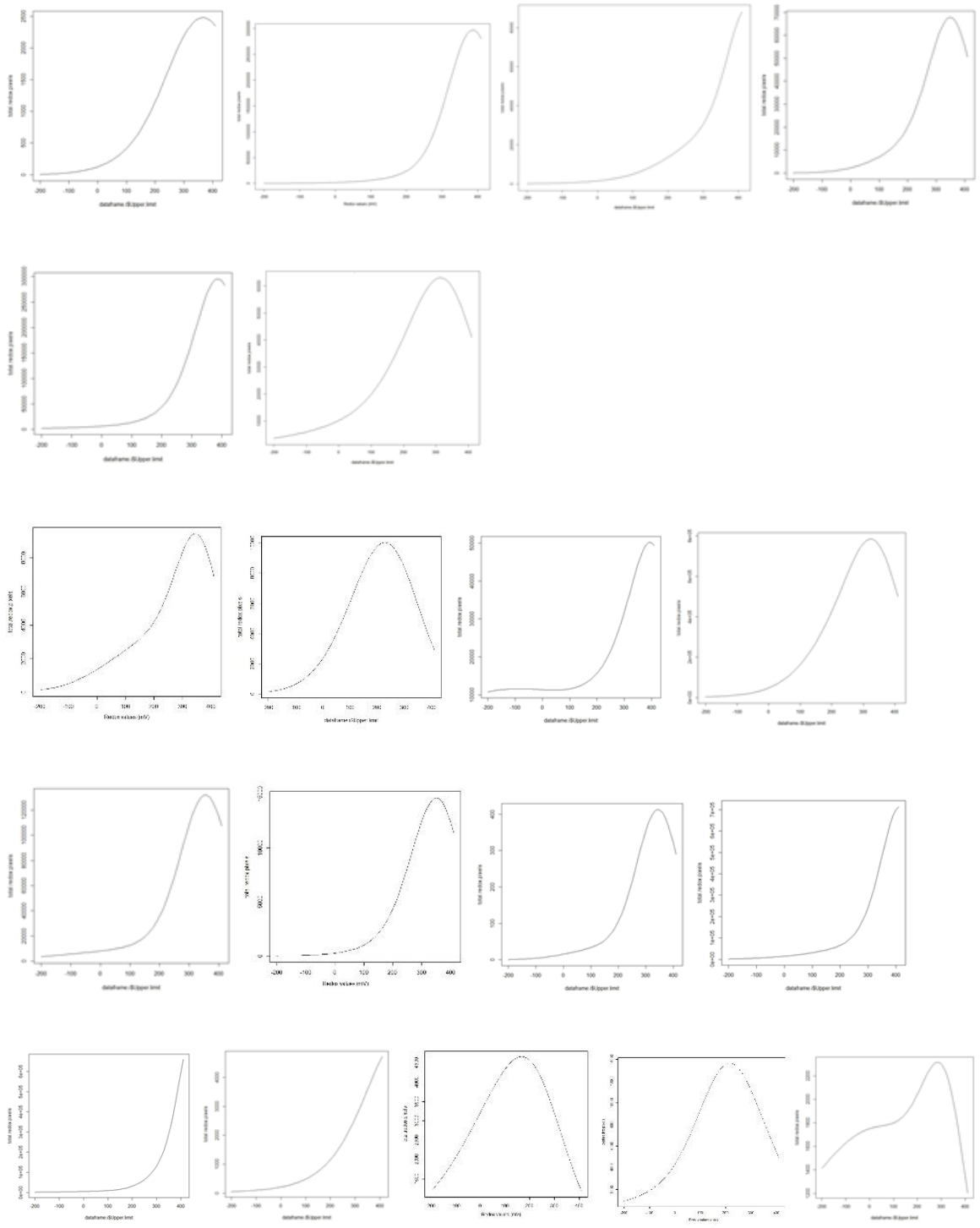

**Appendix 5.1 Predicted distribution of redox values averaged across the whole area of the marsh at each individual marsh in this study.**